

Habilitation à diriger des recherches

INSTITUT DE
RECHERCHE
MATHÉMATIQUE
AVANCÉE

UMR 7501

Strasbourg

Université de Strasbourg
Spécialité MATHÉMATIQUES

Yohann Le Floch

**Quantification de Berezin-Toeplitz et systèmes
semi-toriques**

Soutenue le 17 novembre 2023
devant la commission d'examen

Semyon Klevtsov, garant
Benoît Douçot, rapporteur
Sonja Hohloch, rapporteuse
George Marinescu, rapporteur
Nalini Anantharaman, examinatrice
Thomas Delzant, examinateur
Gabriel Rivière, examinateur

<https://irma.math.unistra.fr>



Université

de Strasbourg

Quantification de Berezin-Toeplitz et systèmes semi-toriques

—

Berezin-Toeplitz quantization and semitoric systems

Yohann Le Floch

Remerciements

Me voici rendu à la partie à la fois la plus agréable et la plus délicate de la rédaction de ce mémoire. En effet, si j’apprécie cette occasion rare de pouvoir exprimer ma reconnaissance à l’écrit, l’exercice est difficile: parler de mes mathématiques est une chose que je sais faire (suffisamment bien, je l’espère), mais parler de moi et de ce que je dois aux autres constitue une tâche autrement plus ardue. En outre, je suis bien conscient que c’est la partie de ce texte qui sera lue par le plus grand nombre, et qu’il faut donc la rédiger de manière particulièrement méticuleuse.

Il s’agit tout de même d’être relativement synthétique. Ainsi, ne m’en voulez pas si vous ne vous trouvez pas explicitement dans les paragraphes qui suivent; de toute manière, si vous comptez pour moi, vous n’avez sans doute pas besoin de ces lignes pour le savoir. Cependant, je vais quand même m’employer à citer quelques noms afin que vous tous et toutes, qui lisez ces remerciements cinq minutes après le début de ma soutenance en regardant votre montre et en vous maudissant d’être venus, ayez de quoi passer le temps en attendant la délivrance, même si vous n’y trouverez sans doute rien de bien original, en tout cas rien qu’un membre aléatoire de la communauté mathématique n’eût pu écrire. Vous ne pourrez même pas vous amuser à construire un ordre de préférence sur l’ensemble des personnes remerciées ici, puisque j’ai choisi, dans chaque rubrique, de les classer par ordre alphabétique. Tout juste pourrez vous, en matière de détail croustillant, apprendre le nom de mon chat, si vous lisez jusqu’au bout; je vous prie de m’excuser pour cette vie bien peu excitante. Le pot sera, je l’espère, beaucoup plus intéressant.

Avant tout, je souhaite exprimer toute ma gratitude à Benoît Douçot, Sonja Hohloch et George Marinescu qui m’ont fait l’immense honneur d’avoir accepté de rapporter ce mémoire. Je remercie également Nalini Anantharaman, Thomas Delzant et Gabriel Rivière pour avoir bien voulu faire partie de mon jury, et enfin Semyon Klevtsov qui a généreusement accepté de jouer le rôle de garant de cette habilitation.

Je n’aurais sans doute pas réussi à naviguer dans les méandres de la procédure d’habilitation sans les informations précieuses distillées par mes prédécesseurs, Giuseppe Ancona et Thomas Dreyfus, et par Géraldine Schverer qui a toujours su répondre avec efficacité et bonne humeur à mes questions; je les en remercie. Je suis également reconnaissant, comme certainement beaucoup d’autres avant moi, envers notre collègue Pierre Guillot d’avoir détaillé les différentes étapes à franchir sur sa page professionnelle.

De mon point de vue, la recherche serait beaucoup moins enthousiasmante sans collaborateur. Ainsi, je remercie chaleureusement Michele Ancona, Laurent Charles, Joseph Palmer, Álvaro Pelayo et San Vĩ Ngọc pour ces moments, mathématiques ou non, partagés ensemble. Je dois en fait remercier tout spécialement Joseph Palmer, pour son soutien alors que je jonglais entre l’écriture de ce mémoire et l’interminable gestation de notre dernier article, et pour sa relecture attentive d’une bonne partie de ce manuscrit. J’ai cité les collègues avec qui nous avons rédigé au moins un article, mais je pourrais ajouter Alix Deleporte (pour nos aventures non auto-adjointes et nos rejets par l’ANR), ainsi que Leonid Polterovich et Ood Shabtai (pour ce “petit problème” concernant les commutateurs de signes de spins) à cette liste. Je suis également reconnaissant envers tous les collègues croisés en conférence, en séminaire ou en d’autres occasions, et avec qui nous avons pu échanger malgré ma propension à esquiver les interactions sociales.

Je ne serai pas le premier (et sûrement pas le dernier) à l’écrire, mais à l’IRMA et à l’UFR

de mathématique et informatique nous jouissons de conditions de travail particulièrement favorables. Je salue donc tous les collègues, personnels d'enseignement et/ou de recherche ou administratifs, et plus particulièrement celles et ceux de l'équipe Analyse (au sens large), dans laquelle j'ai été extrêmement bien accueilli dès mon arrivée à Strasbourg. Bien entendu, ceux qui ont partagé mon bureau, Olivier Benoist puis Giuseppe Ancona, méritent une place spéciale dans ces remerciements; la vie quotidienne aurait été plus fade sans leur joie de vivre et leurs précieux conseils mathématiques ou non. Je remercie également les étudiants et étudiantes qui rendent la partie enseignement de mon travail très agréable; ils et elles sont globalement formidables et de ce point de vue, j'ai l'impression que nous sommes gâtés à Strasbourg. J'en profite pour exprimer ma gratitude à Adriano Marmora qui m'a fait confiance en me proposant ce nouveau défi avec les MPA; j'en suis honoré.

Je remercie également Nicolas Juillet de m'avoir embarqué dans l'aventure MATH.en.JEANS il y a quelques années. L'enthousiasme des élèves et des enseignants et enseignantes que j'ai pu rencontrer par ce biais fait chaud au cœur, et fournit de la motivation quand le reste est compliqué. Merci à toutes et tous.

Il est enfin temps d'aborder les aspects plus personnels de ces remerciements. Merci aux habitués du mercredi soir à l'Urban Soccer pour ces moments de détente bienvenus, avec une pensée spéciale pour Bora grâce à qui tout a commencé. Merci aux grimpeurs et grimpeuses pour ces nombreuses séances passées à réfléchir à des problèmes non mathématiques; merci en particulier à Adèle et Valdo pour leur positivité et leur mignonnerie. Merci aux rennais et à leurs petites familles d'être là depuis toutes ces années et pour ces weekends et vacances passés ensemble. Merci à Quentin et Romain pour les soirées jeux.

Merci enfin à ma famille pour tant de choses qu'essayer de les énoncer serait vain. D'abord merci à Nabla, qui est entré dans ma vie sans crier gare et au meilleur moment possible; sans lui, je ne sais pas si j'aurais supporté les mois d'isolement pendant lesquels notre bon gouvernement nous protégeait du grave danger de se promener en forêt, ni la période d'écriture de ce texte durant laquelle je remettais mes connaissances en question quasiment quotidiennement. Merci également à son cousin Émile qui me fait bien rire. Merci, enfin, à mes proches: Andrée, Bruno, Damien, Ewan, Ida, Killian, Nathalie, merci pour tout.

Contents

1	Introduction	7
1.1	Context and motivations	7
1.2	Works presented in the manuscript	8
1.3	Symplectic preliminaries and notation	9
1.4	Structure of the manuscript	10
1.5	Disclaimers	11
2	Some results in Berezin-Toeplitz quantization	12
2.1	The semiclassical limit of geometric quantization	12
2.2	Lagrangian states and fidelity	16
2.3	Random holomorphic sections and Berezin-Toeplitz operators	25
2.4	Quantum propagation and trace formulas	34
2.4.1	Quantum propagators and smoothed spectral projectors	34
2.4.2	Traces of quantum propagators	40
2.4.3	The Gutzwiller trace formula	43
2.5	Perspectives	47
3	Generalities on semitoric systems	49
3.1	Toric systems	49
3.2	Singularities of four-dimensional integrable systems	50
3.3	Semitoric systems	53
3.4	Symplectic invariants of semitoric systems	55
3.4.1	Marked semitoric polygons	56
3.4.2	The Taylor series invariant	64
3.4.3	Twisting numbers and twisting index	66
3.4.4	Complete invariant and symplectic classification	68
3.5	Hamiltonian S^1 -spaces	69
4	Semitoric families and beyond	72
4.1	Context and motivations	72
4.2	Strictly minimal semitoric systems	73
4.2.1	Toric type blowups	73
4.2.2	Semitoric type blowups	74
4.2.3	Strictly minimal polygons	76
4.3	Semitoric families	80
4.4	Obtaining semitoric systems via toric type blowups and blowdowns	83
4.4.1	Systems of type (3a)	84
4.4.2	Systems of type (3c)	87
4.4.3	Systems of type (3b)	89
4.5	Explicit semitoric systems	90
4.5.1	Systems of type (2) and (3) with $n = 2$	92

4.5.2	Systems of type (1)	94
4.5.3	Systems of type (3a), (3b) and (3c)	95
4.5.4	General strategy	99
4.6	Perspectives	103
5	Inverse spectral theory for semitoric systems	104
5.1	Quantum semitoric systems	104
5.2	The inverse spectral result	107
5.3	Asymptotic lattices and half-lattices	108
5.4	Recovering the invariants	111
5.4.1	Taylor series and height invariants	111
5.4.2	Global labelings, semitoric polygons and complete invariant	119
5.5	Perspectives	123

Résumé

Dans ce mémoire, nous présentons quelques-unes de nos contributions dans le cadre de la quantification de Berezin-Toeplitz, qui correspond à la limite semi-classique de la quantification des espaces de phases compacts, et de l'étude des systèmes semi-toriques, qui sont des systèmes intégrables en dimension quatre avec une symétrie S^1 sous-jacente.

Ce manuscrit est divisé en cinq chapitres, incluant un premier chapitre introductif. Le deuxième chapitre expose des résultats purement semi-classiques: une estimation de la fidélité d'états lagrangiens mixtes, l'étude de la distribution des zéros de certaines sections holomorphes, et une description du propagateur quantique d'un opérateur de Berezin-Toeplitz avec des applications aux formules de traces. Le troisième chapitre constitue une préparation aux chapitres suivants en présentant les prérequis sur les systèmes semi-toriques. Dans le quatrième chapitre, nous décrivons nos résultats concernant la construction d'exemples explicites de systèmes semi-toriques avec certains invariants symplectiques donnés. Enfin, dans le cinquième chapitre, nous présentons un résultat spectral inverse pour les systèmes semi-toriques quantiques, qui combine l'analyse semi-classique et la géométrie des systèmes semi-toriques.

Summary

In this thesis, we present some of our contributions in the setting of Berezin-Toeplitz quantization, corresponding to the semiclassical limit of the quantization of compact phase spaces, and of the study of semitoric systems, which are four-dimensional integrable systems with an underlying S^1 -symmetry.

This manuscript is divided into five chapters, including a first introductory chapter. The second chapter describes purely semiclassical results: an estimate for the fidelity of mixed Lagrangian states, the study of the distribution of zeros of certain holomorphic sections, and a description of the quantum propagator associated with a Berezin-Toeplitz operator, with applications to trace formulas. The third chapter constitutes a preparation to the next ones by reviewing the prerequisites about semitoric systems. In the fourth chapter, we describe our results regarding the construction of explicit examples of semitoric systems with certain prescribed symplectic invariants. Finally, in the fifth chapter we present an inverse spectral result for semitoric systems, combining semiclassical analysis and the geometry of semitoric systems.

Chapter 1

Introduction

In this chapter, we start by reviewing the context underlying our works and some general motivations for them. Afterwards, we list the papers that will be discussed in the memoir and briefly describe our other works. Then we introduce some notation and detail the structure of the manuscript. We conclude with a few disclaimers regarding the text.

1.1 Context and motivations

The works that we describe in this memoir deal with two main topics: Berezin-Toeplitz quantization and semitoric systems.

The framework of Berezin-Toeplitz quantization is the semiclassical limit of the geometric quantization procedure due to Kostant [Kos70] and Souriau [Sou66]. The relevant quantum observables in this setting are Berezin-Toeplitz operators [Ber75, BdMG81, BMS94, Gui95, BPU98, Zel98b, Cha03a, MM08a]. In our work we are essentially interested in the quantization of a compact Kähler manifold; a typical example is given by quantum spins where the classical phase space is a two-sphere, see Example 2.1.1. Recently, Berezin-Toeplitz quantization has proved useful in several fields of mathematics and mathematical physics such as the study of magnetic Laplacians and of the quantum Hall effect [Kle16, KMMW17, CE20, Cha21b, Cha20, Kor22], Kähler and algebraic geometry [Don01, MM07, BMZ11, GW11, RZ12, Fin12, Ber18, Anc21, Ioo22, DZ22, IP23], symplectic topology [Pol12, Pol14, CP18, CP22] and topological quantum field theory [AB11, CM15a, CM15b, MP15, Det18]. This list is in fact far from exhaustive.

Semitoric systems, introduced in [VuN07], also lie at the crossroad of several interesting research areas. A semitoric system is a type of Liouville integrable system on a four-dimensional symplectic manifold for which one component of the momentum map generates an effective Hamiltonian S^1 -action. As such, semitoric systems constitute a natural first generalization of four-dimensional toric systems. Another point of view is that they are integrable systems lifting Hamiltonian S^1 -spaces (see [Kar99] and Section 3.5) with the mildest singularities, except for toric systems (which, in fact, constitute a special class of semitoric systems). Semitoric systems also form a particular class of the almost toric fibrations [Sym03] which have recently been playing an important part in symplectic topology, see for instance [Via14, Via16, ES18, CV22]. Finally, semitoric systems constitute natural examples of systems displaying a non-trivial monodromy [Zou92, Mat96, Zun97] preventing the existence of global action variables [Dui80], and which induces quantum monodromy [CD88, SZ99a] in their quantum counterparts.

In this manuscript we will also mix these two topics by discussing an inverse spectral problem for quantum semitoric systems. Such inverse problems have been popularized by Kac in his celebrated paper [Kac66] and have been broadly studied since. The most popular one is the inverse spectral question for the Riemannian Laplacian, see the survey [DH13]. In this setting the effect of the presence of an S^1 -symmetry has been investigated in [Zel98a, DMSD16] for example. Here we are interested in an inverse problem for general semiclassical (\hbar -pseudodifferential or

Berezin-Toeplitz) operators, in the spirit of [VuN11, CPVuN13, PPVuN14] for instance. For semitoric systems, the inverse question that we will discuss was first advertized in [PVN11] and partial results were obtained in [PVN14, LFPVN16, LFPVN19].

1.2 Works presented in the manuscript

In this memoir, we have chosen to discuss the articles that were completed (or are being prepared) after we started our current position in Strasbourg. These are the works listed below (in chronological order of completion), which will be described in detail later.

- [LF18a] Johann Le Floch. Bounds for fidelity of semiclassical Lagrangian states in Kähler quantization. *J. Math. Phys.*, 59(8):082103, 35, 2018;
- [LFP22] Johann Le Floch and Joseph Palmer. Semitoric families. To appear in *Mem. Amer. Math. Soc.*, <https://arxiv.org/abs/1810.06915>, 2022;
- [CLF20] Laurent Charles and Johann Le Floch. Quantum propagation for Berezin-Toeplitz operators. Preprint, <https://arxiv.org/abs/2009.05279v2>, 43 pages, 2020;
- [LFVuN21] Johann Le Floch and San Vũ Ngọc. The inverse spectral problem for quantum semitoric systems. Preprint, <https://arxiv.org/abs/2104.06704>, 105 pages, 2021;
- [ALF22] Michele Ancona and Johann Le Floch. Berezin-Toeplitz operators, Kodaira maps, and random sections. Preprint, <https://arxiv.org/abs/2206.15112>, 32 pages, 2022;
- [LFP23] Johann Le Floch and Joseph Palmer. Families of four-dimensional integrable systems with S^1 -symmetries. Preprint, <https://arxiv.org/abs/2307.10670>, 145 pages, 2023;
- [CLF23b] Laurent Charles and Johann Le Floch. Pairings of Lagrangian states on compact Kähler manifolds. *In preparation*, 2023+;
- [CLF23a] Laurent Charles and Johann Le Floch. The Gutzwiller trace formula for Berezin-Toeplitz operators on compact Kähler manifolds. *In preparation*, 2023+.

Let us briefly describe our other works. The papers

- [LF14a] Johann Le Floch. Singular Bohr-Sommerfeld conditions for 1D Toeplitz operators: elliptic case. *Comm. Partial Differential Equations*, 39(2):213–243, 2014;
- [LF14b] Johann Le Floch. Singular Bohr-Sommerfeld conditions for 1D Toeplitz operators: hyperbolic case. *Anal. PDE*, 7(7):1595–1637, 2014

formed the core of our PhD thesis and dealt with the semiclassical description of the spectrum of a Berezin-Toeplitz operator with Morse principal symbol on a surface, near non-degenerate singular values of this symbol. In

- [LFP16] Johann Le Floch and Álvaro Pelayo. Euler–MacLaurin formulas via differential operators. *Adv. in Appl. Math.*, 73:99–124, 2016

with Álvaro Pelayo, we studied some Euler-Maclaurin formulas on polytopes. In the article (and erratum)

- [LFPVN16] Johann Le Floch, Álvaro Pelayo, and San Vũ Ngọc. Inverse spectral theory for semiclassical Jaynes–Cummings systems. *Mathematische Annalen*, 364(3):1393–1413, 2016;

- [LFPVN19] Yohann Le Floch, Álvaro Pelayo, and San Vũ Ngọc. Correction to: “Inverse spectral theory for semiclassical Jaynes-Cummings systems”. *Math. Ann.*, 375(1-2):917–920, 2019

with Álvaro Pelayo and San Vũ Ngọc, we obtained a partial inverse spectral result for semitoric systems. In

- [LFP19a] Yohann Le Floch and Álvaro Pelayo. Spectral asymptotics of semiclassical unitary operators. *Journal of Mathematical Analysis and Applications*, 473(2):1174–1202, 2019

with Álvaro Pelayo, we investigated the semiclassical joint spectrum of commuting unitary operators for some axiomatic quantization. In

- [LFP19b] Yohann Le Floch and Álvaro Pelayo. Symplectic geometry and spectral properties of classical and quantum coupled angular momenta. *J. Nonlinear Sci.*, 29(2):655–708, 2019

with Álvaro Pelayo, we studied the coupled angular momenta system (see Example 3.3.4) from the point of view of semitoric systems, in particular we computed some of its symplectic invariants. Finally, the book

- [LF18b] Yohann Le Floch. *A brief introduction to Berezin-Toeplitz operators on compact Kähler manifolds*. CRM Short Courses. Springer, Cham, 2018

constitutes an introduction to Berezin-Toeplitz quantization.

1.3 Symplectic preliminaries and notation

In this section we recall a few definitions from symplectic geometry that will be useful throughout the text. This essentially serves as a way to define our conventions and notation, in particular our sign choices.

Hamiltonian flows. Let (M, ω) be a connected symplectic manifold, and let $f \in \mathcal{C}^\infty(M, \mathbb{R})$. We define the Hamiltonian vector field of f as the unique vector field X_f on M satisfying $df + \omega(X_f, \cdot) = 0$. The Poisson bracket of two smooth functions $f, g \in \mathcal{C}^\infty(M, \mathbb{R})$ is the smooth function $\{f, g\} = \mathcal{L}_{X_f}g = \omega(X_f, X_g)$ where \mathcal{L} is the Lie derivative. If X_f is complete, the Hamiltonian flow of f is the one-parameter family of symplectomorphisms $(\phi_{t,f})_{t \in \mathbb{R}}$ defined as

$$\forall m \in M \quad \begin{cases} \frac{d}{dt}\phi_{t,f}(m) = X_f(\phi_{t,f}(m)), \\ \phi_{0,f}(m) = m. \end{cases}$$

We will sometimes also consider time-dependent functions $f \in \mathcal{C}^\infty(\mathbb{R} \times M, \mathbb{R})$, in which case by setting $f_t = f(t, \cdot)$ the Hamiltonian vector field X_{f_t} and the Hamiltonian flow ϕ_{t,f_t} are defined in the same way. When the function f is clear from the context, we will simply write ϕ_t for its Hamiltonian flow.

Hamiltonian actions. Let G be a Lie group, let \mathfrak{g} be its Lie algebra and let $\exp : \mathfrak{g} \rightarrow G$ be the exponential map. Recall that the *adjoint action* of G on \mathfrak{g} is the left action given by $(g, \xi) \in G \times \mathfrak{g} \mapsto \text{Ad}_g(\xi) = \frac{d}{dt}\big|_{t=0} g \exp(t\xi) g^{-1}$. This induces a left action of G on the dual \mathfrak{g}^* , called the *coadjoint action*, defined by $(g, \alpha) \in G \times \mathfrak{g}^* \mapsto \text{Ad}_{g^{-1}}^*(\alpha)$. Here for $g \in G$, Ad_g^* is the dual of Ad_g , which means that for every $\alpha \in \mathfrak{g}^*$ and every $\xi \in \mathfrak{g}$, $\langle \text{Ad}_g^*(\alpha), \xi \rangle = \langle \alpha, \text{Ad}_g(\xi) \rangle$ with $\langle \cdot, \cdot \rangle$ the duality bracket between \mathfrak{g} and \mathfrak{g}^* .

Now, let (M, ω) be a connected symplectic manifold as above, and assume that G acts on M ; we will write $\phi_g(m) = g \cdot m \in M$ for the action of an element $g \in G$ on a point $m \in M$.

The action is called *symplectic* if for every $g \in G$, $\phi_g : M \rightarrow M$ is a symplectomorphism, i.e. a diffeomorphism such that $\phi_g^* \omega = \omega$. For $\xi \in \mathfrak{g}$, let ξ_M be the vector field defined as

$$\forall m \in M \quad \xi_M(m) = \left. \frac{d}{dt} \right|_{t=0} \phi_{\exp(t\xi)}(m).$$

The action is said to be *Hamiltonian* if there exists a map $\mu : M \rightarrow \mathfrak{g}^*$ such that

- for every $\xi \in \mathfrak{g}$, $d\mu^\xi + \iota_{\xi_M} \omega = 0$ where ι is the interior product and $\mu^\xi : M \rightarrow \mathbb{R}$ is defined as

$$\forall m \in M \quad \mu^\xi(m) = \langle \mu(m), \xi \rangle;$$

- μ is equivariant with respect to the coadjoint action, i.e.

$$\forall g \in G, \forall m \in M, \quad \mu(\phi_g(m)) = \text{Ad}_{g^{-1}}^*(\mu(m)).$$

Such a map is called a *momentum map* for the action of G on M .

For instance, the Hamiltonian flow ϕ_t of $f \in C^\infty(M, \mathbb{R})$ gives a Hamiltonian action of \mathbb{R} on M as $t \cdot m = \phi_t(m)$, and f is a momentum map for this action. Here we have identified the Lie algebra of \mathbb{R} with \mathbb{R} , and more generally we will do the same for \mathbb{R}^n . In fact we will also often work with \mathbb{T}^n -actions, and in this case we will use the standard identification of $(\mathfrak{t}^n)^*$ with \mathbb{R}^n .

1.4 Structure of the manuscript

The rest of this manuscript is divided into four chapters. Chapter 2 deals with Berezin-Toeplitz quantization, Chapters 3 and 4 cover semitoric systems, and Chapter 5 contains results mixing both semitoric systems and quantization in a crucial way.

More precisely, in Chapter 2, we briefly review the semiclassical limit of geometric quantization in the Kähler setting, in particular the Berezin-Toeplitz operators. Then we describe the contents of [LF18a], which deals with the estimation, in the semiclassical limit, of the fidelity of two mixed states associated with Lagrangian submanifolds with densities in a compact Kähler manifold. We also review the results from [ALF22], obtained with Michele Ancona, about the distribution of zeros of certain holomorphic sections of a large power of some complex line bundle over a Kähler manifold; these sections are obtained by applying a fixed Berezin-Toeplitz operator to random holomorphic sections. Finally, we discuss the works [CLF20, CLF23b, CLF23a], joint with Laurent Charles, in which we investigated the asymptotic behavior of the quantum propagator associated with a Berezin-Toeplitz operator on a compact Kähler manifold, with some applications to trace formulas.

In Chapter 3, we lay the ground for the subsequent chapters by introducing the objects and concepts that will be used throughout the rest of the text. In particular, we review toric systems, define semitoric systems, describe their symplectic classification and the corresponding invariants, and discuss their relationship with Hamiltonian S^1 -spaces. This chapter can probably be skipped by experts, as it is mainly aimed at introducing consistent notation and terminology and setting the stage for the questions studied in the subsequent chapters, but we nevertheless hope that it constitutes a pedestrian introduction to the topic of semitoric systems for the reader who is not acquainted to it. There are of course more detailed references on this subject, see for instance the lecture notes [SVuN18] or the recent review [AH19]. Additionally, the more general topic of almost toric fibrations is covered in the nice recent lecture notes [Eva23].

In Chapter 4, we describe the contents of the two papers [LFP22, LFP23], joint with Joseph Palmer. The main goal of these papers is to obtain a recipe to construct a semitoric system with given number of focus-focus singularities, semitoric polygon, and height invariant, three invariants that are bundled in the so-called marked semitoric polygon of the system. We explain how we managed to come up with semitoric systems (either fully explicitly or by applying certain

sequences of blowups and blowdowns to fully explicit systems) for all the marked semitoric polygons which are minimal with respect to some natural blowup operations, by considering certain one-parameter families of integrable systems bifurcating between systems that are either of toric type or semitoric with one or two focus-focus singularities.

In Chapter 5, we introduce the inverse spectral problem for semitoric systems that we considered in [LFVuN21] with San Vũ Ngọc, and describe the steps in its resolution. Concretely, we define semiclassical integrable systems quantizing semitoric systems, and we explain how from the joint spectrum of such a system, one can recover, in a constructive way, all the symplectic invariants of the underlying semitoric system, and hence this system up to isomorphism.

We conclude each of the Chapters 2, 4 and 5 by giving some perspectives for future works. Our aim is not to describe an exhaustive and precise list of future projects but rather to give an idea of some natural questions that arise from our works. We believe that some of the questions evoked there could constitute good projects for prospective students.

1.5 Disclaimers

Before going any further, we must warn the reader about a few aspects of this manuscript.

But first, which reader are we talking about? After all, the primary goal of this memoir is to allow its author to be granted his Habilitation à Diriger des Recherches, and to this end the most important readers are the referees who generously accepted to delve into it. They may in fact be disconcerted by the length of this text, which is partly explained by the fact that we also (perhaps naively) envisioned another type of reader, namely students (or colleagues) wanting to learn the topics discussed here. We tried to satisfy both audiences by implementing different depths in each chapter: informal discussions, ideas of proofs, more technical details, but also explicit examples, sometimes with detailed computations and numerical illustrations. We sincerely hope that we did not completely fail, and that the outcome remains digestible for all readers.

This choice to produce a document which may be useful to students also explains why we chose to write it in English instead of French, so that it is accessible to a broader audience. We hope that this did not have too big of an impact on the quality of the writing.

The other warnings concern two particular parts of the text. First, in Sections 2.4.2 and 2.4.3 we describe two articles which are still in preparation; we still chose to discuss their contents because they both are at a quite advanced stage and the results that they contain are interesting applications of the article [CLF20]. However, the consequence is that in these sections, we do not cite precise statements in the corresponding manuscripts, and we give less details about the ideas of the proofs. Second, at the time that we finish writing this memoir, the paper [LFVuN21], discussed in Chapter 5, is still undergoing the refereeing process at a journal, after a round of revision which led to some changes in the numbering of the various statements, figures, etc. Here all the numbers that we give refer to the latest arXiv version [LFVuN21], which corresponds to the pre-revision stage of the paper.

Chapter 2

Some results in Berezin-Toeplitz quantization

In this chapter, we start by briefly reviewing, in Section 2.1, the procedure of geometric quantization in the Kähler case, in the semiclassical setting, and describe the corresponding Berezin-Toeplitz operators. We then summarize the contents of the works [LF18a], [ALF22], [CLF20] and of the upcoming [CLF23b] and [CLF23a], which are inscribed in this context.

In [LF18a], described in Section 2.2, we study how the fidelity of two mixed states constructed from Lagrangian submanifolds of a quantizable compact Kähler manifold reflects, in the semiclassical limit, geometric properties of the intersection of these submanifolds. In [ALF22], which is the object of Section 2.3, we study the distribution of zeros of a section of a large power of a certain complex line bundle over a compact Kähler manifold, obtained by applying a Berezin-Toeplitz operator to a random holomorphic section. In Section 2.4 we describe the paper [CLF20], which deals with the asymptotic behavior of the quantum propagator associated with a Berezin-Toeplitz operator, and the upcoming [CLF23b] and [CLF23a], which propose some applications of the results of [CLF20] to trace formulas. Finally, in Section 2.5, we propose some ideas for future works in these directions.

2.1 The semiclassical limit of geometric quantization

Geometric quantization, introduced independently by Kostant [Kos70] and Souriau [Sou66], is a procedure that aims to construct a quantum state space and quantum observables from classical mechanics on a compact phase space. Our framework is the semiclassical limit of geometric quantization, in which case the quantum observables are Berezin-Toeplitz operators.

Berezin-Toeplitz operators were introduced by Berezin [Ber75], their microlocal analysis was initiated by Boutet de Monvel and Guillemin [BdMG81], and they now form a well-established subject thanks to the work of many authors, see for instance [BMS94, Gui95, BPU98, Zel98b, Cha03a, MM08a]. Our goal here is not to describe the technical aspects of this theory but rather to introduce notation and give an idea of the objects, allowing to understand the motivations and contents of our works; actually, for more details and references we refer the reader to our book [LF18b].

Throughout this text we will always work in the Kähler case. Concretely, let (M, ω, j) be a compact, connected, Kähler manifold, and let $n = \dim_{\mathbb{C}} M$; recall that M is a complex manifold and that ω is a symplectic form on M which is compatible with the complex structure j . In particular M is endowed with a Riemannian metric $g = \omega(\cdot, j\cdot)$. Assume moreover that there exists a Hermitian, holomorphic line bundle $(L, h) \rightarrow M$ whose Chern connection ∇ has curvature $\text{curv}(\nabla) = -i\omega$, called a *prequantum line bundle*. It is standard that the existence of a prequantum line bundle amounts to the fact that the cohomology class $[\frac{\omega}{2\pi}]$ is integral; when this condition is satisfied, we say that M is quantizable.

It is sometimes convenient to introduce an auxiliary Hermitian, holomorphic line bundle $(L', h') \rightarrow M$. In particular, several statements become simpler when using $(L', h') = (\delta, h_\delta)$ a half-form bundle, *i.e.* a square root of the canonical bundle $K = \Omega^{n,0}(M) \rightarrow M$, when it exists; this corresponds to the metaplectic correction of geometric quantization. Note that K carries a natural Hermitian metric h_K given by

$$\forall m \in M \quad \forall \alpha, \beta \in K_m \quad h_K(\alpha, \beta) = i^{n^2} \frac{\alpha \wedge \bar{\beta}}{\mu}$$

with $\mu = \frac{\omega^{\wedge n}}{n!}$ the Liouville volume form on M . Any half-form bundle $\delta \rightarrow M$ inherits a holomorphic structure and a Hermitian metric h_δ from h_K ; the latter is the unique metric satisfying

$$\forall m \in M \quad \forall s \in \delta_m \quad (h_\delta)_m(s, s) = \sqrt{(h_K)_m(s^{\otimes 2}, s^{\otimes 2})}.$$

The Chern connection ∇^δ associated with this Hermitian metric is such that

$$\forall s, t \in \mathcal{C}^\infty(M, \delta) \quad \nabla^K(s \otimes t) = (\nabla^\delta s) \otimes t + s \otimes (\nabla^\delta t)$$

with ∇^K the Chern connection of K .

The semiclassical parameter is an integer $k \geq 1$, and the quantum spaces are the spaces

$$\mathcal{H}_k = H^0(M, L^{\otimes k} \otimes L')$$

of holomorphic sections of $L^{\otimes k} \otimes L' \rightarrow M$. The inner product $\langle \cdot, \cdot \rangle_k$ on the space \mathcal{H}_k is given by

$$\forall \psi, \phi \in \mathcal{H}_k \quad \langle \psi, \phi \rangle_k = \int_M h_k(\psi, \phi) \mu \quad (2.1)$$

where h_k is the Hermitian form induced by h and h' on $L^{\otimes k} \otimes L'$. For every $k \geq 1$, \mathcal{H}_k is finite-dimensional, and in the semiclassical limit $k \rightarrow +\infty$ its dimension satisfies

$$\dim \mathcal{H}_k = \left(\frac{k}{2\pi} \right)^n \int_M (\omega + k^{-1} \beta)^{\wedge n} + O(k^{n-2}) \quad (2.2)$$

where $\beta = i \operatorname{curv}(\nabla') - \frac{i}{2} \operatorname{curv}(\nabla^K)$ and ∇' is the Chern connection of (L', h') , see for instance [Cha06, Section 1.2]. In particular when $(L', h') = (\delta, h_\delta)$, this formula simplifies since $\beta = 0$.

Let $L^2(M, L^{\otimes k} \otimes L')$ be the completion of the space of smooth sections of $L^{\otimes k} \otimes L' \rightarrow M$ with respect to $\langle \cdot, \cdot \rangle_k$, and let $\Pi_k : L^2(M, L^{\otimes k} \otimes L') \rightarrow \mathcal{H}_k$ be the orthogonal projection on \mathcal{H}_k . The Berezin-Toeplitz operator associated with $f \in \mathcal{C}^\infty(M)$ is (the sequence of) operator(s)

$$T_k(f) : \mathcal{H}_k \rightarrow \mathcal{H}_k, \quad \psi \mapsto \Pi_k(f\psi).$$

More generally, Berezin-Toeplitz operators are operators of the form

$$T_k = \Pi_k f(\cdot, k) + R_k : H^0(M, L^{\otimes k}) \rightarrow H^0(M, L^{\otimes k})$$

where $(f(\cdot, k))_{k \in \mathbb{N}}$ is a sequence of elements of $\mathcal{C}^\infty(M)$ with an asymptotic expansion of the form

$$f(\cdot, k) = f_0 + k^{-1} f_1 + k^{-2} f_2 + \dots$$

in the \mathcal{C}^∞ topology, and the operator norm of R_k is a $O(k^{-\infty})$, *i.e.* a $O(k^{-N})$ for every $N \in \mathbb{N}$. The first term f_0 in the asymptotic expansion of $f(\cdot, k)$ is called the *principal symbol* of T_k . The function $f_1 + \frac{1}{2} \Delta f_0$, where Δ is the holomorphic Laplacian associated with the Kähler structure, is the *subprincipal symbol* of T_k . In Section 2.4, we will also consider time-dependent Berezin-Toeplitz operators, obtained by choosing sequences $(f(\cdot, \cdot, k))_{k \in \mathbb{N}}$ of elements of $\mathcal{C}^\infty(\mathbb{R} \times M)$.

Any Berezin-Toeplitz operator T_k is an integral operator whose Schwartz kernel, for which we use the notation $T_k(\cdot, \cdot)$, is an element of

$$H^0(M \times \bar{M}, (L^{\otimes k} \otimes L') \boxtimes (\bar{L}^{\otimes k} \otimes \bar{L}')) \simeq H^0(M, L^{\otimes k} \otimes L') \otimes H^0(\bar{M}, \bar{L}^{\otimes k} \otimes \bar{L}')$$

(see the discussion after Example 2.1.1 regarding the isomorphism), where \boxtimes is the external tensor product, \bar{M} is M endowed with $-\omega$ (and $-j$) and (\bar{L}, \bar{h}) is the conjugate of (L, h) (and similarly for (L', h')). Concretely,

$$\forall \psi \in \mathcal{H}_k \quad \forall x \in M \quad (T_k \psi)(x) = \int_M T_k(x, y) \cdot \psi(y) \mu(y)$$

where the dot stands for contraction with respect to h_k :

$$\forall m \in M \quad \forall u, v \in L_m^{\otimes k} \otimes L'_m \quad \bar{v} \cdot u = (h_k)_m(u, v).$$

Equivalently, one can see $T_k(x, y)$ as a map from $L_y^{\otimes k} \otimes L'_y$ to $L_x^{\otimes k} \otimes L'_x$, sending $v \in L_y^{\otimes k} \otimes L'_y$ to $T(x, y) \cdot v$. In particular, the study of the asymptotic properties of the Schwartz kernel of Π_k , called the Bergman kernel, is a crucial aspect of the theory of Berezin-Toeplitz operators, and has been carried out by many authors. In this semiclassical context, for the Kähler case, Catlin [Cat99] and Zelditch [Zel98b], using a result of [BdMG81] on the Szegő projector associated with a strictly pseudoconvex domain, proved independently the existence of an asymptotic expansion of $\Pi_k(x, x)$ in integral powers of k^{-1} and computed the first term in this expansion. Then Lu [Lu00] studied this asymptotic expansion, and in particular computed explicitly its next three terms. Charles [Cha03a] generalized the result of [Zel98b], still using [BdMG81], to obtain a general asymptotic expansion for Π_k including the off-diagonal behavior. In this manuscript we will mostly refer to this expansion to first order, namely

$$\Pi_k(x, y) = \left(\frac{k}{2\pi} \right)^n S^k(x, y) (a_0(x, y) + O(k^{-1})) \quad (2.3)$$

where $S \in \mathcal{C}^\infty(M \times \bar{M}, L \boxtimes \bar{L})$ satisfies $S(x, x) = 1$ (identifying $L_x \otimes \bar{L}_x$ with \mathbb{C} by means of the Hermitian metric h on L) and $|S(x, y)| < 1$ whenever $x \neq y$, $a_0 \in \mathcal{C}^\infty(M \times \bar{M}, L' \boxtimes \bar{L}')$ is such that $a_0(x, x) = 1$ and the remainder $O(k^{-1})$ is uniform in $(x, y) \in M^2$. A direct approach for the derivation of the full asymptotic expansion of Π_k was later given in [BBS08]. Moreover, in the analytic setting one can obtain exponentially small remainders in this asymptotic expansion, see [RSN20, DHS20, Del21, Cha21a].

These results have been extended to the symplectic, not necessarily Kähler, case by many authors, see [BU00, SZ02, DLM04, MZ08, MM08b, Kor18, KMM19, ILMM20] for instance.

Let us now describe a very simple but enlightening example which will follow us throughout the text. Indeed, this example appears in several of the works that we describe in this manuscript and serves as a good illustration of the various phenomena that we bring to light. This is also why we describe it in detail in order to obtain a consistent notation.

Example 2.1.1 (Spin components). The unit sphere $S^2 \subset \mathbb{R}^3$ with coordinates (x, y, z) , endowed with $-\frac{1}{2}\omega_{S^2}$ where ω_{S^2} is its usual symplectic form given by

$$\forall u \in S^2 \quad \forall v, w \in T_u S^2 \quad (\omega_{S^2})_u(v, w) = \langle u, v \wedge w \rangle_{\mathbb{R}^3}$$

(equivalently, in cylindrical coordinates, $\omega_{S^2} = d\theta \wedge dz$), can be quantized as follows. Let π_N be the stereographic projection from the north pole of S^2 to its equatorial plane; π_N realizes a diffeomorphism between S^2 and the complex projective line \mathbb{CP}^1 . The latter is endowed with the Fubini-Study symplectic form ω_{FS} , normalized in such a way that the volume of \mathbb{CP}^1 equals 2π . A straightforward computation shows that $\pi_N^* \omega_{\text{FS}} = -\frac{1}{2}\omega_{S^2}$, hence the problem amounts to the quantization of $(\mathbb{CP}^1, \omega_{\text{FS}})$.

Recall that the hyperplane bundle $L = \mathcal{O}(1) \rightarrow \mathbb{CP}^1$ is the dual of the tautological line bundle

$$\mathcal{O}(-1) = \{([u], v) \in \mathbb{CP}^1 \times \mathbb{C}^2 \mid v \in \mathbb{C}u\} \rightarrow \mathbb{CP}^1, \quad ([u], v) \mapsto [u],$$

which is endowed with the natural holomorphic and Hermitian structures. These in turn induce holomorphic and Hermitian structures on $L \rightarrow \mathbb{CP}^1$, and one readily checks that the corresponding Chern connection has curvature $-i\omega_{\text{FS}}$, so that $L \rightarrow \mathbb{CP}^1$ is a prequantum line bundle. Recall also that the canonical bundle of \mathbb{CP}^1 identifies with $\mathcal{O}(-2)$, and hence the tautological line bundle $\mathcal{O}(-1)$ is a half-form bundle.

So the quantum spaces quantizing $(\mathbb{CP}^1, \omega_{\text{FS}})$, taking into account the metaplectic correction, are

$$\mathcal{H}_k = H^0(\mathbb{CP}^1, \mathcal{O}(k) \otimes \mathcal{O}(-1)) = H^0(\mathbb{CP}^1, \mathcal{O}(k-1)), \quad k \geq 1.$$

It is standard that there is a canonical isomorphism between \mathcal{H}_k and the space $\mathbb{C}_{k-1}^{\text{hom}}[w_1, w_2]$ of homogeneous polynomials of degree $k-1$ in two complex variables, obtained by considering the duality pairing of the value of a section at $[u] \in \mathbb{CP}^1$ with $u^{\otimes k-1} \in \mathcal{O}(-k+1)_{[u]}$; through this isomorphism, $\mathbb{C}_{k-1}^{\text{hom}}[w_1, w_2]$ inherits an inner product from the inner product $\langle \cdot, \cdot \rangle_k$ on \mathcal{H}_k (see Equation (2.1)), and an orthonormal basis for this inner product is

$$e_{\ell,k} = \sqrt{\frac{k \binom{k-1}{\ell}}{2\pi}} w_1^\ell w_2^{k-1-\ell}, \quad 0 \leq \ell \leq k-1. \quad (2.4)$$

It is convenient to work in a chart of \mathbb{CP}^1 , say $U_2 = \{[w_1 : w_2] \mid w_2 \neq 0\}$ with holomorphic coordinate $w = \frac{w_1}{w_2}$, and the corresponding trivialization of L via the local section s dual to the local section

$$\tau : U_2 \rightarrow U_2 \times \mathbb{C}^2, \quad w \mapsto ([w : 1], (w, 1)) \quad (2.5)$$

of $\mathcal{O}(-1)$, which has pointwise norm $|\tau(w)| = \sqrt{1 + |w|^2}$. Note also that in this local holomorphic coordinate w , the Fubini-Study form reads

$$\omega_{\text{FS}} = \frac{i \, dw \wedge d\bar{w}}{(1 + |w|^2)^2}. \quad (2.6)$$

This yields an identification of \mathcal{H}_k with the space $\mathbb{C}_{k-1}[w]$ of polynomials of degree at most $k-1$ in one complex variable, in which the inner product reads

$$\langle P, Q \rangle_k = \int_{\mathbb{C}} \frac{P(w) \overline{Q(w)}}{(1 + |w|^2)^{k+1}} |dw \wedge d\bar{w}|.$$

In this identification the Bergman kernel is computed to be

$$\Pi_k(v, w) = \frac{k}{2\pi} (1 + v\bar{w})^{k-1} s^{\otimes k-1}(v) \otimes \overline{s^{\otimes k-1}(w)}. \quad (2.7)$$

Observe that this is indeed consistent with Equation (2.3).

In this setting, and with a slight abuse of notation (writing $T_k(f)$ instead of $T_k(f \circ \pi_N^{-1})$ for $f \in \mathcal{C}^\infty(S^2)$), the operators $T_k(x)$, $T_k(y)$ and $T_k(z)$ are given by

$$T_k(x) = \frac{1}{k+1} \left((1 - w^2) \frac{d}{dw} + (k-1)w \right)$$

and

$$T_k(y) = \frac{i}{k+1} \left((1 + w^2) \frac{d}{dw} - (k-1)w \right), \quad T_k(z) = \frac{1}{k+1} \left(2w \frac{d}{dw} - (k-1)\text{Id} \right).$$

In the rest of the text, we will often work with the operators

$$\hat{X}_k = T_k \left(x - \frac{1}{2k} \Delta x \right) = \frac{k+1}{k} T_k(x), \quad \hat{Y}_k = \frac{k+1}{k} T_k(y), \quad \hat{Z}_k = \frac{k+1}{k} T_k(z),$$

whose subprincipal symbols vanish (indeed $\Delta x = -2x$ and similarly for y and z). The action of each of these operators in the above orthonormal basis is given by

$$\begin{cases} \hat{X}_k e_{\ell,k} = \frac{1}{k} \left(\sqrt{\ell(k-\ell)} e_{\ell-1,k} + \sqrt{(\ell+1)(k-\ell-1)} e_{\ell+1,k} \right), \\ \hat{Y}_k e_{\ell,k} = \frac{i}{k} \left(\sqrt{\ell(k-\ell)} e_{\ell-1,k} - \sqrt{(\ell+1)(k-\ell-1)} e_{\ell+1,k} \right), \\ \hat{Z}_k e_{\ell,k} = \left(\frac{2\ell+1-k}{k} \right) e_{\ell,k}, \end{cases} \quad (2.8)$$

for $0 \leq \ell \leq k-1$, using the convention $e_{p,k} = 0$ if $p \notin \{0, \dots, k-1\}$. For more details, see for instance Examples 4.4.5 and 5.2.4 in [LF18b]. Note that if we do not need to work with the metaplectic correction, it suffices to change k to $k+1$; this remark will be useful when discussing the examples illustrating the papers in which we did not use this correction, namely [LF18a] (in Section 2.2, in particular Example 2.2.5) and [ALF22] (in Section 2.3, in particular Example 2.3.2).

In Chapter 5 we will work intensively with an example (Example 5.1.2) whose underlying phase space is $S^2 \times S^2$. The previous example will suffice to describe its properties because the quantum spaces associated with a product is the tensor product of the two quantum spaces: if $(L_1, h_1) \rightarrow (M_1, \omega_1, j_1)$ and $(L_2, h_2) \rightarrow (M_2, \omega_2, j_2)$ are two prequantum line bundles over compact Kähler manifolds, then $(L_1 \boxtimes L_2, h_1 \boxtimes h_2)$ is a prequantum line bundle over $M_1 \times M_2$ and

$$H^0(M_1 \times M_2, L_1^{\otimes k} \boxtimes L_2^{\otimes k}) \simeq H^0(M_1, L_1^{\otimes k}) \otimes H^0(M_2, L_2^{\otimes k}).$$

We briefly review another example with a non-compact classical phase space, but which will nonetheless be useful in Chapter 5.

Example 2.1.2 (Bargmann spaces). Let $(M, \omega) = (\mathbb{C}, \omega_0)$ where $\omega_0 = i dz \wedge d\bar{z}$, and let $\alpha = \frac{i}{2}(z d\bar{z} - \bar{z} dz)$. Let $L_0 = \mathbb{C} \times \mathbb{C} \rightarrow \mathbb{C}$ be the trivial bundle equipped with its standard Hermitian structure, with the connection $\nabla = d - i\alpha$, and with the unique holomorphic structure making ∇ its Chern connection. The Hilbert spaces $\mathcal{B}_k = H^0(\mathbb{C}, L_0^{\otimes k}) \cap L^2(\mathbb{C}, L_0^{\otimes k})$ coincide with the Bargmann spaces

$$\mathcal{B}_k = \left\{ f \psi^k \mid f : \mathbb{C} \rightarrow \mathbb{C} \text{ holomorphic, } \int_{\mathbb{C}} |f(z)|^2 e^{-k|z|^2} |dz \wedge d\bar{z}| < +\infty \right\}$$

where $\psi(z) = e^{-\frac{|z|^2}{2}}$ for $z \in \mathbb{C}$. The Bargmann transform $B_k : f \in L^2(\mathbb{R}) \mapsto B_k f$, where

$$\forall z \in \mathbb{C} \quad (B_k f)(z) = 2^{\frac{1}{4}} \left(\frac{k}{2\pi} \right)^{\frac{3}{4}} \left(\int_{\mathbb{R}} e^{-\frac{k}{2}(z^2 + x^2 - 2\sqrt{2}zx)} f(x) dx \right) \psi^k(z),$$

is a unitary operator from $L^2(\mathbb{R})$ to \mathcal{B}_k . See [Bar61] for more details.

2.2 Lagrangian states and fidelity

In [LF18a], we introduced some quantum states associated with submanifolds with densities in quantizable compact Kähler manifolds, and tried to recover some geometric information on pairs of such submanifolds from the study of a quantity associated with the corresponding pair of states, and coming from quantum information, called fidelity. Obtaining precise asymptotics for this fidelity turned out to be too complicated and instead we estimated a lower and an upper bound

for it, called the sub-fidelity and super-fidelity, in the case of a pair of Lagrangian submanifolds; the asymptotics of these two bounds involved some interesting geometric quantities describing the intersection of these submanifolds.

More precisely, as above, let (M, ω) be a compact Kähler manifold equipped with a prequantum line bundle $(L, h) \rightarrow M$; given a submanifold $\Sigma \subset M$, we want to construct a quantum state (or rather, a sequence of states) in $\mathcal{H}_k = H^0(M, L^{\otimes k})$ that quantizes it in some sense. There are two standard examples of such a construction: when $\Sigma = \{m\}$ is a point, the state being the coherent state at m (see below), and when Σ is a Bohr-Sommerfeld Lagrangian submanifold, *i.e.* a Lagrangian submanifold with trivial holonomy with respect to the connection ∇^k induced by ∇ on $L^{\otimes k}$ (see [BPU95] and [Cha03b]), which is useful, for instance, to obtain quasimodes for Berezin-Toeplitz operators. In both cases, the state is a pure state $[\psi_k] \in \mathbb{P}(\mathcal{H}_k)$, and its microsupport $\text{MS}(\psi_k)$ is contained in Σ . Recall that for a pure state, the microsupport $\text{MS}(\psi_k)$ is defined as follows: $m \notin \text{MS}(\psi_k)$ if and only if there exists a neighborhood Ω of m such that for every $N \geq 0$, $|\psi_k| = O(k^{-N})$ uniformly on Ω (here $|\cdot|$ stands for the pointwise norm associated with the Hermitian metric h_k on $L^{\otimes k}$). The states that we constructed in [LF18a] are mixed quantum states, obtained as a probabilistic mixture of an infinite number of coherent states.

Recall that a mixed quantum state (or rather the density operator of a mixed state) on a Hilbert space \mathcal{H} is a positive semi-definite Hermitian operator $\rho : \mathcal{H} \rightarrow \mathcal{H}$ with $\text{Tr}(\rho) = 1$. A pure state $[\psi] \in \mathbb{P}(\mathcal{H})$ is a particular type of mixed state with density operator $\rho_{[\psi]} = \frac{\langle \cdot, \psi \rangle}{\|\psi\|^2} \psi$ the orthogonal projection on $\text{Span}(\psi)$. A typical example of mixed state is the probabilistic mixture of pure states

$$\rho = p_1 \rho_{[\psi_1]} + \dots + p_N \rho_{[\psi_N]}, \quad p_1, \dots, p_N \geq 0, \quad p_1 + \dots + p_N = 1,$$

meaning that this state is in the state $[\psi_j]$ with probability p_j , for $j \in \{1, \dots, N\}$. To measure how far from being pure a state ρ is, one can compute its purity $\text{Tr}(\rho^2)$, which equals one if and only if ρ is a pure state.

One can measure the closeness of two mixed quantum states ρ and η by computing their fidelity [Uhl76, Joz94]

$$F(\rho, \eta) = \|\sqrt{\rho} \sqrt{\eta}\|_{\text{Tr}}^2 = \text{Tr} \left(\sqrt{\sqrt{\rho} \eta \sqrt{\rho}} \right)^2 \in [0, 1].$$

Observe that when $\rho = \rho_{[\psi]}$ and $\eta = \rho_{[\phi]}$ are pure, then

$$F(\rho, \eta) = \text{Tr}(\rho \eta) = \frac{|\langle \psi, \phi \rangle|^2}{\|\phi\|^2 \|\psi\|^2}.$$

For any two mixed states ρ, η , $F(\rho, \eta) = 1$ if and only if $\rho = \eta$, and $F(\rho, \eta) = 0$ if and only if $\rho(\mathcal{H})$ and $\eta(\mathcal{H})$ are orthogonal. This fidelity can be complicated to compute, and in [MPH⁺09] the authors obtained the bounds $E(\rho, \eta) \leq F(\rho, \eta) \leq G(\rho, \eta)$ for every ρ, η , where the sub-fidelity E and the super-fidelity G , which can be measured experimentally, keep some of the good properties of the fidelity and are defined as

$$E(\rho, \eta) = \text{Tr}(\rho \eta) + \sqrt{2} \sqrt{\text{Tr}(\rho \eta)^2 - \text{Tr}((\rho \eta)^2)} \quad (2.9)$$

and

$$G(\rho, \eta) = \text{Tr}(\rho \eta) + \sqrt{(1 - \text{Tr}(\rho^2))(1 - \text{Tr}(\eta^2))}. \quad (2.10)$$

These two quantities only involves products of ρ and η and not their square roots, and they are thus more tractable than the fidelity itself. Note that the fidelity and super-fidelity coincide when at least one of the states is pure.

Let $\Sigma \subset M$ be a closed, connected smooth submanifold of M of dimension $d \geq 1$ equipped with a smooth positive density σ such that $\int_{\Sigma} \sigma = 1$. For k large enough, the state that we associate with (Σ, σ) is

$$\rho_k(\Sigma, \sigma) = \int_{\Sigma} P_k^m \sigma(m)$$

where P_k^m is the coherent projector at the point m , defined as follows (after [Cha03a, Section 5]). Let $U \subset L$ be the set of elements u of L such that $h(u, u) = 1$ and let $\pi : U \rightarrow M$ be the natural projection; for $k \geq 1$ and $u \in U$, consider the holomorphic section

$$\xi_k^u : p \mapsto \Pi_k(p, \pi(u)) \cdot u^k$$

of $L^{\otimes k} \rightarrow M$. Because of the asymptotic properties of the Bergman kernel Π_k recalled in Section 2.1 (see in particular Equation (2.3)), there exists $k_0 \geq 1$ such that for every $k \geq k_0$ and every $u \in U$, $\xi_k^u \neq 0$. Therefore for $k \geq k_0$ and $u \in U$ the state $[\xi_k^u]$ is well-defined, and one readily checks that it only depends on the point $m = \pi(u)$; $[\xi_k^u]$ is the *coherent state* at m , and the *coherent projector* at m is the orthogonal projector $P_k^m = \rho_{[\xi_k^u]}$.

Note that states of this type on the non-compact manifold $M = \mathbb{C}^n$ have been studied in [PEU20].

One readily checks that $\rho_k(\Sigma, \sigma)$ is indeed a state, and a first result is the computation of its purity.

Proposition 2.2.1 ([LF18a, Proposition 3.3]). *Let μ_{Σ} be the Riemannian volume on Σ corresponding to the Riemannian metric induced by the Kähler metric g on Σ . The purity of $\rho_k(\Sigma, \sigma)$ satisfies*

$$\mathrm{Tr}(\rho_k(\Sigma, \sigma)^2) = \left(\frac{2\pi}{k}\right)^{\frac{d}{2}} \left(\int_{\Sigma} f \sigma + O(k^{-1})\right) = \left(\frac{2\pi}{k}\right)^{\frac{d}{2}} \left(\int_{\Sigma} f^2 \mu_{\Sigma} + O(k^{-1})\right)$$

where f is the function such that $\sigma = f \mu_{\Sigma}$.

In particular, as k goes to infinity, the state $\rho_k(\Sigma, \sigma)$ will become further and further away from pure, since this purity will go to zero.

Moreover, it is rather simple to show that the state $\rho_k(\Sigma, \sigma)$ concentrates on Σ , by computing its microsupport. For a mixed state $\rho_k : \mathcal{H}_k \rightarrow \mathcal{H}_k$, the following definition of the microsupport $\mathrm{MS}(\rho_k)$, coinciding with the above one when the state is pure, is given in [CP18, Section 4]: $m \notin \mathrm{MS}(\rho_k)$ if and only if there exists $f \in \mathcal{C}^{\infty}(M)$ such that $f(m) \neq 0$ and $\|T_k(f)\rho_k\|_{\mathrm{op}} = O(k^{-\infty})$ where $\|\cdot\|_{\mathrm{op}}$ is the operator norm.

Proposition 2.2.2 ([LF18a, Corollary 3.6]). *The microsupport of the state $\rho_k(\Sigma, \sigma)$ coincides with Σ .*

As explained earlier, given two submanifolds with densities (Σ_1, σ_1) and (Σ_2, σ_2) , we would like to compute the fidelity $F(\rho_k(\Sigma_1, \sigma_1), \rho_k(\Sigma_2, \sigma_2))$ of the corresponding states. Of course, if $(\Sigma_1, \sigma_1) = (\Sigma_2, \sigma_2)$ then $\rho_k(\Sigma_1, \sigma_1) = \rho_k(\Sigma_2, \sigma_2)$ and this fidelity equals one. Another extreme case is when Σ_1 and Σ_2 are disjoint.

Proposition 2.2.3 ([LF18a, Proposition 3.8]). *Assume that $\Sigma_1 \cap \Sigma_2 = \emptyset$. Then there holds $F(\rho_k(\Sigma_1, \sigma_1), \rho_k(\Sigma_2, \sigma_2)) = O(k^{-\infty})$.*

In intermediate cases, we do not expect this fidelity to be easily computable. So in [LF18a] we chose to compute the sub-fidelity and super-fidelity of the states $\rho_{k,1} = \rho_k(\Sigma_1, \sigma_1)$ and $\rho_{k,2} = \rho_k(\Sigma_2, \sigma_2)$ in a situation that makes the computations tractable. More precisely, assume that $\Sigma_1 = \Gamma_1$ and $\Sigma_2 = \Gamma_2$ are Lagrangian submanifolds of M intersecting transversally at a finite number of points m_1, \dots, m_s . Our results involve geometric quantities called the principal angles at each intersection point.

Let V be a real vector space equipped with an inner product $(\cdot|\cdot)$, and let W and Z be two subspaces of V such that $\alpha = \dim W \geq \beta = \dim Z \geq 1$. The *principal angles* $0 \leq \theta_1 \leq \dots \leq \theta_\beta \leq \frac{\pi}{2}$ between W and Z are defined recursively by the formula

$$\forall \ell \in \{1, \dots, \beta\} \quad \cos(\theta_\ell) = (u_\ell|v_\ell) := \max_{u,v \in \mathcal{V}_\ell} (u|v)$$

where $\mathcal{V}_1 = \{(u, v) \in W \times Z \mid \|u\| = 1 = \|v\|\}$ and for $\ell \in \{2, \dots, \beta\}$,

$$\mathcal{V}_\ell = \{(u, v) \in \mathcal{V}_1 \mid \forall p \in \{1, \dots, \ell-1\}, (u|u_p) = 0 = (v|v_p)\}.$$

Observe that $\theta_1 = 0$ if and only if $W \cap Z \neq \{0\}$.

Back to our problem, for every $r \in \{1, \dots, s\}$, let $0 < \theta_1(m_r) \leq \theta_2(m_r) \leq \dots \leq \theta_n(m_r) \leq \frac{\pi}{2}$ be the principal angles between the subspaces $T_{m_r}\Gamma_1$ and $T_{m_r}\Gamma_2$ of $T_{m_r}M$, computed using the inner product g_{m_r} , where we recall that $g = \omega(\cdot, j\cdot)$ is the Kähler metric. Moreover, as in Proposition 2.2.1, for $\ell \in \{1, 2\}$ let μ_{Γ_ℓ} be the Riemannian volume coming from the Riemannian metric induced by g on Γ_ℓ , and let f_ℓ be the function such that $\sigma_\ell = f_\ell \mu_{\Gamma_\ell}$. Moreover, for $r \in \{1, \dots, s\}$ we define the number

$$(\sigma_1, \sigma_2)_{m_r} = f_1(m_r)f_2(m_r) > 0. \quad (2.11)$$

Theorem 2.2.4 ([LF18a, Theorems 4.2 and 4.9]). *The super-fidelity of $\rho_{k,1}$ and $\rho_{k,2}$ satisfies:*

$$G(\rho_{k,1}, \rho_{k,2}) = 1 - \frac{1}{2} \left(\frac{2\pi}{k} \right)^{\frac{n}{2}} \left(\int_{\Gamma_1} f_1 \sigma_1 + \int_{\Gamma_2} f_2 \sigma_2 \right) + O(k^{-\min(n, \frac{n}{2}+1)}).$$

The sub-fidelity of $\rho_{k,1}$ and $\rho_{k,2}$ satisfies:

$$E(\rho_{k,1}, \rho_{k,2}) = \left(\frac{2\pi}{k} \right)^n C((\Gamma_1, \sigma_1), (\Gamma_2, \sigma_2)) + O(k^{-(n+1)}),$$

where $C((\Gamma_1, \sigma_1), (\Gamma_2, \sigma_2)) = C_1 + \sqrt{2(C_2 + C_3)}$ with

$$C_1 = \sum_{r=1}^s \frac{(\sigma_1, \sigma_2)_{m_r}}{\prod_{\ell=1}^n \sin(\theta_\ell(m_r))}, \quad C_2 = \sum_{r=1}^s \sum_{\substack{q=1 \\ q \neq r}}^s \frac{(\sigma_1, \sigma_2)_{m_r} (\sigma_1, \sigma_2)_{m_q}}{\prod_{\ell=1}^n \sin(\theta_\ell(m_r)) \sin(\theta_\ell(m_q))}$$

and

$$C_3 = \sum_{r=1}^s \frac{(\sigma_1, \sigma_2)_{m_r}^2}{\prod_{\ell=1}^n \sin(\theta_\ell(m_r))} \left(\prod_{\ell=1}^n \frac{1}{\sin(\theta_\ell(m_r))} - \prod_{\ell=1}^n \frac{1}{\sqrt{1 + \sin^2(\theta_\ell(m_r))}} \right).$$

This shows that for this choice of submanifolds, the sub-fidelity is a $O(k^{-n})$ while the super-fidelity is a $O(1)$. This leaves a large possible range of behaviors for the fidelity itself; however, recall that the states that we consider are far from being pure so we do not expect the super-fidelity to give a good bound. To get a better intuition on this issue, it is interesting to study an example.

Example 2.2.5. We work in the setting of Example 2.1.1, but without metaplectic correction, which means that $(M, \omega) = (S^2, -\frac{1}{2}\omega_{S^2})$, and the Hilbert spaces that we consider are $\mathcal{H}_k = H^0(\mathbb{CP}^1, \mathcal{O}(k))$ (no metaplectic correction). The Lagrangian submanifolds that we consider are the two great circles $\Gamma_1 = \{z = 0\}$ and its image Γ_2^α by the rotation R_α of angle $\alpha \in (0, \frac{\pi}{2}]$ about the y -axis, namely

$$\Gamma_2^\alpha = \begin{cases} \{(x, y, z) \in S^2 \mid z = x \tan \alpha\} & \text{if } \alpha \neq \frac{\pi}{2}, \\ \{(x, y, z) \in S^2 \mid x = 0\} & \text{if } \alpha = \frac{\pi}{2}. \end{cases}$$

For the densities, we choose $\sigma_1 = \frac{|d\theta|}{2\pi}$ where (θ, φ) are the usual spherical coordinates, and σ_2^α the density induced on Γ_2^α by σ_1 through R_α .

The matrix of $\rho_{k,1} = \rho_k(\Gamma_1, \sigma_1)$ in the orthonormal basis $(e_{\ell,k+1})_{0 \leq \ell \leq k}$ from Equation (2.4) can be easily computed using the explicit formula (2.7) for the Bergman kernel, and reads

$$\rho_{k,1} = \frac{1}{2^k} \text{diag} \left(\binom{k}{0}, \binom{k}{1}, \dots, \binom{k}{k} \right);$$

in other words, $\rho_{k,1}$ is a probabilistic mixture of the pure states $(e_{\ell,k+1})_{0 \leq \ell \leq k}$ according to a binomial distribution $B(k, \frac{1}{2})$. Note that

$$\text{Tr}(\rho_{k,1}^2) = \frac{1}{4^k} \sum_{\ell=0}^k \binom{k}{\ell}^2 = \frac{1}{4^k} \binom{2k}{k} \sim_{k \rightarrow +\infty} \frac{1}{\sqrt{k\pi}};$$

this agrees with Proposition 2.2.1 which gives

$$\text{Tr}(\rho_{k,1}^2) \sim_{k \rightarrow +\infty} \sqrt{\frac{2\pi}{k}} \int_0^{2\pi} \frac{d\theta}{2\pi\sqrt{2}} = \frac{1}{\sqrt{k\pi}}$$

since $\mu_{\Gamma_1} = \frac{|d\theta|}{\sqrt{2}}$ so $\sigma_1 = \frac{1}{\pi\sqrt{2}}\mu_{\Gamma_1}$.

Computing the matrix elements of $\rho_{k,2}^\alpha = \rho_k(\Gamma_2^\alpha, \sigma_2^\alpha)$ in the orthonormal basis $(e_{\ell,k+1})_{0 \leq \ell \leq k}$ is more involved but can be done as follows, by exploiting the natural actions of $\text{SU}(2)$ on \mathbb{CP}^1 and \mathcal{H}_k . Let

$$\tau_2 = \frac{1}{2} \begin{pmatrix} 0 & -1 \\ 1 & 0 \end{pmatrix} \in \mathfrak{su}(2)$$

and let $U_k(\alpha) : \mathcal{H}_k \rightarrow \mathcal{H}_k$ be the unitary operator corresponding to the action of $\exp(\alpha\tau_2) \in \text{SU}(2)$:

$$\forall \psi \in \mathcal{H}_k \quad U_k(\alpha)\psi = \exp(\alpha\tau_2) \cdot \psi$$

Then (see [LF18a, Lemma 5.3]) $\rho_{k,2}^\alpha = U_k(\alpha)\rho_{k,1}U_k(\alpha)^*$. One can check that $U_k(\alpha)$ is the exponential of the operator A_k whose action in $(e_{\ell,k+1})_{0 \leq \ell \leq k}$ reads

$$A_k e_{\ell,k+1} = \frac{\alpha}{2} \sqrt{(\ell+1)(k-\ell)} e_{\ell+1,k+1} - \frac{\alpha}{2} \sqrt{\ell(k-\ell+1)} e_{\ell-1,k+1}$$

for every $\ell \in \{0, \dots, k\}$. Using these results, one can compute numerically the fidelity, sub-fidelity and super-fidelity of $\rho_{k,1}$ and $\rho_{k,2}^\alpha$.

Moreover, one can compute explicitly the quantities involved in the estimates of Theorem 2.2.4. Since, as we will see below, the estimate for the super-fidelity is a direct consequence of Proposition 2.2.1, that we have checked for $\rho_{k,1}$ above and holds for $\rho_{k,2}^\alpha$ as well because

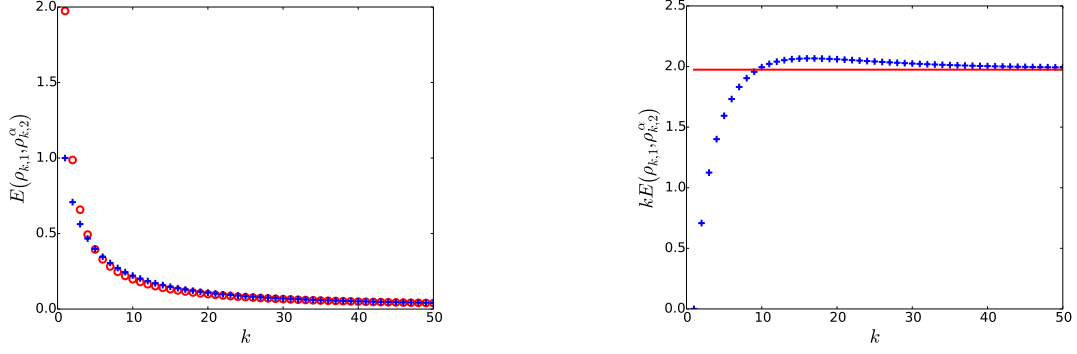
$$\text{Tr}(\rho_{k,2}^\alpha)^2 = \text{Tr}((U_k(\alpha)\rho_{k,1}U_k(\alpha)^*)^2) = \text{Tr}(\rho_{k,1}),$$

we will focus on the sub-fidelity. Note that Γ_1 and Γ_2^α intersect transversally at the two points $m_1 = (0, -1, 0)$ and $m_2 = (0, 1, 0)$, and for each of these points there is one principal angle $\theta_1(m_1) = \theta_1(m_2) = \alpha$. Moreover, since $\sigma_1 = \frac{1}{\pi\sqrt{2}}\mu_{\Gamma_1}$, by construction $\sigma_2^\alpha = \frac{1}{\pi\sqrt{2}}\mu_{\Gamma_2^\alpha}$ and so

$$(\sigma_1, \sigma_2)_{m_1} = (\sigma_1, \sigma_2)_{m_2} = \frac{1}{2\pi^2}.$$

Consequently, the constants in Theorem 2.2.4 read

$$C_1 = \frac{1}{\pi^2 \sin \alpha}, \quad C_2 = \frac{1}{2\pi^4 \sin^2 \alpha}, \quad C_3 = \frac{1}{2\pi^4 \sin \alpha} \left(\frac{1}{\sin \alpha} - \frac{1}{\sqrt{1 + \sin^2 \alpha}} \right)$$



(a) The blue crosses correspond to $E(\rho_{k,1}, \rho_{k,2}^\alpha)$, and the red circles correspond to the first term on the right-hand side of Equation (2.12).

(b) The blue crosses correspond to the quantity $kE(\rho_{k,1}, \rho_{k,2}^\alpha)$, while the solid red line represents the constant $\frac{2}{\pi \sin \alpha} \left(1 + \sqrt{2 - \frac{\sin \alpha}{\sqrt{1 + \sin^2 \alpha}}} \right)$ from Equation (2.12).

Figure 2.1: Sub-fidelity $E(\rho_{k,1}, \rho_{k,2}^\alpha)$ and $kE(\rho_{k,1}, \rho_{k,2}^\alpha)$, as functions of k , for $1 \leq k \leq 50$ and $\alpha = \frac{\pi}{4}$.

and we obtain after some simplifications:

$$E(\rho_{k,1}, \rho_{k,2}^\alpha) = \frac{2}{k\pi \sin \alpha} \left(1 + \sqrt{2 - \frac{\sin \alpha}{\sqrt{1 + \sin^2 \alpha}}} \right) + O(k^{-2}). \quad (2.12)$$

We compare this theoretical estimate with the numerically computed sub-fidelity in Figure 2.1 for $\alpha = \frac{\pi}{4}$ and various values of k , and in Figure 2.2 for $k = 500$ and various values of α . Note that the remainder in Equation (2.12) may depend on α so if k is fixed, it does not make sense to consider arbitrarily small values of α .

For this family of examples, one can in fact estimate more precisely the fidelity, at the cost of rather involved technicalities. The statement itself reflects the technical aspect of this work.

Theorem 2.2.6 ([LF18a, Theorem 5.9]). *Let $\alpha \in (0, \frac{\pi}{2}]$ and let $\rho_{k,1}$ and $\rho_{k,2}^\alpha$ be as in Example 2.2.5. The fidelity of $\rho_{k,1}$ and $\rho_{k,2}^\alpha$ satisfies*

$$F(\rho_{k,1}, \rho_{k,2}^\alpha) \leq \frac{16k^{3\delta-1}}{\pi \sin^2 \alpha} + O(k^{\frac{25\delta}{12}-1})$$

for every $\delta \in (0, \frac{1}{2}]$.

This means that morally, this fidelity is of order $O(k^{-1})$, and comparing this with Equation (2.12) shows that the sub-fidelity gives the correct order for the fidelity in this case. This is also confirmed numerically in Figure 2.3, where we compare the fidelity and sub-fidelity of $\rho_{k,1}$ and $\rho_{k,2}^\alpha$ when $\alpha = \frac{\pi}{3}$. It is tempting to conjecture that this remains true in our general setting of two Lagrangian submanifolds intersecting transversally in (M^{2n}, ω) , meaning that the fidelity will be a $O(k^{-n})$, but we have not explored this path and the difficulty to obtain Theorem 2.2.6 in this simple example where symmetries help does not lead to optimism.

Let us now give some ideas of the proofs of the different results. The proof of Proposition 2.2.2 relies on a characterization of the microsupport in terms of semiclassical measures obtained in [CP18, Proposition 4.4]. Then, except for Theorem 2.2.6 that we will discuss later, the crucial point is always to apply a version of the stationary phase lemma after having reduced the problem to the computation of an oscillatory integral by exploiting the asymptotic behavior

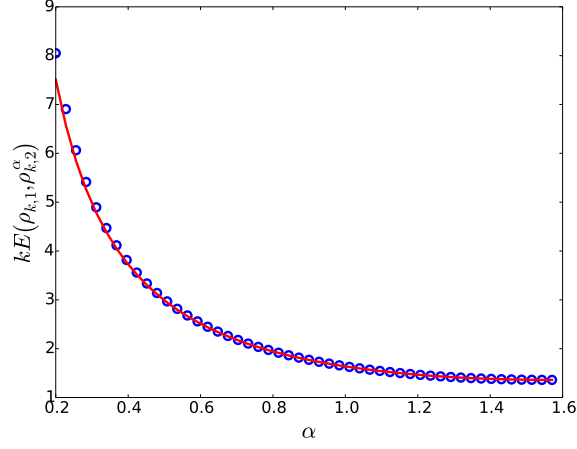
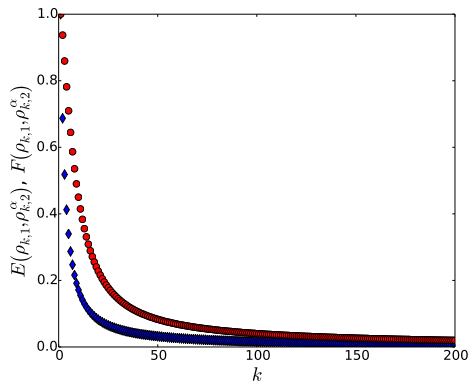
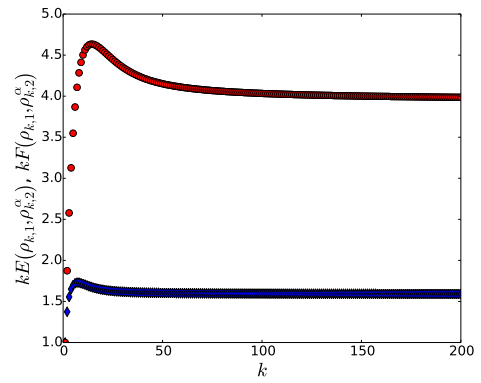


Figure 2.2: The blue circles represent the value of $kE(\rho_{k,1}, \rho_{k,2}^\alpha)$ as a function of α for $k = 500$ and $0.2 \leq \alpha \leq \frac{\pi}{2}$. The red line corresponds to the theoretical equivalent $\alpha \mapsto \frac{2}{\pi \sin \alpha} \left(1 + \sqrt{2 - \frac{\sin \alpha}{\sqrt{1 + \sin^2 \alpha}}} \right)$ obtained in Equation (2.12).



(a) $E(\rho_{k,1}, \rho_{k,2}^\alpha)$ and $F(\rho_{k,1}, \rho_{k,2}^\alpha)$.



(b) $kE(\rho_{k,1}, \rho_{k,2}^\alpha)$ and $kF(\rho_{k,1}, \rho_{k,2}^\alpha)$.

Figure 2.3: Comparison between the fidelity and sub-fidelity of $\rho_{k,1}$ and $\rho_{k,2}^\alpha$ for $\alpha = \frac{\pi}{3}$, as functions of k , $1 \leq k \leq 200$. The blue diamonds correspond to the sub-fidelity, while the red circles represent the fidelity.

of the Bergman kernel Π_k (see Section 2.1). Here we will use the formulation from [Cha03a] given in Equation (2.3). Actually we will need more properties, which we will describe later, of the section S from this equation. In order to outline the proofs and compare their relative difficulties, we will need to further enter into technical details.

For Proposition 2.2.1, preliminary computations lead to

$$\mathrm{Tr}(\rho_k(\Sigma, \sigma)^2) = \int_{\Sigma} \int_{\Sigma} \frac{|\Pi_k(x, y)|^2}{|\Pi_k(x, x)| |\Pi_k(y, y)|} \sigma(x) \sigma(y).$$

Because of the off-diagonal behavior of Π_k , we obtain $\mathrm{Tr}(\rho_k(\Sigma, \sigma)^2)$ up to $O(k^{-\infty})$ by computing this integral on a neighborhood of the diagonal in $\Sigma \times \Sigma$. Writing the section S from Equation (2.3) locally near this diagonal as $S = e^{-\varphi}$, this can in turn be computed by applying the stationary phase lemma where the phase φ has a submanifold of critical points (the diagonal in $\Sigma \times \Sigma$). Computing carefully the transverse Hessian of this phase, using properties of S from [Cha03a], gives the result.

To prove Proposition 2.2.2 regarding the microsupport of $\rho_k(\Sigma, \sigma)$, we estimate the operator norm $\|T_k(\chi)\rho_k(\Sigma, \sigma)\|_{\mathrm{op}}$ for some appropriate cutoff functions χ on M . Since $\dim \mathcal{H}_k = O(k^n)$ (see Equation (2.2)), it suffices, actually, to estimate the trace $\mathrm{Tr}(T_k(\chi)\rho_k(\Sigma, \sigma))$. This can be done see by means of the asymptotic expansion of the Schwartz kernel of T_k given in [Cha03a] as a consequence of the asymptotic expansion of Π_k ; see [LF18a, Lemma 3.5] for more details.

To prove Proposition 2.2.3, we first derive the inequality

$$F(\rho_k(\Sigma_1, \sigma_1), \rho_k(\Sigma_2, \sigma_2)) \leq \dim(\mathcal{H}_k) \mathrm{Tr}(\rho_k(\Sigma_1, \sigma_1)\rho_k(\Sigma_2, \sigma_2))$$

and see that it suffices to estimate the trace on the right-hand side since $\dim(\mathcal{H}_k) = O(k^n)$ (see Equation (2.2)). Then, similarly as above, we obtain

$$\mathrm{Tr}(\rho_{k,1}\rho_{k,2}) = \int_{\Sigma_1} \int_{\Sigma_2} \frac{|\Pi_k(x, y)|^2}{|\Pi_k(x, x)| |\Pi_k(y, y)|} \sigma_1(x) \sigma_2(y)$$

and, because of Equation (2.3) again, the integrand is a $O(k^{-\infty})$ uniformly on $\Sigma_1 \times \Sigma_2$ since the latter does not intersect the diagonal of $M \times M$.

We now come to the proof of Theorem 2.2.4. We see from Equations (2.9) and (2.10) that for both the sub-fidelity and super-fidelity of $\rho_{k,1}$ and $\rho_{k,2}$, we need to estimate the term $\mathrm{Tr}(\rho_{k,1}\rho_{k,2})$. This is the content of [LF18a, Theorem 4.4], which states that

$$\mathrm{Tr}(\rho_{k,1}\rho_{k,2}) = \left(\frac{2\pi}{k}\right)^n \left(\sum_{r=1}^s \frac{(\sigma_1, \sigma_2)_{m_r}}{\prod_{\ell=1}^n \sin(\theta_{\ell}(m_r))}\right) + O(k^{-(n+1)}), \quad (2.13)$$

where we recall that $0 < \theta_1(m_r) \leq \dots \leq \theta_n(m_r) \leq \frac{\pi}{2}$ are the principal angles between $T_{m_r}\Gamma_1$ and $T_{m_r}\Gamma_2$, and that $(\sigma_1, \sigma_2)_{m_r}$ is defined in Equation (2.11). From this and Proposition 2.2.1 we readily obtain the part of Theorem 2.2.4 regarding the super-fidelity, and the leading term in this trace estimate gives the terms C_1 and C_2 in the result about the sub-fidelity.

To derive Equation (2.13), we once again write

$$\mathrm{Tr}(\rho_{k,1}\rho_{k,2}) = \int_{\Gamma_1} \int_{\Gamma_2} \frac{|\Pi_k(x, y)|^2}{|\Pi_k(x, x)| |\Pi_k(y, y)|} \sigma_1(x) \sigma_2(y),$$

and conclude as above that the only non-negligible contributions come from neighborhoods of the intersection points m_1, \dots, m_s . Each of these contributions is computed from a stationary phase lemma applied to a phase with a single critical point, again by writing locally near the corresponding intersection point the section S from Equation (2.3) as $S = e^{-\varphi}$. The explicit computation of the Hessian determinant at the critical point is not completely trivial and involves a nice equality between the product of the sines of the principal angles between two n -dimensional

subspaces W and Z of a $2n$ -dimensional vector space and a determinant involving a Gram-like matrix containing the scalar products of elements of orthonormal bases of W and Z (see [LF18a, Lemma 2.2]).

To conclude, we need to estimate the more involved term $\text{Tr}((\rho_{k,1}\rho_{k,2})^2)$. The idea is the same as before, but this time we have the rather intimidating equality

$$\text{Tr}((\rho_{k,1}\rho_{k,2})^2) = \int_{\Gamma_1} \int_{\Gamma_2} \int_{\Gamma_1} \int_{\Gamma_2} \text{Tr}(P_k^{x_1} P_k^{x_2} P_k^{y_1} P_k^{y_2}) \sigma_1(x_1) \sigma_2(x_2) \sigma_1(y_1) \sigma_2(y_2)$$

and the term $\text{Tr}(P_k^{x_1} P_k^{x_2} P_k^{y_1} P_k^{y_2})$ can again be written by means of the Bergman kernel, but not only using its pointwise norm. Concretely, the contribution away from the intersection points m_1, \dots, m_s is negligible, and near each of these points we write the section S from Equation (2.3) as $S(x, y) = e^{i\psi(x, y)} t(x) \otimes \bar{t}(y)$ where t is a local section of L with pointwise norm equal to one. Then we need to integrate

$$e^{ik\Psi(x_1, x_2, y_1, y_2)} a_0(y_1, y_2) a_0(x_2, y_1) a_0(x_1, x_2) a_0(y_2, x_1)$$

where the phase Ψ is given by

$$\Psi(x_1, x_2, y_1, y_2) = \psi(y_1, y_2) + \psi(x_2, y_1) + \psi(x_1, x_2) + \psi(y_2, x_1).$$

The computation of the Hessian of Ψ is delicate and relies on an explicit expression for the Hessian of ψ , obtained in [Cha06], in terms of the Kähler data. After using another equality involving the sines of the principal angles and the symplectic form (see [LF18a, Lemma 2.3]), we get

$$\text{Tr}((\rho_{k,1}\rho_{k,2})^2) = \left(\frac{2\pi}{k}\right)^{2n} \left(\sum_{r=1}^s \frac{(\sigma_1, \sigma_2)_{m_r}^2}{\prod_{\ell=1}^n \sin(\theta_\ell(m_r)) \sqrt{1 + \sin^2(\theta_\ell(m_r))}} \right) + O(k^{-(2n+1)})$$

and by combining this estimate with Equation (2.13) we obtain the term C_3 in Theorem 2.2.4.

An important remark is that, while the assumption that Γ_1 and Γ_2 are Lagrangian is crucial in this computation of $\text{Tr}((\rho_{k,1}\rho_{k,2})^2)$, it does not play any part in the derivation of Equation (2.13) regarding $\text{Tr}(\rho_{k,1}\rho_{k,2})$. We suspect that this equation still holds for two submanifolds of respective dimensions d and $2n - d$ (with $1 \leq d \leq n$) intersecting transversally at a finite number of points, up to adapting the notation: in this case only d principal angles $\theta_1 \leq \dots \leq \theta_d$ are well-defined, and we should set $\theta_{d+1} = \dots = \theta_n = \frac{\pi}{2}$.

Another remark is that one can see on these proofs why the computation of the sub-fidelity and super-fidelity is tractable. The density operators of our states are integral operators, and these quantities involves their products (and powers); but the Schwartz kernel of a product can be explicitly computed from the Schwartz kernels of the original operators, and this constitutes the preliminary computations in the above proofs. However, there is no such general formula for the Schwartz kernel of a square root, and this is why estimating the fidelity itself is a difficult problem.

This is also why we needed to resort to different techniques to prove Theorem 2.2.6. The first step is to compare the states $\rho_{k,1}$ and $\rho_{k,2}^\alpha$ to Berezin-Toeplitz operators with Gaussian symbols. More precisely, we show that for every $c \geq 2$ and every $k \geq 1$

$$\rho_{k,1} \leq \frac{1}{\sqrt{k+1}} T_k(f_k^c), \quad \rho_{k,2}^\alpha \leq \frac{1}{\sqrt{k+1}} T_k(f_k^c \circ R_{-\alpha})$$

where $f_k^c : S^2 \rightarrow \mathbb{R}^+$ is defined as $f_k^c(x, y, z) = \sqrt{\frac{2(2c+1)}{\pi}} \exp(-c(k+1)z^2)$ and we recall that $R_{-\alpha}$ is the rotation of angle $-\alpha$ about the y -axis. Using the monotonicity of the fidelity, this gives (see [LF18a, Proposition 5.7]), setting $g_k^c = f_k^c \circ R_{-\alpha}$,

$$F(\rho_{k,1}, \rho_{k,2}^\alpha) \leq \frac{1}{k+1} F(T_k(f_k^c), T_k(g_k^c)),$$

and it suffices to estimate the fidelity on the right-hand side. What have we gained? The point is that for Berezin-Toeplitz operators in reasonable symbol classes, symbolic calculus allows to approximate $\sqrt{T_k(f)}$ by $T_k(\sqrt{f})$. Unfortunately, f_k^c is precisely a bad symbol, since it is of the form $f_k^c = f(\sqrt{c(k+1)}\cdot)$, with $f(x, y, z) = \sqrt{\frac{2(2c+1)}{\pi}} \exp(-z^2)$, and $k^{\frac{1}{2}}$ is the critical scale at which symbolic calculus fails.

This can be circumvented by considering instead, for $0 < \delta < \frac{1}{2}$, the functions $f_k^{c,\delta} = f(\sqrt{c(k+1)}^{\frac{1}{2}-\delta}\cdot)$ and $g_k^{c,\delta} = f_k^{c,\delta} \circ R_{-\alpha}$, which belong in good symbol classes. Then

$$F(T_k(f_k^c), T_k(g_k^c)) \leq F(T_k(f_k^{c,\delta}), T_k(g_k^{c,\delta})) = \left\| \sqrt{T_k(f_k^{c,\delta})} \sqrt{T_k(g_k^{c,\delta})} \right\|_{\text{Tr}}^2.$$

Then we use symbolic calculus to approximate $\sqrt{T_k(f_k^{c,\delta})} \sqrt{T_k(g_k^{c,\delta})}$ by $T_k(\sqrt{f_k^{c,\delta} g_k^{c,\delta}})$, whose trace norm can be easily estimated using a very explicit stationary phase computation carried out in [LF18a, Appendix B]. The tricky and very technical part is to carefully control the remainders appearing in these approximations. For this we need to discriminate between the interactions near and away from the intersection points of Γ_1 and Γ_2^α , and this analysis involves another parameter r controlling the size of cutoffs near these points. The final step in the proof of Theorem 2.2.6 is to optimize the parameters c , δ and r appearing in these remainders.

2.3 Random holomorphic sections and Berezin-Toeplitz operators

We will now describe the results obtained with Michele Ancona in [ALF22] regarding the expected zero locus of a holomorphic section obtained as the image of a random holomorphic section under the action of a Berezin-Toeplitz operator.

Trying to understand the distribution of the (real or complex) zeros of random polynomials of large degree is a classical and well-established topic, dating back to the 1930s [BP31, LO38] at least, and popularized by the seminal article by Kac [Kac43]. Here we are interested in the complex zeros of holomorphic sections of high powers of a complex line bundle, chosen at random according to a suitable Gaussian distribution, using a framework that has been introduced and investigated by Shiffman and Zelditch (see [SZ99b]) and has been intensively studied since (see for instance [BCHM18] for a recent survey on these topics).

Of course the particular case of random homogenous polynomials in two complex variables falls into the study of random holomorphic sections, since such polynomials naturally arise as the holomorphic sections of a suitable line bundle over \mathbb{CP}^1 , see Example 2.1.1. But in fact this case was already studied by Bogomolny, Bohigas and Leboeuf without using the language of sections in [BBL96], where the authors proved that the zeros of such a random homogeneous polynomial are uniformly distributed. In order to explain this result, and its generalization by Shiffman and Zelditch in [SZ99b], we now introduce some notation and describe the problem more precisely.

Let (M, ω, j) be a compact Kähler manifold of complex dimension n , and let $(L, h) \rightarrow M$ be a prequantum line bundle over M . As before, for $k \geq 1$, let $\mathcal{H}_k = H^0(M, L^{\otimes k})$ be the space of holomorphic sections of $L^{\otimes k} \rightarrow M$, equipped with the inner product $\langle \cdot, \cdot \rangle_k$ defined in Equation (2.1) (here we do not consider any auxiliary line bundle L'). Let $N_k = \dim \mathcal{H}_k$ and let $(e_{\ell,k})_{1 \leq \ell \leq N_k}$ be any orthonormal basis of \mathcal{H}_k . Then we pick a holomorphic section at random by considering:

$$s_k = \sum_{\ell=1}^{N_k} \alpha_{\ell,k} e_{\ell,k} \quad (2.14)$$

where the coefficients $\alpha_{\ell,k}$ are independent and identically distributed complex random variables with distribution $\mathcal{N}_{\mathbb{C}}(0, 1)$. Equivalently, the probability distribution of the random section s_k

is the measure μ_k on \mathcal{H}_k defined as

$$d\mu_k(s) = \frac{1}{\pi N_k} e^{-\|s\|_k^2} ds$$

with ds the Lebesgue measure induced on \mathcal{H}_k by the inner product $\langle \cdot, \cdot \rangle_k$.

The result of [BBL96] is the following: choose a random homogeneous polynomial $P_k = s_k$ of degree k using this procedure with $(M, \omega) = (\mathbb{CP}^1, \omega_{\text{FS}})$ and $L \rightarrow M$ the hyperplane bundle, see Examples 2.1.1 and 2.3.2. Then for any measurable set $U \subset \mathbb{CP}^1$,

$$\mathbb{E}[\#(Z_{P_k} \cap U)] = \frac{k}{2\pi} \omega_{\text{FS}}(U)$$

where Z_{P_k} is the set of zeros of P_k . Note that in this case the zeros are uniformly distributed for every $k \geq 1$; this is an effect of the $U(2)$ -symmetry present in this example, but in what follows, we will state asymptotic results as $k \rightarrow +\infty$.

In order to state higher-dimensional results, we need to use the language of currents, the form-valued analogues of distributions. Recall in particular that a current of degree p on a smooth manifold N of dimension d is an element of the topological dual $\mathcal{D}'_p(N)$ of the space $\mathcal{D}^{d-p}(N)$ of smooth compactly supported $(d-p)$ -forms on N (we define similarly, if N is a complex manifold, currents of bidegree (p, q)), and that a sequence $(\eta_\ell)_{\ell \geq 0}$ of currents of degree p converges to a current η of degree p if and only if for every compactly supported $(d-p)$ -form φ , the sequence $(\langle \eta_\ell, \varphi \rangle)_{\ell \geq 0}$ converges to $\langle \eta, \varphi \rangle$. Two typical examples are the current associated with a locally integrable differential form $\eta \in \Omega^p(N)$, defined by

$$\forall \varphi \in \mathcal{D}^{n-p}(N) \quad \langle \eta, \varphi \rangle = \int_N \eta \wedge \varphi$$

and the integration current η_V associated with a smooth submanifold V of codimension p of N , defined by

$$\forall \varphi \in \mathcal{D}^{n-p}(N) \quad \langle \eta_V, \varphi \rangle = \int_V \varphi.$$

In fact, even when V is only an analytic subset of N , one can define a current of integration by integrating along the regular part of V , see [Lel57].

In particular, back to our setting, both the Kähler form ω and the zero locus $Z_s = \{s = 0\}$ of any holomorphic section $s \in \mathcal{H}_k$ define currents of bidegree $(1, 1)$ on M . The expectation of the current-valued random variable given by the integration current associated with the zero locus Z_{s_k} of the random holomorphic section s_k is itself a $(1, 1)$ -current defined as

$$\forall \varphi \in \Omega^{n-1, n-1}(M) \quad \langle \mathbb{E}[Z_{s_k}], \varphi \rangle = \mathbb{E}[\langle Z_{s_k}, \varphi \rangle] = \int_{s \in \mathcal{H}_k} \langle Z_{s_k}, \varphi \rangle d\mu_k(s).$$

We can now state one of the results of [SZ99b], with a slightly different normalization due to our different convention regarding the prequantum line bundle: recall that we assume that $\text{curv}(\nabla) = -i\omega$, while in [SZ99b] it is assumed that $\text{curv}(\nabla) = -2i\pi\omega$. It is useful to keep this difference in mind when comparing results.

Theorem 2.3.1 ([SZ99b, Theorem 1.1]). *Let s_k be a random holomorphic section as above and let $\mathbb{E}[Z_{s_k}]$ be its expected zero locus. Then $\frac{1}{k}\mathbb{E}[Z_{s_k}]$ converges to $\frac{\omega}{2\pi}$ in the sense of currents when $k \rightarrow +\infty$.*

In fact their proof gives the more precise:

$$\forall \varphi \in \Omega^{n-1, n-1}(M) \quad \langle \mathbb{E}[Z_{s_k}], \varphi \rangle = \frac{k}{2\pi} \langle \omega, \varphi \rangle + \frac{i}{2\pi} \langle \partial \bar{\partial} \log \Pi_k, \varphi \rangle. \quad (2.15)$$

Here we slightly abuse notation and still write Π_k for the restriction of the Bergman kernel to the diagonal of $M \times M$. But for any $\varphi \in \Omega^{n-1, n-1}(M)$, by Stokes' formula,

$$\langle \partial \bar{\partial} \log \Pi_k, \varphi \rangle = \int_M \partial \bar{\partial} \log \Pi_k \wedge \varphi = \int_M \log \Pi_k \partial \bar{\partial} \varphi = O(k^{-1}) \sup_M |\psi|$$

where $\partial \bar{\partial} \varphi = \psi \omega^{\wedge n}$, since $\Pi_k = 1 + O(k^{-1})$ uniformly on M (see Equation (2.3)). Therefore

$$\langle \mathbb{E}[Z_{s_k}], \varphi \rangle = \frac{k}{2\pi} \langle \omega, \varphi \rangle + O(k^{-1}) \sup_M |\psi|. \quad (2.16)$$

We will compare this to our own results below.

Theorem 2.3.1 follows from results on the Kodaira map

$$\Phi_k : M \rightarrow \mathbb{CP}^{N_k-1}, \quad m \in M \mapsto [e_{1,k}(m) : \cdots : e_{N_k,k}(m)],$$

which is an embedding for k large enough by the Kodaira embedding theorem. It is standard that the pullback $\Phi_k^* \omega_{\text{FS}}$ of the Fubini-Study form ω_{FS} on \mathbb{CP}^{N_k-1} does not depend on the choice of the orthonormal basis $(e_{\ell,k})_{1 \leq \ell \leq N_k}$ and lies in the cohomology class $k[\omega]$. In fact,

$$\Phi_k^* \omega_{\text{FS}} = k\omega + i\partial \bar{\partial} \log \Pi_k. \quad (2.17)$$

Tian's asymptotic isometry theorem then shows that

$$\forall p \geq 0 \quad \left\| \frac{1}{k} \Phi_k^* \omega_{\text{FS}} - \omega \right\|_{\mathcal{C}^p} = O(k^{-1}). \quad (2.18)$$

Consequently, $\frac{1}{k} \Phi_k^* \omega_{\text{FS}}$ converges to ω in the \mathcal{C}^∞ topology when $k \rightarrow +\infty$. This result is due to Tian [Tia90] for the \mathcal{C}^2 convergence and Zelditch [Zel98b] for the general \mathcal{C}^∞ convergence; additionally Bouche [Bou90] showed the uniform convergence of the metric induced by Φ_k on L in the case of a positive L whose curvature does not necessarily equal $-i\omega$, and Borthwick and Uribe [BU00] study the symplectic, not necessarily Kähler, case. Moreover, one can check by using the Poincaré-Lelong formula (see for instance [GH78, p. 388]) that

$$\mathbb{E}[Z_{s_k}] = \frac{1}{2\pi} \Phi_k^* \omega_{\text{FS}} \quad (2.19)$$

as currents. Combining Equations (2.18) and (2.19) gives Theorem 2.3.1, and combining Equations (2.17) and (2.19) yields Equation (2.15).

In [ALF22], we were interested in answering the following question: what happens to the zero locus of a random holomorphic section when we apply a Berezin-Toeplitz operator to this section? In particular, what kind of information about the operator can be recovered from a close inspection of this zero locus? More precisely, let $T_k : \mathcal{H}_k \rightarrow \mathcal{H}_k$ be a Berezin-Toeplitz operator with principal symbol $f \in \mathcal{C}^\infty(M, \mathbb{R})$, and let s_k be a random holomorphic section as above. From the data of the sequence of the zero loci of $T_k s_k$, what can one recover about f ? This interrogation was the motivation for the results explained below, and can be seen as part of the popular family of inverse questions discussed in Section 1.1. Unlike in Chapter 5 where we recover classical data from a quantum spectrum, here the idea is to try to retrieve information on the classical observable f underlying the quantum observable T_k by testing T_k against a large number of quantum states obtained as random combinations of pure states.

A first intuition can be obtained as follows. Since the operator T_k is analogous to the operator of multiplication by f , one can naively expect $T_k s_k$ to behave “like $f s_k$ ”; this, of course, does not make sense since the section $f s_k$ will not be holomorphic unless f is constant, but let us nevertheless look at this section. Its zero locus is the union of the zero locus of the original section s_k and of the zero locus of f . So one is tempted to conjecture that the zero locus of f

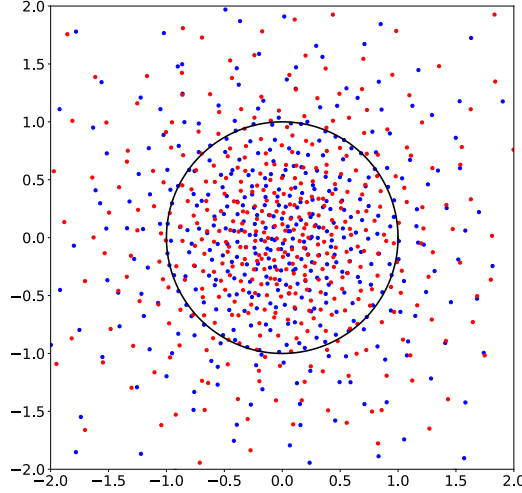


Figure 2.4: Zeros of s_k (in red) and of $T_k s_k$ (in blue) for one sample of the random polynomial s_k from Example 2.3.2 when $k = 500$, in the window $[-2, 2]^2 \subset \mathbb{C}$. Here we work in the image of $S^2 \setminus \{(0, 0, 1)\}$ by the stereographic projection π_N . The solid black line is the unit circle, image by π_N of the zero set of f . Recall also from Equation (2.6) that the Fubini-Study form puts more weight on points with small modulus.

will play a part in the story, and more precisely that $T_k s_k$ will have “more zeros” near $f^{-1}(0)$ than elsewhere.

As we will now explain, this naive intuition is correct to some extent, in the setting that we work with in [ALF22]. Namely, we assume that 0 is a regular value of f . A natural reflex is to look at a simple example of this situation.

Example 2.3.2 (Height function on S^2). We work in the setting of Example 2.1.1, but without metaplectic correction; thus we consider the Hilbert spaces $\mathcal{H}_k = H^0(\mathbb{CP}^1, \mathcal{O}(k)) \simeq \mathbb{C}_k^{\text{hom}}[w_1, w_2]$, $k \geq 1$, with dimension $N_k = k + 1$, and random homogeneous polynomials s_k of the form (2.14) with $(e_{\ell, k+1})_{0 \leq \ell \leq k}$ the orthonormal basis given in Equation (2.4) (after replacing k by $k + 1$). Let $T_k = T_{k+1}(z)$, with principal symbol $f = z$; in Figure 2.4 we display the zeros of s_k and of $T_k s_k$, computed numerically, for one sample of s_k .

It can be visualized on this example that on the one hand, there seems to be a slightly bigger concentration of the zeros of $T_k s_k$ near $f^{-1}(0)$, but on the other hand, the zeros of $T_k s_k$ appear to be uniformly distributed, as are the zeros of s_k . Hence we expect the effect of T_k to be subtle and would like to quantify it. This is the object of the next two statements, Theorems 2.3.3 and 2.3.4.

Theorem 2.3.3 ([ALF22, Theorem 1.9]). *Let $f \in C^\infty(M, \mathbb{R})$ be a smooth function such that 0 is a regular value of f , and let T_k be a Berezin-Toeplitz operator with principal symbol f . Then $\frac{1}{k} \mathbb{E}[Z_{T_k s_k}]$ converges to $\frac{\omega}{2\pi}$ in the sense of currents when $k \rightarrow +\infty$. Moreover,*

$$\mathbb{E}[Z_{T_k s_k}] - \frac{k}{2\pi} \omega \xrightarrow[k \rightarrow +\infty]{} \frac{i}{2\pi} \partial \bar{\partial} \log f^2$$

in the sense of currents.

A simple computation shows that under the assumptions of the theorem, the function $\log f^2$ is locally integrable, so that the current $\partial \bar{\partial} \log f^2$ is well-defined. The first part of the statement shows that the zeros of $T_k s_k$ tend to become equidistributed in the semiclassical limit, as is the case for the zeros of s_k . Naturally, when $T_k = \Pi_k$, then $f = 1$ and $T_k s_k = s_k$, and from

the second part of the statement we recover the fact that the difference $\mathbb{E}[Z_{s_k}] - \frac{k}{2\pi}\omega$ goes to zero when $k \rightarrow +\infty$, as can be deduced from Equation (2.16). But as soon as $f^{-1}(0) \neq \emptyset$, the situation radically changes because this difference is morally a $O(1)$ instead of a $O(k^{-1})$.

In order to get a finer comprehension of the role of $f^{-1}(0)$ in the distribution of zeros of $T_k s_k$, we studied what happens at the quantum mechanical scale $k^{-\frac{1}{2}}$. Before stating the result, we need to introduce more notation. The Kähler structure induces a Hermitian metric on $T^*M \otimes \mathbb{C}$ that we denote by $|\cdot|_\omega$. Moreover, for $m \in M$ and $r > 0$, we denote by $B(m, r)$ the geodesic ball (with respect to the Kähler metric) of radius r around m .

Theorem 2.3.4 ([ALF22, Theorem 1.10]). *Let $f \in C^\infty(M, \mathbb{R})$ be a smooth function such that 0 is a regular value of f , and let T_k be a Berezin-Toeplitz operator with principal symbol f . Let $m \in M$, and let $\varphi \in \Omega^{n-1, n-1}(M)$. For every $R > 0$,*

$$\int_{B(m, \frac{R}{\sqrt{k}})} \left(\mathbb{E}[Z_{T_k s_k}] - \frac{k\omega}{2\pi} \right) \wedge \varphi = \begin{cases} k^{-n+1} \frac{F_\varphi(m)}{\pi |df(m)|_\omega^2} C_n(R) + O(k^{-n+\frac{1}{2}}) & \text{if } m \in f^{-1}(0), \\ k^{-n} \frac{R^{2n} L_\varphi(m) \text{Vol}(B_{\mathbb{R}^{2n}}(0,1))}{2\pi} + O(k^{-n-\frac{1}{2}}) & \text{if } m \notin f^{-1}(0). \end{cases}$$

Here, $C_n(R)$ is an explicit constant and F_φ and L_φ are the functions defined as

$$i \partial f \wedge \bar{\partial} f \wedge \varphi = F_\varphi \frac{\omega^{\wedge n}}{n!}, \quad i \partial \bar{\partial} \log f^2 \wedge \varphi = L_\varphi \frac{\omega^{\wedge n}}{n!}.$$

This result allows to quantify the influence of the zero set $f^{-1}(0)$: the zero locus of $T_k s_k$ tends to concentrate a little more on $f^{-1}(0)$, as can be seen from comparing the orders k^{-n+1} and k^{-n} in the cases $f(m) = 0$ and $f(m) \neq 0$.

The constant $C_n(R)$ in Theorem 2.3.4 is given by

$$C_n(R) = \frac{2^n \pi^n (n-1)!}{(2n-2)!} \left(\sum_{\ell=0}^{n-1} \binom{n-\frac{3}{2}}{\ell} 2^\ell R^{2\ell} - (1+2R^2)^{n-\frac{3}{2}} \right) \quad (2.20)$$

with $\binom{\alpha}{\ell} = \frac{\alpha(\alpha-1)\dots(\alpha-\ell+1)}{\ell!}$ for $\alpha \in \mathbb{R}$, $\ell \in \mathbb{N}_{>0}$ and $\binom{\alpha}{0} = 1$.

We can check the numerical validity of Theorem 2.3.4 on the following example.

Example 2.3.5. We keep working in the setting of Example 2.3.2; the principal symbol f of T_k is the height function on S^2 . Taking $\varphi = 1$ in the statement of Theorem 2.3.4 allows us to compare the number of zeros of $T_k s_k$ in the geodesic ball $B(m, \frac{R}{\sqrt{k}})$ with the volume of this ball, which can be computed explicitly. More precisely, for this choice of φ , the quantity from Theorem 2.3.4 equals

$$E(m, R, k) = \mathbb{E} \left[\# \left(Z_{T_k s_k} \cap B \left(m, \frac{R}{\sqrt{k}} \right) \right) \right] - k \left(1 - \frac{1}{1 + \tan^2(\frac{R}{\sqrt{k}})} \right).$$

We numerically approximate the quantity on the left-hand side by the sample mean

$$\mathcal{E}(m, R, k, N) = \frac{1}{N} \sum_{j=1}^N \# \left(Z_{T_k s_k^{(j)}} \cap B \left(m, \frac{R}{\sqrt{k}} \right) \right) - k \left(1 - \frac{1}{1 + \tan^2(\frac{R}{\sqrt{k}})} \right), \quad (2.21)$$

which, for a fixed k , converges to the quantity $E(m, R, k)$ when $N \rightarrow +\infty$ by the law of large numbers. Here $s_k^{(1)}, \dots, s_k^{(N)} \in H^0(\mathbb{CP}^1, \mathcal{O}(k))$ are N independent random holomorphic sections, and we locate the zeros of $T_k s_k^{(j)}$ numerically, after computing this section from the explicit expression for T_k given in Example 2.1.1. By computing explicitly the quantities F_1 , L_1 , $|df|_\omega$ and $C_1(R)$, we see that Theorem 2.3.4 yields

$$E(m, R, k) = \begin{cases} 1 - \frac{1}{\sqrt{1+2R^2}} + O(k^{-\frac{1}{2}}) & \text{if } m \in f^{-1}(0), \\ -\frac{2k^{-1}R^2(1+|z|^4)}{(|z|^2-1)^2} + O(k^{-\frac{3}{2}}) & \text{if } m \notin f^{-1}(0), \end{cases}$$

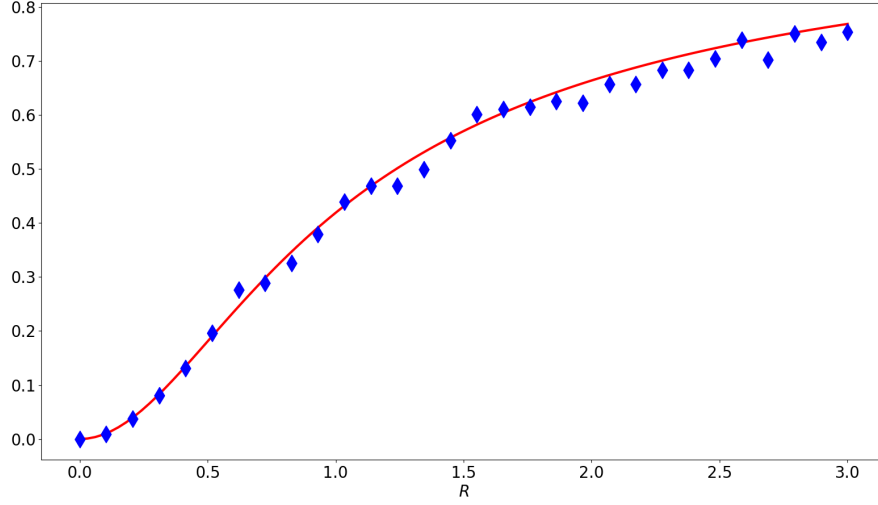


Figure 2.5: The blue diamonds are the numerical values of $\mathcal{E}(m, R, k, N)$ (see Equation (2.21)) for $m = (1, 0, 0)$, $k = 400$, $N = 1000$ and various values of R , in the setting of Example 2.3.5. The solid red line is the graph of $R \mapsto 1 - \frac{1}{\sqrt{1+2R^2}}$.

where $z = \pi_N(m)$. We compare this quantity with $\mathcal{E}(m, R, k, N)$ in Figures 2.5 (for the case $m \in f^{-1}(0)$) and 2.6 (for the case $m \notin f^{-1}(0)$).

We can also view Theorem 2.3.4 as a positive answer to our original question: we can indeed recover the zero set of f from the knowledge of $\mathbb{E}[Z_{T_k s_k}]$, by looking at its action at the quantum mechanical scale $k^{-\frac{1}{2}}$. This is illustrated in the next example.

Example 2.3.6. We keep working on S^2 as in Examples 2.3.2 and 2.3.5, but this time we consider the operator $T_k = T_k(x)T_k(y) - \lambda \text{Id}$ with $\lambda \in (0, \frac{1}{2})$, where $T_k(x)$ and $T_k(y)$ are as in Example 2.1.1. T_k is a Berezin-Toeplitz operator with principal symbol $f_\lambda = xy - \lambda$. Using the formulas from Example 2.1.1, one readily checks that for every $\ell \in \{0, \dots, k\}$,

$$T_k e_{\ell, k+1} = \frac{-i}{(k+2)^2} (\mu_{\ell, \ell-2, k+1} e_{\ell-2, k+1} - \mu_{\ell+2, \ell, k+1} e_{\ell+2, k+1}) - \lambda e_{\ell, k+1}$$

where $(e_{\ell, k+1})_{0 \leq \ell \leq k}$ is the orthonormal basis from Equation (2.4),

$$\mu_{p, q, k+1} = \sqrt{p(p-1)(k-q)(k-q-1)} \quad \text{if } p, q \in \{2, \dots, k-2\}$$

and $\mu_{p, q, k+1} = 0$ otherwise. So again, we can compute explicitly $T_k s_k$ for a random holomorphic section s_k and locate its zeros numerically. Hence we numerically evaluate the quantity $\mathcal{E}(m, R, k, N)$ from Equation (2.21) for various $m \in S^2$, and display its absolute value in Figure 2.7. Thanks to the different order of magnitudes in Theorem 2.3.4 according to whether m belongs to $f_\lambda^{-1}(0)$ or not, we can observe the quantum footprints of this zero set in this figure. Of course, we can vary λ and recover all the regular level sets of the function $f = xy$ in this way.

Similarly to the results from [SZ99b] explained above, Theorems 2.3.3 and 2.3.4 follow from properties of a “twisted” Kodaira map

$$\Phi_{T_k} : M \dashrightarrow \mathbb{CP}^{N_k-1}, \quad m \mapsto [(T_k e_{1, k})(m) : \dots : (T_k e_{N_k, k})(m)],$$

which is only well-defined outside $\bigcap_{s \in H^0(M, L^{\otimes k})} \{T_k s = 0\}$. A first result (Theorem 1.1 in [ALF22]) shows that when 0 is a regular value of the principal symbol f of T_k , then for k

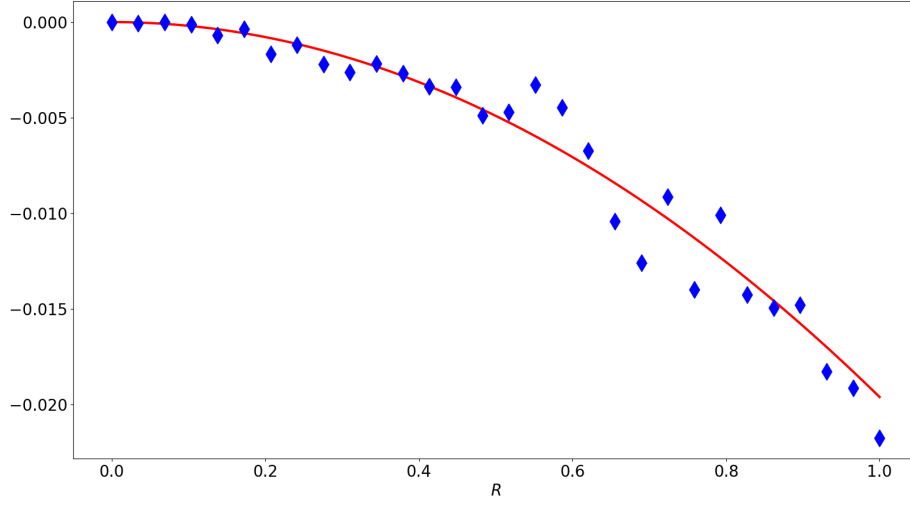


Figure 2.6: The blue diamonds are the numerical values of $\mathcal{E}(m, R, k, N)$ (see Equation (2.21)) for $m = (0, 0, 1)$, $k = 100$, $N = 100000$ and various values of R , in the setting of Example 2.3.5. The solid red line is the graph of $R \mapsto -\frac{2k^{-1}R^2(1+|z|^4)}{(|z|^2-1)^2} = -2k^{-1}R^2$ for these values of k and $z = \pi_N(m) = 0$.

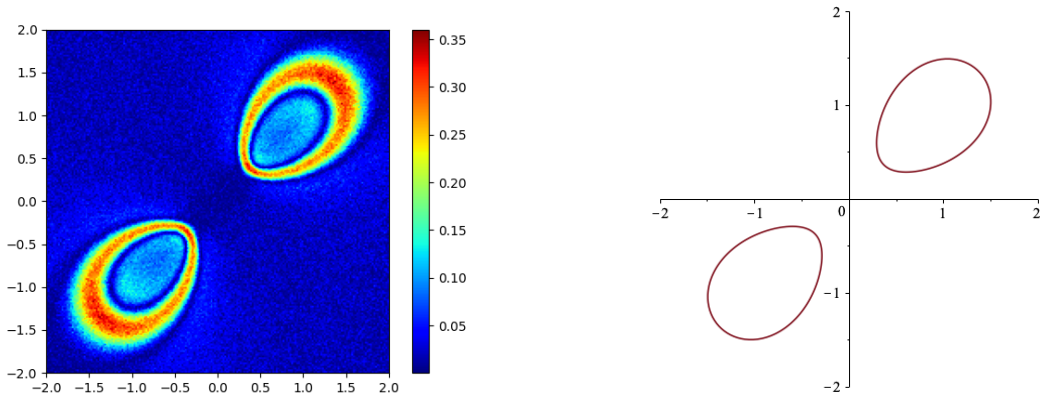


Figure 2.7: Reconstruction of the set $f_\lambda^{-1}(0)$ for $f_\lambda = xy - \lambda$ on S^2 as in Example 2.3.6, with $\lambda = \frac{1}{3}$, after stereographic projection. On the left we display the values of $|\mathcal{E}(m, R, k, N)|$ (see Equation (2.21)) for $R = \frac{1}{\sqrt{2}}$, $k = 100$, $N = 1000$, and $z = \pi_N(m)$ taken on a 200×200 grid discretizing the square $\{|\Re(z)|, |\Im(z)| \leq 2\}$. On the right we show the level set $f_\lambda^{-1}(0)$ for $\lambda = \frac{1}{3}$.

large enough $\bigcap_{s \in H^0(M, L^{\otimes k})} \{T_k s = 0\} = \emptyset$, so that Φ_{T_k} is defined everywhere on M . We can then study the pullback form $\Phi_{T_k}^* \omega_{\text{FS}}$, and obtain the following convergence result.

Theorem 2.3.7 ([ALF22, Theorem 1.2]). *Assume that 0 is a regular value of the principal symbol $f \in \mathcal{C}^\infty(M, \mathbb{R})$ of T_k . Then $\frac{1}{k} \Phi_{T_k}^* \omega_{\text{FS}}$ converges to ω in the sense of currents when $k \rightarrow +\infty$.*

We also have access to the error term in this convergence.

Theorem 2.3.8 ([ALF22, Theorem 1.3]). *Assume that 0 is a regular value of the principal symbol $f \in \mathcal{C}^\infty(M, \mathbb{R})$ of T_k . Then*

$$\Phi_{T_k}^* \omega_{\text{FS}} - k\omega \xrightarrow[k \rightarrow +\infty]{} i\partial\bar{\partial} \log f^2$$

in the sense of currents.

This hints at the fact that as long as $f^{-1}(0) \neq \emptyset$, we cannot expect more than the convergence in the sense of currents in Theorem 2.3.7, which is confirmed by the next statement. This is a striking difference with the case of $f = 1$ studied in [SZ99b] and recalled above, for which the convergence was in the \mathcal{C}^∞ topology.

Theorem 2.3.9 ([ALF22, Theorem 1.4]). *Assume that 0 is a regular value of the principal symbol $f \in \mathcal{C}^\infty(M, \mathbb{R})$ of T_k . Then $\frac{1}{k} \Phi_{T_k}^* \omega_{\text{FS}}$ converges to ω locally uniformly on $M \setminus f^{-1}(0)$ for the \mathcal{C}^∞ topology. However, $\frac{1}{k} \Phi_{T_k}^* \omega_{\text{FS}}$ does not converge to ω in the \mathcal{C}^0 topology (and even pointwise) on $f^{-1}(0)$. More precisely,*

$$\left(\frac{1}{k} \Phi_{T_k}^* \omega_{\text{FS}} \right)_m - \omega_m \xrightarrow[k \rightarrow +\infty]{} \begin{cases} 0 & \text{if } f(m) \neq 0, \\ \frac{4i(\partial f \wedge \bar{\partial} f)_m}{|df(m)|_\omega^2} & \text{if } f(m) = 0. \end{cases}$$

We also have results about this pullback form at scale $k^{-\frac{1}{2}}$.

Theorem 2.3.10 ([ALF22, Theorems 1.5 and 1.7]). *Assume that 0 is a regular value of the principal symbol $f \in \mathcal{C}^\infty(M, \mathbb{R})$ of T_k . Let φ be a smooth $(n-1, n-1)$ -form on M . Then*

$$\int_{B(m, \frac{R}{\sqrt{k}})} (\Phi_{T_k}^* \omega_{\text{FS}} - k\omega) \wedge \varphi = \begin{cases} k^{-n+1} \frac{2F_\varphi(m)}{|df(m)|_\omega^2} C_n(R) + O(k^{-n+\frac{1}{2}}) & \text{if } m \in f^{-1}(0), \\ k^{-n} R^{2n} L_\varphi(m) \text{Vol}(B_{\mathbb{R}^{2n}}(0, 1)) + O(k^{-n-\frac{1}{2}}) & \text{if } m \notin f^{-1}(0). \end{cases}$$

Here we have used the same notation as in Theorem 2.3.4, in particular the functions F_φ and L_φ and the constant $C_n(R)$ are the same as in this theorem.

An application of the Poincaré-Lelong formula gives the following generalization of Equation (2.19):

$$\mathbb{E}[Z_{T_k s_k}] = \frac{1}{2\pi} \Phi_{T_k}^* \omega_{\text{FS}}.$$

This allows us to derive Theorem 2.3.3 from Theorems 2.3.7 and 2.3.8, and Theorem 2.3.4 from Theorem 2.3.10.

To prove Theorems 2.3.7, 2.3.8, 2.3.9 and 2.3.10, we use the following generalization of Equation (2.17):

$$\Phi_{T_k}^* \omega_{\text{FS}} = k\omega + i\partial\bar{\partial} \log B_k, \quad (2.22)$$

where B_k is the restriction to the diagonal of $M \times M$ of the Schwartz kernel of the Berezin-Toeplitz operator $T_k^* T_k$. Then we need to expand B_k up to the subprincipal term:

$$\forall m \in M \quad B_k(m, m) = \left(\frac{k}{2\pi} \right)^n (f(m)^2 + k^{-1} b_1(m) + O(k^{-2})) \quad (2.23)$$

where the remainder $O(k^{-2})$ is uniform on M and

$$b_1 = 2f\Re(g) + 2f\Delta f + \frac{r}{2}f^2 + \frac{1}{2}|df|_\omega^2.$$

Here $g \in \mathcal{C}^\infty(M)$ is the contravariant subprincipal symbol of T_k , meaning that $T_k = \Pi_k(f + k^{-1}g) + O(k^{-2})$. Comparing Equations (2.22) and (2.23) morally gives Theorems 2.3.7 and 2.3.8; to obtain a rigorous proof, we need to be careful and are helped by the fact that when $f(m) = 0$, $b_1(m) = \frac{1}{2}|df(m)|_\omega^2$, which is positive by assumption. So $f^2 + k^{-1}b_1 > ck^{-1}$ for some constant $c > 0$ everywhere on M . This allows us to obtain that for every $\varphi \in \Omega^{n-1, n-1}(M)$,

$$\left| \int_M \partial\bar{\partial} \log B_k \wedge \varphi \right| = \|\partial\bar{\partial}\varphi\|_\infty O(\log k).$$

In particular Equation (2.22) gives the convergence in Theorem 2.3.9 in the case $f(m) \neq 0$. To obtain the result for the case $f(m) = 0$ in Theorem 2.3.9, we effectively compute $\partial\bar{\partial} \log B_k$ and finally obtain that if $f(m) = 0$, then

$$(\partial\bar{\partial} \log B_k)_m = \frac{4k(\partial f \wedge \bar{\partial} f)_m}{|df(m)|_\omega^2} + O(1).$$

Finally, still in view of Equation (2.22), to prove Theorem 2.3.10 we need to estimate the quantity

$$\int_{B(m, \frac{R}{\sqrt{k}})} i\partial\bar{\partial} \log B_k \wedge \varphi$$

where φ is a $(n-1, n-1)$ -form. We will outline the proof of this theorem, and for the sake of simplicity we will not talk about the remainders, which, in [ALF22], are carefully estimated in each of the steps below. A preliminary work on remainders leaves us with the task of estimating

$$\int_{B(m, \frac{R}{\sqrt{k}})} i\partial\bar{\partial} \log(f^2 + k^{-1}b_1) \wedge \varphi. \quad (2.24)$$

When $m \notin f^{-1}(0)$, the leading order in this quantity is $\int_{B(m, \frac{R}{\sqrt{k}})} \partial\bar{\partial} \log f^2 \wedge \varphi$, and the result follows from a Taylor expansion of the function L_φ around m . The case $m \in f^{-1}(0)$ is more involved. First, computing $\partial\bar{\partial} \log(f^2 + k^{-1}b_1)$ and checking carefully the remainders yields that the leading term in (2.24) reads

$$4i \int_{B(m, \frac{R}{\sqrt{k}})} \frac{k^{-1}|df|_\omega^2 - 2f^2}{(2f^2 + k^{-1}|df|_\omega^2)^2} \partial f \wedge \bar{\partial} f \wedge \varphi.$$

By working in normal coordinates at m , using Hadamard's lemma and performing a well-chosen change of variables, this can in turn be approximated by the quantity

$$\frac{4k^{-n+1}F_\varphi(m)}{|df(m)|_\omega^2} \int_{B_{\mathbb{R}^{2n}}(0, R)} \frac{1 - 2t_1^2}{(1 + 2t_1^2)^2} dt_1 \dots dt_{2n}.$$

The constant $C_n(R)$ from Equation (2.20) appears in the explicit computation of the integral involved in this quantity. This computation follows from suitable changes of variables which lead to expressing the integral in terms of hypergeometric functions, and then from using some of the identities relating these functions. The emergence of these hypergeometric functions gave the problem an arithmetic flavor that surprised us.

To conclude, note that Drewitz, Liu and Marinescu [DLM23] studied random holomorphic sections in a non-compact setting and in particular proved similar results as the above ones. In particular, they derived estimates similar to those of Theorem 2.3.10 in the case that $f \geq 0$ and $\Delta f(m) \neq 0$ whenever $f(m) = 0$. So they allow for one additional order of vanishing of f , which requires to look for the next term in the expansion of B_k from Equation (2.23). However in our results f can change sign.

2.4 Quantum propagation and trace formulas

We end this chapter by describing the contents of the manuscript [CLF20] and of the two papers in preparation [CLF23b, CLF23a], all joint with Laurent Charles. These manuscripts deal with a description, in the semiclassical limit, of the quantum propagator generated by a Berezin-Toeplitz operator [CLF20], and the applications of this description to obtain trace formulas for Berezin-Toeplitz operators: in [CLF23b], we obtain an asymptotic formula for the trace of the quantum propagator at a fixed time, and in [CLF23a], we derive the famous Gutzwiller trace formula. We focus on the precise description of the geometric quantities, especially the topological indices, involved in these formulas.

Concretely, let $T_{k,t}$ be a time-dependent Berezin-Toeplitz operator on $\mathcal{H}_k = H^0(M, L^{\otimes k} \otimes L')$ as in Section 2.1, with principal symbol H_t and with subprincipal symbol H_t^{sub} . Here we recall that (L, h) is a Hermitian holomorphic line bundle whose Chern connection ∇ has curvature $-i\omega$, and that (L', h') is an auxiliary Hermitian holomorphic line bundle. The quantum propagator of $T_{k,t}$ is the smooth path $(U_{k,t})_{t \in \mathbb{R}}$ of endomorphisms of \mathcal{H}_k obtained as the unique solution of the Schrödinger equation

$$\begin{cases} \frac{d}{dt} U_{k,t} = -ikT_{k,t}U_{k,t}, \\ U_{k,0} = \text{Id}. \end{cases} \quad (2.25)$$

In particular, if $T_{k,t} = T_k$ does not depend on the time t , then $U_{k,t} = \exp(-iktT_k)$. If $T_{k,t}$ is self-adjoint, then $U_{k,t}$ is unitary.

Now we assume that H_t is real-valued. The quantum propagator $U_{k,t}$ is the quantum analogue of the Hamiltonian flow ϕ_t of H_t , and is expected to reflect the properties of this flow in the semiclassical limit. In [CLF20] we precised this by describing the Schwartz kernel of $U_{k,t}$ (that we still call $U_{k,t}$) as a quantum state in $H^0(M \times \overline{M}, (L^{\otimes k} \otimes L') \boxtimes (\overline{L}^{\otimes k} \otimes \overline{L}'))$ supported on the Lagrangian submanifold

$$\Gamma_{\phi_t} = \{(\phi_t(x), x) \mid x \in M\} \subset M \times \overline{M} \quad (2.26)$$

given by the graph of ϕ_t . In fact the precise result is that $U_{k,t}$ is a Lagrangian state associated with this graph, see the discussion following Theorem 2.4.1. In [CLF23b] we obtain an asymptotic formula for the pairing of two such Lagrangian states under an assumption of clean intersection of the underlying Lagrangian submanifolds, see Theorem 2.4.5; applying this formula to $U_{k,t}$ and the Bergman kernel Π_k yields asymptotic estimates for the trace of the time-one propagator $\text{Tr}(U_{k,1})$ under some natural assumptions on the time-one flow ϕ_1 . In [CLF23a] we use the asymptotic description of $U_{k,t}$ from [CLF20] and an adaptation of the pairing formula from [CLF23b] to obtain the Gutzwiller trace formula: an asymptotic expansion of the trace $\text{Tr}(f(k(E - T_{k,t})))$ where $T_{k,t}$ is a Berezin-Toeplitz operator with time-independent principal symbol H , E is a regular value of H and f is a smooth function with smooth compactly supported Fourier transform. This formula relates the distribution of the eigenvalues of $T_{k,t}$ in a window of size $O(k^{-1})$ around E to the properties of the Hamiltonian flow of H in the level $H^{-1}(E)$.

2.4.1 Quantum propagators and smoothed spectral projectors

In order to describe the results of [CLF20] in more detail, we need to introduce some notation related to lifts of the Hamiltonian flow ϕ_t to L and to the canonical bundle $K \rightarrow M$.

First, for $x \in M$, let $\mathcal{T}_t^L(x) : L_x \rightarrow L_{\phi_t(x)}$ be the parallel transport associated with ∇ on L along the path $s \in [0, t] \mapsto \phi_s(x)$ (and define $\mathcal{T}_t^{L'}(x)$ similarly). We define the *prequantum lift* ϕ_t^L of ϕ to L as

$$\forall x \in M \quad \phi_t^L(x) = e^{-i \int_0^t H_r(\phi_r(x)) dr} \mathcal{T}_t^L(x) : L_x \rightarrow L_{\phi_t(x)}.$$

In particular, if $\gamma = (\phi_t(x))_{t \in [0, T]}$ is a contractible periodic orbit of the flow, then $\phi_T^L(x)$ is the operator of multiplication by $e^{i\mathcal{A}(x, T)}$ where \mathcal{A} is the usual action functional:

$$\mathcal{A}(x, T) = \int_{\mathbb{D}^2} u^* \omega - \int_0^T H_r(\phi_r(x)) dr \quad (2.27)$$

for any smooth $u : \mathbb{D}^2 \rightarrow M$ with $u(\partial \mathbb{D}^2) = \gamma$.

Second, the Hamiltonian flow can be lifted to the canonical bundle in two ways. On the one hand, for $x \in M$ we can consider the parallel transport $\mathcal{T}_t^K(x)$ in K along the trajectory $s \in [0, t] \mapsto \phi_s(x)$, with respect to the Chern connection ∇^K of K . On the other hand, we can consider the linear map $\mathcal{D}_t(x) : K_x \rightarrow K_{\phi_t(x)}$ defined by

$$\forall (\alpha, v) \in K_x \times \Lambda^n T_x M \quad \mathcal{D}_t(x)(\alpha)((T_x \phi_t)_* v) = \alpha(v). \quad (2.28)$$

Or equivalently

$$\forall (\alpha, v) \in K_x \times \Lambda^{n,0} T_x M \quad \mathcal{D}_t(x)(\alpha)((\det(T_x \phi_t)^{1,0})v) = \alpha(v)$$

where $(T_x \phi_t)^{1,0} : T_x^{1,0} M \rightarrow T_{\phi_t(x)}^{1,0} M$ is the first block in the matrix decomposition of

$$T_x \phi_t \otimes \text{Id}_{\mathbb{C}} : T_x M \otimes \mathbb{C} = T_x^{1,0} M \oplus T_x^{0,1} M \rightarrow T_{\phi_t(x)} M \otimes \mathbb{C} = T_{\phi_t(x)}^{1,0} M \oplus T_{\phi_t(x)}^{0,1} M.$$

Here $T^{1,0} M$ (respectively $T^{0,1} M$) is the holomorphic (respectively anti-holomorphic) tangent bundle of M . Let $\rho_t(x) \in \mathbb{C}$ be the complex number such that $\mathcal{D}_t(x) = \rho_t(x) \mathcal{T}_t^K(x)$.

Theorem 2.4.1. *Let $U_{k,t}$ be the quantum propagator of a time-dependent Berezin-Toeplitz operator $T_{k,t}$ with real-valued principal symbol H_t . If $x, y \in M$ and $t \in \mathbb{R}$ are such that $y \neq \phi_t(x)$, then $U_{k,t}(y, x) = O(k^{-\infty})$. Moreover, for any $t \in \mathbb{R}$ and $x \in M$,*

$$U_{k,t}(\phi_t(x), x) = \left(\frac{k}{2\pi}\right)^n \rho_t(x)^{\frac{1}{2}} e^{-i \int_0^t H_r^{\text{sub}}(\phi_r(x)) dr} \left[\phi_t^L(x)\right]^{\otimes k} \otimes \mathcal{T}_t^{L'}(x) + O(k^{n-1}) \quad (2.29)$$

where $\rho_t^{\frac{1}{2}}$ is the continuous square root of the function ρ_t which is equal to 1 at $t = 0$.

In this statement we view $U_{k,t}(y, x)$ as a map from $L_x^{\otimes k} \otimes L'_x$ to $L_y^{\otimes k} \otimes L'_y$, see Section 2.1. In fact, we proved that $U_{k,t}(\phi_t(x), x)$ has a complete asymptotic expansion in integral powers of k^{-1} , and we also gave a uniform description of $U_{k,t}(x, y)$ with respect to (x, y, t) on compact regions, see [CLF20, Theorem 4.2]. More precisely, we showed that the Schwartz kernel $U_{k,t}$ (multiplied by $(\frac{2\pi}{k})^{\frac{n}{2}}$) is a Lagrangian state family in the sense of [CLF20, Section 2.1], generalizing the definition of Lagrangian state from [Cha03b].

If Γ is a closed Lagrangian submanifold of M and $s \in \mathcal{C}^\infty(\Gamma, L)$ is a flat unitary section, a *Lagrangian state* associated with (Γ, s) and with principal symbol $\sigma \in \mathcal{C}^\infty(\Gamma, L')$ is a sequence $\Psi_k \in \mathcal{H}_k$ of the form

$$\Psi_k(x) = \left(\frac{k}{2\pi}\right)^{\frac{n}{4}} F^{\otimes k}(x) \otimes a(x, k) + O(k^{-\infty})$$

where

- $F \in \mathcal{C}^\infty(M, L)$ is such that $\bar{\partial} F$ vanishes to infinite order along Γ ;
- $F|_\Gamma = s$ and $|F(x)| < 1$ for $x \notin \Gamma$;
- $a(\cdot, k)$ is a sequence of elements of $\mathcal{C}^\infty(M, L')$ with an asymptotic expansion $a(\cdot, k) = \sum_{\ell \geq 0} k^{-\ell} a_\ell$ for the \mathcal{C}^∞ topology, where the sections a_ℓ are such that $\bar{\partial} a_\ell$ vanishes to infinite order along Γ , and $a_0|_\Gamma = \sigma$;

- $|\Psi_k| = O(k^N)$ uniformly on M for some integer N .

For instance, it is proved in [Cha03a] that the Bergman kernel Π_k (multiplied by $(\frac{2\pi}{k})^{\frac{n}{2}}$) is a Lagrangian state in $H^0(M \times \overline{M}, (L^{\otimes k} \otimes L') \boxtimes (\overline{L}^{\otimes k} \otimes \overline{L}'))$ associated with the diagonal in $M \times \overline{M}$ equipped with $s = 1$ and with principal symbol $\sigma = 1$, see Equation (2.3) and the discussion surrounding it. The normalization $(\frac{k}{2\pi})^{\frac{n}{4}}$ is here so that the norm of a Lagrangian state is a $O(1)$, see [Cha03b, Proposition 2.6]. Roughly, a *Lagrangian state family* is a smooth one-parameter family of Lagrangian states associated with a smooth one-parameter family of Lagrangian submanifolds.

Assume that M has a half-form bundle δ (see Section 2.1) and let L_1 be the holomorphic line bundle such that $L' = L_1 \otimes \delta$. First, in this case we can define $\mathcal{D}_t(x)^{\frac{1}{2}} : \delta_x \rightarrow \delta_{\phi_t(x)}$ as the continuous square root of $\mathcal{D}_t(x)$ equal to the identity at $t = 0$. Second, L_1 inherits a Hermitian metric from the metrics of L' and δ , and as above we consider the parallel transport $\mathcal{T}_t^{L_1}(x) : (L_1)_x \rightarrow (L_1)_{\phi_t(x)}$ with respect to the corresponding Chern connection. Then Equation (2.29) becomes

$$U_{k,t}(\phi_t(x), x) = \left(\frac{k}{2\pi}\right)^n e^{-i \int_0^t H_r^{\text{sub}}(\phi_r(x)) \, dr} \left[\phi_t^L(x)\right]^{\otimes k} \otimes \mathcal{T}_t^{L_1}(x) \otimes [\mathcal{D}_t(x)]^{\frac{1}{2}} + O(k^{n-1}) \quad (2.30)$$

Note that in fact, to obtain this result we only need to define the half-form bundle δ over the trajectory $s \in [0, t] \mapsto \phi_s(x)$, which is always possible.

Example 2.4.2. We use once again our favorite example of $(M, \omega) = (S^2, -\frac{1}{2}\omega_{S^2})$ described in Example 2.1.1. We consider the quantum propagator $U_{k,t}$ associated with the Berezin-Toeplitz operator \hat{Z}_k on \mathcal{H}_k , see Equation (2.8). The Schwartz kernel of $U_{k,t}$ can be computed thanks to the general formula

$$U_{k,t}(w, v) = \sum_{\ell=0}^{k-1} (U_{k,t} e_{\ell,k})(w) \otimes \overline{e_{\ell,k}(v)}$$

where we use the local coordinates on the chart U_2 introduced in Example 2.1.1, and with $(e_{\ell,k})_{0 \leq \ell \leq k-1}$ the orthonormal basis from Equation (2.4), which in this trivialization reads

$$e_{\ell,k}(w) = \sqrt{\frac{k \binom{k-1}{\ell}}{2\pi}} w^\ell s^{\otimes k}(z), \quad 0 \leq \ell \leq k-1,$$

where s is the local section of L dual to the section τ defined in Equation (2.5). Since \hat{Z}_k acts diagonally in this basis, with eigenvalues $\frac{2\ell+1-k}{k}$, $0 \leq \ell \leq k-1$, we obtain that

$$U_{k,t}(w, v) = \sum_{\ell=0}^{k-1} e^{-it(2\ell+1-k)} e_{\ell,k}(w) \otimes \overline{e_{\ell,k}(v)},$$

which can be rearranged as

$$U_{k,t}(w, v) = \frac{k}{2\pi} e^{i(k-1)t} \sum_{\ell=0}^{k-1} \binom{k-1}{\ell} (e^{-2it} w \bar{v})^\ell s^{\otimes k-1}(w) \otimes \overline{s^{\otimes k-1}(v)}$$

and finally yields

$$U_{k,t}(w, v) = \frac{k}{2\pi} e^{i(k-1)t} (1 + e^{-2it} w \bar{v})^{k-1} s^{\otimes k-1}(w) \otimes \overline{s^{\otimes k-1}(v)}.$$

In particular,

$$|U_{k,t}(w, v)| = \frac{k}{2\pi} \left| \frac{1 + e^{-2it} w \bar{v}}{\sqrt{(1 + |w|^2)(1 + |v|^2)}} \right|^{k-1}$$

is a $O(k^{-\infty})$ whenever $w \neq e^{2it}v = \phi_t(v)$ (recall the $\frac{1}{2}$ in the symplectic form). Furthermore,

$$U_k(\phi_t(v), v) = \frac{k}{2\pi} e^{i(k-1)t} (1 + |v|^2)^{k-1} s^{\otimes k-1}(\phi_t(v)) \otimes \overline{s^{\otimes k-1}(v)}. \quad (2.31)$$

Since there exists a global half-form bundle $\delta = \mathcal{O}(-1)$, we will compare this with Equation (2.30). Recall that the principal symbol of T_k is $H = z = \frac{|w|^2 - 1}{1 + |w|^2}$ and that its subprincipal symbol vanishes. In particular Equation (2.30) yields

$$U_k(\phi_t(v), v) \sim_{k \rightarrow +\infty} \frac{k}{2\pi} (\phi_t^L(v))^{\otimes k} \otimes \mathcal{D}_t(v)^{\frac{1}{2}} \quad (2.32)$$

with

$$\phi_t^L(v)s(v) = e^{-i \int_0^t H(\phi_r(v)) dr} \mathcal{T}_t^L(v)s(v) = e^{-itH(v) + i \int_0^t \alpha_{\phi_r(v)}(X_H(\phi_r(v))) dr} s(\phi_t(v))$$

where X_H is the Hamiltonian vector field of H and α is any primitive of ω_{FS} on U_2 , for instance $\alpha = \frac{iwd\bar{w}}{1+|w|^2}$. A straightforward computation yields

$$\int_0^t \alpha_{\phi_r(v)}(X_H(\phi_r(v))) dr = \frac{2t|v|^2}{1 + |v|^2}$$

so $\phi_t^L(v)s(v) = e^{it} s(\phi_t(v))$. Moreover, the flow ϕ_t preserves the complex structure so

$$\mathcal{D}_t(v)^{\frac{1}{2}} \tau(v) = \det_{\mathbb{C}}(T_v \phi_t)^{-\frac{1}{2}} \tau(\phi_t(v)) = e^{-it} \tau(\phi_t(v))$$

(recall that here the square root is chosen to be continuous in t and equal to 1 at $t = 0$). Consequently, Equation (2.32) gives

$$U_k(\phi_t(v), v)(s^{\otimes k}(v) \otimes \tau(v)) \sim_{k \rightarrow +\infty} \frac{k}{2\pi} e^{i(k-1)t} s^{\otimes k}(\phi_t(v)) \otimes \tau(\phi_t(v)) = e^{i(k-1)t} s^{\otimes k-1}(\phi_t(v))$$

and this agrees with Equation (2.31) which gives

$$U_k(\phi_t(v), v)(s^{\otimes k}(v) \otimes \tau(v)) = \frac{k}{2\pi} e^{i(k-1)t} \underbrace{h_1(s(v), \tau(v))}_{=1} s^{\otimes k-1}(\phi_t(v))$$

since $h(s(v), s(v)) = (1 + |v|^2)^{-1}$.

This example is perhaps too simple since the Hamiltonian flow of H preserves the complex structure. In [CLF20, Appendix A], we verify the validity of our results numerically on another example on the torus \mathbb{T}^2 , in which the Hamiltonian flow of the principal symbol of T_k does not preserve the complex structure.

In [CLF20] we also obtained an asymptotic description of the Schwartz kernel of the smoothed spectral projector $f(k(E - T_k))$, where T_k is a time-independent self-adjoint Berezin-Toeplitz operator with principal symbol H and subprincipal symbol H^{sub} , f is a smooth function with a smooth compactly supported Fourier transform and $E \in \mathbb{R}$ is a regular value of H .

We introduce another lift \mathcal{D}'_t of the Hamiltonian flow ϕ_t of H to the canonical bundle as follows. Let E be a regular value of H and let $x \in H^{-1}(E)$. Then $T_x \phi_t(X_H(x)) = X_H(\phi_t(x))$ so $T_x \phi_t$ descends to a symplectic map

$$T_x H^{-1}(E) / \text{Span}(X_H(x)) \xrightarrow{T_x \phi_t} T_{\phi_t(x)} H^{-1}(E) / \text{Span}(X_H(\phi_t(x))).$$

Moreover, if $F_x = \text{Span}(X_H(x), j_x X_H(x))$ (where we recall that j is the complex structure on M), then its symplectic orthogonal $G_x = F_x^\perp$ is a complement of $\text{Span}(X_H(x))$ in $T_x H^{-1}(E)$ so it is isomorphic to $T_x H^{-1}(E) / \text{Span}(X_H(x))$. Moreover, since F_x and G_x are symplectic

subspaces preserved by j_x , the canonical line K_x decomposes as the product of their canonical lines: $K_x \simeq K(F_x) \otimes K(G_x)$. We set

$$\mathcal{D}'_t(x) = A_x \otimes B_x : K_x \simeq K(F_x) \otimes K(G_x) \rightarrow K_{\phi_t(x)} \simeq K(F_{\phi_t(x)}) \otimes K(G_{\phi_t(x)})$$

where A_x and B_x are two maps that we define now. First, let $\lambda \in K(F_x)$ and $\kappa \in K(F_{\phi_t(x)})$ be such that $\lambda(X_H(x)) = 1 = \kappa(X_H(\phi_t(x)))$, and let

$$A_x : K(F_x) \rightarrow K(F_{\phi_t(x)}), \quad \lambda \mapsto \frac{2}{|X_H(x)|^2} \kappa$$

where $|\cdot|$ is the pointwise norm associated with the Kähler metric. Second, let ψ be the linear symplectomorphism given by

$$\psi : G_x \simeq T_x H^{-1}(E) / \text{Span}(X_H(x)) \xrightarrow{T_x \phi_t} T_{\phi_t(x)} H^{-1}(E) / \text{Span}(X_H(\phi_t(x))) \simeq G_{\phi_t(x)}$$

and define $B_x : K(G_x) \rightarrow K(G_{\phi_t(x)})$ by the property that

$$\forall (\alpha, v) \in K(G_x) \times \Lambda^n G_x \quad B_x(\alpha)(\psi_* v) = \alpha(v)$$

similarly as in Equation (2.28).

Finally, let $\rho'_t(x)$ be the complex number such that $\mathcal{D}'_t(x) = \rho'_t(x) \mathcal{T}_t^K(x)$. Note that by definition, $\rho'_0(x) = \frac{2}{|X_H(x)|^2}$. Note also that in the particular case where $T_x \phi_t$ sends $j_x X_H(x)$ to $j_{\phi_t(x)} X_H(\phi_t(x))$, then $\mathcal{D}'_t(x) = \frac{2}{|X_H(x)|^2} \mathcal{D}_t(x)$ so $\rho'_t(x) = \frac{2}{|X_H(x)|^2} \rho_t(x)$.

Consider also the Lagrangian immersion

$$\iota_E : \mathbb{R} \times H^{-1}(E) \rightarrow M \times \overline{M}, \quad (t, x) \mapsto (\phi_t(x), x).$$

Note that it is indeed only an immersion in general because of periodic trajectories of the Hamiltonian flow.

Theorem 2.4.3 ([CLF20, Theorem 1.2]). *Let T_k be a time-independent Berezin-Toeplitz operator with principal symbol H and subprincipal symbol H^{sub} , let E be a regular value of H and let f be a smooth function with smooth compactly supported Fourier transform. For any $x, y \in H^{-1}(E)$,*

$$f(k(E - T_k))(y, x) = \left(\frac{k}{2\pi}\right)^n k^{-\frac{1}{2}} \sum_{\substack{t \in \text{supp}(\hat{f}) \\ \phi_t(x) = y}} \hat{f}(t) \rho'_t(x)^{\frac{1}{2}} e^{-i \int_0^t H^{\text{sub}}(\phi_r(x)) \, dr} \mathcal{T}_t^L(x)^{\otimes k} \otimes \mathcal{T}_t^{L'}(x) + O(k^{n-\frac{3}{2}})$$

where $\rho'_t(x)^{\frac{1}{2}}$ is the continuous square root of $\rho'_t(x)$ equal to $\frac{\sqrt{2}}{|X_H(x)|}$ at $t = 0$. Furthermore, for any $(y, x) \in M \times \overline{M}$ not belonging to $\iota_E(\text{supp}(\hat{f}) \times H^{-1}(E))$, we have $f(k(E - T_k))(y, x) = O(k^{-\infty})$.

Here our convention for the Fourier transform is

$$\forall t \in \mathbb{R} \quad \hat{f}(t) = \frac{1}{\sqrt{2\pi}} \int_{\mathbb{R}} e^{-itE} f(E) \, dE.$$

In fact this statement slightly differs from [CLF20, Theorem 1.2] because in the latter there was a factor $\sqrt{2\pi}$ that should not have appeared. And as before, the real statement (see [CLF20, Theorem 6.3]) is that $\left(\frac{2\pi}{k}\right)^{\frac{n}{2}} k^{-\frac{1}{2}} f(k(E - T_k))$ is a Lagrangian state; in fact, the Lagrangian it is associated with is the image of ι_E , so it is only an immersed Lagrangian state; but this is too technical for the present discussion, see [CLF20, Section 5.2] for details.

As for Theorem 2.4.1 above, the statement of Theorem 2.4.3 simplifies in the presence of a half-form bundle $\delta \rightarrow M$. As in the discussion following Theorem 2.4.1, by writing $L' = L_1 \otimes \delta$ we obtain in this case that

$$f(k(E - T_k))(y, x) = \left(\frac{k}{2\pi}\right)^n k^{-\frac{1}{2}} \sum_{\substack{t \in \text{supp} \hat{f} \\ \phi_t(x) = y}} \hat{f}(t) e^{-i \int_0^t H^{\text{sub}}(\phi_r(x)) \, dr} \mathcal{T}_t^L(x)^{\otimes k} \otimes \mathcal{T}_t^{L_1}(x) \otimes \mathcal{D}'_t(x)^{\frac{1}{2}} + O(k^{n-\frac{3}{2}}) \quad (2.33)$$

where $\mathcal{D}'_t(x)^{\frac{1}{2}} : \delta_x \rightarrow \delta_{\phi_t(x)}$ is continuous and equal to $\sqrt{2}|X_x|^{-1} \text{Id}_{\delta_x}$ at $t = 0$.

Example 2.4.4. In this example, we will illustrate at the same time the statement of Theorem 2.4.3 and its proof. We work in the exact same context as in Example 2.4.2, and with the same notation. Let E be a regular value of H , and let $S_k = f(k(E - T_k))$. Let $v, w \in H^{-1}(E)$; then

$$S_k(w, v) = \frac{k}{2\pi} \left(\sum_{\ell=0}^{k-1} f(kE - (2\ell + 1 - k)) \binom{k-1}{\ell} (w\bar{v})^\ell \right) s^{\otimes k-1}(w) \otimes \overline{s^{\otimes k-1}(v)}.$$

By writing f as the inverse Fourier transform of \hat{f} , this gives

$$S_k(w, v) = \frac{k}{(2\pi)^{\frac{3}{2}}} \left(\int_{\mathbb{R}} e^{iu(k(1+E)-1)} \hat{f}(u) \left(\sum_{\ell=0}^{k-1} \binom{k-1}{\ell} (e^{-2iu} w\bar{v})^\ell \right) du \right) s^{\otimes k-1}(w) \otimes \overline{s^{\otimes k-1}(v)},$$

which yields

$$S_k(w, v) = \frac{k}{(2\pi)^{\frac{3}{2}}} \left(\int_{\mathbb{R}} e^{iu(k(1+E)-1)} \hat{f}(u) (1 + e^{-2iu} w\bar{v})^{k-1} du \right) s^{\otimes k-1}(w) \otimes \overline{s^{\otimes k-1}(v)}.$$

We see as in Example 2.4.2 that the contributions coming from times t such that $w \neq e^{2it}v = \phi_u(v)$ are $O(k^{-\infty})$, so it suffices to integrate on neighborhoods of the points $t \in \text{supp}(\hat{f})$ for which $w = e^{2it}v$. In a sufficiently small neighborhood U of such a point t , the contribution to $S_k(w, v)$ is $I_k s^{\otimes k-1}(w) \otimes \overline{s^{\otimes k-1}(v)}$ where

$$I_k = \frac{k}{(2\pi)^{\frac{3}{2}}} \int_U e^{ik\varphi(u)} \hat{f}(u) \frac{e^{-iu}}{1 + e^{-2iu} w\bar{v}} du \quad \text{with } \varphi(u) = 1 + E + \log(1 + e^{-2iu} w\bar{v}).$$

The only critical point of the phase function φ is t , and $\varphi''(t) = \frac{4|v|^2}{(1+|v|^2)^2} > 0$. Therefore the stationary phase lemma [Hör83, Theorem 7.7.5] gives

$$I_k = \frac{\sqrt{k}}{2\pi} e^{ik(1+E)t} \frac{(1 + |v|^2)^k}{2|v|} e^{-it} \hat{f}(t) + O(k^{-\frac{1}{2}})$$

so finally

$$S_k(w, v) = \frac{\sqrt{k}}{2\pi} \sum_{\substack{t \in \text{supp} \hat{f} \\ \phi_t(v) = w}} e^{ik(1+E)t} \frac{(1 + |v|^2)^k}{2|v|} e^{-it} \hat{f}(t) s^{\otimes k-1}(w) \otimes \overline{s^{\otimes k-1}(v)} + O(k^{-\frac{1}{2}}). \quad (2.34)$$

We are working with a half-form bundle, so we will compare this with the estimate (2.33). In Example 2.4.2, we already computed

$$\mathcal{T}_t^L(v) s(v) = e^{\frac{2it|v|^2}{1+|v|^2}} s(\phi_t(v)) = e^{it(1+E)} s(\phi_t(v)).$$

For the second equality, we have used that $v \in H^{-1}(E)$ so $|v|^2 = \frac{1+E}{1-E}$. Since in this example the tangent map to the flow and j commute, the discussion before Theorem 2.4.3 yields

$$\mathcal{D}'_t(v)^{\frac{1}{2}} \tau(v) = \frac{\sqrt{2}}{|X_H(v)|} \mathcal{D}_t(v)^{\frac{1}{2}} \tau(v) = \frac{1 + |v|^2}{2|v|} e^{-it} \tau(\phi_t(v)).$$

Here we have used the computation of $\mathcal{D}_t(v)^{\frac{1}{2}}$ in Example 2.4.2. Therefore, Equation (2.33) yields

$$S_k(w, v) (s^{\otimes k}(v) \otimes \tau(v)) = \frac{\sqrt{k}}{2\pi} \sum_{\substack{t \in \text{supp} \hat{f} \\ \phi_t(v) = w}} \hat{f}(t) e^{ikt(1+E)} \frac{1 + |v|^2}{2|v|} e^{-it} s^{\otimes k-1}(v) + O(k^{-\frac{1}{2}})$$

which is the same as what Equation (2.34) gives since $h(s, s) = (1 + |v|^2)^{-1}$.

Let us give a few words about the proofs. To prove Theorem 2.4.1 (and its more general formulation in [CLF20, Theorem 4.2]), we first showed in [CLF20, Theorem 2.4] that the solution of the Schrödinger equation

$$-ik^{-1}\partial_t\Psi_k + T_{k,t}\Psi_k = 0$$

with initial data a Lagrangian state associated with the Lagrangian submanifold Γ_0 is a Lagrangian state family associated with the image of Γ_0 under the Hamiltonian flow ϕ_t , and the delicate and technical part is then to compute the principal symbol of this Lagrangian state family [CLF20, Theorem 2.5]. These results come from a careful application of the stationary phase lemma, with a close inspection of the coefficients of the expansion that it yields. Then the idea is simply to view Equation (2.25) in this context, by interpreting the product $T_{k,t}U_{k,t}$ as the action of the Berezin-Toeplitz operator $T_{k,t} \otimes \text{Id}$ on $U_{k,t}$, and recalling that $U_{k,0} = \Pi_k$ is a Lagrangian state (up to a multiplicative factor).

Then Theorem 2.4.3 results from the fact that

$$f(k(E - T_k)) = k^{-\frac{1}{2}}\mathcal{F}_k^{-1}(\hat{f}(t)U_{k,t})(E)$$

where \mathcal{F}_k is the semiclassical Fourier transform:

$$\mathcal{F}_k(f)(t) = \left(\frac{k}{2\pi}\right)^{\frac{1}{2}} \int_{\mathbb{R}} e^{-iktE} f(E) dE, \quad \mathcal{F}_k^{-1}(g)(E) = \left(\frac{k}{2\pi}\right)^{\frac{1}{2}} \int_{\mathbb{R}} e^{iktE} g(t) dt.$$

Indeed, we proved in [CLF20, Theorem 5.4] that if Ψ_k is a Lagrangian state family, then $\mathcal{F}_k^{-1}(\Psi_k)(E)$ is a Lagrangian state, and it suffices to apply this to $\hat{f}(t)U_{k,t}$ which is, thanks to [CLF20, Theorem 4.2] and up to a multiplicative factor, a Lagrangian state family. Again, we skip the details about the computation of the principal symbol of this Lagrangian state.

The study of the quantum propagator and the smoothed spectral projectors of a Berezin-Toeplitz operators is not new [BPU98, ZZ18, Ioo20]. One of the main novelties of our results is the explicit, precise, and simple computation of the invariants $\rho_t(x)$ and $\rho'_t(x)$ from Theorems 2.4.1 and 2.4.3, which did not seem to exist in the literature, even in the recent [ZZ18, Ioo20]. Moreover our direct approach of seeing the quantum propagator as a Lagrangian state evolved under Schrödinger's equation leads to relatively simple computations. Further explanations are given in [CLF20, Section 1.4].

2.4.2 Traces of quantum propagators

In [CLF23b], Theorem 2.4.1 allows us to estimate the trace $\text{Tr}(U_{k,1})$ of the time-one quantum propagator, in the semiclassical limit, thanks to a pairing formula for Lagrangian states that we describe now. Let Ψ_k, Ψ'_k be two Lagrangian states associated with (Γ, s) and (Γ', s') respectively and with respective principal symbols $\sigma \in \mathcal{C}^\infty(\Gamma, L')$ and $\sigma' \in \mathcal{C}^\infty(\Gamma', L')$ (see the discussion after Theorem 2.4.1). Assume that the Lagrangian submanifolds Γ and Γ' of M intersect cleanly in the sense that

- $\Gamma \cap \Gamma'$ is a finite (disjoint) union of connected submanifolds $\mathcal{C}_1, \dots, \mathcal{C}_m$ of M ;
- for every $\ell \in \{1, \dots, m\}$ and every $x \in \mathcal{C}_\ell$, $T_x\mathcal{C}_\ell = T_x\Gamma \cap T_x\Gamma'$.

Note in particular that if Γ and Γ' intersect transversally at a finite number of points, they intersect cleanly.

Theorem 2.4.5 ([CLF23b]). *There exist natural densities $\delta_{\mathcal{C}_\ell}$ on each \mathcal{C}_ℓ such that*

$$\langle \Psi_k, \Psi'_k \rangle_k = \sum_{\ell=1}^m \left(\frac{2\pi}{k}\right)^{\frac{n-d_\ell}{2}} \int_{\mathcal{C}_\ell} h(s, s')^k h'(\sigma, \sigma') \delta_{\mathcal{C}_\ell} + O\left(k^{\frac{d_\ell-n}{2}-1}\right)$$

where $d_\ell = \dim \mathcal{C}_\ell$. Recall that h and h' are the Hermitian metrics on L and L' , respectively.

This result extends [Cha10, Theorem 6.1] in which the two Lagrangians intersect transversally. We will not describe the densities $\delta_{\mathcal{C}_1}, \dots, \delta_{\mathcal{C}_m}$ in all generality here, but more details will appear in [CLF23b].

The above results, in particular Theorem 2.4.1, can be combined with Theorem 2.4.5 to estimate the trace $\text{Tr}(U_{k,1})$ of the time-one propagator of a time-dependent Berezin-Toeplitz operator $T_{k,t}$. Indeed, we may write $\text{Tr}(U_{k,1}) = \langle U_{k,1}, \Pi_k \rangle_k$ where $\langle \cdot, \cdot \rangle_k$ is the inner product on $H^0(M \times \overline{M}, (L^{\otimes k} \otimes L') \boxtimes (\overline{L}^{\otimes k} \otimes \overline{L}'))$, and recall that $(\frac{2\pi}{k})^{\frac{n}{2}} U_{k,1}$ is a Lagrangian state in this Hilbert space associated with the Lagrangian submanifold Γ_{ϕ_1} of $M \times \overline{M}$ defined in Equation (2.26), and that $(\frac{2\pi}{k})^{\frac{n}{2}} \Pi_k$ is also a Lagrangian state, see the discussion after Theorem 2.4.1. One of the quantities involved in the estimate that we obtain is the action functional \mathcal{A} from Equation (2.27), but the other ones are more delicate to define.

First, if g is a linear symplectomorphism on a symplectic vector space V , there is a natural way to define a density δ_g on $N = \ker(g - \text{Id})$, such that if $N = \{0\}$, then $\delta_g = |\det(g - \text{Id})|^{-\frac{1}{2}}$ and if $N = V$, then δ_g is the Liouville density; more details will be given in [CLF23b], and these densities are similar to the ones discussed in [DG75, Section 4]. In particular, if the graph of ϕ_1 and the diagonal of $M \times \overline{M}$ intersect cleanly, the fixed point set M^{ϕ_1} of ϕ_1 is a finite union of connected submanifolds and if \mathcal{C} is one of these components, then for every $x \in \mathcal{C}$,

$$T_x \mathcal{C} = \{X \in T_x M \mid (T_x \phi_1)(X) = X\} = \ker(T_x \phi_1 - \text{Id}).$$

Consequently, \mathcal{C} can be endowed with the density $\delta_{\phi_1, \mathcal{C}}$ which coincides at $x \in \mathcal{C}$ with the density $\delta_{T_x \phi_1}$ on $T_x \mathcal{C}$.

Second, let $x \in M$ be a fixed point of ϕ_1 and let $\gamma : [0, 1] \rightarrow M, t \mapsto \phi_t(x)$ be the corresponding closed trajectory of ϕ_t . Let s be any frame of $\gamma^* L$ such that $s(0) = s(1)$, and let f be the function such that $\nabla s = -if(t)dt \otimes s$. The holonomy

$$h(L, x) = \int_0^1 f(r) dr \quad (2.35)$$

of γ in L is well-defined modulo $2\pi\mathbb{Z}$. The holonomy $h(L', x)$ of γ in L' is defined similarly. We also define the action

$$\mathcal{A}(L, x) = h(L, x) - \int_0^1 H_r(\phi_r(x)) dr,$$

which coincides with the action $\mathcal{A}(x, 1)$ from Equation (2.27) if the orbit is contractible.

Third, let $a(t) : T_{\gamma(t)} M \rightarrow \mathbb{R}^{2n}$ be a trivialization of $\gamma^* TM$ by symplectomorphisms, so that

$$g_t = a(t)(T_{\gamma(0)} \phi_t) a(0)^{-1}, \quad t \in [0, 1]$$

is a path of linear symplectomorphisms of \mathbb{R}^{2n} . Let $\mu_{\text{RS}}(\text{graph}(g_t), \mathcal{D})$ be the Robbin-Salamon index associated with this path relative and to the diagonal \mathcal{D} of $M \times \overline{M}$, as defined in [RS93]. This depends on the choice of the trivialization a , but we will now make some particular choices and add a correction term to obtain a well-defined invariant $I(x)$. Let $(\alpha_\ell, \beta_\ell)_{1 \leq \ell \leq n}$ be an orthosymplectic frame of $\gamma^* TM$, meaning that

$$\forall \ell, m \in \{1, \dots, n\} \quad \beta_\ell = j\alpha_\ell, \quad \omega(\alpha_\ell, \alpha_m) = \omega(\beta_\ell, \beta_m) = 0, \quad \omega(\alpha_\ell, \beta_m) = \delta_{\ell, m},$$

and such that for every $\ell \in \{1, \dots, n\}$, $\alpha_\ell(1) = \alpha_\ell(0)$ and $\beta_\ell(1) = \beta_\ell(0)$. Let s be the frame of $\gamma^* K$ such that $s(\alpha_1 \wedge \dots \wedge \alpha_n) = 1$ and write $\nabla^K s = -if_K dt \otimes s$ for some function f_K , where we recall that ∇^K is the Chern connection of the canonical line bundle $K \rightarrow M$. If we compute $\mu_{\text{RS}}(\text{graph}(g_t), \mathcal{D})$ using the trivialization a of $\gamma^* TM$ corresponding to the orthosymplectic frame $(\alpha_\ell, \beta_\ell)_{1 \leq \ell \leq n}$, then the quantity

$$I(x) = \frac{1}{2} \int_0^1 f_K(t) dt + \frac{\pi}{2} \mu_{\text{RS}}(\text{graph}(g_t), \mathcal{D})$$

does not depend on this choice of orthosymplectic frame.

We bundle these ingredients into the quantity

$$\theta(x) = - \int_0^1 H_r^{\text{sub}}(\phi_r(x)) dr + h(L', x) - I(x).$$

If M has a half-form bundle δ , by setting $L' = \delta$ these quantities become simpler. Indeed, in this case $h(L', x) - I(x) = -\frac{\pi}{2}m$ where m is a half-integer, well-defined modulo 4, which coincides with $\mu_{\text{RS}}(\text{graph}(g_t), \mathcal{D})$ modulo 4 if we define g_t as above by using any trivialization associated with an orthosymplectic frame $(\alpha_\ell, \beta_\ell)_{1 \leq \ell \leq n}$ such that the corresponding frame s of γ^*K has a square root $t \in \mathcal{C}^\infty([0, 1], \delta)$ with $t(0) = t(1)$. And in fact, as before, we do not need a global half-form bundle, as it suffices to introduce one over the trajectory γ .

Theorem 2.4.6 ([CLF23b]). *Assume that the graph of ϕ_1 and the diagonal of $M \times \overline{M}$ intersect cleanly. Then*

$$\text{Tr}(U_{k,1}) = \sum_{\mathcal{C} \text{ component of } M^{\phi_1}} \left(\frac{k}{2\pi} \right)^{\frac{\dim \mathcal{C}}{2}} e^{ik\mathcal{A}(\mathcal{C})} \int_{\mathcal{C}} e^{i\theta} \delta_{\phi_1, \mathcal{C}} + O(k^{\frac{\dim \mathcal{C}}{2}-1})$$

where $\mathcal{A}(\mathcal{C})$ is the value of $\mathcal{A}(L, x)$ for any $x \in \mathcal{C}$.

This theorem has a simpler statement when ϕ_1 is non-degenerate, which means that for each fixed point $x \in M^{\phi_1}$, 1 is not an eigenvalue of $T_x \phi_1$ (in which case the clean intersection assumption is automatically satisfied).

Theorem 2.4.7. *Assume that ϕ_1 is non-degenerate. Then*

$$\text{Tr}(U_{k,1}) = \sum_{x \in M^{\phi_1}} \frac{e^{ik\mathcal{A}(x) + i\theta(x)}}{|\det(T_x \phi_1 - \text{Id})|^{\frac{1}{2}}} + O(k^{-1}).$$

Example 2.4.8. Let $\alpha \notin \pi\mathbb{Z}$. We work in the setting of Example 2.4.2 and consider $U_{k,1} = e^{-ik\alpha \hat{Z}_k}$, the time-one propagator of the operator $\alpha \hat{Z}_k$ with \hat{Z}_k is as in Equation (2.8), which has principal symbol $H = \alpha z$ on $(S^2, -\frac{1}{2}\omega_{S^2})$ and vanishing subprincipal symbol. On the one hand, the eigenvalues of \hat{Z}_k are $\frac{2\ell+1-k}{k}$, $0 \leq \ell \leq k-1$, so

$$\text{Tr}(U_{k,1}) = \sum_{\ell=0}^{k-1} e^{-i(2\ell+1-k)\alpha} = e^{i(k-1)\alpha} \frac{1 - e^{-2ik\alpha}}{1 - e^{-2i\alpha}} = \frac{\sin(k\alpha)}{\sin \alpha}.$$

On the other hand, the time-one Hamiltonian flow ϕ_1 of H is non-degenerate, and has two fixed points $S = (0, 0, -1)$ and $N = (0, 0, 1)$. One readily computes

$$\mathcal{A}(S) = -1, \quad \mathcal{A}(N) = 1, \quad \theta(S) = -\frac{\pi}{2} - \pi \left\lfloor \frac{\alpha}{\pi} \right\rfloor, \quad \theta(N) = \frac{\pi}{2} - \pi \left\lfloor \frac{\alpha}{\pi} \right\rfloor.$$

Moreover,

$$\delta_{\phi_1, S} = |\det(T_S \phi_1 - \text{Id})|^{-\frac{1}{2}} = \left| \det \begin{pmatrix} \cos \alpha - 1 & -\sin \alpha \\ \sin \alpha & \cos \alpha - 1 \end{pmatrix} \right|^{-\frac{1}{2}} = |2(1 - \cos \alpha)|^{-\frac{1}{2}} = \frac{1}{2|\sin \alpha|}$$

and similarly $\delta_{\phi_1, N} = \frac{1}{2|\sin \alpha|}$. Consequently, Theorem 2.4.7 yields

$$\text{Tr}(U_{k,1}) = \frac{ie^{-i\pi \lfloor \frac{\alpha}{\pi} \rfloor} (e^{-ik\alpha} - e^{ik\alpha})}{2|\sin \alpha|} + O(k^{-1}) = \frac{e^{-i\pi \lfloor \frac{\alpha}{\pi} \rfloor} \sin(k\alpha)}{|\sin \alpha|} + O(k^{-1}),$$

which is consistent with the above exact formula since $e^{-i\pi \lfloor \frac{\alpha}{\pi} \rfloor}$ equals the sign of $\sin \alpha$.

Example 2.4.9. One readily generalizes this example to one in which the time-one flow ϕ_1 is degenerate although its graph intersects cleanly the diagonal. In order to do so, we consider the function $H = \alpha z_1$, with $\alpha \notin \pi\mathbb{Z}$, on $(S^2 \times S^2, \omega \oplus \omega)$ with $\omega = -\frac{1}{2}\omega_{S^2}$ and coordinates $(x_1, y_1, z_1, x_2, y_2, z_2)$. The operator $\alpha \hat{Z}_k \otimes \text{Id}$ acting on $\mathcal{H}_k \otimes \mathcal{H}_k$, where \hat{Z}_k and \mathcal{H}_k are as in Example 2.1.1, is a Berezin-Toeplitz operator with principal symbol H and vanishing subprincipal symbol. Its eigenvalues are $\frac{(2\ell+1-k)\alpha}{k}$, $0 \leq \ell \leq k-1$, each with multiplicity k , so

$$\text{Tr}(U_{k,1}) = k \sum_{\ell=0}^{k-1} e^{-i(2\ell+1-k)\alpha} = k \frac{\sin(k\alpha)}{\sin \alpha}.$$

The fixed point set M^{ϕ_1} of the time-one flow ϕ_1 of H is the disjoint union of two spheres $\Sigma_{\pm} = \{(0, 0, \pm 1)\} \times S^2$. One readily computes

$$\mathcal{A}(\Sigma_-) = -\alpha, \quad \mathcal{A}(\Sigma_+) = \alpha, \quad \theta(\Sigma_-) = -\frac{\pi}{2} - \pi \left\lfloor \frac{\alpha}{\pi} \right\rfloor, \quad \theta(\Sigma_+) = \frac{\pi}{2} - \pi \left\lfloor \frac{\alpha}{\pi} \right\rfloor.$$

Moreover, $\delta_{\phi_1, \Sigma_-} = |\omega| = \delta_{\phi_1, \Sigma_+}$. Thus, Theorem 2.4.6 yields

$$\text{Tr}(U_{k,1}) = \frac{ik}{2\pi} \left(e^{ik\alpha} e^{-i\pi \lfloor \frac{\alpha}{\pi} \rfloor} \text{Vol}(\Sigma_+) - e^{-ik\alpha} e^{-i\pi \lfloor \frac{\alpha}{\pi} \rfloor} \text{Vol}(\Sigma_-) \right) + O(1) = k \frac{e^{-i\pi \lfloor \frac{\alpha}{\pi} \rfloor} \sin(k\alpha)}{|\sin \alpha|} + O(1)$$

which is consistent with the above result.

In fact, in these two examples the function $\frac{1}{2}H$ is the momentum map for an effective Hamiltonian S^1 -action, and the quantities involved in Theorem 2.4.6 can be computed in this general setting in terms of the weights (see Section 3.5) and volume of the components of the fixed point set of the action.

The key part of the proof of Theorem 2.4.6 is the computation of the geometric quantities appearing in its statement, and in particular the index contained in θ . The idea is to compare the densities $\delta_{\mathcal{C}_\ell}$ from Theorem 2.4.5 obtained on the components of the intersections $\Gamma_0 \cap \Gamma'$ and $\Gamma_1 \cap \Gamma'$ where Γ_0 and Γ' are two Lagrangian submanifolds and $\Gamma_1 = \phi_1(\Gamma_0)$, and in particular to control precisely how their phases differ.

The main novelty that was seemingly missing in the literature is the precise computation of the Robbin-Salamon indices appearing in Theorems 2.4.6 and 2.4.7. For instance, in [Ioo20] a similar formula for the trace of the time-one propagator of a time-independent Berezin-Toeplitz operator was provided, but these indices did not seem to appear explicitly.

2.4.3 The Gutzwiller trace formula

Another application of the results from [CLF20] is the computation of the quantities involved in the Gutzwiller trace formula, performed in [CLF23a]. This formula is a popular topic in quantum mechanics, both in the physics [BB70, BB71, BB72, Gut71] and mathematics [CdV73, Cha74] literature, and describes the asymptotic distribution of the eigenvalues in a window of size of order the semiclassical parameter around a given energy.

Concretely, let $T_{k,t}$ be a Berezin-Toeplitz operator with time-independent principal symbol H , let E be a regular value of H and let f be a smooth function with smooth compactly supported Fourier transform. The Gutzwiller trace formula is an asymptotic estimate of the trace $\text{Tr}(f(k(E - T_k)))$, and stating our result requires to introduce some invariants which are similar to the ones defined in Section 2.4.2.

First, we work under the following clean intersection condition: we assume that

$$\{(t, -H(x), \phi_t(x), x) \mid t \in \text{supp}(\hat{f}), x \in M\} \text{ and } \{(t, -E, x, x) \mid t \in \text{supp}(\hat{f}), x \in M\}$$

intersect cleanly. Under this assumption, the set

$$\mathcal{N}_E = \left\{ (t, x) \mid t \in \text{supp}(\hat{f}), x \in H^{-1}(E) \text{ with } \phi_t(x) = x \right\} \quad (2.36)$$

is a finite union of smooth connected submanifolds $\mathcal{N}_1, \dots, \mathcal{N}_p$ and for every $\ell \in \{1, \dots, p\}$ and every $(t, x) \in \mathcal{N}_\ell$,

$$T_{(t,x)}\mathcal{N}_\ell = \{(s, Y) \in \mathbb{R} \oplus T_x M \mid \omega_x(X_x, Y) = 0, T_x \phi_t(Y) + sX_x = Y\}.$$

Second, let g be a linear symplectomorphism of a symplectic vector space (V, ω_V) and let $\xi \in \ker(g - \text{Id}) \setminus \{0\}$. Then there is a natural density $\delta_{g,\xi}$ on

$$N = \{(s, Y) \in \mathbb{R} \oplus V \mid \omega(\xi, Y) = 0, g(Y) + s\xi = Y\}.$$

Indeed, one can relate N to $N' = \ker(G - \text{Id})$ with

$$G : \mathbb{R}^2 \oplus V \rightarrow \mathbb{R}^2 \oplus V, \quad (s, \tau, Y) \mapsto (s, \tau + \omega(\xi, Y), g(Y) + s\xi)$$

and define $\delta_{g,\xi}$ by means on the density δ_G on N' described in Section 2.4.2. In particular, each component \mathcal{N}_ℓ of \mathcal{N}_E can be equipped with the density δ_ℓ which coincides with $\delta_{T_x \phi_t, X_H(x)}$ on $T_{(t,x)}\mathcal{N}_\ell$.

Third, let $(t, x) \in \mathbb{R} \times H^{-1}(E)$ be such that $\phi_t(x) = x$ (note that $t = 0$ is allowed, and the quantities below will still be defined with a slight abuse of notation). Define the holonomy $h(L, t, x)$ of the trajectory $\gamma : r \in [0, t] \mapsto \phi_r(x)$ as in Equation (2.35): for any frame s of γ^*L such that $s(0) = s(t)$,

$$h(L, t, x) = \int_0^t f(r) dr, \quad \nabla s = -if(r)dr \otimes s.$$

Under the above clean intersection condition, the holonomy map $(t, x) \mapsto h(L, t, x)$ is constant on each component \mathcal{N}_ℓ . Define similarly the holonomy $h(L', t, x)$ of the trajectory γ in L' . Now, consider the linear maps $\eta_0 : \mathbb{R} \oplus T_x M \rightarrow \mathbb{R}^2 \oplus T_x M \oplus T_x M$ and $\xi_r : \mathbb{R} \oplus T_x M \rightarrow \mathbb{R}^2 \oplus T_x M \oplus T_x M$, $r \in [0, t]$, defined as

$$\eta_0(s, Y) = (s, 0, Y, Y), \quad \tilde{\xi}_r(s, Y) = (s, \omega_x(X_H(x), Y), T_x \phi_r(Y) + sX_H(\phi_r(x)), Y).$$

We define the Robbin-Salamon index

$$\nu(t, x) := \mu_{\text{RS}}((\text{Im } \tilde{\xi}_r)_{r \in [0, t]}, \text{Im } \eta_0)$$

by viewing $\text{Im } \tilde{\xi}_r$ and $\text{Im } \eta_0$ as subspaces of a fixed symplectic vector space as follows. Choose an orthosymplectic frame $(\alpha_\ell, \beta_\ell)_{1 \leq \ell \leq n}$ of γ^*TM such that $\alpha_\ell(t) = \alpha_\ell(0)$ and $\beta_\ell(t) = \beta_\ell(0)$ for every $\ell \in \{1, \dots, n\}$, and use this frame to identify $T_{\phi_r(x)}M$ with $T_x M$ for every $r \in [0, t]$. Then $\text{Im } \tilde{\xi}_r$ can be viewed as a Lagrangian subspace of $\mathbb{R}^2 \oplus T_x M \oplus T_x M$ for every $r \in [0, t]$. Moreover, let s_K be the frame of γ^*K such that $s_K(\alpha_1 \wedge \dots \wedge \alpha_n) = 1$, and write $\nabla s_K = -if_K dt \otimes s_K$ for some function f_K . Then

$$J(t, x) = \frac{1}{2} \int_0^t f_K(r) dr + \frac{\pi}{2} \nu(t, x)$$

does not depend on the choice of the orthosymplectic frame. Finally, define

$$\Theta(t, x) = h(L', t, x) - J(t, x) - \int_0^t H_r^{\text{sub}}(\phi_r(x)) dr.$$

As in Section 2.4.2, these quantities simplify in the presence of a half-form bundle $\delta \rightarrow M$. If $L' = \delta$, then $h(L', t, x) - J(t, x) = -\frac{\pi}{2}m$ where m is a half-integer, well-defined modulo 4, which coincides with $\mu_{\text{RS}}((\text{Im } \tilde{\xi}_r)_{r \in [0, t]}, \text{Im } \eta_0)$ modulo 4 if the orthosymplectic frame $(\alpha_\ell, \beta_\ell)_{1 \leq \ell \leq n}$ chosen to define this index is such that the corresponding frame s of γ^*K has a square root $\tau \in \mathcal{C}^\infty([0, t], \delta)$ with $\tau(0) = \tau(t)$.

Theorem 2.4.10 ([CLF23a]). *Under the above clean intersection assumption,*

$$\mathrm{Tr}(f(k(E - T_k))) = \frac{1}{\sqrt{2\pi}} \sum_{\ell=1}^p \left(\frac{k}{2\pi}\right)^{\frac{d_\ell-1}{2}} e^{ikh(L, \mathcal{N}_\ell)} \int_{\mathcal{N}_\ell} \hat{f}(t) e^{i\Theta(t, x)} \delta_\ell(t, x) + O(k^{\frac{d_\ell-1}{2}-1})$$

where $d_\ell = \dim \mathcal{N}_\ell$ and $h(L, \mathcal{N}_\ell) = h(L, t, x)$ for any $(t, x) \in \mathcal{N}_\ell$.

In fact the more precise result is that the contribution of each component \mathcal{N}_ℓ has a complete asymptotic expansion.

It is interesting to state the version of Theorem 2.4.10 obtained in the particular case of isolated periodic orbits, meaning that the components of \mathcal{N}_E are either $\mathcal{N}_0 = \{0\} \times H^{-1}(E)$ or $\mathcal{N}_\ell = \{T_\ell\} \times \gamma_\ell$, $1 \leq \ell \leq p$, where γ_ℓ is a periodic orbit of the Hamiltonian flow with period T_ℓ . In this case, the quantities in the statement of Theorem 2.4.10 can be simplified as follows.

First, recall that since E is a regular value of H , the Liouville volume form $\mu = \frac{\omega^{\wedge n}}{n!}$ induces a volume form ν_E (hence a density, that we still write ν_E) on the hypersurface $H^{-1}(E)$. Namely, if α is any differential form such that $\mu = \alpha \wedge dH$ near $H^{-1}(E)$, then ν_E is the pullback of α to $H^{-1}(E)$. It is standard that ν_E does not depend on the choice of α , and that if Y is a vector field such that $\omega(X_H, Y) = 1$ near $H^{-1}(E)$, then one can choose $\alpha = \iota_Y \mu_M$ where ι is the interior product.

Second, for $\ell \in \{1, \dots, p\}$ and for $x \in \gamma_\ell$, let S_x be the generalized eigenspace of $T_x \phi_{T_\ell}$ associated with the eigenvalue 1, and let S_x^\perp be its symplectic orthogonal. Then the quantity $D(\gamma_\ell) = \det(T_x \phi_{T_\ell} - \mathrm{Id})|_{S_x^\perp}$ does not depend on the choice of $x \in \gamma_\ell$.

Theorem 2.4.11 ([CLF23a]). *For every $\ell \in \{1, \dots, p\}$, let T_ℓ^\sharp be the positive primitive period of γ_ℓ . Then*

$$\begin{aligned} \mathrm{Tr}(f(k(E - T_k))) &= \frac{1}{\sqrt{2\pi}} \left(\frac{k}{2\pi}\right)^{n-1} \hat{f}(0) \int_{H^{-1}(E)} \nu_E + O(k^{n-2}) \\ &\quad + \sum_{\ell=1}^p \frac{1}{\sqrt{2\pi}} \frac{\hat{f}(T_\ell) e^{ikh(L, \gamma_\ell)}}{|D(\gamma_\ell)|^{\frac{1}{2}}} \int_0^{T_\ell^\sharp} e^{i\Theta(T_\ell, \phi_t(x))} dt + O(k^{-1}). \end{aligned}$$

The first term in this estimate is the so-called *Weyl term* giving the volume of the energy level $H^{-1}(E)$.

As above, the main novelty of our results is the explicit computation of the Robbin-Salamon indices appearing in Theorems 2.4.10 and 2.4.11, which was not directly accessible in the existing literature [BPU98, Pao18, Ioo20]. We will discuss this point in more detail in [CLF23a].

Example 2.4.12. We consider the Hamiltonian $H = z_1^2 + z_2$ on $(M = S^2 \times S^2, \omega \oplus \omega)$ with $\omega = -\frac{1}{2}\omega_{S^2}$ and coordinates $(x_1, y_1, z_1, x_2, y_2, z_2)$. So we use once again the setting and notation of Example 2.1.1. The operator

$$T_k = T_k \left(z_1^2 - \frac{1}{2k} \Delta z_1^2 \right) \otimes \mathrm{Id} + \mathrm{Id} \otimes \hat{Z}_k = \frac{k+3}{k} T_k(z_1^2) - \frac{1}{k} \mathrm{Id} \otimes \mathrm{Id} + \mathrm{Id} \otimes \hat{Z}_k$$

acting on $\mathcal{H}_k \otimes \mathcal{H}_k$ is a Berezin-Toeplitz operator with principal symbol H and vanishing subprincipal symbol. A straightforward computation shows that in the identification of \mathcal{H}_k with $\mathbb{C}_{k-1}[w]$,

$$T_k(z_1^2) = \frac{1}{(k+1)(k+2)} \left(4w^2 \frac{d^2}{dw^2} - 4(k-2)w \frac{d}{dw} + (k^2 - k + 2) \mathrm{Id} \right).$$

This leads to the fact that the eigenvalues of T_k are

$$\lambda_{\ell, m}(k) = \frac{(k+3)(k-2\ell-1)^2}{k(k+1)(k+2)} + \frac{1}{k(k+2)} + \frac{k-2m-1}{k}, \quad 0 \leq \ell, m \leq k-1.$$

Of course, we have that

$$\mathrm{Tr}(f(k(E - T_k))) = \sum_{\ell=0}^{k-1} \sum_{m=0}^{k-1} f(k(E - \lambda_{\ell,m}(k))). \quad (2.37)$$

Below we will choose a suitable \hat{f} and evaluate numerically the trace $\mathrm{Tr}(f(k(E - T_k)))$ thanks to this formula, by computing each quantity $f(k(E - \lambda_{\ell,m}(k)))$ thanks to numerical integration routines.

In order to justify our choice of \hat{f} and to compare the numerical outcomes with the estimate of Theorem 2.4.10, we need to understand the Hamiltonian flow of H . In cylindrical coordinates, the Hamiltonian vector field reads $X_H = 4z_1\partial_{\theta_1} + 2\partial_{\theta_2}$, hence ϕ_t is the rotation with angle $4z_1t$ about the vertical axis in the first sphere and with angle $2t$ about the vertical axis in the second sphere. Hence, only the elements of $\pi\mathbb{Z}$ can be periods of this flow; we will select the period $T = \pi$ only. In order to do so, we consider the bump function

$$\hat{f}(t) = \chi\left(\frac{t - \pi}{c}\right), \quad \chi(s) = \begin{cases} e^{1 - \frac{1}{1-s^2}} & \text{if } -1 < s < 1, \\ 0 & \text{otherwise} \end{cases}$$

with $0 < c < \pi$, so that $\hat{f}(\pi) = 1$ and $\mathrm{supp}(\hat{f})$ does not contain any other integer multiple of π , and obtain the numerical values of its inverse Fourier transform f at the points $k(E - \lambda_{\ell,m}(k))$ by computing the integral in

$$f(\xi) = c\sqrt{\frac{2}{\pi}} e^{i\pi\xi} \int_0^1 \cos(cs\xi) \chi(s) \, ds$$

thanks to the *quad* numerical integration routine from Python.

Now, we choose the regular value E of H such that $-1 < E < -\frac{3}{4}$; then the points $m = (x_1, y_1, z_1, x_2, y_2, z_2) \in H^{-1}(E)$ with period π are the elements of the surface $\Sigma_E = \{z_1 = 0, z_2 = E\}$. Indeed, necessarily $2z_1 = q$ is an integer, but since

$$-1 \leq z_2 = E - z_1^2 = E - \frac{q^2}{4} < -\frac{(3+q^2)}{4},$$

the only possibility is $q = 0$. Consequently, with our choice of f , the set \mathcal{N}_E from Equation (2.36) is $\mathcal{N}_E = \{\pi\} \times \Sigma_E$.

Let $m \in \Sigma_E$; then $X_H(m) = 2\partial_{\theta_2}$, so $X_H(m)^\perp = \mathrm{Span}(\partial_{\theta_1}, \partial_{\theta_2}, \partial_{z_1})$. Since moreover $T_m\phi_\pi$ leaves ∂_{θ_1} , ∂_{θ_2} and ∂_{z_2} invariant and sends ∂_{z_1} to $\partial_{z_1} + 4\pi\partial_{\theta_1}$, one readily checks that the space

$$A = \left\{ (s, Y) \in \mathbb{R} \oplus T_m M \mid Y \in X_H(m)^\perp, T_m\phi_\pi(Y) + sX_H(m) = Y \right\}$$

satisfies

$$A = \{0\} \times \mathrm{Span}(\partial_{\theta_1}, \partial_{\theta_2}) = T_{(\pi, m)}\mathcal{N}_E,$$

so the clean intersection condition from Theorem 2.4.10 is satisfied.

The density δ_E on \mathcal{N}_E in this theorem can be computed to be

$$\delta_E = \frac{d\theta_1 d\theta_2}{4\sqrt{2\pi}}.$$

Moreover, the holonomy $h(L, \pi, m)$ reads

$$h(L, \pi, m) = \int_0^\pi \alpha_{\phi_t(m)}(X_H(\phi_t(m))) \, dt,$$

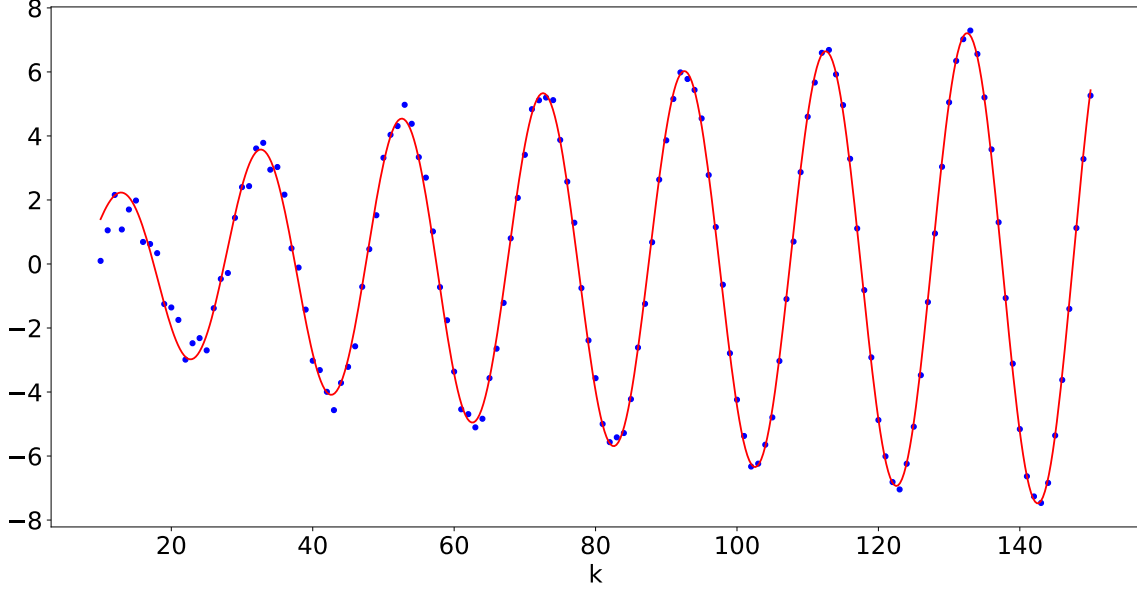


Figure 2.8: The blue dots represent the real part of $\text{Tr}(f(k(E - T_k)))$ from Example 2.4.12, computed using Formula (2.37), for $E = -0.9$ and different values of k (and $c = 1$ in the above choice of f). The solid red line is the graph of the real part of $\kappa \mapsto \left(\frac{\kappa}{2\pi}\right)^{\frac{1}{2}} \frac{\pi}{2} e^{i(\kappa\pi(1+E) - \frac{5\pi}{4})}$, which gives the equivalent obtained in (2.38) for integral values $\kappa = k$.

where

$$\alpha = \frac{1}{2} \left((1 + z_1) d\theta_1 + \frac{dz_1}{\sqrt{1 - z_1}} + (1 + z_2) d\theta_2 + \frac{dz_2}{\sqrt{1 - z_2}} \right).$$

This gives $h(L, \pi, m) = \pi(1 + E)$. The computation of the Robbin-Salamon index $\nu(\pi, m)$ is straightforward but tedious (details will appear in an appendix of [CLF23a]); the final result is that $\nu(\pi, m) = \frac{5}{2}$. Hence, finally, Theorem 2.4.10 yields (recall from Example 2.1.1 that we are working with the global half-form bundle $L' = \delta = \mathcal{O}(-1)$)

$$\text{Tr}(f(k(E - T_k))) = \left(\frac{k}{2\pi}\right)^{\frac{1}{2}} \frac{\pi}{2} e^{i(k\pi(1+E) - \frac{5\pi}{4})} + O(k^{-\frac{1}{2}}). \quad (2.38)$$

We compare this asymptotic estimate with the numerical evaluation of Formula (2.37) in Figures 2.8 and 2.9.

The idea of the proof of Theorem 2.4.11 is quite similar to the idea of the proof of Theorem 2.4.6, with a few subtleties. First, we apply a Bargmann transform (see Example 2.1.2) to interpret the Schwartz kernel $U_{k,t}$ as a Lagrangian section of the quantization of $\mathbb{C} \times M \times \overline{M}$. Then we compute the trace $\text{Tr}(f(k(E - T_k)))$ thanks to a pairing formula similar to Theorem 2.4.5 and adapted to this non-compact setting.

2.5 Perspectives

We conclude this chapter by giving a few ideas about future research directions building on the results that we just described.

Recall that in the paper [LF18a] discussed in Section 2.2, we only obtained, in the general case, estimates for the sub-fidelity and super-fidelity of two states supported on Lagrangian submanifolds intersecting transversally. Obtaining asymptotic estimates for the fidelity itself, even in this Lagrangian setting, seems too complicated; it was already quite difficult in the

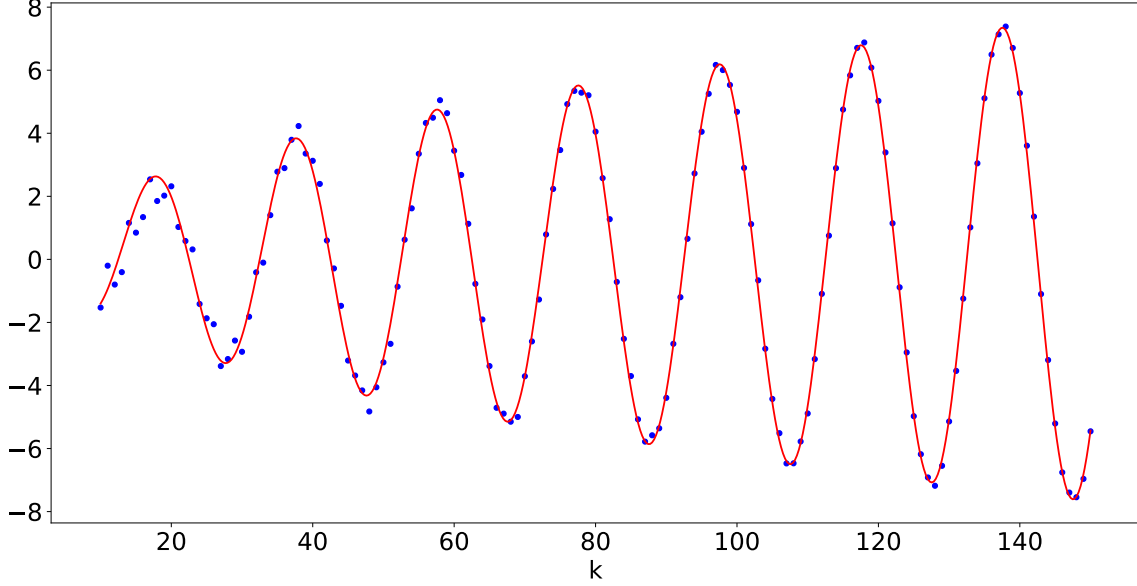


Figure 2.9: The blue dots represent the imaginary part of $\text{Tr}(f(k(E - T_k)))$ from Example 2.4.12, computed using Formula (2.37), for $E = -0.9$ and different values of k (and $c = 1$ in the above choice of f). The solid red line is the graph of the imaginary part of $\kappa \mapsto \left(\frac{\kappa}{2\pi}\right)^{\frac{1}{2}} \frac{\pi}{2} e^{i(\kappa\pi(1+E) - \frac{5\pi}{4})}$, which gives the equivalent obtained in (2.38) for integral values $\kappa = k$.

simple case of two great circles on S^2 , but maybe our proofs could be simplified. But perhaps this complicated analysis could be carried on for the case of two curves on a surface; one caveat is that we heavily used the symmetries in the case of S^2 . Another direction would be to estimate the sub-fidelity and super-fidelity, which are more tractable, for states supported on more general submanifolds, and possibly under weaker assumptions about the intersections.

The possible extensions of the results from [ALF22] discussed in Section 2.3 are numerous, as suggests the substantial literature on zeros of random holomorphic sections. For instance, one could try to obtain variance estimates, similar to the ones in [SZ99b], for the current associated with the zero locus $Z_{T_k s_k}$ of the section $T_k s_k$ with s_k a random holomorphic section and T_k a Berezin-Toeplitz operator with principal symbol f for which 0 is a regular value. In another direction, it would be interesting to allow, as in [DLM23] but without restriction on the sign of f , 0 to be a singular value of f , say non-degenerate, and to study the expectation of $Z_{T_k s_k}$; in particular, the case of a hyperbolic singular value on a surface already seems intriguing and solving it could perhaps allow one to recover all the level sets of f from the application of T_k on a large number of random holomorphic sections in the case of a Morse function f on a surface. This would already become more technical than the results in [ALF22] because it would require to work with the term of order k^{-2} in the asymptotic expansion of B_k from Equation (2.23). Another possible extension would be to study the common zero set of $T_k^{(1)} s_k, \dots, T_k^{(d)} s_k$, where s_k is a random holomorphic section and each $T_k^{(\ell)}$ is a Berezin-Toeplitz operator with principal symbol f_ℓ , under appropriate assumptions on f_1, \dots, f_d .

Finally, let (M, ω, J) be a Hamiltonian S^1 -space, see Section 3.5: (M, ω) is a compact symplectic manifold and J is the momentum map for an effective Hamiltonian S^1 -action. Let \hat{J}_k be a Berezin-Toeplitz operator with principal symbol J . We believe that we can use the results of [CLF20] and [CLF23b] discussed in Section 2.4 to describe the cluster structure of the spectrum of \hat{J}_k and to count the number of eigenvalues in each spectral cluster, as was done for the homogeneous pseudodifferential case in [DG75] and [CdV79], respectively. This could constitute a first step in the investigation of the inverse spectral question for Hamiltonian S^1 -spaces alluded to in Section 5.5.

Chapter 3

Generalities on semitoric systems

Our goal in this chapter is to introduce the main characters of the rest of the manuscript, namely semitoric systems, and to describe some of their properties. In order to do so, we first quickly review integrable and toric systems in Section 3.1. We then recall, in Section 3.2, some useful facts about the singularities of integrable systems in dimension four. In Section 3.3, we define semitoric systems and give some important examples of such systems. We then describe, in Section 3.4, the invariants involved in the symplectic classification of semitoric systems. Finally, in Section 3.5 we define Hamiltonian S^1 -spaces and review their relationship with semitoric systems. Some definitions are quite technical by essence, so we tried to outline the ideas regularly so that the reader who is only interested in the spirit of these definitions can skip the most involved parts.

3.1 Toric systems

Four-dimensional toric systems are the simplest examples of semitoric systems, and exhibit remarkable properties. Here we define toric systems from the integrable systems perspective in any even dimension, and later on we will specialize to dimension four.

An *integrable system* is the data of a connected symplectic manifold (M^{2n}, ω) together with smooth functions $f_1, \dots, f_n \in \mathcal{C}^\infty(M, \mathbb{R})$ such that

1. the functions f_1, \dots, f_n pairwise Poisson commute: for all $i, j \in \{1, \dots, n\}$, $\{f_i, f_j\} = 0$;
2. the Hamiltonian vector fields X_{f_1}, \dots, X_{f_n} (or equivalently df_1, \dots, df_n) are almost everywhere linearly independent.

Now we assume that M is compact. Because of the first condition, the Hamiltonian flows of f_1, \dots, f_n pairwise commute, so we obtain a group action of \mathbb{R}^n on M by composing these flows, namely:

$$\forall (t_1, \dots, t_n) \in \mathbb{R}^n, \forall m \in M, \quad (t_1, \dots, t_n) \cdot m = (\phi_{t_1, f_1} \circ \dots \circ \phi_{t_n, f_n})(m). \quad (3.1)$$

By definition, this group action is Hamiltonian (see Section 1.3), and its momentum map is $F = (f_1, \dots, f_n) : M \rightarrow \mathbb{R}^n$.

If all these Hamiltonian flows share the same period, this \mathbb{R}^n -action induces a torus action.

Definition 3.1.1. The integrable system $(M, \omega, F = (f_1, \dots, f_n))$ with M compact is *toric* if

1. the flows of f_1, \dots, f_n are all 2π -periodic;
2. the \mathbb{T}^n -action induced by the composition of these flows is effective.

A celebrated theorem by Atiyah [Ati82] and Guillemin-Sternberg [GS82] states that the image $F(M) \subset \mathbb{R}^n$ of the momentum map of a toric integrable system (M^{2n}, ω, F) is a convex polytope, obtained as the convex hull of the images of the fixed points of the torus action. Later Delzant [Del88] proved that $F(M)$ satisfies the additional properties:



Figure 3.1: The two Delzant polygons from Example 3.1.2.

1. there are n edges meeting at each vertex (simplicity);
2. the edges emanating from a vertex p are of the form $p + tu_j$, $t \geq 0$, for some $u_j \in \mathbb{Z}^n$ (rationality);
3. for each vertex, the above u_1, \dots, u_n can be chosen to form a \mathbb{Z} -basis of \mathbb{Z}^n (smoothness);

a convex polytope satisfying these properties is now commonly called a *Delzant polytope*. He also proved that two isomorphic (*i.e.* equivariantly symplectomorphic) compact toric systems share the same polytope, and that the set of classes of toric systems up to isomorphism is in bijection with the set of Delzant polytopes, through the map $[(M, \omega, F)] \mapsto F(M)$. Furthermore, he described explicitly an inverse for this map: starting from a given Delzant polytope, one can construct a toric system producing this polytope by symplectic reduction of \mathbb{C}^d with its standard symplectic form with respect to some Hamiltonian torus action. We insist on the fact that the dimension d and the momentum map for this torus action are obtained completely explicitly from the polygon, see [Del88, Section 3] or [CdS03, Section 2.5].

In the rest of the manuscript we will focus on four-dimensional systems. In this case we will talk about Delzant polygons (instead of polytopes) for toric systems, and the first item in their definition above will be automatically satisfied.

Example 3.1.2. We investigate the two famous Delzant polygons shown in Figure 3.1.

1. For the triangle from Figure 3.1a, Delzant's algorithm yields the toric system (M, ω, F) where (M, ω) is obtained as the symplectic reduction of \mathbb{C}^3 by the S^1 -action generated by $N = \frac{1}{2}(|z_1|^2 + |z_2|^2 + |z_3|^2)$ at level $N = 1$ and $F = (\frac{1}{2}|z_1|^2, \frac{1}{2}|z_2|^2)$. The symplectic manifold (M, ω) identifies with $(\mathbb{CP}^2, \omega_{\text{FS}})$ where ω_{FS} is the Fubini-Study form, normalized so that the volume of \mathbb{CP}^2 equals $2\pi^2$.
2. For the square from Figure 3.1b, Delzant's algorithm gives the toric system (M, ω, F) where (M, ω) is obtained as the symplectic reduction of \mathbb{C}^4 by the \mathbb{T}^2 -action generated by $N = \frac{1}{2}(|z_1|^2 + |z_2|^2, |z_3|^2 + |z_4|^2)$ at level $N = (2, 2)$. The symplectic manifold (M, ω) identifies with $(S^2 \times S^2, \omega_{S^2} \oplus \omega_{S^2})$ where ω_{S^2} is the standard symplectic form on S^2 .

Here we have only discussed compact toric systems for the sake of clarity, but one can also consider non-compact toric systems. In this context, and under the assumption that the momentum map is proper, the convexity result described above has been extended in [LMTW98].

3.2 Singularities of four-dimensional integrable systems

In order to define semitoric systems, we first need to discuss singularities of integrable systems. Now and for the rest of the text, (M, ω) is a connected, four-dimensional symplectic manifold.

A *regular point* of the integrable system $(M, \omega, F = (f_1, f_2))$ is a point $m \in M$ where $X_{f_1}(m)$ and $X_{f_2}(m)$ are linearly independent; $c \in F(M)$ is a *regular value* if every point in the fiber $F^{-1}(c)$ is regular. Let $c \in \mathbb{R}^2$ be a regular value of the momentum map F , and assume that the fiber $F^{-1}(c)$ is compact and connected; the celebrated action-angle theorem (see [Min47] and [Dui80]) states that there exist a symplectomorphism ϕ from a neighborhood of $F^{-1}(c)$ in M to a neighborhood of the zero section in $T^*\mathbb{T}^2$ and a local diffeomorphism $G_0 : (\mathbb{R}^2, 0) \rightarrow (\mathbb{R}^2, c)$ such that

$$F \circ \phi^{-1} = G_0(I_1, I_2),$$

where $T^*\mathbb{T}^2$ is endowed with the coordinates $(\theta_1, \theta_2, I_1, I_2) \in (\mathbb{R}/2\pi\mathbb{Z})^2 \times \mathbb{R}^2$ and the symplectic form $dI_1 \wedge d\theta_1 + dI_2 \wedge d\theta_2$. The coordinates (I_1, I_2) are commonly called *action coordinates* or *action variables* and form a local toric momentum map. We call G_0^{-1} an *action diffeomorphism*; in what follows, in particular in Chapter 5, we will often consider *oriented* action diffeomorphisms and variables, meaning that $\det(dG_0(0)) > 0$. These are not unique: any two pairs of action variables (I_1, I_2) and (L_1, L_2) near $F^{-1}(c)$ are related by

$$\begin{pmatrix} L_1 \\ L_2 \end{pmatrix} = A \begin{pmatrix} I_1 \\ I_2 \end{pmatrix} + \kappa$$

for some $A \in \text{GL}(2, \mathbb{Z})$ (or $A \in \text{SL}(2, \mathbb{Z})$ if both pairs are oriented action variables) and $\kappa \in \mathbb{R}^2$.

In general (and automatically if M is compact), the momentum map will possess some singularities, which may prevent one from obtaining global action variables. A point $m \in M$ (respectively a value $c \in F(M)$) is called a *singular point* (respectively a *singular value*) if it is not regular. The *rank* of the singular point m is the rank of the family $(X_{f_1}(m), X_{f_2}(m))$, and it is also equal to the dimension of the orbit passing through m for the \mathbb{R}^2 -action defined in Equation (3.1). One can define a good notion of non-degenerate singular point, and in order to do so it is convenient to distinguish between rank one and rank zero points.

Non-degenerate rank zero singular points. Let $m \in M$ be a rank zero singular point of the momentum map F .

Definition 3.2.1 ([BF04, Definition 1.23]). The rank zero point m is *non-degenerate* if the Hessians $d^2f_1(m), d^2f_2(m)$ span a Cartan subalgebra of the Lie algebra $(\mathcal{Q}_m, \{\cdot, \cdot\}_m)$ of quadratic forms on T_mM , with Lie bracket the Poisson bracket.

The classification of the Cartan subalgebras of \mathcal{Q}_m (see for instance [BF04, Theorem 1.3]) yields a classification of non-degenerate rank zero points in different types, which are usually called Williamson types. One can understand this classification through the properties of the eigenvalues of a matrix belonging to $\mathfrak{sp}(4, \mathbb{R})$, which can be identified with \mathcal{Q}_m in the following way. Let \mathcal{B} be any basis of T_mM and let Ω_m be the matrix of ω_m in \mathcal{B} . Moreover, if $q \in \mathcal{Q}_m$, let B_q be its matrix in \mathcal{B} . Then we get a Lie algebra isomorphism

$$\mathcal{Q}_m \rightarrow \mathfrak{sp}(4, \mathbb{R}), \quad q \mapsto \Omega_m^{-1} B_q.$$

Using this identification (and slightly abusing notation by writing q instead of B_q), for any $\nu, \mu \in \mathbb{R}$, the characteristic polynomial of the matrix $A_{\nu, \mu} = \Omega_m^{-1} (\nu d^2f_1(m) + \mu d^2f_2(m))$ is of the form $X \mapsto \chi_{\nu, \mu}(X^2)$ with $\chi_{\nu, \mu}$ a quadratic polynomial (see for instance [BF04, Proposition 1.2]) that we call the *reduced characteristic polynomial* of $A_{\nu, \mu}$.

Definition 3.2.2 ([BF04, Section 1.8.2]). The rank zero point m is non-degenerate if and only if there exists $(\nu, \mu) \in \mathbb{R}^2$ such that the reduced characteristic polynomial $\chi_{\nu, \mu}$ has two distinct nonzero roots $\lambda_1, \lambda_2 \in \mathbb{C}$. In this case, m is

- an *elliptic-elliptic* point if $\lambda_1 < 0$ and $\lambda_2 < 0$;

- a *hyperbolic-elliptic* point if $\lambda_1 > 0$ and $\lambda_2 < 0$ or $\lambda_1 < 0$ and $\lambda_2 > 0$;
- a *hyperbolic-hyperbolic* point if $\lambda_1 > 0$ and $\lambda_2 > 0$;
- a *focus-focus* point if $\Im(\lambda_1) \neq 0$ (and hence $\Im(\lambda_2) \neq 0$).

If m is non-degenerate, the set \mathcal{D} of $(\nu, \mu) \in \mathbb{R}^2$ such that $\chi_{\nu, \mu}$ has two distinct nonzero roots $\lambda_1(\nu, \mu), \lambda_2(\nu, \mu)$ is open and dense, and for any $(\nu, \mu), (\nu', \mu') \in \mathcal{D}$, the roots $\lambda_1(\nu, \mu), \lambda_2(\nu, \mu)$ and $\lambda_1(\nu', \mu'), \lambda_2(\nu', \mu')$ share the same properties in the above list. So these types are well-defined.

Non-degenerate rank one singular points. Now, let $m \in M$ be a rank one singular point of F , so that there exist $\nu, \mu \in \mathbb{R}$ such that $\nu df_1(m) + \mu df_2(m) = 0$. The orbit through m of the \mathbb{R}^2 -action (3.1) is one-dimensional; let $L \subset T_m M$ be the tangent line to this orbit at m , and let L^\perp be the symplectic orthogonal of L . Note that $L \subset L^\perp$, that ω_m descends to a symplectic form on the quotient L^\perp/L and that $L \subset \ker(d^2(\nu f_1 + \mu f_2)(m))$, so that $d^2(\nu f_1 + \mu f_2)(m)$ descends to the quotient L^\perp/L .

Definition 3.2.3 ([BF04, Definition 1.21], see also [HP18, Section 2.1.3]). The rank one singular point m is *non-degenerate* if $d^2(\nu f_1 + \mu f_2)(m)$ is an isomorphism of L^\perp/L .

Again, there are different types of non-degenerate rank one singular points according to the eigenvalues of this isomorphism. Fix a basis of L^\perp/L , and let $\tilde{\Omega}_m$ be the matrix of the quotient symplectic form in this basis. Consider the matrix $A_{\nu, \mu} = \tilde{\Omega}_m^{-1} d^2(\nu f_1 + \mu f_2)(m)$ (where we abuse notation by writing $d^2(\nu f_1 + \mu f_2)(m)$ for the matrix of the induced endomorphism of L^\perp/L). The eigenvalues of $A_{\nu, \mu}$ are of the form $\pm \lambda$ for some $\lambda \in \mathbb{C}$, see for instance [BF04, Proposition 1.2].

Definition 3.2.4 (See [BF04, Section 1.8] and [LFP22, Definition 2.5]). The rank one singular point m is non-degenerate if $\det A_{\nu, \mu} \neq 0$, and m is

- an *elliptic-regular* point if the eigenvalues of $A_{\nu, \mu}$ are of the form $\pm i\alpha$ for some $\alpha \in \mathbb{R} \setminus \{0\}$ (or equivalently if $\det A_{\nu, \mu} > 0$);
- a *hyperbolic-regular* point if the eigenvalues of $A_{\nu, \mu}$ are of the form $\pm \alpha$ for some $\alpha \in \mathbb{R} \setminus \{0\}$ (or equivalently if $\det A_{\nu, \mu} < 0$).

In the literature, one also often encounters the terms *elliptic-transverse* and *hyperbolic-transverse*.

Near each non-degenerate singular point of an integrable system, there exists a convenient symplectic normal form, named Eliasson's normal form. This normal form is valid in any dimension, but here we only state it for four-dimensional systems since we only need this. To the best of our knowledge, the literature only contains a complete proof for the analytic case, in [Vey78] (see also [Rüs64] for the case $n = 2$). For the smooth case, there exist complete proofs for fully elliptic singularities in any dimension (see [DM91, Eli90]), for the general case in dimension two (see [CdVV79]), and for the focus-focus case in dimension four (see [VuNW13, Cha13]). In [CdVVuN03] the authors gave a normal form near an elliptic-regular fiber in dimension four, and in [MZ04] the authors studied normal forms in the presence of an additional group action.

Theorem 3.2.5 ([Eli84]). *Let $m \in M$ be a non-degenerate singular point of the integrable system $(M, \omega, F = (f_1, f_2))$. Then there exist local symplectic coordinates $(x, \xi) = (x_1, x_2, \xi_1, \xi_2)$ on an open neighborhood $U \subset M$ of m and a map $Q = (q_1, q_2) : U \rightarrow \mathbb{R}^2$ whose components are taken from the following list:*

- $q_j(x, \xi) = \frac{1}{2}(x_j^2 + \xi_j^2)$ (*elliptic*);
- $q_j(x, \xi) = x_j \xi_j$ (*hyperbolic*);

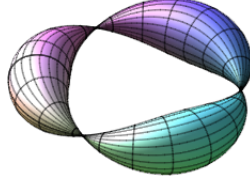


Figure 3.2: A focus-focus fiber containing three focus-focus points.

- $q_j(x, \xi) = \xi$ (regular);
- $q_1(x, \xi) = x_1\xi_2 - x_2\xi_1$, $q_2(x, \xi) = x_1\xi_1 + x_2\xi_2$ (focus-focus)

such that m corresponds to $(x, \xi) = (0, 0)$ and $\{q_j, f_\ell\} = 0$ for every $j, \ell \in \{1, 2\}$. Moreover, if none of the components q_j is hyperbolic, then there exists a local diffeomorphism $g : (\mathbb{R}^2, 0) \rightarrow (\mathbb{R}^2, F(m))$ such that for every $(x, \xi) \in U$, $F(x, \xi) = (g \circ Q)(x, \xi)$.

In this statement, the symplectic form on \mathbb{R}^4 is $d\xi_1 \wedge dx_1 + d\xi_2 \wedge dx_2$.

3.3 Semitoric systems

The definition of semitoric systems that we give now was introduced in [PVuN09, Definition 2.1]. The original definition, [VuN07, Definition 3.1], was slightly more general.

Definition 3.3.1. A *semitoric system* is an integrable system $(M, \omega, F = (J, H))$ on a four-dimensional symplectic manifold (M, ω) such that

1. J is the momentum map for an effective Hamiltonian S^1 -action;
2. J is proper;
3. the singular points of $F = (J, H)$ are all non-degenerate, with no hyperbolic component.

As a consequence of this definition, the singularities of a semitoric system are either of elliptic type (elliptic-regular or elliptic-elliptic), or focus-focus. Therefore, the new type of singularities, compared to toric systems, are focus-focus points; the corresponding singular fibers are tori that are pinched at one or several points, which are precisely the focus-focus points, see Figure 3.2 (note that the fact that the fibers of a semitoric system are connected is proved in [VuN07, Theorem 3.4]). Note that by [VuN07, Corollary 5.10], the total number of focus-focus points of a semitoric system is finite.

A four-dimensional toric integrable system is of course a particular case of semitoric system, with no focus-focus singularity; the fixed points of the \mathbb{T}^2 -action, whose images by the momentum map are the vertices of the Delzant polygon, are the elliptic-elliptic points of the system, while the elliptic-regular points are sent to the interior of the edges of this polygon. In fact, by [VuN07, Corollary 3.5], a semitoric system $(M, \omega, F = (J, H))$ has no focus-focus singularity if and only if it is of *toric type*: there exists a diffeomorphism g defined on a neighborhood of $F(M)$ and with values in \mathbb{R}^2 such that $g \circ F$ is the momentum map of a toric integrable system. This toric momentum map is obtained by extending action variables to the whole image $F(M)$; using the normal form from Theorem 3.2.5 near elliptic-elliptic points and the normal form from [MZ04] near elliptic-regular fibers, one readily checks that there is no obstruction in doing so.

In Chapter 4, we will focus on the case where (M, ω) is compact, in which case the second item in Definition 3.3.1 is automatically satisfied. In Chapter 5, we will allow for non-compact manifolds, but we will need to assume that our systems are simple, as defined now.

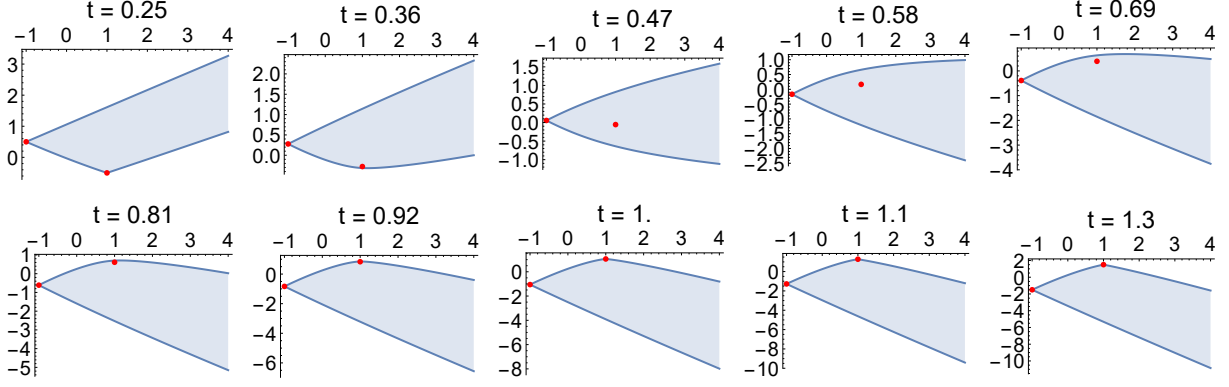


Figure 3.3: Image of the momentum map $F_t = (J, H_t)$ of the spin-oscillator system from Example 3.3.3, with J, H_t defined in Equation (3.2), for various values of $t \in \mathbb{R}$.

Definition 3.3.2. A semitoric system $(M, \omega, F = (J, H))$ is *simple* if each fiber of J contains at most one focus-focus point.

Note that there are two ways to not be simple. The first one is when there are at least two focus-focus points in the same fiber of J , but not of F (meaning that this fiber of J contains several tori pinched at one point each), and the second one is when there are at least two focus-focus points in the same fiber of F (which is then a torus with two or more pinches, as is the case in Figure 3.2). As discussed at the beginning of Chapter 5, in principle the results described in that chapter should extend without any difficulty to the former case; however, in the latter case it is possible that the joint spectrum does not contain enough information to recover all the symplectic invariants.

Below we give two historical examples of semitoric systems coming from physics.

Example 3.3.3 (Spin-oscillator). Endow \mathbb{R}^2 with coordinates (u, v) and its standard symplectic form $\omega_{\mathbb{R}^2} = du \wedge dv$, and S^2 with coordinates (x, y, z) and its usual symplectic form ω_{S^2} , as in Example 2.1.1. On $(M, \omega) = (S^2 \times \mathbb{R}^2, \omega_{S^2} \oplus \omega_{\mathbb{R}^2})$, we consider, for $t \in \mathbb{R}$,

$$J = \frac{1}{2}(u^2 + v^2) + z, \quad H_t = (1 - 2t) \left(\frac{1}{2}(u^2 + v^2) - z \right) + t(ux + vy). \quad (3.2)$$

For every $t \in \mathbb{R} \setminus \{\frac{1}{3}, 1\}$, the system $(M, \omega, F_t = (J, H_t))$ is a semitoric system, with no focus-focus singularity for $t \in (-\infty, \frac{1}{3}) \cup (1, +\infty)$, and with one focus-focus singular point $m = (0, 0, 0, 0, 1)$ for $t \in (\frac{1}{3}, 1)$ (see [VuN07, Proposition 6.1]). The S^1 -action generated by J corresponds to rotating at the same time about the origin in \mathbb{R}^2 and about the vertical axis in S^2 . The image of the momentum map F_t is displayed in Figure 3.3. This system was studied from the semitoric point of view in [PVN12] and [ADH19].

The quantum version of this system is known as the Jaynes-Cummings model [JC64] and plays an important part in quantum optics, see for instance [LFVuN21, Section 1] for an extended discussion and references. The classical spin-oscillator system and some of its generalizations, also including focus-focus singularities in dimension four or higher, were studied in [BCD09, BD12, BD15].

Example 3.3.4 (Coupled angular momenta). Let $R_1, R_2 > 0$. On $(M, \omega) = (S^2 \times S^2, -(R_1 \omega_{S^2} \oplus R_2 \omega_{S^2}))$ with coordinates $(x_1, y_1, z_1, x_2, y_2, z_2)$, we consider, for $t \in [0, 1]$,

$$J = R_1 z_1 + R_2 z_2, \quad H_t = (1 - t) z_1 + t(x_1 x_2 + y_1 y_2 + z_1 z_2). \quad (3.3)$$

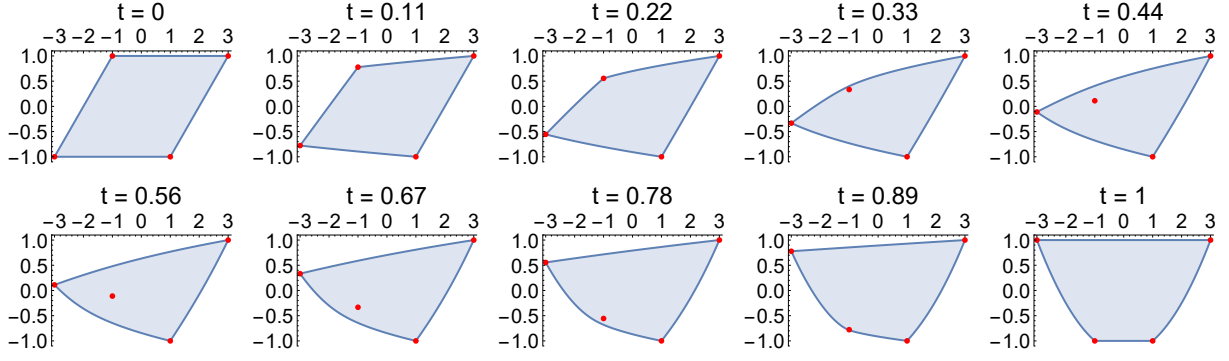


Figure 3.4: Image of the momentum map $F_t = (J, H_t)$ of the coupled angular momenta system from Example 3.3.4, with J, H_t defined in Equation (3.3), for $R_1 = 1, R_2 = 2$ and various values of $t \in [0, 1]$. Note that in this case Equation (3.4) gives $t^- = \frac{2}{5+2\sqrt{2}} \approx 0.26$ and $t^+ = \frac{2}{5-2\sqrt{2}} \approx 0.92$.

Let $0 < t^- < t^+ \leq 1$ be defined as

$$t^\pm = \frac{R}{1 + 2R \mp 2\sqrt{R}} \quad \text{with } R = \frac{R_2}{R_1}. \quad (3.4)$$

If $R_1 \neq R_2$, then $t^+ < 1$ and $(M, \omega, F_t = (J, H_t))$ is of toric type when $t \in [0, t^-) \cup (t^+, 1]$, and semitoric with one focus-focus point $m = (0, 0, 1, 0, 0, -1)$ when $t \in (t^-, t^+)$. When $R_1 = R_2$, then $t^+ = 1$ and the statements for $t \in [0, t^-)$ and $t \in (t^-, t^+)$ still hold, but when $t = t^+ = 1$ the system cannot be semitoric because the point m and the fixed point $(0, 0, -1, 0, 0, 1)$ lie in the same fiber of F (and we know from [VuN07, Theorem 1] that the fibers of the momentum map of a semitoric system are connected). In any case, when $t = t^-$ or $t = t^+$, the point m is degenerate. The image of the momentum map F_t is displayed in Figure 3.4. This system was originally introduced in [SZ99a] where the authors exhibited the non-trivial monodromy of its quantum counterpart (described in Example 5.1.2), and studied through the semitoric lens in [LFP19b]. For $R_1 \neq R_2$, this is an example of semitoric family, see Example 4.3.3.

The system from Example 3.3.4 was generalized in [HP18]: the authors produced a two-parameter family $(S^2 \times S^2, -(R_1\omega_{S^2} \oplus R_2\omega_{S^2}), F_{s_1, s_2} = (J, H_{s_1, s_2}))$, $s_1, s_2 \in [0, 1]$, which is either (when $R_1 \neq R_2$) of toric type, or semitoric with one focus-focus point, or semitoric with two focus-focus points, according to the values of the parameters s_1, s_2 .

The systems from Examples 3.3.3 and 3.3.4 were also recently generalized to the b -symplectic setting in [BHMM23].

3.4 Symplectic invariants of semitoric systems

In [PVuN09, PVuN11], Pelayo and Vũ Ngọc completely classified simple semitoric systems up to isomorphism, in terms of symplectic invariants that we will describe now. This classification has later been generalized to non-simple semitoric systems by Palmer, Pelayo and Tang in [PPT19]; in this case the semi-local invariants near the focus-focus fibers (Taylor series) are more involved (see [PT19]), but we will not need them in the rest of the manuscript. The so-called twisting index invariant is also a bit more delicate to define in the non-simple case, but we will not need them in this case either. In fact the only invariants that we will need in the non-simple case, in Chapter 4, are the number of focus-focus points, polygon, and height invariants, that are bundled into the so-called marked semitoric polygon, see Section 3.4.1 below. Therefore we will essentially describe the invariants in the simple case, except when describing this marked semitoric polygon; note that the first construction of this invariant in [VuN07] contained the non-simple case.

We use the following notion of semitoric isomorphism. Two semitoric systems $(M, \omega, F = (J, H))$ and $(M', \omega', F' = (J', H'))$ are said to be isomorphic if and only if there exist a symplectomorphism $\phi : M \rightarrow M'$ and a smooth function $f \in C^\infty(\mathbb{R}^2, \mathbb{R})$ with $\partial_y f > 0$ such that $F' \circ \phi = g \circ F$ where for every $(x, y) \in \mathbb{R}^2$, $g(x, y) = (x, f(x, y))$. In particular, such an isomorphism respects the generator of the S^1 -action ($J' \circ \phi = J$).

Roughly speaking, the classification of simple semitoric systems up to isomorphism is given in terms of five invariants:

1. the number N_f (which is finite) of focus-focus points of the system;
2. a rational convex polygon $\Delta \subset \mathbb{R}^2$ obtained as the image of a “generalized toric momentum map” $\mu : M \rightarrow \mathbb{R}^2$;
3. for each focus-focus point m :
 - (a) the height of $\mu(m)$ in Δ , obtained as some symplectic volume;
 - (b) a formal series in two variables, encoding the dynamics near the singularity;
 - (c) an integer describing how some natural local toric momentum map compares with μ .

However this rough description is a bit simplistic because, in practice, these invariants are all related. So we will now give a more precise definition of those. For the sake of simplicity we will assume that the systems that we consider have at least one focus-focus point; if there is no such singularity, only the polygonal invariant remains, and its definition can easily be adapted from what follows by using the convention that any finite set indexed by $\{1, \dots, s\}$ is empty when $s = 0$. Alternatively, the construction of the polygonal invariant of a system of toric type is explicitly discussed in [SVuN18, Section 5.2.2]; we also give a brief description of this construction after Example 3.4.5.

3.4.1 Marked semitoric polygons

From now on and until further notice, the semitoric systems that we consider are allowed to be non-simple. The idea behind the construction of the polygon Δ is to try to obtain global actions variables over the set $B_{\text{reg}} \subset F(M)$ of regular values (which is not simply connected because of the focus-focus values); this is prevented by the non-trivial monodromy above loops circling focus-focus values, exhibited in [Zou92, Mat96, Zun97]. This monodromy is always given by the matrix T^k , where T is as in Equation (3.5) below and $|k|$ is the number of focus-focus points with image in the interior of the chosen loop. If the system is simple, by introducing vertical cuts emanating from the focus-focus values in B_{reg} to obtain a simply connected set \tilde{B}_{reg} , so that global action variables can be constructed over \tilde{B}_{reg} , and by taking into account this monodromy to glue back at the cuts, one manages to construct the aforementioned map μ , such that $\Delta = \mu(M)$ is a convex polygon. In the non-simple case the picture is a bit more involved, but the idea is similar, except that in this context the cuts will be associated with focus-focus points.

This construction depends on two choices: the choice of some initial action variables of the form (J, K) near some $c_0 \in B_{\text{reg}}$, and the choice of the direction (upwards or downwards) of each cut. Therefore the actual invariant is an equivalence class of such polygons, that we will define now. Actually, it is convenient to bundle this invariant together with the number of focus-focus points and height invariant, thus obtaining the so-called marked semitoric polygon of $(M, \omega, (J, H))$.

Marked semitoric polygons. We start by defining the possible (classes of) polygons that we will obtain in this way. When constructing these polygons from semitoric systems, it will be necessary to keep track of the cut directions, so we will need to define some rather involved

notation. But first of all, when M is not compact (a situation that we will encounter in Chapter 5), one must be careful with the meaning of the word “polygon”.

Definition 3.4.1. A *polygon* is a closed subset Δ of \mathbb{R}^2 whose boundary $\partial\Delta$ is a continuous piecewise linear curve such that for any $K \subset \mathbb{R}^2$ compact, $\partial\Delta \cap K$ is differentiable except at finitely many points that are called *vertices* of Δ . Each linear piece of $\partial\Delta$ is called an *edge* of Δ . A polygon is called

- *convex* if it is the convex hull of isolated points in \mathbb{R}^2 ;
- *rational* if the slope of every edge is a rational number.

Of course, a compact convex polygon with a finite number of vertices is a polygon in the usual sense.

Let $\Delta \subset \mathbb{R}^2$ be a convex, rational polygon, and let

$$T = \begin{pmatrix} 1 & 0 \\ 1 & 1 \end{pmatrix} \in \mathrm{SL}(2, \mathbb{Z}). \quad (3.5)$$

Let q be a vertex of Δ . Since Δ is rational, the edges emanating from q are directed by integral vectors (vectors with integer coefficients), and we can choose normal vectors to these edges that are also integral. Let $v_1, v_2 \in \mathbb{Z}^2$ be the primitive inwards pointing normal vectors to these edges (recall that a vector $\begin{pmatrix} a \\ b \end{pmatrix} \in \mathbb{Z}^2$ is primitive if and only if a and b are relatively prime), ordered in such a way that $\det(v_1, v_2) > 0$.

Definition 3.4.2. Let k be a positive integer; we say that q satisfies:

1. the *Delzant* condition if $\det(v_1, v_2) = 1$;
2. the *k-hidden Delzant* condition if $\det(v_1, (T^*)^k v_2) = 1$;
3. the *k-fake* condition if $v_1 = (T^*)^k v_2$ (which, in this context, amounts to $\det(v_1, (T^*)^k v_2) = 0$).

In the literature one can also encounter an equivalent definition involving vectors directing the edges instead of normal vectors, but it is more natural for us to use the normal vectors; this was important in particular in [LFP23] where we intensively used the relationship between semitoric systems and their helices, see Section 4.2.3.

Let $\pi_1, \pi_2 : \mathbb{R}^2 \rightarrow \mathbb{R}$ be the canonical projections to the first and second factor, respectively. For $c, c' \in \mathbb{R}^2$, write $c \leq_{\mathrm{lex}} c'$ if and only if c is smaller than c' for the lexicographic order. Let $s \in \mathbb{Z}_{\geq 0}$, let $\vec{c} = (c_1, \dots, c_s) \in (\mathbb{R}^2)^s$ and let $\vec{\epsilon} = (\epsilon_1, \dots, \epsilon_s) \in \{-1, 1\}^s$. Assume that all the points c_1, \dots, c_s belong to the interior of Δ and that $c_1 \leq_{\mathrm{lex}} \dots \leq_{\mathrm{lex}} c_s$. Then $(\Delta, \vec{c}, \vec{\epsilon})$ is called a *marked weighted polygon*. For marked weighted polygons constructed from semitoric systems, $s = N_f$ will be the number of focus-focus points of the system, the marked points c_1, \dots, c_{N_f} will be the images of the focus-focus points m_1, \dots, m_{N_f} in the polygon, and $\epsilon_1, \dots, \epsilon_{N_f}$ will give the direction of the cut at each focus-focus point (upwards if $\epsilon_j = 1$, downwards if $\epsilon_j = -1$).

Let \mathcal{T} be the subgroup of $\mathrm{GL}(2, \mathbb{Z}) \ltimes \mathbb{R}^2$ consisting of applications leaving the vertical direction invariant; in other words, an element of \mathcal{T} is the composition of a linear transformation of the form T^ℓ for some $\ell \in \mathbb{Z}$ and of the translation by a vertical vector. Then \mathcal{T} acts on the set of marked weighted polygons in the following way. For $\tau \in \mathcal{T}$ and $(\Delta, \vec{c}, \vec{\epsilon})$ a marked weighted polygon, define

$$\tau \cdot (\Delta, \vec{c}, \vec{\epsilon}) = (\tau(\Delta), \tau(\vec{c}), \vec{\epsilon}) \quad (3.6)$$

where $\tau(\vec{c}) = (\tau(c_1), \dots, \tau(c_s))$.

When constructing the marked semitoric polygon of a semitoric system, the action of \mathcal{T} will correspond to the freedom in the choice of initial action variables of the form (J, K) alluded to

above. To account for the freedom in the choice of cut direction (up or down) at each point c_j , we need to introduce another group action which is a bit more complicated to define.

For $\lambda \in \mathbb{R}$, endow the vertical line $\pi_1^{-1}(\lambda)$ with an origin O , and define the piecewise affine transformation $t_\lambda : \mathbb{R}^2 \rightarrow \mathbb{R}^2$ as the identity on $\pi_1^{-1}((-\infty, \lambda])$ and as T , relative to O , on $\pi_1^{-1}([\lambda, +\infty))$. Explicitly,

$$\forall (x, y) \in \mathbb{R}^2 \quad t_\lambda(x, y) = \begin{cases} (x, y) & \text{if } x \leq \lambda, \\ (x, y + x - \lambda) & \text{if } x \geq \lambda. \end{cases} \quad (3.7)$$

Clearly t_λ does not depend on the choice of the origin O . Additionally, for $\vec{u} = (u_1, \dots, u_s) \in \{-1, 0, 1\}^s$ and $\vec{\lambda} = (\lambda_1, \dots, \lambda_s) \in \mathbb{R}^s$, let $t_{\vec{u}, \vec{\lambda}} = t_{\lambda_1}^{u_1} \circ \dots \circ t_{\lambda_s}^{u_s}$ (one readily checks that for any $\lambda, \lambda' \in \mathbb{R}$, t_λ and $t_{\lambda'}$ commute, so the order of the compositions in the definition of $t_{\vec{u}, \vec{\lambda}}$ does not matter).

Moreover, endow $G_s = \{-1, 1\}^s$ with a group structure by means of the composition law $*$ defined as

$$(\epsilon_1, \dots, \epsilon_s) * (\epsilon'_1, \dots, \epsilon'_s) = (\epsilon_1 \epsilon'_1, \dots, \epsilon_s \epsilon'_s).$$

The action of G_s that we will define now does not necessarily preserve the convexity of polygons (but will preserve convexity when restricted to the class of polygons actually constructed from a semitoric system, which will satisfy the assumptions in Lemma 3.4.3). So we forget convexity for a moment and consider the set

$$\mathcal{P} = \{(P, \vec{c}, \vec{\epsilon}) \mid P \text{ is a polygon, } \vec{c} \in (\mathbb{R}^2)^s, \vec{\epsilon} \in \{-1, 1\}^s\}$$

and define an action of G_s on \mathcal{P} as

$$\vec{\epsilon}' \cdot (P, \vec{c}, \vec{\epsilon}) = (t_{\vec{u}, \vec{\lambda}}(P), t_{\vec{u}, \vec{\lambda}}(\vec{c}), \vec{\epsilon}' * \vec{\epsilon}), \quad (3.8)$$

for $\vec{\epsilon}' \in G_s$ and $(P, \vec{c}, \vec{\epsilon}) \in \mathcal{P}$, with $t_{\vec{u}, \vec{\lambda}}(\vec{c}) = (t_{\vec{u}, \vec{\lambda}}(c_1), \dots, t_{\vec{u}, \vec{\lambda}}(c_s))$ and

$$\vec{u} = \left(\frac{\epsilon_1 - \epsilon'_1 \epsilon_1}{2}, \dots, \frac{\epsilon_s - \epsilon'_s \epsilon_s}{2} \right), \quad \vec{\lambda} = (\pi_1(c_1), \dots, \pi_1(c_s)). \quad (3.9)$$

In practice, the action of G_s consists in changing some cut directions, which also has an effect on the polygon: for instance if we change an upwards cut $\epsilon_j = 1$ to a downwards cut $\epsilon'_j \epsilon_j = -1$ at the marked point c_j , we apply the transformation T from Equation (3.5) to the part of P lying to the right of the vertical line passing through c_j .

The fact that the action of G_s defined above does not necessarily preserve the convexity of Δ can be seen from the very simple example given in [PVuN11, Section 2.2] and displayed in Figure 3.5a, but can also be visualized in the more subtle example of Figure 3.5b. A marked weighted polygon $(\Delta, \vec{c}, \vec{\epsilon})$ is said to be *admissible* if all the polygons in its G_s -orbit are convex. The G_s -action given in Equation (3.8) yields an action of the set of admissible marked weighted polygons, which commutes with the \mathcal{T} -action defined in Equation (3.6). Therefore, one obtains a $(G_s \times \mathcal{T})$ -action on the set of admissible marked weighted polygons.

For the polygons constructed from semitoric systems, this loss of convexity will not be a problem since the image of each cut starting at a focus-focus value will eventually hit a vertex of the polygon with some good properties, which will ensure admissibility. This is what motivates the following definitions.

If $(\Delta, \vec{c}, \vec{\epsilon})$ is a marked weighted polygon, consider the half-line

$$\mathcal{L}_{(\Delta, \vec{c}, \vec{\epsilon})}^j = \{(x, y) \in \mathbb{R}^2 \mid x = \pi_1(c_j), \epsilon_j y \geq \epsilon_j \pi_2(c_j)\},$$

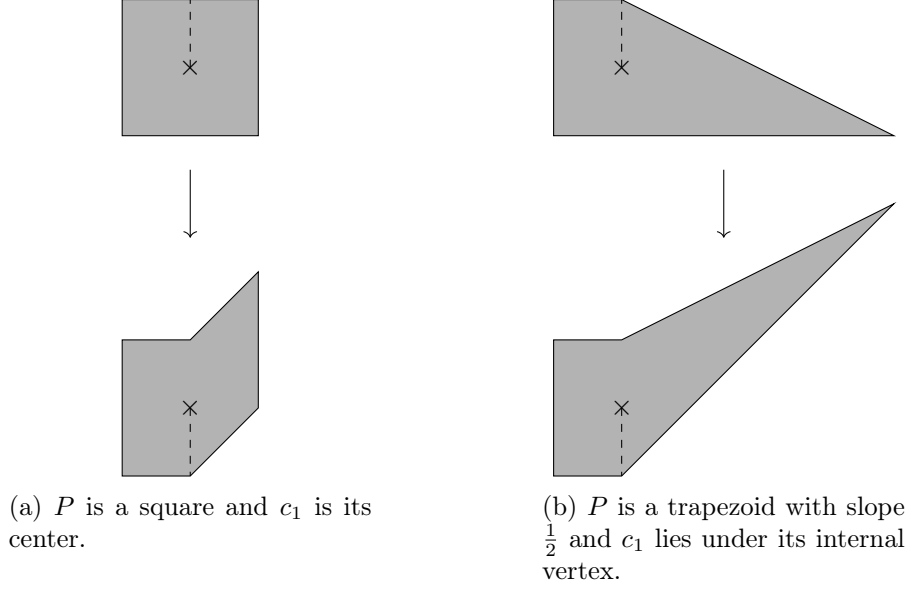


Figure 3.5: In each figure, the top picture displays an element $(P, c_1, 1) \in \mathcal{P}$, and the bottom picture shows its image under the action of $\epsilon'_1 = -1 \in G_1$, see Equation (3.8). In both examples, one can observe that this action breaks convexity.

starting at the point c_j and directed upwards if $\epsilon_j = 1$ and downwards if $\epsilon_j = -1$; we call this half-line a *cut*, and it will be represented as dashed lines in the pictures, such as Figure 3.5. Consider also the union

$$\mathcal{L}_{(\Delta, \vec{c}, \vec{\epsilon})} = \bigcup_{j=1}^s \mathcal{L}_{(\Delta, \vec{c}, \vec{\epsilon})}^j$$

of all these cuts. The next result extends [PVuN09, Lemma 4.2] to the non-simple case, and is stated in [LFP23, Definition 2.10].

Lemma 3.4.3. *Let $(\Delta, \vec{c}, \vec{\epsilon})$ be a marked weighted polygon satisfying the following assumptions:*

1. *each point $q \in \partial\Delta \cap \mathcal{L}_{(\Delta, \vec{c}, \vec{\epsilon})}$ is a vertex of Δ which satisfies either the k -fake or k -hidden Delzant condition (see Definition 3.4.2), where*

$$k = \# \left\{ j \in \{1, \dots, s\} \mid q \in \mathcal{L}_{(\Delta, \vec{c}, \vec{\epsilon})}^j \right\},$$

in which case q is known as a k -fake or k -hidden corner (or vertex), respectively;

2. *all other vertices satisfy the Delzant condition, and are called Delzant corners (or vertices).*

Then it is admissible.

The $(G_s \times \mathcal{T})$ -orbit of a marked weighted polygon $(\Delta, \vec{c}, \vec{\epsilon})$ satisfying the conditions in Lemma 3.4.3, denoted by $[(\Delta, \vec{c}, \vec{\epsilon})]$, is called a *marked semitoric polygon*.

It will also be useful at times, especially in Chapter 4, to talk about unmarked semitoric polygons, which will only contain the information of the respective horizontal positions of the cuts and their directions, or in other words, only the horizontal coordinate $\pi_1(c_j)$ of each marked point c_j and the value of ϵ_j . This corresponds to forgetting the height invariants of the focus-focus points and keeping only the J -value of these points and for each of them, the associated cut direction. Equivalently, one can define an unmarked weighted polygon as the data of $(\Delta, \vec{\lambda}, \vec{\epsilon})$ with $\vec{\lambda} = (\lambda_1, \dots, \lambda_s) \in \mathbb{R}^s$ and define an unmarked semitoric polygon as the $(G_s \times \mathcal{T})$ -orbit of an unmarked weighted polygon satisfying the conditions in Lemma 3.4.3 obtained by using λ_j instead of $\pi_1(c_j)$ in the definition of $\mathcal{L}_{(\Delta, \vec{c}, \vec{\epsilon})}^j$.

The marked semitoric polygon of a semitoric system. Let $(M, \omega, F = (J, H))$ be a semitoric system, and let N_f be its number of focus-focus points; as before, we assume that $N_f > 0$ for the sake of simplicity and refer the reader to [SVuN18, Section 5.2.2] and the discussion following Example 3.4.5 for the case $N_f = 0$. Let $c_j = (x_j, y_j)$, $1 \leq j \leq N_f$ be the corresponding focus-focus values, ordered lexicographically; since we are not requiring the system to be simple, note that these values are not necessarily distinct.

Let $\vec{\epsilon} \in \{-1, 1\}^{N_f}$ and, for every $j \in \{1, \dots, N_f\}$, let $\ell_j^{\epsilon_j}$ be the vertical half-line starting from (x_j, y_j) and going downwards if $\epsilon_j = -1$ and upwards if $\epsilon_j = 1$; consider the union

$$\ell^{\vec{\epsilon}} = \bigcup_{j=1}^{N_f} \ell_j^{\epsilon_j}$$

of all these half-lines. This is a collection of cuts, upwards or downwards, each associated with a given focus-focus point.

As above, let $B_{\text{reg}} \subset F(M)$ be the set of regular values of F ; this set carries an integral affine structure, that is a structure of smooth manifold with transition maps of the form $v \mapsto Av + b$ with $A \in \text{GL}(2, \mathbb{Z})$ and $b \in \mathbb{R}^2$. In the case of B_{reg} , the charts are given by action diffeomorphisms (see Section 3.2). Moreover, \mathbb{R}^2 is endowed with its standard integral affine structure.

The following result originally appeared in [VuN07], but in the statement we essentially adopt the notation and convention from [PPT19]. In [VuN07], there is a one-to-one correspondence between cuts and focus-focus **values** and each point lying on one or several cuts is given a multiplicity according to the number of focus-focus points in the corresponding fibers, while in [PPT19], there is one cut associated with each focus-focus **point**. Both choices come with advantages and drawbacks: the choice made in [VuN07] is better suited to the interpretation in terms of cuts in the set of regular values that we will describe below, while the option taken in [PPT19] directly includes the number of focus-focus points in the polygon and makes more sense when thinking about a system (M, ω, F_t) depending on a parameter t and bifurcating from simple to non-simple, for instance when two focus-focus points are on the same J -fiber but not on the same F_t -fiber for $t \neq 0$, while they lie on the same F_0 -fiber. Indeed, in this example for $t \neq 0$ there would be two marked points and cuts with both conventions, so it is natural to keep these when $t = 0$.

Theorem 3.4.4 ([VuN07, Theorem 3.8]). *There exists a homeomorphism $g_{\vec{\epsilon}} : F(M) \rightarrow \mathbb{R}^2$ of the form*

$$g_{\vec{\epsilon}}(x, y) = \left(x, g_{\vec{\epsilon}}^{(2)}(x, y) \right), \quad \frac{\partial g_{\vec{\epsilon}}^{(2)}}{\partial y} > 0$$

such that

1. the restriction $\tilde{g}_{\vec{\epsilon}}$ of $g_{\vec{\epsilon}}$ to $F(M) \setminus \ell^{\vec{\epsilon}}$ is a diffeomorphism into its image;
2. $\tilde{g}_{\vec{\epsilon}}$ sends the integral affine structure of B_{reg} to the standard integral affine structure of \mathbb{R}^2 ;
3. $\tilde{g}_{\vec{\epsilon}}$ extends to a smooth multi-valued map from B_{reg} to \mathbb{R}^2 and for any $j \in \{1, \dots, N_f\}$

$$\forall c \in \ell_j^{\epsilon_j} \setminus \{c_1, \dots, c_{N_f}\} \quad \lim_{\substack{(x,y) \rightarrow c \\ x < x_j}} d\tilde{g}_{\vec{\epsilon}}(x, y) = T^{k(c)} \lim_{\substack{(x,y) \rightarrow c \\ x > x_j}} d\tilde{g}_{\vec{\epsilon}}(x, y)$$

where $k(c)$ is defined as

$$k(c) = \sum_{\substack{p \in \{1, \dots, N_f\} \\ c \in \ell_p^{\epsilon_p}}} \epsilon_p; \tag{3.10}$$

4. the image $g_{\vec{\epsilon}}(F(M))$ is a rational convex polygon.

Moreover, such a $g_{\vec{e}}$ is unique up to the left composition by an element of \mathcal{T} .

The set $\ell_j^{\epsilon_j} \setminus \{c_1, \dots, c_{N_f}\}$ in this statement is a finite union of intervals, and the function $c \mapsto k(c)$ is constant on each of these intervals. This constant is called the *wall-crossing index* of the interval in [PPT19], see Definition 2.9 and Figure 1 in that paper.

The map $\mu_{\vec{e}} = g_{\vec{e}} \circ F$, with $g_{\vec{e}}$ as in Theorem 3.4.4, is called a *generalized toric momentum map* or *cartographic homeomorphism*. The triple

$$(\Delta_{\vec{e}}, \vec{c} = (g_{\vec{e}}(x_1, y_1), \dots, g_{\vec{e}}(x_{N_f}, y_{N_f})), \vec{e}), \quad (3.11)$$

where $\Delta_{\vec{e}} = g_{\vec{e}}(F(M)) = \mu_{\vec{e}}(M)$, is a marked weighted polygon satisfying the assumptions of Lemma 3.4.3. So one can define the *marked semitoric polygon* $\Delta_{(M, \omega, F)}$ of (M, ω, F) as the $(G_{N_f} \times \mathcal{T})$ -orbit of the marked weighted polygon (3.11).

The idea behind the construction of such a generalized toric momentum map goes as follows. Since it is more visual in the simple case, we may assume for a moment that our semitoric system is simple. Let $c \in B_{\text{reg}}$ be a regular value of F , and choose a pair of action variables of the form (J, L) near c . They cannot be extended over the whole of B_{reg} because of the non-trivial monodromy induced by the focus-focus points discussed earlier. Nevertheless, the action variables (J, L) can be extended over the simply connected set $B_{\text{reg}} \setminus \ell^{\vec{e}}$. By using the normal forms from Theorem 3.2.5 and from [MZ04] to deal with the singularities of elliptic type, they can in fact be extended over $F(M) \setminus \ell^{\vec{e}}$. Taking into account the monodromy to glue back along the cuts allows one to obtain the generalized toric momentum map $\mu_{\vec{e}}$; this gluing rule corresponds to the third item in Theorem 3.4.4. Of course $\mu_{\vec{e}}$ depends on the choice of the signs \vec{e} encoding the cut directions, and changing \vec{e} to $\vec{e}^* \ast \vec{e}$ amounts to acting by $\vec{e}^* \in G_{N_f}$ on the marked weighted polygon $(\mu_{\vec{e}}(M), \vec{c}, \vec{e})$ as in Equation (3.8). Moreover, $\mu_{\vec{e}}$ also depends on the initial choice of action variables (J, L) , and any other choice (J, L') is the image of (J, L) by a transformation $\tau \in \mathcal{T}$, and the resulting marked weighted polygon is obtained as the image of $(\mu_{\vec{e}}(M), \vec{c}, \vec{e})$ under the action of τ as in Equation (3.6).

Example 3.4.5. Let $(M, \omega, (J, H_t))$ be the coupled angular momenta system as in Example 3.3.4. Some representatives of the marked semitoric polygon of this system for $t \in (t^-, t^+)$ are displayed in Figure 3.6.

In the absence of focus-focus singularities ($N_f = 0$), the system is of toric type and its marked semitoric polygon is simply obtained by extending any initial set of action variables of the form (J, L) over the whole of $F(M)$. Of course there is no cut anymore, so only the action of \mathcal{T} , corresponding to the initial choice of action variables, remains. We will use the notation $[(\Delta, \emptyset, \emptyset)]$ for this marked (or unmarked) semitoric polygon. If the system is toric, then there is a preferred representative, since H is also an action variable: the Delzant polygon of the system.

Note that the fact that two marked semitoric polygons which differ by a horizontal translation correspond to non-isomorphic semitoric systems comes from the fact that isomorphisms must respect the first component of the momentum map. But in practice, by starting from a system (M, ω, J) and adding a constant to J , we obtain a new system whose marked semitoric polygon is the image of the original one by a horizontal translation. This will actually be important in Chapter 4.

The height invariant. The marked semitoric polygon of a semitoric system is a convenient object combining the polygon with first coordinates of its cuts, number of focus-focus points and height invariants. Indeed, the latter can be computed from this marked semitoric polygon as follows. Let $(\Delta, \vec{c}, \vec{e})$ be a representative of the marked semitoric polygon of $(M, \omega, F = (J, H))$, and for $j \in \{1, \dots, N_f\}$, let

$$h_j = b_j - \min\{b \mid (a_j, b) \in \Delta\} > 0$$

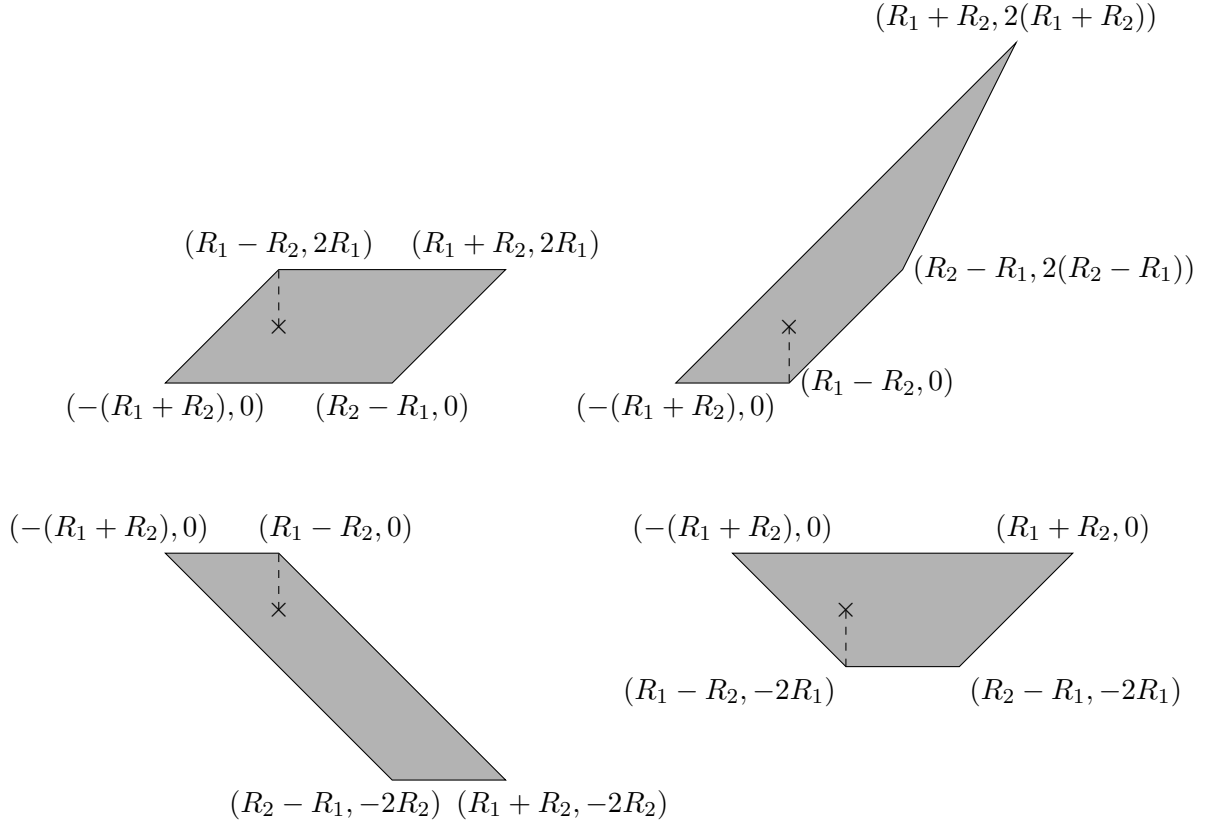


Figure 3.6: A few representatives of the marked semitoric polygon for the coupled angular momenta system of Example 3.3.4. The polygons in the bottom row are obtained from those in the top row by applying the global transformation $T^{-1} \in \mathcal{T}$ with T as in Equation (3.5). The polygons in the rightmost column are obtained from those in the leftmost column by changing the cut direction from upwards ($\epsilon_1 = 1$) to downwards ($\epsilon_1 = -1$), see Equation (3.8).

be the height of the marked point $c_j = (a_j, b_j)$ in the polygon Δ . The value of h_j does not depend on the choice of representative $(\Delta, \vec{c}, \vec{\epsilon})$. Indeed, let $(\tilde{\Delta}, \vec{\tilde{c}}, \vec{\tilde{\epsilon}})$ be another representative of the marked semitoric polygon, and let

$$\psi = \left(\vec{\epsilon}^t, \left(T^\ell, \begin{pmatrix} 0 \\ t \end{pmatrix} \right) \right) \in G_{N_f} \times \mathcal{T}$$

be such that $(\tilde{\Delta}, \vec{\tilde{c}}, \vec{\tilde{\epsilon}}) = \psi \cdot (\Delta, \vec{c}, \vec{\epsilon})$. Moreover, let $b_- = \min\{b \mid (a_j, b) \in \Delta\}$. Then

$$\tilde{c}_j = \left(a_j, \ell a_j + b_j + t + \sum_{p=1}^{j-1} u_p(a_j - a_p) \right), \quad \min\{b \mid (a_j, b) \in \tilde{\Delta}\} = \ell a_j + b_- + t + \sum_{p=1}^{j-1} u_p(a_j - a_p)$$

and so

$$\tilde{b}_j - \min\{b \mid (a_j, b) \in \tilde{\Delta}\} = b_j - b_- = h_j.$$

This common value h_j is the *height invariant* associated with c_j .

In fact, the height invariant h_j of the focus-focus point (x_j, y_j) can also be computed without referring to a generalized toric momentum map. Indeed, let $(M_{x_j}^{\text{red}}, \omega_{x_j}^{\text{red}})$ be the symplectic reduction of M by the S^1 -action generated by J at level $J = x_j$. Then $2\pi h_j$ is the symplectic area, with respect to $\omega_{x_j}^{\text{red}}$, of $\{[m] \in M_{x_j}^{\text{red}} \mid H(m) < y_j\}$. There is another interpretation of this height invariant, which is depicted at the end of Section 3.4.2.

Example 3.4.6. The height invariant of the unique focus-focus point in the coupled angular momenta system $(M, \omega, (J, H_t))$, $t \in (t^-, t^+)$, of Example 3.3.4 was computed in [ADH20, Theorem 5.1], and equals

$$h = 2 \min(R_1, R_2) + \frac{R_1 \left(\sqrt{C(t, R)} - 2Rt \arctan_{\frac{\pi}{2}} \left(\frac{\sqrt{C(t, R)}}{R-t} \right) - 2t \arctan_{\frac{\pi}{2}} \left(\frac{\sqrt{C(t, R)}}{(1-2t)R+t} \right) \right)}{\pi t} \quad (3.12)$$

with $R = \frac{R_2}{R_1}$ and

$$C(t, R) = 2Rt - t^2 - R^2(1 - 2t)^2 = (1 + 4R^2)(t - t^-)(t^+ - t). \quad (3.13)$$

Here $\arctan_{\frac{\pi}{2}}$ is the (discontinuous) determination of the arctangent yielding angles in $(0, \pi)$, namely

$$\arctan_{\frac{\pi}{2}} u = \begin{cases} \arctan u & \text{if } u \geq 0, \\ \arctan u + \pi & \text{if } u \leq 0. \end{cases}$$

In practice, to construct the marked semitoric polygon of a semitoric system, one does not need to come up with an explicit generalized toric momentum map. It suffices to apply the following recipe, based on [VuN07, Theorem 5.3] in which the Duistermaat-Heckman function ρ_J of J (see Section 5.4.2) is computed.

1. Choose the directions of the cuts. Their horizontal locations are given by the first coordinates of the marked points, which are the values of J at each focus-focus point.
2. Let J_{\min} be the global minimum of J . Assume for simplicity that this minimum is attained at a single elliptic-elliptic point. Then Δ will start with a vertex located at $x = J_{\min}$. The angular sector formed by the two edges emanating from this vertex is determined up to the action of an element of \mathcal{T} from the weights of the S^1 -action at the point.
3. Extend the edges of this piece of polygon until they hit a vertical line containing the J -values $J(p_i)$ of one or several elliptic-elliptic or focus-focus point p_1, \dots, p_d , and let c be the corresponding intersection point. Then the change of slopes between the incoming edge and the outgoing edge at c is obtained by summing contributions coming from each p_i , and more precisely:

- (a) if p_i is elliptic-elliptic, its contribution is determined by the weights of the S^1 -action at p_i ;
- (b) if p_i is focus-focus, this contribution equals $k(c)$ from Equation (3.10).

Notice that we have not been precise about the sign of this change of slopes. We do not need to, since we know that Δ must be convex.

4. Continue until Δ is fully drawn.
5. Compute the height of each marked point in Δ by computing a symplectic volume as explained above. Since the first coordinate of each marked point is known, this allows one to locate all the marked points.

If J_{\min} is attained on a fixed surface, the polygon Δ will start with a vertical line segment of length the symplectic area of this surface divided by 2π . The first ordinate of the elements of this segment is $x = J_{\min}$. The difference of the slopes of the edges emanating from the two endpoints of this segment is a bit more complicated to compute, but one can proceed as follows. If the global maximum J_{\max} of J is attained at a single elliptic-elliptic point, then we can apply the same strategy as above but starting from this maximum instead of the minimum of J . Otherwise, the aforementioned difference of slopes will be determined by the length of the vertical line segment with first ordinate J_{\max} . Indeed, the lengths of these two walls are the values of the Duistermaat-Heckman function ρ_J at $x = J_{\min}$ and $x = J_{\max}$, and the changes of slopes computed in Step 3 correspond to changes of slopes between two consecutive affine pieces of ρ_J .

Now we come back to the case of a simple semitoric system $(M, \omega, F = (J, H))$ and define the remaining symplectic invariants (Taylor series and twisting index) in this context. In order to do so, we adopt the notation and presentation of Sections 2.4 and 2.5 from [LFVuN21], but in a slightly different order.

3.4.2 The Taylor series invariant

The Taylor series invariant is a formal series associated with each focus-focus point that describes the singular dynamics near this point. More precisely, it is obtained as the Taylor expansion of a canonical regularization of a singular action variable constructed near the singular fiber.

Let $m_0 \in M$ be a focus-focus point; for the sake of simplicity, we assume that $F(m_0) = 0$ (which amounts to changing F by a constant). Let $\Lambda_0 = F^{-1}(0)$ be the corresponding singular fiber, which is a torus pinched at m_0 only since the system is simple.

Let $\Omega \subset M$ be a small neighborhood of m_0 on which Eliasson's normal form from Theorem 3.2.5 holds and such that $F(\Omega)$ is simply connected, and let (x_1, x_2, ξ_1, ξ_2) be the Darboux coordinates given in this theorem. This normal form implies that there exists a smooth function $f_r : \mathbb{R}^2 \rightarrow \mathbb{R}$ such that, in these coordinates

$$f_r(J, H) = x_1\xi_1 + x_2\xi_2.$$

This function is unique up to sign, addition of a constant, and addition of a function which is flat at the origin; the function f_r obtained by imposing $f_r(0) = 0$ and $\partial_y f_r > 0$ is called the *Eliasson function*. It is only unique up to addition of a flat function, but in what follows only its Taylor expansion at the origin will matter. The corresponding Hamiltonian $H_r = f_r(J, H)$ is called the *radial* Hamiltonian; its trajectories in $\Lambda_0 \cap \Omega$ are straight lines going to the origin in the coordinates (x_1, x_2, ξ_1, ξ_2) . The map $q = (J, H_r)$ must coincide (up to addition of a flat function to f_r) with the quadratic map Q in Eliasson's normal form (Theorem 3.2.5) and hence is called the Eliasson momentum map.

Let $\Omega_0 \subset M$ be a saturated neighborhood of Λ_0 , and let $B \subset F(\Omega_0)$ be a small ball centered at the origin in \mathbb{R}^2 such that $B \setminus \{0\} \subset B_{\text{reg}}$. Let $U \subset B \setminus \{0\}$ be a simply connected open set

such that $U \subset F(\Omega)$ and U is contained in the right half-plane $\{(x, y) \in \mathbb{R}^2 \mid x > 0\}$, and choose action coordinates in $F^{-1}(U)$ of the form (J, L) . Extend L over the simply connected open set $F(\Omega) \setminus \ell$ where ℓ is the vertical half-line $\{(0, y) \in \mathbb{R}^2 \mid y \geq 0\}$. Since X_L is tangent to the fibers of F , it decomposes uniquely as

$$X_L = \tilde{\tau}_1 X_J + \tilde{\tau}_2 X_{H_r} \quad (3.14)$$

where $\tilde{\tau}_j = \tau_j \circ F$ for $j = 1, 2$, with τ_j a smooth function on $F(\Omega) \setminus \ell$.

Let \log be the determination of the complex logarithm obtained by choosing arguments in $(-\frac{3\pi}{2}, \frac{\pi}{2}]$ (which means that the cut coincides with the half-line $\{z \in \mathbb{C} \mid \Re(z) = 0, \Im(z) \geq 0\}$). The following result is the crucial step in obtaining a nice regularized action from L .

Proposition 3.4.7 ([VuN03], [SVuN18, Lemma 4.46]). *The functions*

$$\begin{cases} \sigma_1 : c \mapsto \tau_1(c) + \frac{1}{2\pi} \Im(\log(c_1 + i f_r(c_1, c_2))), \\ \sigma_2 : c \mapsto \tau_2(c) + \frac{1}{2\pi} \Re(\log(c_1 + i f_r(c_1, c_2))) \end{cases}$$

extend smoothly at $c = (0, 0)$.

Now, write $L = \hat{L} \circ q$ where $q = (J, H_r)$ is the Eliasson momentum map and \hat{L} is smooth. Equation (3.14) yields

$$\tilde{\tau}_1 = \frac{\partial \hat{L}}{\partial X} \circ q, \quad \tilde{\tau}_2 = \frac{\partial \hat{L}}{\partial Y} \circ q,$$

hence Proposition 3.4.7 implies that the function

$$S : \mathbb{R}^2 \rightarrow \mathbb{R}, \quad (X, Y) \mapsto \hat{L}(X, Y) + \Im(w \log w - w)$$

with $w = X + iY$, extends to a smooth function S in a neighborhood of the origin, with $(g^{-1})^* dS = \sigma_1 dc_1 + \sigma_2 dc_2$ where g is the local diffeomorphism from Theorem 3.2.5 associated with f_r , in other words $g^{-1}(x, y) = (x, f_r(x, y))$. Let

$$S^\infty = \sum_{\ell, m \geq 0} S_{\ell, m} X^\ell Y^m$$

be the Taylor series of S at the origin.

Definition 3.4.8. The *Taylor series invariant* associated with m_0 is the equivalence class $[S^\infty]$ of S^∞ in $\mathbb{R}[[X, Y]]/(\mathbb{R} \oplus \mathbb{Z}X)$. The first terms $[S_{1,0}] \in \mathbb{R}/\mathbb{Z}$ and $S_{0,1} \in \mathbb{R}$ are called the *linear invariants* of this Taylor series invariant.

The action L being defined only up to a constant term, it is natural to forget the term $S_{0,0}$ in the actual invariant; moreover it is clear from the definition of σ_1 that only the class of $S_{1,0}$ modulo \mathbb{Z} should be considered. It is proved in [VuN03, Theorem 2.1] that $[S^\infty]$ is a complete symplectic invariant for the singular foliation defined by F in a neighborhood of Λ_0 .

Example 3.4.9. The Taylor series invariant of the coupled angular momenta system $(M, \omega, (J, H_t))$, $t \in (t^-, t^+)$ of Example 3.3.4 was computed in [ADH20]. Here we only reproduce the linear invariants, and refer the reader to [ADH20, Theorem A] for more details:

$$S_{1,0} = \frac{1}{2\pi} \arctan \left(\frac{(2t-1)R^2 - R(1+t) + t}{(1-R)\sqrt{C(t, R)}} \right), \quad S_{0,1} = \frac{1}{2\pi} \ln \left(\frac{4R_1^{\frac{5}{2}} C(t, R)^{\frac{3}{2}}}{R_2^{\frac{3}{2}} (1-t)t^2} \right) \quad (3.15)$$

with $R = \frac{R_2}{R_1}$ and $C(t, R)$ as in Equation (3.13).

The functions τ_1 and τ_2 also have an interpretation as “periods” for some dynamics related to the Hamiltonian flows of J and H_r , as was originally explained in [VN00].

The height invariant can also be interpreted in this context, using the constant term $S_{0,0}$ that was discarded in the invariant $[S^\infty]$. Indeed, we may extend the action L which was used to define S^∞ so that it is well-defined where H reaches its minimum on $J^{-1}(0)$, and modify it by a constant so that it vanishes there. With this choice of L , $S_{0,0}$ is the height invariant of the focus-focus point m_0 .

As already stated, we will not construct the Taylor series invariant in the non-simple case, but we still give a quick idea of its nature. The idea of the construction of this invariant was sketched at the end of [VuN03] and the corresponding semi-local symplectic classification was obtained in [PT19]. Roughly, for each focus-focus fiber containing d focus-focus points m_1, \dots, m_d , the invariant is given by d formal series. One of them is the analogue of $[S^\infty]$: it is constructed by combining the regularizations of analogues of the functions τ_1 and τ_2 from Equation (3.14) constructed near every focus-focus point m_i . The $d - 1$ remaining Taylor series encode how the Eliasson normal forms near each m_i are related. In fact one has to be careful because the construction of these Taylor series depends on the ordering m_1, \dots, m_d of the singular points, but the actual invariant does not. We refer the reader to [PT19] or [PPT19, Section 2.2] for more details.

3.4.3 Twisting numbers and twisting index

Keeping the same notation as in the previous section, note that action variables of the form (J, L) on $U \subset F(\Omega)$ are not unique, and that if (J, L) and (J, L') are two sets of such action variables, then there exist an integer n and a real number c such that $L' = L + nJ + c$. The twisting number associated with m_0 is the integer n appearing in this relation for an appropriate choice of L and L' that we describe now. One is local and reflects the singular dynamics near the focus-focus fiber, and is called the *privileged action variable* L_{priv} ; the other comes from the global choice of a generalized toric momentum map. More precisely, let $\vec{\epsilon} \in \{-1, 1\}^{N_f}$, let $g_{\vec{\epsilon}}$ be as in Theorem 3.4.4, and let $\mu_{\vec{\epsilon}} = g_{\vec{\epsilon}} \circ F$ be the corresponding generalized toric momentum map. Since U is contained in the right half-plane, it does not intersect the cut above or below $F(m_0) = 0$, so by construction $\mu_{\vec{\epsilon}}$ is a local toric momentum map on U , with first component J and second component $L_{\vec{\epsilon}}$. The reference action variable that we choose is this $L_{\vec{\epsilon}}$.

The privileged action variable L_{priv} is a bit more involved to describe. Consider action variables of the form (J, L) on U , and extend L to $F(\Omega) \setminus \ell$ as in the previous section. Let σ_1, σ_2 be the functions of Proposition 3.4.7 applied to τ_1, τ_2 appearing in the decomposition (3.14) for X_L . By this proposition, the value $\sigma_1(0)$ of σ_1 at the origin is well-defined, and this value depends only on L . In fact, the integer part of $\sigma_1(0)$ does depend on L but not its fractional part: if σ'_1 is associated with the action variable $L' = L + nJ + c$ with $n \in \mathbb{Z}$ and $c \in \mathbb{R}$, then one readily checks that $\sigma'_1(0) = \sigma_1(0) + n$. We say that $L = L_{\text{priv}}$ is a *privileged action variable* when $\sigma_1(0) \in [0, 1)$, that is when the integer part of $\sigma_1(0)$ vanishes; in this case we write $\sigma_1^{\text{priv}}(0)$ for $\sigma_1(0)$. The action variable L_{priv} is only defined up to addition of a constant, but this constant does not matter in the following definition of the twisting number.

Definition 3.4.10. The *twisting number* associated with m_0 and $g_{\vec{\epsilon}}$ is the unique integer p such that $dL_{\vec{\epsilon}} = dL_{\text{priv}} + p dJ$ on U .

This twisting number is not the actual symplectic invariant, as it depends on the choice of $\vec{\epsilon}$ and of an associated generalized toric momentum map $\mu_{\vec{\epsilon}}$, or in other words on the choice of a representative $(\Delta, \vec{\epsilon}, \vec{e})$ of the marked semitoric polygon of the system. Hence we need to understand how the action of $G_{N_f} \times \mathcal{T}$ impacts the twisting number. So we fix such a representative $(\Delta, \vec{\epsilon}, \vec{e})$ and investigate the effect of the two actions corresponding to the change of initial action variables and the change of cut directions, respectively.

First, let $\tau \in \mathcal{T}$, and let $k \in \mathbb{Z}$ be such that the linear part of τ equals T^k . Let $\mu_{\vec{\epsilon}} = g_{\vec{\epsilon}} \circ F = (J, L_{\vec{\epsilon}})$ and $\mu'_{\vec{\epsilon}} = g'_{\vec{\epsilon}} \circ F = (J, L'_{\vec{\epsilon}}) = \tau \circ \mu_{\vec{\epsilon}}$; then $dL'_{\vec{\epsilon}} = dL_{\vec{\epsilon}} + k dJ$, so if p is the twisting number associated with m_0 and $g_{\vec{\epsilon}}$, the twisting number associated with m_0 and $g'_{\vec{\epsilon}}$ is $p + k$.

Second, let $\vec{\epsilon}' \in \{-1, 1\}^{N_f}$, and let $\vec{u}, \vec{\lambda}$ be as in Equation (3.9), so that $\mu_{\vec{\epsilon}' * \vec{\epsilon}} = t_{\vec{u}, \vec{\lambda}} \circ \mu_{\vec{\epsilon}}$. Assume that the marked point corresponding to m_0 in $(\Delta, \vec{c}, \vec{\epsilon})$ is c_j (in other words that $c_j = \mu_{\vec{\epsilon}}(m_0)$). Then one readily checks, using for instance Equation (3.7), that on U

$$L_{\vec{\epsilon}' * \vec{\epsilon}} = L_{\vec{\epsilon}} + (u_1 + \dots + u_j)J - (\lambda_1 + \dots + \lambda_j);$$

therefore $dL_{\vec{\epsilon}' * \vec{\epsilon}} = dL_{\vec{\epsilon}} + (u_1 + \dots + u_j)dJ$, so the twisting number associated with m_0 and $g_{\vec{\epsilon}' * \vec{\epsilon}}$ is $p + u_1 + \dots + u_j$.

Summing up, if p_1, \dots, p_{N_f} are the twisting indices associated with the focus-focus points m_1, \dots, m_{N_f} respectively and a representative $(\Delta, \vec{c}, \vec{\epsilon})$ of the marked semitoric polygon of (M, ω, F) , and if $(\vec{\epsilon}', \tau)$ is an element of $G_{N_f} \times \mathcal{T}$, then the twisting indices associated with m_1, \dots, m_{N_f} and the representative $(\vec{\epsilon}', \tau) \cdot (\Delta, \vec{c}, \vec{\epsilon})$ (see Equations (3.6) and (3.8)) are

$$p_1 + k + u_1, p_2 + k + u_1 + u_2, \dots, p_{N_f} + k + u_1 + \dots + u_{N_f}$$

if the linear part of τ is T^k . This leads to the following definition.

Definition 3.4.11. The *twisting index* of the semitoric system $(M, \omega, F = (J, H))$ is the $(G_{N_f} \times \mathcal{T})$ -orbit of $(\Delta, \vec{c}, \vec{\epsilon}, \vec{p})$, where $(\Delta, \vec{c}, \vec{\epsilon})$ is a representative of the marked semitoric polygon of (M, ω, F) and $\vec{p} = (p_1, \dots, p_{N_f})$ is the corresponding collection of twisting numbers, under the action given by:

$$\forall (\vec{\epsilon}', \tau) \in G_{N_f} \times \mathcal{T}, \quad (\vec{\epsilon}', \tau) \cdot (\Delta, \vec{c}, \vec{\epsilon}, \vec{p}) = \left(t_{\vec{u}, \vec{\lambda}} \circ \tau(\Delta), t_{\vec{u}, \vec{\lambda}} \circ \tau(\vec{c}), \vec{\epsilon}' * \vec{\epsilon}, \vec{p}' \right) \quad (3.16)$$

where $\vec{u}, \vec{\lambda}$ are as in Equation (3.9) and where

$$\vec{p}' = (p_1 + k + u_1, p_2 + k + u_1 + u_2, \dots, p_{N_f} + k + u_1 + \dots + u_{N_f})$$

with k such that the linear part of τ is T^k .

This invariant is sometimes also called the decorated semitoric polygon invariant of the system, see [SVuN18, Definition 5.38].

This definition differs from the original definition [PVuN09, Definition 5.9] for two reasons. The first one is that the authors had seemingly missed the effect of changing the cut direction associated with a focus-focus point c_i with $i < j$ (this is also discussed in [AHP23], where several equivalent definitions of the twisting index are stated). In systems with only one focus-focus point, as is the case for many explicit examples, this difference is not visible, which explains why this problem was overlooked. The second one is more subtle, and is only a matter of choice: in the original definition, the privileged action was defined in such a way that it changed when the cut at $c_j = \mu_{\vec{\epsilon}}(m_0)$ changed (in other words it depended on the choice of ϵ_j), while here, following the approach of [LFVuN21], it does not. The advantage of the choice made in [PVuN09] is that the twisting number did not change when changing ϵ_j while here, it does; however we prefer the choice that we have made here because the privileged action is then a completely local object, not depending on the global choice of a generalized toric momentum map. Even in the case of a system with a unique focus-focus point, this difference is visible when considering representatives of the marked semitoric polygon with downwards cut ($\epsilon = -1$) (but it is not visible when working with an upwards cut).

Example 3.4.12. Let $(M, \omega, (J, H_t))$ be the coupled angular momenta system from Example 3.3.4 with $t^- < t < t^+$. Then the twisting number associated with the only focus-focus point

and the marked semitoric polygon in the top left corner of Figure 3.6 vanishes; this was proved in [ADH20]. This determines the twisting index of the system. For instance, the twisting numbers associated with the other polygons from Figure 3.6 are 1 (top right), -1 (bottom left) and 0 (bottom right). Note that for the two polygons in the rightmost column, these numbers differ (by 1) from the twisting numbers displayed in [ADH20, Figure 15] because of the different choice made here (see the above discussion).

The twisting index and Taylor series invariants are in fact related, as was understood independently in [PPT19] and [LFVuN21]. In order to understand this relation, consider any pair of action variables of the form (J, L) on U , and let $q \in \mathbb{Z}$ and $c \in \mathbb{R}$ be such that $L = L_{\text{priv}} + nJ + c$. Then $\sigma_1(0) = \sigma_1^{\text{priv}}(0) + n$. Let $\vec{\epsilon} \in \{-1, 1\}^{N_f}$ and let, as above, $L_{\vec{\epsilon}}$ be the action variable associated with a generalized toric momentum map $\mu_{\vec{\epsilon}} = g_{\vec{\epsilon}} \circ F$ coming from Theorem 3.4.4. Let p be the twisting number associated with m_0 and $g_{\vec{\epsilon}}$, see Definition 3.4.10. Then

$$dL_{\vec{\epsilon}} = dL_{\text{priv}} + p dJ = dL + (p - n)dJ.$$

Hence, when $L = L_{\vec{\epsilon}}$ we get $n = p$ and obtain the following link between the Taylor series and twisting index invariants.

Proposition 3.4.13 ([LFVuN21, Proposition 2.14]). *Choose action variables of the form (J, L) on U . The linear terms in the Taylor series invariant and the functions σ_1, σ_2 associated with L are related by:*

$$S_{0,1} = \sigma_1(0) = \sigma_1^{\text{priv}}(0) + p, \quad S_{1,0} = \sigma_2(0),$$

where $p \in \mathbb{Z}$ is the twisting number associated with m_0 and $g_{\vec{\epsilon}}$, with $\vec{\epsilon}$ such that L coincides with $L_{\vec{\epsilon}}$ on U . In particular, $[S_{0,1}] = \sigma_1(0)$ modulo \mathbb{Z} , and $p = \lfloor \sigma_1(0) \rfloor$.

Of course the fact that $[S_{0,1}] = \sigma_1(0)$ modulo \mathbb{Z} was already present in the definition of $[S^\infty]$, so the interesting information is that $p = \lfloor \sigma_1(0) \rfloor$. One can wonder why the link between these two invariants was seemingly overlooked for several years. One reason is that, historically, the semi-global classification near a focus-focus point, achieved through the Taylor series invariant in [VuN03], preceded the classification of semitoric systems; since in this classification the linear term $S_{0,1}$ of the Taylor series was only relevant through its fractional part, it was natural to discard its integer part, which is related to the twisting number.

As for the Taylor series invariant, we will not describe the twisting index invariant in the non-simple case. As in Proposition 3.4.13, in this case the twisting numbers are obtained from the integer parts of certain coefficients of the Taylor series invariant. We refer the reader to [PPT19, Section 4.4] for more details.

3.4.4 Complete invariant and symplectic classification

Let $(M, \omega, F = (J, H))$ be a simple semitoric system; by combining the above invariants, one obtains the complete symplectic invariant of $(M, \omega, F = (J, H))$, which is the main character of the classification results from [PVuN09, PVuN11].

Definition 3.4.14. The *complete symplectic invariant* of the simple semitoric system $(M, \omega, F = (J, H))$ is the $(G_{N_f} \times \mathcal{T})$ -orbit of $(\Delta, \vec{c}, \vec{\epsilon}, \vec{p}, \overrightarrow{[S^\infty]})$ where $(\Delta, \vec{c}, \vec{\epsilon})$ is a representative of the marked semitoric polygon of (M, ω, F) , $\vec{p} = (p_1, \dots, p_{N_f})$ is the corresponding collection of twisting numbers, and $\overrightarrow{[S^\infty]} = ([S_1^\infty], \dots, [S_{N_f}^\infty])$ where $[S_j^\infty]$ is the Taylor series invariant of the focus-focus point m_j . Here $G_{N_f} \times \mathcal{T}$ acts on $(\Delta, \vec{c}, \vec{\epsilon}, \vec{p})$ as in Equation (3.16) and acts trivially on $\overrightarrow{[S^\infty]}$.

The following definition is adapted from [PVuN11, Definition 4.5].

Definition 3.4.15. A *complete semitoric ingredient* is the $(G_{N_f} \times \mathcal{T})$ -orbit of $(\Delta, \vec{c}, \vec{\epsilon}, \vec{p}, \vec{[S]})$, where the action on $(\Delta, \vec{c}, \vec{\epsilon}, \vec{p})$ is given by Equation (3.16) and the action on $\vec{[S]}$ is trivial, and

1. $N_f \geq 0$ is an integer;
2. $(\Delta, \vec{c}, \vec{\epsilon})$ is a marked semitoric polygon (a marked weighted polygon satisfying the conditions of Lemma 3.4.3);
3. $\vec{p} = (p_1, \dots, p_{N_f}) \in \mathbb{Z}^{N_f}$ is an N_f -tuple of integers;
4. $\vec{[S]} = (S_1, \dots, S_{N_f})$ where each S_j , $j = 1, \dots, N_f$, is an equivalence class of formal series in $\mathbb{R}[[X, Y]]/(\mathbb{R} \oplus \mathbb{Z}X)$.

The precise result of [PVuN09, PVuN11] is the following.

Theorem 3.4.16 ([PVuN09, Theorem 6.2] and [PVuN11, Theorem 4.6]). *Two semitoric systems are isomorphic if and only if they have the same complete symplectic invariant. Moreover, given any complete semitoric ingredient, there exists a semitoric system whose complete symplectic invariant coincides with this ingredient.*

The second part of this statement, namely the construction of a semitoric system with given symplectic invariants described in [PVuN11], is divided into the following steps:

1. from the data of the marked semitoric polygon $(\Delta, \vec{c}, \vec{\epsilon})$, construct a symplectic manifold and a momentum map over Δ minus the cuts, by symplectically gluing local models coming from normal forms at elliptic-elliptic, elliptic-regular and regular points;
2. over each marked point c_j , construct a local model (manifold and momentum map) with focus-focus singularity whose Taylor series invariant coincides with $[S_j^\infty]$, using the classification result obtained in [VuN03]. Then compose the momentum map on the left with an appropriate integral affine transformation obtained from the twisting number p_j , and glue this model symplectically to the previous model;
3. finally, it only remains to study what happens at the parts of the cuts that are not concerned by the previous step. For this it suffices, for the j -th cut, to mimic the construction of the first step but for the polygon $t_{\pi_1(c_j)}(\Delta)$ where $t_{\pi_1(c_j)}$ is as in Equation (3.7). By symplectically gluing all the local models in these three steps, one obtains a global momentum map μ ;
4. the momentum map μ is not smooth; compose it on the left with an appropriate homeomorphism to obtain the smooth momentum map (J, H) of a semitoric system with the desired invariants.

We insist once again on the fact that the classification result from Theorem 3.4.16 has been extended to the non-simple case in [PPT19], but we will not describe this case here since it would require to introduce more objects and notation and is not necessary for the next chapters.

3.5 Hamiltonian S^1 -spaces

In Chapter 4, we will exploit a structure underlying compact semitoric systems, and studied in [Kar99].

Definition 3.5.1. A *Hamiltonian S^1 -space* is a triple (M, ω, J) where (M, ω) is a compact, connected four-dimensional symplectic manifold and J is the momentum map for an effective Hamiltonian S^1 -action.

In [Kar99], Karshon constructed a labeled graph which is a complete invariant of Hamiltonian S^1 -spaces: two Hamiltonian S^1 -spaces (M, ω, J) and (M', ω', J') have the same Karshon graph if and only if there exists a symplectomorphism $\Phi : (M, \omega) \rightarrow (M', \omega')$ such that $J = J' \circ \Phi$. As we will recall below, if $(M, \omega, F = (J, H))$ is a compact semitoric system, the Karshon graph of the Hamiltonian S^1 -space (M, ω, J) can be obtained from the marked semitoric polygon of (M, ω, F) .

Before defining this graph, let us recall some properties and notation. Let (M, ω, J) be a Hamiltonian S^1 -space and let M^{S^1} be the fixed point set for the S^1 -action generated by J . Then each component of M^{S^1} is either an isolated fixed point or a symplectic surface; the latter can only happen at the global minimum or maximum of J . For $k \geq 2$, let \mathbb{Z}_k be the cyclic subgroup of S^1 of order k ; each component of the closure of the set of points with stabilizer \mathbb{Z}_k is a closed symplectic sphere, called a \mathbb{Z}_k -sphere. On each \mathbb{Z}_k -sphere, the group S^1/\mathbb{Z}_k acts with two fixed points which are also isolated fixed points of the S^1 -action and are called the *poles* of the \mathbb{Z}_k -sphere.

Given a fixed point $p \in M^{S^1}$, one can determine whether it is a pole of a \mathbb{Z}_k -sphere by investigating the weights of J at p . By [Kar99, Corollary A.7], near p , there exist local complex coordinates z_1, z_2 on \mathbb{C}^2 with symplectic form $\omega_{\mathbb{C}} = \frac{i}{2}(dz_1 \wedge d\bar{z}_1 + dz_2 \wedge d\bar{z}_2)$ and relatively prime integers $m, n \in \mathbb{Z}$, called the (isotropy) *weights* of J at p , such that

$$J = J(p) + \frac{m}{2}|z_1|^2 + \frac{n}{2}|z_2|^2. \quad (3.17)$$

If $|m| \geq 2$ (respectively $|n| \geq 2$) then p is a pole of a $\mathbb{Z}_{|m|}$ -sphere (respectively $\mathbb{Z}_{|n|}$ -sphere).

The *Karshon graph* of (M, ω, J) consists of two types of vertices: each isolated fixed point $p \in M^{S^1}$ corresponds to a regular vertex of the graph, labeled with the value $J(p)$, while each fixed surface $\Sigma \subset M^{S^1}$ corresponds to a fat vertex of the graph (drawn as a large oval), labeled with the common value $J(\Sigma)$ of its elements, its genus g , and its normalized volume $\frac{1}{2\pi} \int_{\Sigma} \omega$. Any two vertices corresponding to the two poles of the same \mathbb{Z}_k -sphere are joined by an edge labeled with k .

In practice, when drawing such a graph (see for instance the bottom of Figure 3.7), we omit the labels corresponding to J -values and represent these values by the horizontal positions of the vertices. Note that in [Kar99] these values were instead represented by the vertical positions of the vertices.

Let $(M, \omega, F = (J, H))$ be a compact semitoric system. The underlying S^1 -space (M, ω, J) has the property that every fixed surface is a sphere (see [HSS15, Proposition 3.4]). Therefore in this context we will simply omit the genus labels when drawing its Karshon graph. Moreover, the weights of J at any focus-focus point of F are always -1 and 1 (see [Zun02, Theorem 1.2]), so no focus-focus point can be a pole of a \mathbb{Z}_k -sphere. As explained in [HSS15, Section 3], the Karshon graph of (M, ω, J) can be deduced from any representative $(\Delta, \vec{c}, \vec{\epsilon})$ of the marked semitoric polygon of (M, ω, F) as follows:

- the fixed surfaces of J correspond to vertical edges of the polygon (called *vertical walls*), so any such vertical edge yields a fat vertex of the Karshon graph. This vertex is labeled with its J -value and the normalized volume of the fixed surface, which is obtained as the length of the vertical wall;
- the marked points c_1, \dots, c_{N_f} correspond to regular vertices that are not connected to any edge, labeled with their J -values $J(c_\ell)$, $1 \leq \ell \leq N_f$;
- the Delzant and hidden Delzant vertices of Δ correspond to regular vertices, labeled with their J -values;
- each \mathbb{Z}_k -sphere corresponds to a chain of edges of the polygon connecting exactly two Delzant or hidden Delzant vertices, whose interior vertices are all fake, and such that one,

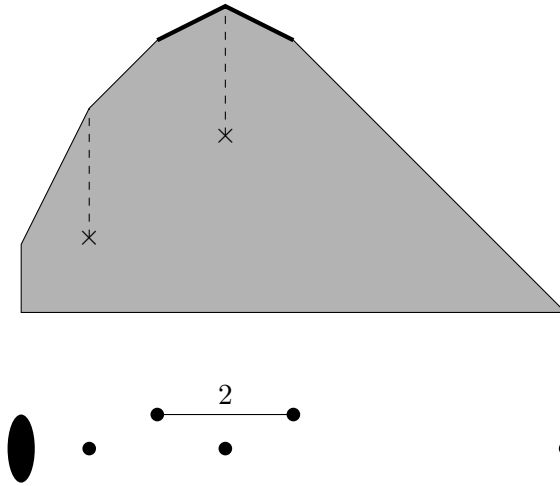


Figure 3.7: A marked semitoric polygon and the Karshon graph corresponding to the underlying Hamiltonian S^1 -space. The chain of edges indicated in bold corresponds to a \mathbb{Z}_2 -sphere.

and hence all, of the edges in the chain has slope of the form b/k for some $b \in \mathbb{Z}$ relatively prime to k . Hence to such a chain of edges we associate an edge in the graph, labeled with the integer k .

This is illustrated in Figure 3.7.

Chapter 4

Semitoric families and beyond

In this chapter, we describe the results of [LFP22, LFP23], joint with Joseph Palmer, dealing with the construction of explicit semitoric systems from the data of their marked semitoric polygons. In [LFP22], we constructed such explicit systems on Hirzebruch surfaces, as members of certain one-parameter families of integrable systems in which one point undergoes Hamiltonian-Hopf bifurcations, transitioning between elliptic-elliptic and focus-focus type. These systems are some of the strictly minimal semitoric systems with respect to some type of blowups, which we explain in detail in this chapter. In [LFP23] we extended these definitions and constructions to obtain explicit semitoric systems for each of these strictly minimal models. We also proposed a recipe to come up with such constructions.

In Section 4.1 we explain the motivations behind these questions and constructions. In Section 4.2 we describe the relevant notions of blowups and the associated strictly minimal semitoric systems. In Section 4.3 we define the one-parameter families introduced in [LFP22, LFP23] and state our main result that every strictly minimal semitoric system can be obtained as a member of such a family. This result is obtained from two constructions. One consists in performing sequences of blowups followed by blowdowns on a fully explicit starting system, and is explained in Section 4.4. The other consists in creating new fully explicit semitoric systems and is detailed in Section 4.5.

Throughout this whole chapter, all semitoric systems will be of the form $(M, \omega, (J, H))$ with (M, ω) a **compact**, connected symplectic manifold. They need not be simple (see Definition 3.3.2), and actually in [LFP23] we adapted several notions and results to the non-simple case.

4.1 Context and motivations

As explained at the end of Section 3.4, the construction of a semitoric system with given symplectic invariants is rather involved, and the gluing procedure that it contains is an obstacle to the obtainment of fully explicit, global formulas defining the system, in contrast with Delzant's algorithm which yields a completely explicit toric system with given Delzant polygon, see Section 3.1. This is of course to be expected because of the much richer nature and complexity of semitoric systems. But one can then wonder what happens if we forget some of the invariants: if we are not interested in the value of the twisting index and Taylor series invariants, the constraints appearing in the second step in the construction of a system from its invariants described in Section 3.4.4 disappear (since any local focus-focus model will do, with no need to be modified by an affine transformation involving the twisting number). Moreover in this case we are left with the marked Delzant semitoric polygon, and we are closer to the toric case with the Delzant polygon as the sole invariant, so one might hope to find a simpler procedure to construct an explicit system.

Consequently, a natural question is the following: can one come up with a procedure which, given a marked semitoric polygon, produces a semitoric system $(M, \omega, F = (J, H))$ with this

polygon as its polygonal invariant? Additionally, can one expect to obtain $(M, \omega, F = (J, H))$ fully explicitly?

It is probably too optimistic to hope for a positive answer to these questions. Nevertheless, in [LFP22, LFP23], we proposed some general strategies to answer them in some cases. In these works, we considered one-parameter families $F = (J, H_t)$, $0 \leq t \leq 1$, with fixed J and H_t varying smoothly with the parameter t (and often obtained as a convex combination $H_t = (1-t)H_0 + tH_1$). This choice was originally motivated by the historical examples of the spin-oscillator (Example 3.3.3) and of coupled angular momenta (Example 3.3.4), and allows one to take advantage of the underlying structure of Hamiltonian S^1 -space of (M, ω, J) , see Section 3.5.

In fact, another motivation came from the scarcity of explicit examples of semitoric systems with at least one focus-focus singularity. When we first started working on [LFP22], the two above systems, along with a generalization of the example of coupled angular momenta due to Hohloch and Palmer [HP18], were the only explicit examples in the literature. Consequently, we wanted to construct fully explicit examples on manifolds other than $S^2 \times S^2$ or $S^2 \times \mathbb{R}^2$.

Actually, we were also motivated by the classification of minimal semitoric systems, i.e. semitoric systems on which no blowdown can be performed (or equivalently from which one can obtain all semitoric systems by performing sequences of blowups) obtained by Kane, Palmer and Pelayo in [KPP18]. Here by blowup we mean toric type blowup, see Section 4.2.1, and we restrict our attention to compact semitoric systems with at least one focus-focus singularity. These authors introduced an invariant of semitoric systems called the semitoric helix, on which the blowups can be read, and listed all the minimal semitoric helices. It was then natural to look for explicit semitoric systems with such a helix.

4.2 Strictly minimal semitoric systems

Actually, there exist two notions of blowups (and the corresponding reverse operations, called blowdowns) that are relevant in the semitoric world: toric type and semitoric type blowups. The systems that we were interested in in [LFP22, LFP23], that we called strictly minimal and discuss in Section 4.2.3, are minimal with respect to both types: they do not admit any toric type or semitoric type blowdown.

Roughly speaking, in dimension four, blowing up at a point amounts to removing an open ball around this point and collapsing its boundary along the fibers of a Hopf fibration. This operation can be performed in the presence of a symplectic structure, by removing a symplectically embedded ball: the new manifold obtained after the blowup can be endowed with a symplectic form which coincides with the original one away from the removed ball, see for instance [MS17, Section 7.1].

One can then consider symplectic blowups respecting some additional structure. For instance, Karshon introduced and studied in [Kar99, Section 6] blowups sending a Hamiltonian S^1 -space (see Section 3.5) to another Hamiltonian S^1 -space. The two kinds of blowups that we will discuss now lift these S^1 -equivariant blowups and send a semitoric system to another semitoric system.

4.2.1 Toric type blowups

Toric type blowups, introduced in [LFP22, Chapter 4], are not specific to semitoric systems and can be performed at any elliptic-elliptic (or completely elliptic in higher dimension) point of any integrable system to obtain a new integrable system. The idea is to perform a \mathbb{T}^2 -equivariant blowup (see for instance [CdS03, Section 3.5]) for the local toric integrable system given by Eliasson's normal form of Theorem 3.2.5 at such an elliptic-elliptic point. Of course if the original system is toric then this is nothing but the usual toric blowup, which corresponds to performing a corner chop at the associated vertex of the Delzant polygon (i.e. removing a certain triangular region based at this vertex and with two sides directed by the edges emanating from

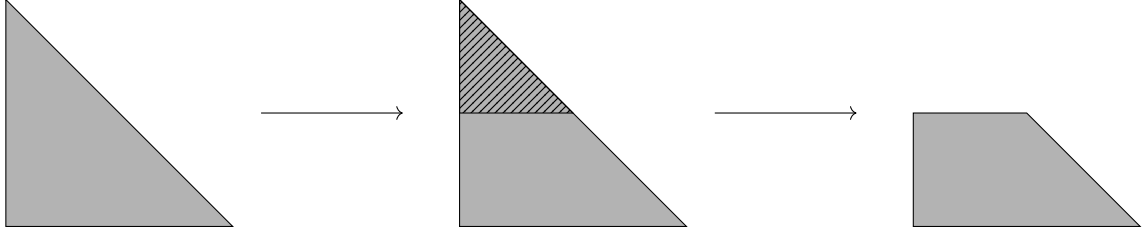


Figure 4.1: Performing a corner chop on the Delzant polygon (left) of a toric system (here the standard \mathbb{T}^2 -action on \mathbb{CP}^2 , see Example 3.1.2) results in another Delzant polygon (right). The region which is chopped off is shaded in the central figure.

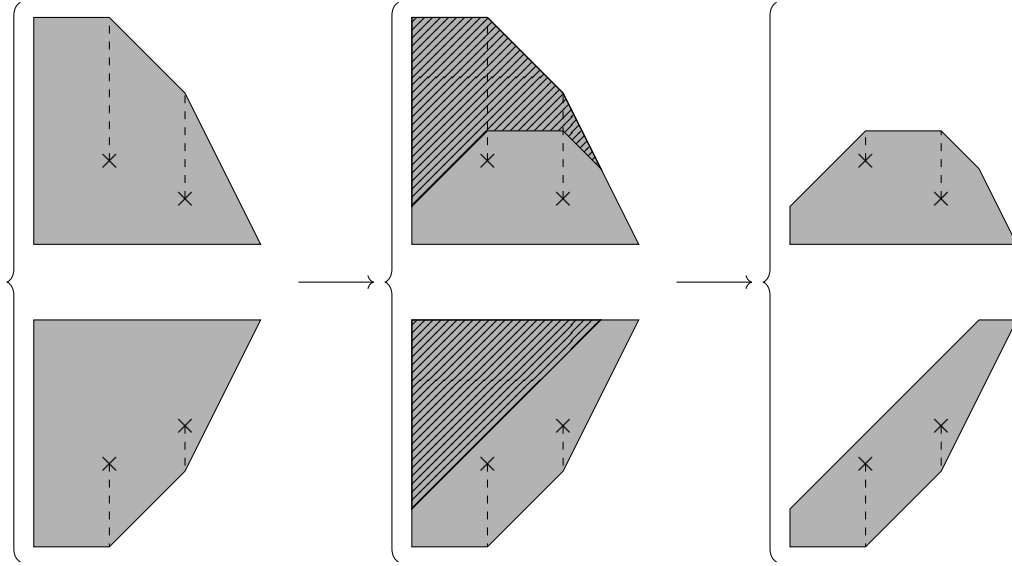


Figure 4.2: Performing a corner chop on a marked semitoric polygon. Note that the removed region (shaded in the central figure) only has to be a triangle for one representative of the polygon.

this vertex) to obtain another Delzant polygon, see Figure 4.1.

If the original system is semitoric, there is still a correspondence between toric type blowups and corner chops, but it is quite subtle. The system $(M, \omega, F = (J, H))$ admits a toric type blowup at an elliptic-elliptic point $p \in M$ if and only if there exists one representative of its marked semitoric polygon $\Delta_{(M, \omega, F)}$ on which a corner chop can be performed at the vertex corresponding to p . This means in particular that the triangle to be removed from this representative should neither contain any marked point nor intersect any cut. This is illustrated in Figure 4.2; for more details, see [LFP22, Section 4.3].

4.2.2 Semitoric type blowups

Semitoric type blowups are a special case of the almost toric blowups introduced by Symington in [Sym03, Section 5.4]. A specific example of such a blowup is described in [Aur09, Example 3.1.2]. This type of blowups was discussed by Zung for general integrable systems in [Zun03], and will be studied for general four-dimensional integrable systems in the upcoming [HSSS]. For our purpose in [LFP23] it was sufficient to define these blowups from their action on marked semitoric polygons (using the classification results from [PVuN09, PVuN11, PPT19]), following [HP21].

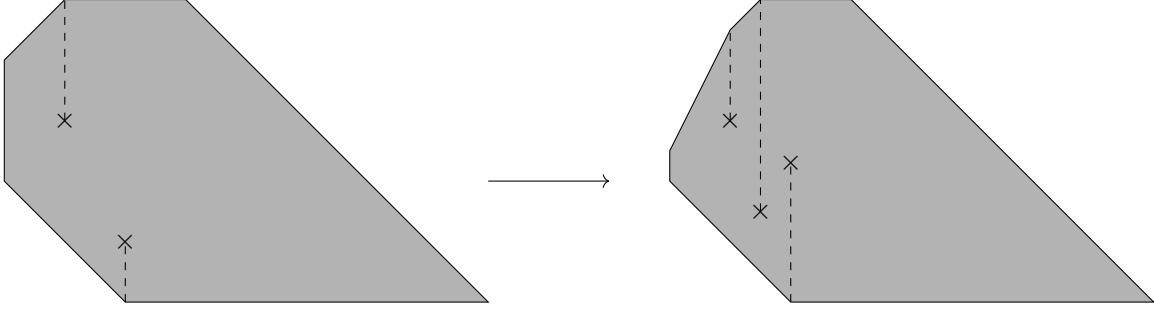


Figure 4.3: Performing a wall chop on a marked weighted polygon; the resulting polygon has one additional marked point and a smaller vertical wall, and the height of each of the original marked points is allowed to change.

Roughly speaking, a semitoric type blowup of a semitoric system $(M, \omega, F = (J, H))$ consists in trading part of a fixed surface of J to create a new focus-focus point. This corresponds to performing a *wall chop* (i.e. removing a certain triangle with one side on a vertical wall) on any representative of the marked semitoric polygon of (M, ω, F) and introducing a new marked point. This operation is illustrated in Figure 4.3, and can be described formally as followed. This description is a bit involved because in fact, the original marked points are allowed to move vertically during this process.

Let $(\Delta, \vec{c}, \vec{\epsilon})$ be a representative of $\Delta_{(M, \omega, F)}$. Assume that J has a fixed surface corresponding to its minimum, which means that the leftmost edge of Δ is a vertical wall W . Let $\lambda > 0$ be smaller than the length of this vertical wall and than the width of Δ . For $\mu \in \mathbb{R}$, let $\tilde{t}_\mu : \mathbb{R}^2 \rightarrow \mathbb{R}^2$ be defined as the identity on $\{x \geq \mu\}$ and as T , relative to a given origin on the vertical line $\pi_1^{-1}(\mu)$, on $\{x \leq \mu\}$, where we recall that $\pi_1 : \mathbb{R}^2 \rightarrow \mathbb{R}$ is the projection to the first factor. Explicitly,

$$\tilde{t}_\mu(x, y) = \begin{cases} (x, y) & \text{if } x \geq \mu, \\ (x, y + x - \mu) & \text{if } x \leq \mu. \end{cases}$$

Let Δ' be the unique convex polygon such that

$$\partial^- \Delta' = \partial^- \Delta, \quad \partial^+ \Delta' = \tilde{t}_{\pi_1(W) + \lambda}(\partial^+ \Delta),$$

where $\partial^- \Delta$ and $\partial^+ \Delta$ stand for the top and bottom boundary of Δ , respectively, i.e.

$$\partial^- \Delta = \left\{ (x, y_-) \in \Delta \mid y_- = \min_{(x, y) \in \Delta} y \right\}, \quad \partial^+ \Delta = \left\{ (x, y_+) \in \Delta \mid y_+ = \max_{(x, y) \in \Delta} y \right\}.$$

Choose any $c'_b \in \Delta' \cap (\pi_1)^{-1}(\pi_1(W) + \lambda)$, and let $c'_1 \leq_{\text{lex}} \dots \leq_{\text{lex}} c'_s$ be such that

$$\forall \ell \in \{1, \dots, s\} \quad c'_\ell \in \text{int}(\Delta') \cap (\pi_1)^{-1}(c_\ell).$$

Let $\ell \in \{1, \dots, s\}$ be such that $c'_\ell \leq_{\text{lex}} c'_b \leq_{\text{lex}} c'_{\ell+1}$. We call the marked weighted polygon

$$(\Delta', \vec{c}' = (c'_1, \dots, c'_\ell, c'_b, c'_{\ell+1}, \dots, c'_s), \vec{\epsilon}' = (\epsilon_1, \dots, \epsilon_\ell, 1, \epsilon_{\ell+1}, \dots, \epsilon_s))$$

a wall chop of size λ of $(\Delta, \vec{c}, \vec{\epsilon})$. This new polygon satisfies the conditions of Lemma 3.4.3, and its $(G_s \times \mathcal{T})$ -orbit (recall the actions defined in Equations (3.6) and (3.8)) is a marked semitoric polygon. Any semitoric system corresponding to this new marked semitoric polygon is called a semitoric type blowup of (M, ω, F) .

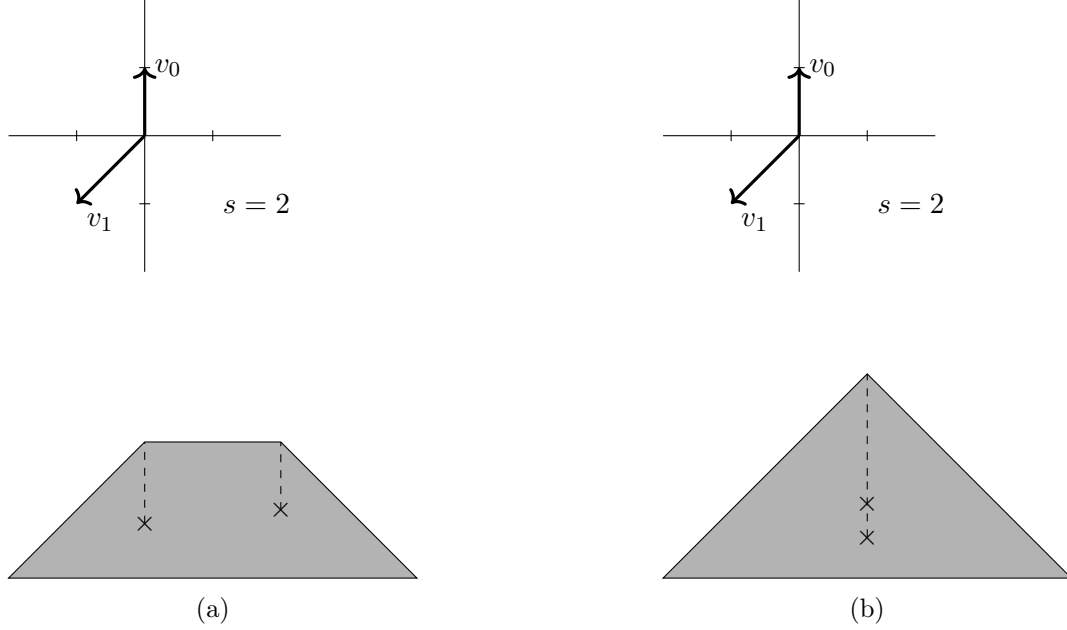


Figure 4.4: Two semitoric polygons giving the same helix. The system in (b) is not simple.

4.2.3 Strictly minimal polygons

We would like to classify the compact semitoric systems with at least one focus-focus singularity that do not admit any toric type or semitoric type blowdown, which we call *strictly minimal*. In [KPP18], the authors studied this question for toric type blowdowns only. In order to do so, they introduced a semitoric invariant called the semitoric helix (the analogue of a toric fan), which is a sequence of vectors that can be constructed from the marked semitoric polygon of the system. This construction is explained in [KPP18, Section 5.3] for simple semitoric systems, and in [LFP23, Section 3.2] for possibly non-simple systems.

The idea is to start from the counter-clockwise ordered primitive inwards pointing normal vectors w_0, \dots, w_{p-1} of a given representative of the marked semitoric polygon, to account for the monodromy induced by focus-focus points by replacing the vectors w_{j+1}, \dots, w_{p-1} with $(T^*)^k w_{j+2}, \dots, (T^*)^k w_{p-1}$ (with T as in Equation (3.5)) in this list each time that the vertex associated with w_j and w_{j+1} is k -fake or k -hidden Delzant (see Definition 3.4.2), and to extend the final outcome v_0, \dots, v_{d-1} to an infinite sequence of vectors $(v_n)_{n \in \mathbb{Z}}$ satisfying a particular periodicity relation. In fact, more precisely, the semitoric helix is the triple $(d, s, [v])$ where s is the number of marked points and $[v]$ is the class of the sequence $v = (v_n)_{n \in \mathbb{Z}}$ for some equivalence relation. In practice, such a helix is represented by the data of the vectors v_0, \dots, v_{d-1} and the number s , as in the example displayed in Figure 4.4. The helix is also defined intrinsically, see [KPP18, Section 5.1].

As explained above, toric type blowups correspond to corner chops on marked semitoric polygons, and these corner chops can in turn easily be read off of the semitoric helix. Namely, a blowdown is possible on the helix $(d, s, [v])$ if and only if there exists $\ell \in \mathbb{Z}$ such that $v_j = v_{j-1} + v_{j+1}$. A semitoric helix not satisfying this condition is called minimal, and the main result of [KPP18] is the classification of minimal semitoric helices. In fact, some degrees of freedom are missing in the list obtained in [KPP18], and in [LFP23] we introduced the following operations on helices in order to fix this.

The J -reflection of a semitoric helix $(d, s, [v])$ is the helix $(d, s, [\tilde{v}])$ defined by

$$\forall j \in \{0, \dots, d-1\}, \quad \tilde{v}_j = \begin{pmatrix} -1 & 0 \\ 0 & 1 \end{pmatrix} v_{d-1-j};$$

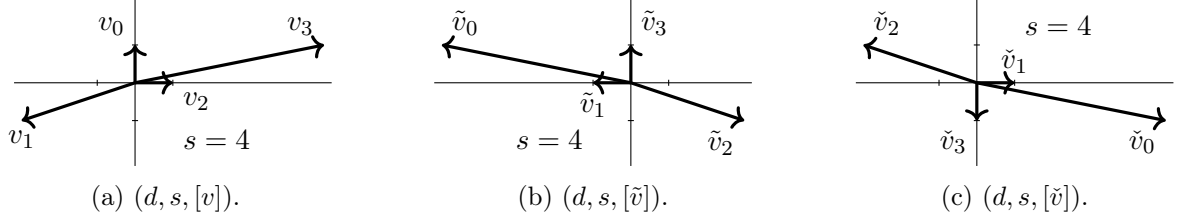


Figure 4.5: A semitoric helix $(d, s, [v])$ and its J -reflection $(d, s, [\tilde{v}])$ and H -reflection $(d, s, [\check{v}])$. These are the semitoric helices associated with the marked semitoric polygons in Figure 4.6 (in the same order).

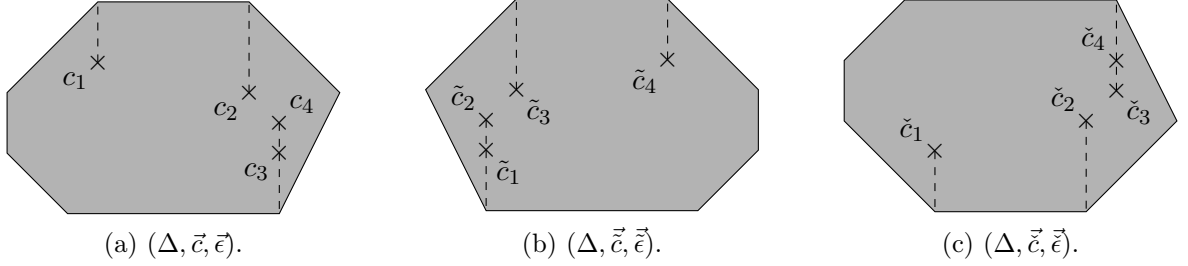


Figure 4.6: A representative of a marked semitoric polygon $[(\Delta, \vec{c}, \vec{e})]$ and of its J -reflection $[(\Delta, \vec{\tilde{c}}, \vec{\tilde{e}})]$ and H -reflection $[(\Delta, \vec{\check{c}}, \vec{\check{e}})]$.

the H -reflection of $(d, s, [v])$ is the helix $(d, s, [\check{v}])$ defined by

$$\forall j \in \{0, \dots, d-1\}, \quad \check{v}_j = \begin{pmatrix} 1 & 0 \\ 0 & -1 \end{pmatrix} v_{d-1-j}.$$

These operations are illustrated in Figure 4.5. They have natural analogues for marked semitoric polygons, but for the sake of clarity we will not reproduce their precise definitions here and refer the reader to [LFP23, Definition 3.20]; the idea is to perform reflections with respect to the vertical and horizontal axis respectively, but one should respect the fact that in a marked semitoric polygon the marked points are ordered lexicographically. An example can be seen in Figure 4.6. In particular, these operations correspond to changing J to $-J$ or H to $-H$ in a semitoric system.

The minimal semitoric helices are obtained from seven types and their J and H -reflections. The first six types are illustrated in Figure 4.7 and more precisely, $(d, s, [v])$ is:

- of type (1) if $d = 2$, $s = 1$, $v_0 = \begin{pmatrix} 0 \\ 1 \end{pmatrix}$ and $v_1 = \begin{pmatrix} -1 \\ -2 \end{pmatrix}$;
- of type (2) if $d = 2$, $s = 2$, $v_0 = \begin{pmatrix} 0 \\ 1 \end{pmatrix}$ and $v_1 = \begin{pmatrix} -1 \\ -1 \end{pmatrix}$;
- of type (3) if $d = 3$, $s = 1$, $v_0 = \begin{pmatrix} 0 \\ 1 \end{pmatrix}$, $v_1 = \begin{pmatrix} -1 \\ 1-n \end{pmatrix}$ and $v_2 = \begin{pmatrix} 0 \\ -1 \end{pmatrix}$ for some $n \geq 1$, $n \neq 3$;
- of type (4) if $d = 3$, $s \neq 2$, $v_0 = \begin{pmatrix} 1 \\ 0 \end{pmatrix}$, $v_1 = \begin{pmatrix} 0 \\ 1 \end{pmatrix}$ and $v_2 = \begin{pmatrix} -1 \\ -1 \end{pmatrix}$;
- of type (5) if $d = 4$, $s \neq 1$, $v_0 = \begin{pmatrix} 1 \\ 0 \end{pmatrix}$, $v_1 = \begin{pmatrix} 0 \\ 1 \end{pmatrix}$, $v_2 = \begin{pmatrix} -1 \\ 1-n \end{pmatrix}$ and $v_3 = \begin{pmatrix} 0 \\ -1 \end{pmatrix}$ for some $n \geq 3$;

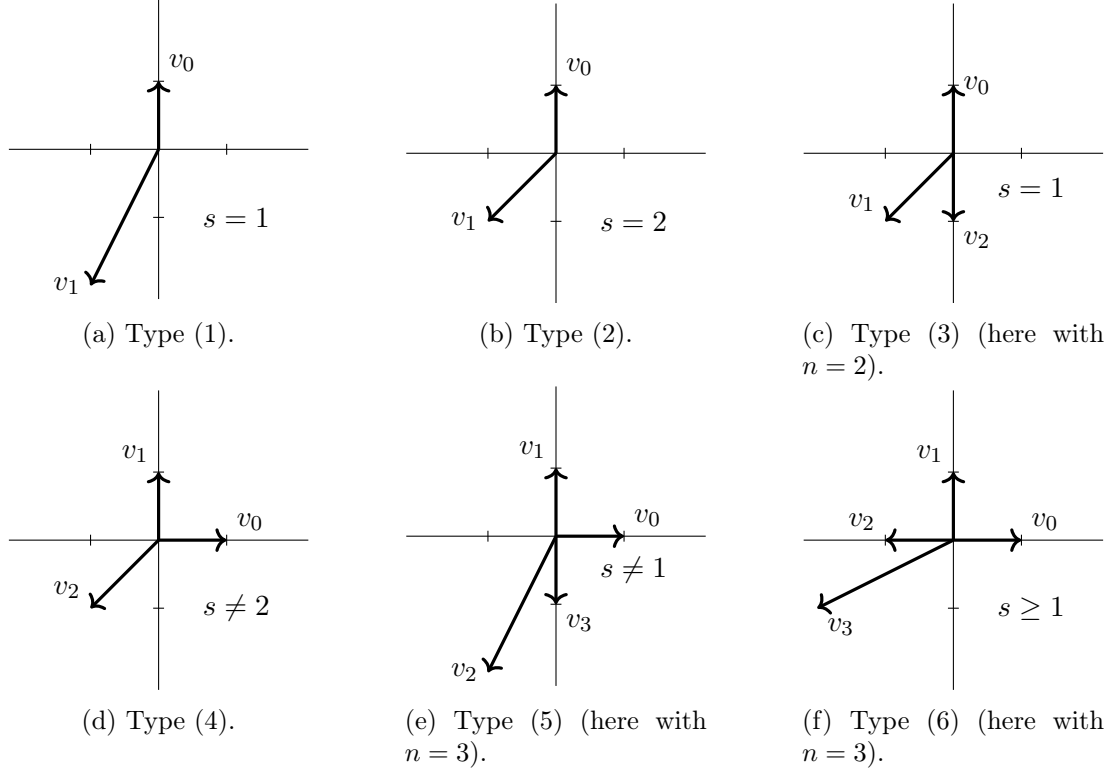


Figure 4.7: The first six types of minimal helices.

- of type (6) if $d = 4$, $s \geq 1$, $v_0 = \begin{pmatrix} 1 \\ 0 \end{pmatrix}$, $v_1 = \begin{pmatrix} 0 \\ 1 \end{pmatrix}$, $v_2 = \begin{pmatrix} -1 \\ 0 \end{pmatrix}$ and $v_3 = \begin{pmatrix} 1-n \\ -1 \end{pmatrix}$ for some $n \in \mathbb{Z} \setminus \{2, s\}$.

The seventh type of helix is more complicated to describe but it always contains a horizontal vector. This is the only necessary information for our purpose, because a semitoric system admits a semitoric type blowdown if and only if its helix includes a horizontal vector (because this vector indicates the presence of a vertical wall in the marked semitoric polygon). By combining this observation with the fact that the helices of type (3) with parameter $n = 1$, (4), (5) and (6) all contain a horizontal vector, we obtain the list of strictly minimal semitoric helices.

Proposition 4.2.1 ([LFP23, Proposition 4.5]). *A compact semitoric system with at least one focus-focus point is strictly minimal if and only if the associated helix is of type (1), (2), or (3) with $n \geq 2$ or $n \geq 4$, or the J -reflection of H -reflection of one of these.*

Proposition 4.2.1 is a statement about semitoric helices, and we would like a statement about semitoric systems. Unfortunately the semitoric helix does not determine the semitoric system, for two reasons. First, many non-isomorphic semitoric systems share the same marked semitoric polygon, since fixing this polygon still allows one to change the Taylor series and twisting index invariants of the system. Second, the semitoric helix does not even uniquely determine the marked semitoric polygon, see for instance Figure 4.4; in fact the map associating to a marked semitoric polygon its semitoric helix is far from injective, essentially because one can change the relative positions of some of the marked points without changing the helix. Moreover, finding all marked semitoric polygons corresponding to a given helix is a very complicated problem in general.

Fortunately, for the helices of types (1), (2) and (3) this question remains tractable, though tedious: one can find all the corresponding marked semitoric polygons by exhaustion. These polygons are defined as follows.

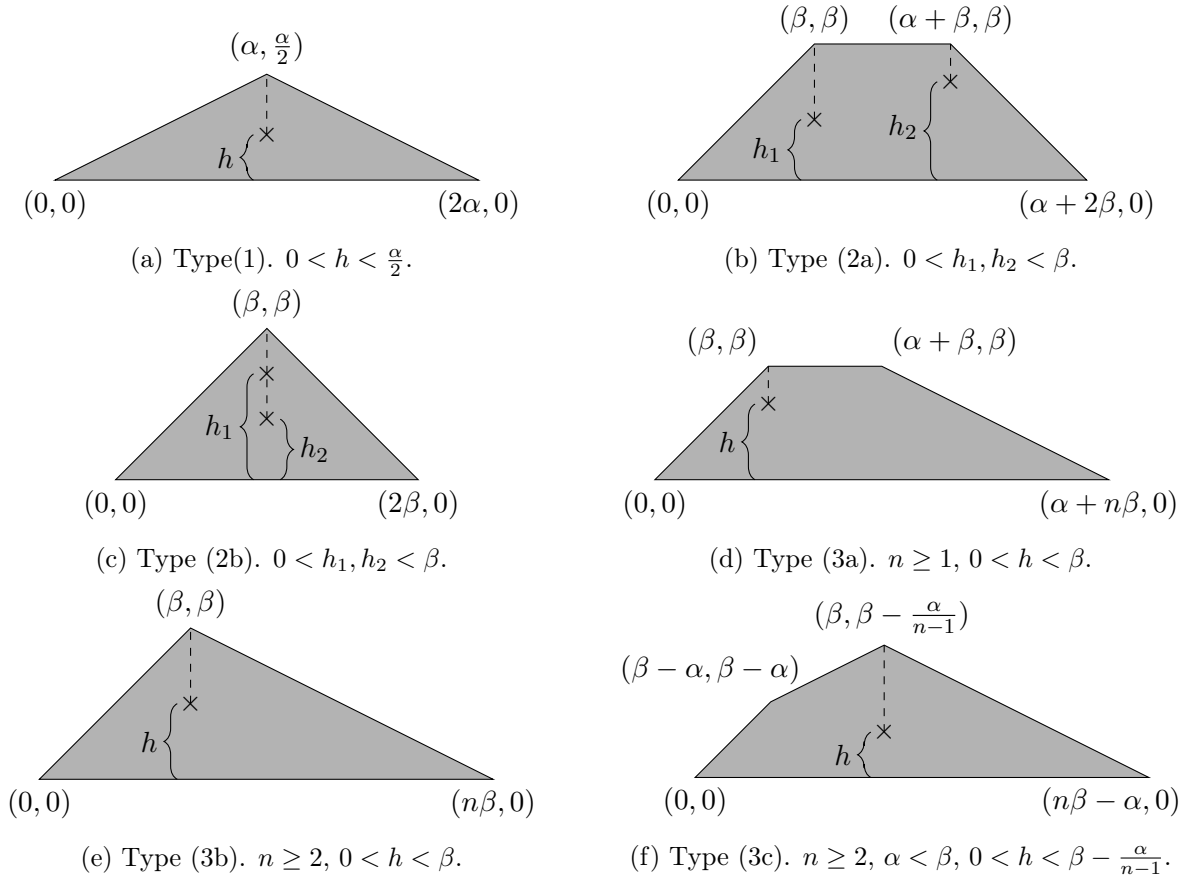


Figure 4.8: A representative of the marked semitoric polygon of each type among (1), (2a), (2b), (3a), (3b), (3c).

Definition 4.2.2. A marked semitoric polygon is said to be of type (1), (2a), (2b), (3a), (3b) or (3c) if and only if one of its representatives is as in Figure 4.8. In this figure the parameters α, β are positive real numbers, the parameter n is an integer, and the height invariants are either h (one marked point) or (h_1, h_2) (two marked points); the constraints on these parameters are precised in the captions.

Using the above arguments, we showed in [LFP23] that these types constitute all the marked semitoric polygons of strictly minimal semitoric systems.

Theorem 4.2.3 ([LFP23, Theorem 4.8]). *Let (M, ω, F) be a semitoric system with at least one focus-focus singularity. This system does not admit a toric or semitoric type blowdown if and only if its marked semitoric polygon is of type (1), (2a), (2b), (3a) with $n = 2$ or $n \geq 4$, (3b) or (3c) (with $n \neq 3$ for these last two), see Definition 4.2.2, or the J -reflection or H -reflection of one of these.*

In this statement we omit the freedom in the horizontal translation of the polygon. But as we explained earlier, it suffices to add a constant to J to translate the marked semitoric polygon horizontally, so this degree of freedom is not very interesting for our purposes.

In fact the polygons of types (2b) and (3b) with $n = 2$ (and their J and H -reflections) are exactly the polygons which admit perfect packings by equivariantly embedded balls, as proved in [DKL+22]. This gives another reason to be interested in them.

The remaining step to obtain a classification of all strictly minimal semitoric systems is to understand the relationship between two systems with the same marked semitoric polygon. Natu-

rally, this involves an isomorphism between the underlying Hamiltonian S^1 -spaces and conditions on the positions of the images of rank zero singular points in the polygons.

Theorem 4.2.4 ([LFP23, Corollary 4.17]). *Two semitoric systems $(M, \omega, F = (J, H))$ and $(M', \omega', F' = (J', H'))$ have the same marked semitoric polygon if and only if there exists a symplectomorphism $\Phi: M \rightarrow M'$ such that $\Phi^* J' = J$ and for all fixed points p of J that are not a global maximum or minimum of J , p is a maximum (respectively minimum) of H on $J^{-1}(J(p))$ if and only if $\Phi(p)$ is a maximum (respectively minimum) of H' on $J'^{-1}(J'(p))$ and for each such p which is not a maximum or minimum of H on $J^{-1}(J(p))$ the volumes of $J^{-1}(J(p)) \cap \{H < H(p)\}$ and $(J')^{-1}(J'(\Phi(p))) \cap \{H' < H'(\Phi(p))\}$ are equal.*

Note that here we focused on semitoric systems with at least one focus-focus singularity. But by performing all possible semitoric type blowdowns on a semitoric system with helix of type (4), (5) or (6), we obtain a system of toric type. Of course these strictly minimal models with no focus-focus point are related to the usual toric minimal models (discussed in [Ful93]), and in [LFP23, Section 4.4] we described which of these toric minimal models appears when starting from each of these types.

4.3 Semitoric families

In [LFP22] and [LFP23], in order to find explicit systems with strictly minimal marked semitoric polygons (hence of the types from Definition 4.2.2), we considered several kinds of families of integrable systems, inspired by the two historical systems of Examples 3.3.3 and 3.3.4. Our idea was to work with one-parameter families lifting a fixed Hamiltonian S^1 -space (see Section 3.5), and which are semitoric for almost all values of the parameter. The more general type of such families that we studied is the following.

Definition 4.3.1 ([LFP22, Definition 1.4]). *A semitoric family with degenerate times $t_1, \dots, t_k \in [0, 1]$, is a family of integrable systems (M, ω, F_t) , $0 \leq t \leq 1$ on a four-dimensional symplectic manifold (M, ω) such that:*

- $F_t = (J, H_t)$ where H_t is of the form $H_t = H(t, \cdot)$ for some smooth $H : [0, 1] \times M \rightarrow \mathbb{R}$;
- (M, ω, F_t) is semitoric if and only if $t \in [0, 1] \setminus \{t_1, \dots, t_k\}$.

By a slight abuse of terminology, and with obvious changes to the definition, we will sometimes consider semitoric families with parameter $t \in [0, b]$ for some $b > 0$. Moreover, given a semitoric family with parameter $t \in [0, b]$, we will call the same systems restricted to $t \in [0, c]$ for some $c \leq b$ a sub-family.

In [LFP22] we considered some specific semitoric families, in which one point transitions from elliptic-elliptic to focus-focus and back to elliptic-elliptic, undergoing at each transition a Hamiltonian-Hopf bifurcation (see for instance [vdM85]), also called nodal trade in this setting.

Definition 4.3.2 ([LFP22, Definition 1.6]). *A semitoric transition family with transition point $p \in M$ and transition times t^-, t^+ , with $0 < t^- < t^+ < 1$, is a family of integrable systems $(M, \omega, F_t)_{0 \leq t \leq 1}$ on a four-dimensional symplectic manifold (M, ω) such that:*

- $F_t = (J, H_t)$ where H_t is of the form $H_t = H(t, \cdot)$ for some smooth $H : [0, 1] \times M \rightarrow \mathbb{R}$;
- (M, ω, F_t) is semitoric for $t \in [0, 1] \setminus \{t^-, t^+\}$;
- for $t < t^-$ and $t > t^+$ the point p is singular of elliptic-elliptic type;
- for $t^- < t < t^+$ the point p is singular of focus-focus type;
- for $t = t^-$ and $t = t^+$ there are no degenerate singular points in $M \setminus \{p\}$;

- if p is a maximum (respectively minimum) of $(H_0)|_{J^{-1}(J(p))}$ then p is a minimum (respectively maximum) of $(H_1)|_{J^{-1}(J(p))}$.

Example 4.3.3. Let $(M, \omega, F_t = (J, H_t))_{0 \leq t \leq 1}$ be the family of systems of coupled angular momenta from Example 3.3.4. If $R_1 \neq R_2$, this system is a semitoric transition family with transition point $m = (0, 0, 1, 0, 0, -1)$ and transition times t^-, t^+ defined in Equation (3.4). If $R_1 = R_2$, it is not a semitoric transition family but it is a semitoric family with degenerate times t^- and $t^+ = 1$. In both cases, when $t \in (t^-, t^+)$ the semitoric system (M, ω, F_t) is strictly minimal, of type:

- (3a) (up to H -reflection, see Section 4.2.3) with parameters $n = 2$, $\alpha = 2(R_2 - R_1)$ and $\beta = 2R_1$ if $R_2 > R_1$;
- (3b) (up to H -reflection) with parameters $n = 2$ and $\beta = 2R_1$ if $R_2 = R_1$;
- (3c) (up to H -reflection) with parameters $n = 2$, $\alpha = 2(R_1 - R_2)$ and $\beta = 2R_1$ if $R_2 < R_1$.

Another example which also existed before [LFP22] is given by the two-parameter families of systems on $S^2 \times S^2$ introduced in [HP18] and generalizing the coupled angular momenta system. By fixing one of the parameters, one obtains different one-parameter families that constitute semitoric families (and most of the time, semitoric transition families) including systems of type (2a), (2b), (3a) with $n = 2$, (3b) with $n = 2$ and (3c) with $n = 2$.

For reasons that we will explain below, in [LFP23] we needed to introduce another kind of semitoric family, more general than semitoric transition families, in which one point still undergoes two Hamiltonian-Hopf bifurcations, going from elliptic-elliptic to focus-focus and back to elliptic-elliptic. The difference with a semitoric transition family is that we do not require the system to be semitoric after the second transition.

Definition 4.3.4. A *half-semitoric transition family* with transition point $p \in M$ and transition times t^-, t^+ , $t^- < t^+$, is a family of integrable systems $(M, \omega, F_t)_{0 \leq t \leq 1}$ on a four-dimensional symplectic manifold (M, ω) such that:

- $F_t = (J, H_t)$ where H_t is of the form $H_t = H(t, \cdot)$ for some smooth $H : [0, 1] \times M \rightarrow \mathbb{R}$;
- (M, ω, F_t) is semitoric for $t \in [0, t^+) \setminus \{t^-\}$;
- for $t < t^-$ and $t > t^+$ the point p is singular of elliptic-elliptic type;
- for $t^- < t < t^+$ the point p is singular of focus-focus type;
- for $t = t^-$ and $t = t^+$ there are no degenerate singular points in $M \setminus \{p\}$.

An example of half-semitoric transition family is described in Section 4.5.2 below, see in particular Theorem 4.5.2 and Figure 4.23. In this example we see one of the possible behaviors of a half-semitoric transition family for $t > t^+$: the transition point p is the elliptic-elliptic corner in a triangular flap, see the discussion after Theorem 4.5.2.

One of the main results that we obtained in [LFP23] is that these one-parameter families suffice to describe all the strictly minimal systems.

Theorem 4.3.5 ([LFP23, Theorem 1.12]). *Every strictly minimal semitoric system $(M, \omega, F = (J, H))$ can be obtained as part of a semitoric family, i.e. as the $t = t_0$ system in such a family, for some $t_0 \in [0, 1]$. Moreover, this semitoric family can be chosen as*

- a semitoric transition family if (M, ω, F) is of type (2a) or (3a);
- a sub-family of a half-semitoric transition family if (M, ω, F) is of type (1).

This statement is obtained by combining many different results from [LFP22] and [LFP23] (together with some already existing results from other authors) that we will describe in the rest of this chapter. First, by invoking Theorem 4.2.4, it can be derived from the following statement about marked semitoric polygons.

Theorem 4.3.6 ([LFP23, Theorem 1.11]). *Every strictly minimal marked semitoric polygon $[(\Delta, \vec{c}, \vec{\epsilon})]$ can be obtained as the marked semitoric polygon of the $t = t_0$ system in a semitoric family for some $t_0 \in [0, 1]$. Moreover, this semitoric family can be chosen as*

- *a semitoric transition family if $[(\Delta, \vec{c}, \vec{\epsilon})]$ is of type (2a) or (3a);*
- *a sub-family of a half-semitoric transition family if $[(\Delta, \vec{c}, \vec{\epsilon})]$ is of type (1).*

Second, this statement about polygons is obtained by two main arguments. On the one hand, we can construct (or obtain from the literature) a fully explicit system in a semitoric family with unmarked semitoric polygon any of the strictly minimal ones from Definition 4.2.2, and for some of these types we can even obtain every marked semitoric polygon in this way (in other words, for some of these types we can obtain all possible values of the height invariants by varying the different parameters). More precisely, in Section 4.5.1 we describe systems of type (2a), (3a) and (3c) (with $n = 2$ for the last two) which are members of semitoric transition families and were constructed in [LFP22]; by varying the different parameters in these systems we obtain all possible marked semitoric polygons of these types. We also recall how systems of type (2b) and (3b) with $n = 2$, again with every possible marked semitoric polygon, can be obtained as members of semitoric families by choosing appropriate values of the parameters in the existing systems from [SZ99a] and [HP18]. Then in Section 4.5.2 we present systems of type (1), allowing us to obtain all marked semitoric polygons of this type, constructed as part of half-semitoric transition families; we also discuss another family of systems of type (1) from [CDEW19]. Finally, in Section 4.5.3 we introduce half-semitoric transition families containing systems with every possible unmarked semitoric polygon of type (3a), (3b) or (3c), for any $n \geq 3$.

On the other hand, we can in fact obtain every strictly minimal marked semitoric polygon in another, albeit less explicit, way, namely by performing alternatively toric type blowups and blowdowns on a fully explicit starting system. We explain this strategy in the next section, Section 4.4, and discuss the former regarding explicit systems in Section 4.5.

Both sections contain some results from [LFP22] and some results from [LFP23], for the sake of clarity. Nevertheless, there is a crucial difference between the systems obtained in these two papers: the explicit systems obtained in [LFP22], all part of semitoric transition families, were either of type (2a) or (2b), or of type (3a) or (3c) with $n = 2$. In particular, the underlying Hamiltonian S^1 -spaces do not include any \mathbb{Z}_k -sphere, since their marked semitoric polygons do not contain any edge with slope b/k with $k \geq 2$ and $b \in \mathbb{Z}$ relatively prime to k (see Section 3.5). This is fundamental because, as explained in [LFP23, Section 5], the presence of such \mathbb{Z}_k -spheres may constitute an obstruction to being part of a semitoric transition family (and it indeed does for some of the other types of strictly minimal systems).

More precisely, these obstructions are related to the relative positions of the different elliptic-elliptic points, focus-focus points and \mathbb{Z}_k -spheres. They can be stated directly in terms of the system (see [LFP23, Proposition 5.2]), but for our purpose it is clearer to state them using marked semitoric polygons.

Corollary 4.3.7 ([LFP23, Corollary 5.3]). *Let (M, ω, F) be a semitoric system and let $p \in M$ be a focus-focus point. Let $(\Delta, \vec{c}, \vec{\epsilon})$ be any representative of the marked semitoric polygon of (M, ω, F) , let c_j be the marked point corresponding to p , and let ℓ be the vertical line passing through c_j . If ℓ contains a Delzant or hidden Delzant vertex of Δ , or intersects an edge of Δ of non-integer slope (or one of its vertices), then (M, ω, F) can not be obtained as the $t = t_0$ system, $t_0 \in (t^-, t^+)$, in a semitoric transition family with p as the transition point.*

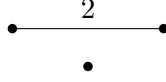


Figure 4.9: The Karshon graph of the Hamiltonian S^1 -space underlying a semitoric system of type (1), which cannot be obtained as part of a semitoric transition family. Indeed, this is prevented by the interior fixed point lying below an edge (here, coming from a \mathbb{Z}_2 -sphere).

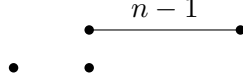


Figure 4.10: The Karshon graph of the Hamiltonian S^1 -space underlying a semitoric system of type (3b), which cannot be obtained as part of a semitoric transition family.

These obstructions can also be read off of the Karshon graph of the underlying Hamiltonian S^1 -space, which can in turn be deduced from the marked semitoric polygon of the system $(M, \omega, F = (J, H))$, as recalled in Section 3.5. Indeed, if the regular vertex corresponding to the fixed point p of J lies below or above an edge with weight $k \geq 2$ (corresponding to a \mathbb{Z}_k -sphere), then (M, ω, F) cannot be obtained as the $t = t_0$ system, $t_0 \in (t^-, t^+)$, in a semitoric transition family with transition point p .

In particular, by inspecting the Karshon graphs of the strictly minimal systems (see Figures 4.9, 4.10 and 4.11), we obtain that systems of type (1), (3b) with $n \geq 2$ and (3c) with $n \geq 3$ cannot be obtained as part of a semitoric transition family (this is the content of Corollaries 5.4 and 5.5 in [LFP23]).

In [LFP23, Proposition 5.7] we also gave some obstructions to being part of a half-semitoric transition family, but these obstructions do not occur in any of the strictly minimal semitoric systems and we do not detail them here.

4.4 Obtaining semitoric systems via toric type blowups and blowdowns

In this section we explain how we obtained semitoric systems with all possible marked semitoric polygons of type (3a) and of types (3b) and (3c) by means of toric type blowups and blowdowns. In all these cases the idea is the same: start with a well-known fully explicit semitoric system, and perform a sequence of successive toric type blowups and blowdowns to arrive to the desired system.

In fact, we also proved that these systems are part of semitoric families (and sometimes semitoric transition families). In order to do so, we started with a system which is itself part of a semitoric (transition) family, and used the fact that, under some natural conditions, toric type blowups and blowdowns can be performed to all the members of a semitoric family, yielding another semitoric family. This is the content of [LFP22, Section 4.4], that we do not reproduce

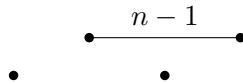


Figure 4.11: The Karshon graph of the Hamiltonian S^1 -space underlying a semitoric system of type (3c), which cannot be obtained as part of a semitoric transition family if $n \geq 3$. Indeed, this is prevented by the interior fixed point lying below an edge (here, coming from a \mathbb{Z}_{n-1} -sphere).

here since it is quite technical.

In what follows, we present the results in a chronological order: systems of type (3a) were obtained in [LFP22], while systems of type (3b) and (3c) were obtained in [LFP23]. And since type (3c) is slightly subtler than type (3b), we start with the former. In each case we give the starting system, the statement and a visual idea of its proof. All these systems will take place on Hirzebruch surfaces, which are certain \mathbb{CP}^1 -bundles over \mathbb{CP}^1 , but which are more convenient to define from symplectic reduction for our purposes.

Let $n \geq 0$ and $\alpha, \beta > 0$; the n -th Hirzebruch surface $(W_n(\alpha, \beta), \omega_{W_n(\alpha, \beta)})$ is the symplectic reduction of \mathbb{C}^4 with its standard symplectic form with respect to the \mathbb{T}^2 -action generated by

$$N(z_1, z_2, z_3, z_4) = \frac{1}{2} (|z_1|^2 + |z_2|^2 + n|z_3|^2, |z_3|^2 + |z_4|^2)$$

at level $N = (\alpha + n\beta, \beta)$. Note that for $n = 0$, $(W_0(\alpha, \beta), \omega_{W_0(\alpha, \beta)})$ identifies with the product $S^2 \times S^2$ of two spheres, each equipped with its standard symplectic form rescaled in such a way that the volume of the first (respectively second) factor is $2\pi\alpha$ (respectively $2\pi\beta$).

In what follows, we will consider Hamiltonians which are invariant under the \mathbb{T}^2 -action generated by N . In this case, slightly abusing notation, we will keep the same formulas for the Hamiltonians that they induce in the reduced space. We will also abuse notation in this way in the rest of the manuscript.

4.4.1 Systems of type (3a)

The case of systems of type (3a) was studied in [LFP22]. Here we start with the system of coupled angular momenta from Example 3.3.4, which it is best to translate to a system on the zeroth Hirzebruch surface for our purposes. The following lemma (stated slightly differently as Lemma 5.1 in [LFP22]) follows from the explicit identification between $S^2 \times S^2$ and $W_0(\alpha, \beta)$ and the explicit formulas of Equation (3.3) (see also the discussion in Example 4.3.3).

Lemma 4.4.1. *Let $0 < \alpha' < \beta'$. The family of systems $(W_0(\alpha', \beta'), \omega_{W_0(\alpha', \beta')}, (J, H_t))$ where*

$$J = \frac{1}{4} (|z_2|^2 - |z_1|^2) + \frac{1}{4} (|z_4|^2 - |z_3|^2) = \frac{1}{2} (|z_2|^2 + |z_4|^2) - \frac{1}{2} (\alpha' + \beta')$$

and

$$H_t = \frac{(1-t)}{2\alpha'} (|z_2|^2 - |z_1|^2) + \frac{t}{\alpha'\beta'} \left(\Re(z_1 \bar{z}_2 \bar{z}_3 z_4) + \frac{1}{4} (|z_2|^2 - |z_1|^2) (|z_4|^2 - |z_3|^2) \right)$$

is a semitoric transition family with transition point $m = [\sqrt{2\alpha'}, 0, 0, \sqrt{2\beta'}]$ and transition times

$$t^- = \frac{\beta'}{2\beta' + \alpha' + 2\sqrt{\alpha'\beta'}}, \quad t^+ = \frac{\beta'}{2\beta' + \alpha' - 2\sqrt{\alpha'\beta'}}.$$

More precisely, it is

- of toric type with (unmarked) semitoric polygon $[(\Delta_{2,a}(\alpha', \beta'), \emptyset, \emptyset)]$ as in Figure 4.12b when $0 < t < t^-$;
- semitoric with one focus-focus point m and marked semitoric polygon $[(\Delta_{2,a}(\alpha', \beta'), (\beta', h(t)), -1)]$ as in Figure 4.12a when $t^- < t < t^+$, where $h(t)$ is the height invariant of m for the system $(W_0(\alpha', \beta'), \omega_{W_0(\alpha', \beta')}, (J, H_t))$;
- of toric type with (unmarked) semitoric polygon $[(\tilde{\Delta}_{2,a}(\alpha', \beta'), \emptyset, \emptyset)]$ as in Figure 4.12c when $t^+ < t \leq 1$.

Furthermore, the system $(J, \frac{\alpha'}{2} H_0)$ is actually toric, with Delzant polygon $\Delta_{2,a}(\alpha', \beta')$.

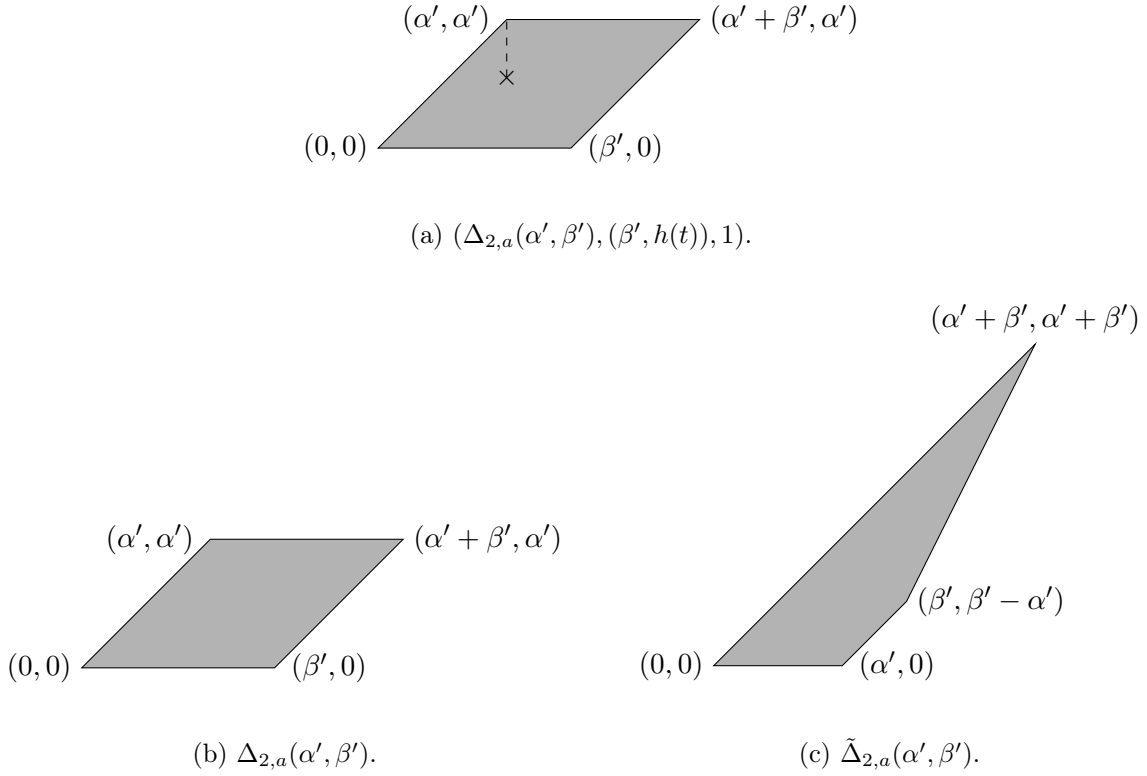


Figure 4.12: Representatives of the marked semitoric polygons associated with the semitoric transition family of Lemma 4.4.1 for (a) $t^- < t < t^+$, (b) $t < t^-$, and (c) $t > t^+$.

The next statement slightly differs from the original statement in [LFP22] since we wanted to use a consistent notation throughout this section.

Theorem 4.4.2 ([LFP22, Theorem 5.2]). *For every $n \in \mathbb{Z}_{\geq 0}$ and $\alpha, \beta > 0$ there exists a semitoric transition family on $W_n(\alpha, \beta)$ with transition point $[\sqrt{2\alpha}, 0, \sqrt{2\beta}, 0]$ and transition times $t_n^-, t_n^+ \in (0, 1)$ satisfying*

$$\frac{\beta}{2\beta + \alpha + 2\sqrt{\alpha\beta}} \leq t_n^- < \frac{1}{2} < t_n^+ \leq \frac{\beta}{2\beta + \alpha - 2\sqrt{\alpha\beta}}$$

with equality on both sides if and only if $n = 0$, such that

1. for $t_n^- < t < t_n^+$ the system is semitoric and has associated marked semitoric polygon $[(\Delta_{n,a}, (\beta, y(t)), 1)]$ where $y(t)$ belongs to the interval $(0, \beta)$, see Figure 4.13a (in particular, it is of type (3a) with parameters α, β, n and $y(t)$);
2. if $t = t_n^-$ or $t = t_n^+$ the system has exactly one degenerate point at $[\sqrt{2\alpha}, 0, \sqrt{2\beta}, 0]$;
3. if $t < t_n^-$ the system is of toric type with marked semitoric polygon $[(\Delta_{n,a}, \emptyset, \emptyset)]$, shown in Figure 4.13b;
4. if $t > t_n^+$ the system is of toric type with marked semitoric polygon $[(\tilde{\Delta}_{n,a}, \emptyset, \emptyset)]$, shown in Figure 4.13c;

Moreover, such a system can be obtained from the system of Lemma 4.4.1 for some appropriate choice of α' and β' , by alternately performing blowups and blowdowns, each n times.

The proof of Theorem 4.4.2 goes by induction on n , and is illustrated in Figure 4.14.

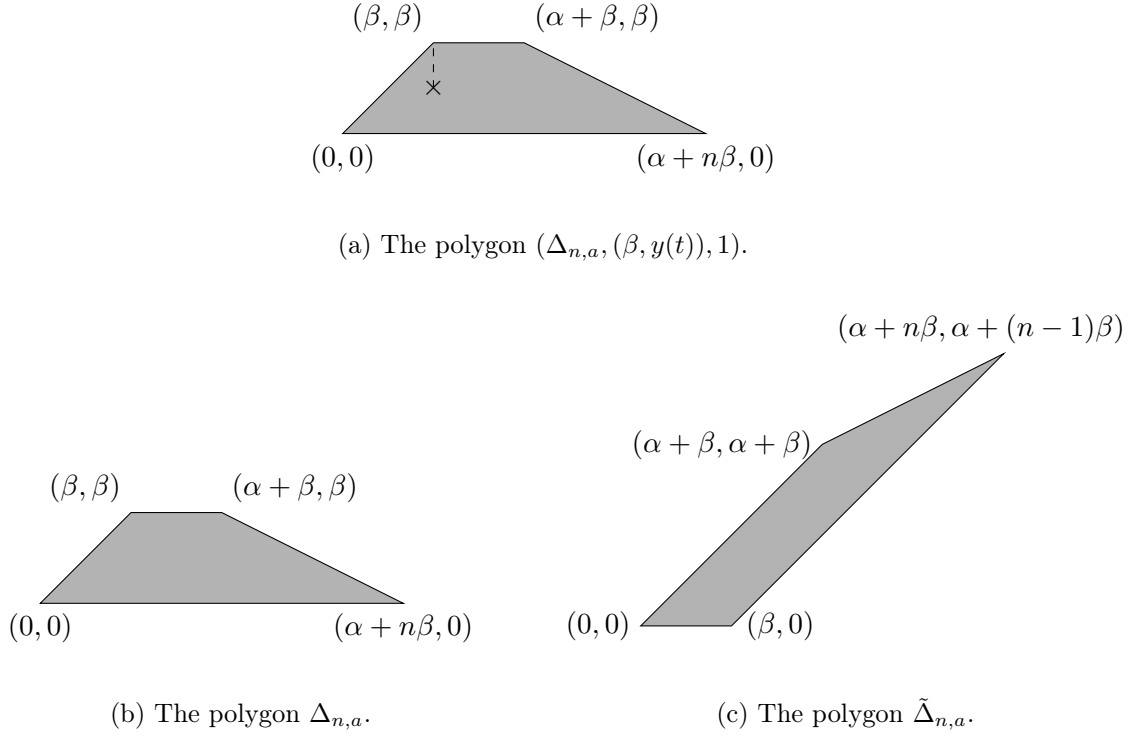


Figure 4.13: Polygons associated with the semitoric transition family of Theorem 4.4.2. Here we chose different representatives than in [LFP22, Figure 20] in order to compare more easily this case with the cases of types (3b) and (3c) described in the next two sections.

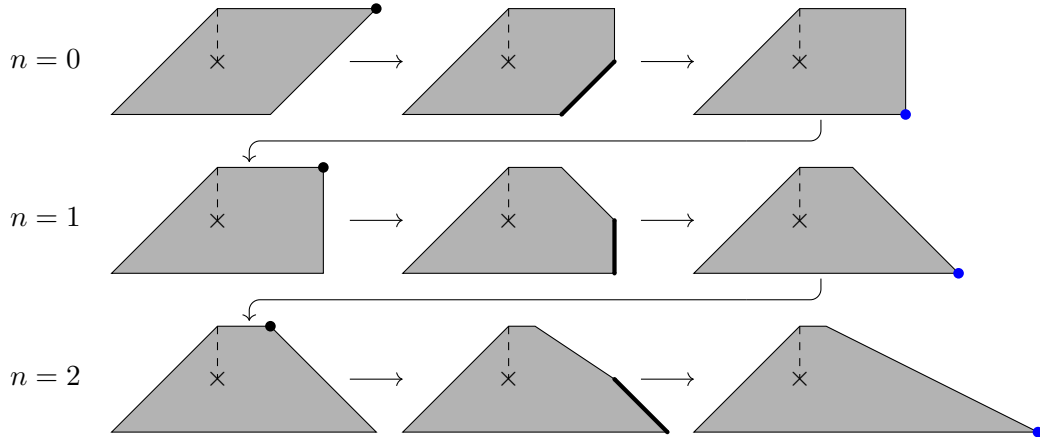


Figure 4.14: A visual proof of Theorem 4.4.2. Here we display one representative of the marked semitoric polygon of the semitoric system obtained at each step of the proof, starting from the system in Lemma 4.4.1. At each step, we perform a corner chop (corresponding to a toric type blowup) at the black point and then a corner unchop (corresponding to a toric type blowdown) at the bold edge, thus creating a new vertex indicated by the blue point.

4.4.2 Systems of type (3c)

In this case the starting system is a subset of the two-parameter family on $S^2 \times S^2$ described in [HP18], which we translate here to a family of systems on the zeroth Hirzebruch surface.

Lemma 4.4.3 ([LFP23, Lemma 6.2]). *Let $0 < \alpha' < \beta'$. The family of systems*

$$(W_0(\alpha', \beta'), \omega_{W_0(\alpha', \beta')}, (J, H_t))_{0 \leq t \leq 1}$$

where

$$J = \frac{1}{4} (|z_2|^2 - |z_1|^2) + \frac{1}{4} (|z_4|^2 - |z_3|^2) = \frac{1}{2} (|z_2|^2 + |z_4|^2) - \frac{1}{2} (\alpha' + \beta')$$

and

$$H_t = \frac{(1-t)}{2\alpha'} (|z_2|^2 - |z_1|^2) + \frac{t}{\alpha'\beta'} \left(\Re(z_1 \bar{z}_2 \bar{z}_3 z_4) - \frac{1}{4} (|z_2|^2 - |z_1|^2) (|z_4|^2 - |z_3|^2) \right)$$

is a semitoric transition family with transition point $m = [\sqrt{2\alpha'}, 0, 0, \sqrt{2\beta'}]$ and transition times

$$t^- = \frac{\beta'}{2\beta' + \alpha' + 2\sqrt{\alpha'\beta'}}, \quad t^+ = \frac{\beta'}{2\beta' + \alpha' - 2\sqrt{\alpha'\beta'}}.$$

More precisely, it is

- of toric type with (unmarked) semitoric polygon $[(\Delta_{2,c}(\alpha', \beta'), \emptyset, \emptyset)]$ as in Figure 4.15b when $0 < t < t^-$;
- semitoric with one focus-focus point m and marked semitoric polygon $[(\Delta_{2,c}(\alpha', \beta'), (\beta', h(t)), -1)]$ as in Figure 4.15a when $t^- < t < t^+$, where $h(t)$ is the height invariant of m for the system $(W_0(\alpha', \beta'), \omega_{W_0(\alpha', \beta')}, (J, H_t))$;
- of toric type with (unmarked) semitoric polygon $[(\tilde{\Delta}_{2,c}(\alpha', \beta'), \emptyset, \emptyset)]$ as in Figure 4.15c when $t^+ < t \leq 1$.

Furthermore, the system $(J, \frac{\alpha'}{2} H_0)$ is actually toric, with Delzant polygon $\Delta_{2,c}(\alpha', \beta')$.

By performing sequences of successive blowups and blowdowns, we obtain the following result.

Theorem 4.4.4. *For any $n \geq 2$, any $\alpha, \beta > 0$ with $\alpha < \beta$ and any $h \in (0, \beta - \frac{\alpha}{n-1})$, there exist $b \in (0, 1)$ and a semitoric family*

$$(W_{n-2}(\beta - \alpha, \beta), \omega_{W_{n-2}(\beta - \alpha, \beta)}, F_t^n = (J, H_t^n))_{0 \leq t \leq b}$$

with one degenerate time t_n^- satisfying

$$\frac{\beta}{3\beta - \alpha + 2\sqrt{\beta(\beta - \alpha)}} \leq t_n^- < \frac{1}{2}$$

with equality on the left if and only if $n = 2$, such that there exists one point $p_n \in W_{n-2}(\beta - \alpha, \beta)$ such that

1. $F_{t_n^-}$ has no degenerate singular point in $M \setminus \{p_n\}$;
2. if $t \in (t_n^-, b)$, the system is semitoric with one focus-focus point p_n and its marked semitoric polygon is $[(\Delta_{n,c}(\beta - \alpha, \beta), (\beta, h_n(t)), -1)]$ as in Figure 4.16 where the image of $t \mapsto h_n(t)$ is the interval $(0, h)$ (in particular, it is of type (3c) with parameters $\alpha, \beta, n, h_n(t)$);
3. if $t \in [0, t_n^-)$, the system is of toric type (p_n being elliptic-elliptic) and its (unmarked) semitoric polygon is $[(\Delta_{n,c}(\beta - \alpha, \beta), \emptyset, \emptyset)]$. Furthermore, for $t = 0$ it is toric up to multiplication of H_0 by a constant, with Delzant polygon $\Delta_{n,c}(\beta - \alpha, \beta)$.

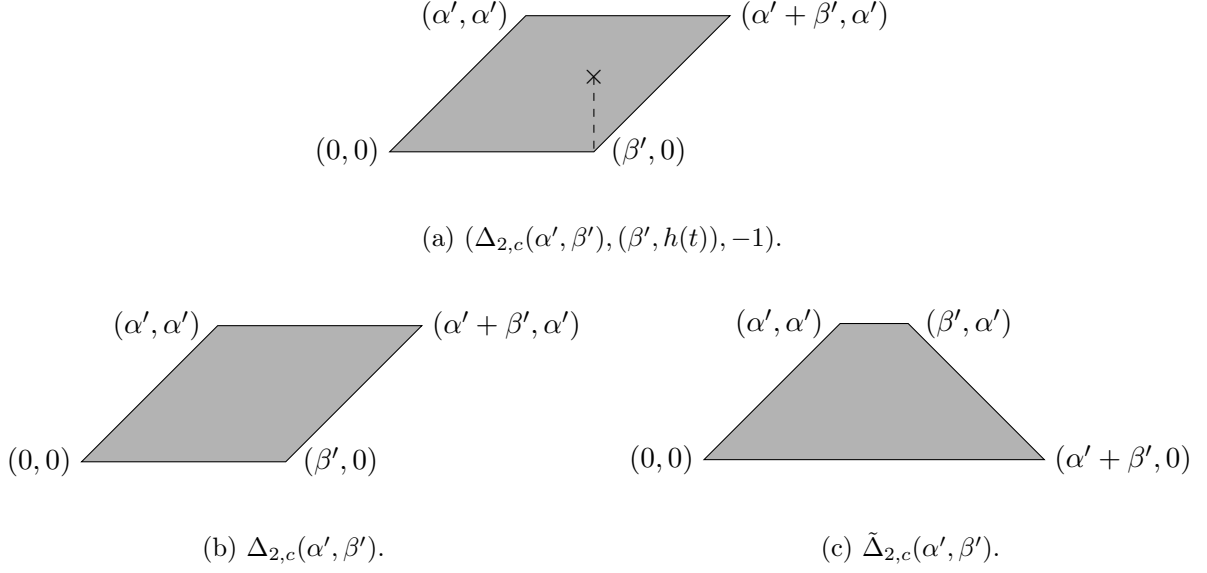


Figure 4.15: Representatives of the marked semitoric polygons associated with the semitoric transition family of Lemma 4.4.3 for (a) $t^- < t < t^+$, (b) $t < t^-$, and (c) $t > t^+$.

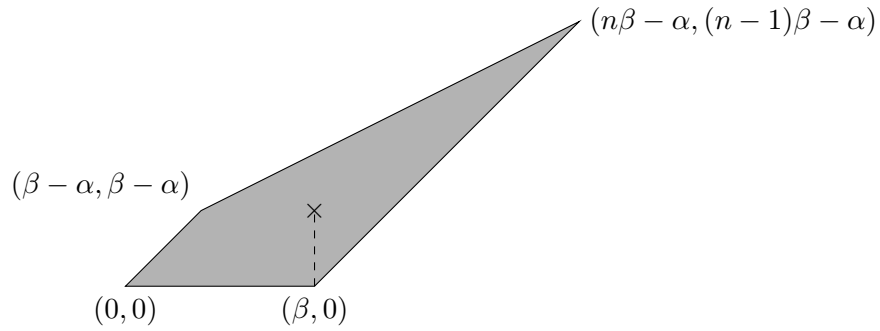


Figure 4.16: The marked weighted polygon $(\Delta_{n,c}(\beta - \alpha, \beta), (\beta, h_n(t)), -1)$.

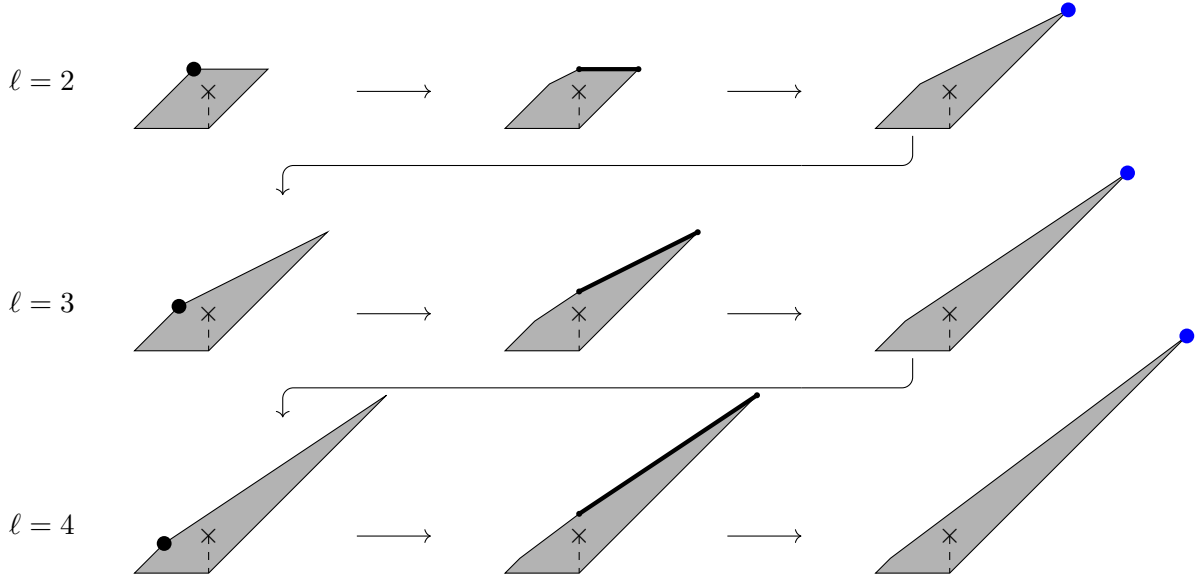


Figure 4.17: A visual proof of Theorem 4.4.4. As in Figure 4.14, we display one representative of the marked semitoric polygon of the semitoric system obtained at each step of the proof, starting from the system in Lemma 4.4.3. At each step, we perform a corner chop (corresponding to a toric type blowup) at the black point and then a corner unchop (corresponding to a toric type blowdown) at the bold edge, thus creating a new vertex indicated by the blue point.

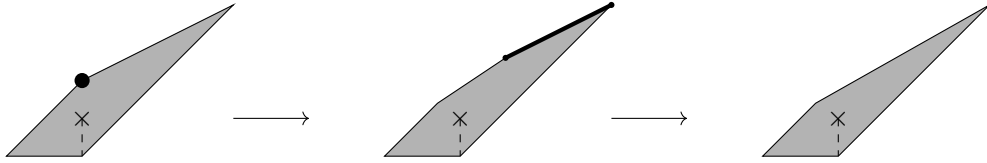


Figure 4.18: Performing a corner chop at the vertex indicated by the black dot, then a corner unchop along the bold segment, to a marked semitoric polygon of type (3b) does not yield a marked semitoric polygon of type (3b).

Moreover, such a family can be obtained by alternatively performing toric type blowups and blow-downs, each $n - 2$ times, to the system of Lemma 4.4.3 for some appropriate choice of α' and β' .

The fact that the system is of type (3c) for $t \in (t_n^-, b)$ comes from the fact that the polygon $\Delta_n(\beta - \alpha, \beta)$ is obtained from the polygon of Figure 4.8f by changing the cut direction. Note that the maximal height invariant of a system of type (3c) with this polygon is $\beta - \frac{\alpha}{n-1}$; consequently, the statement allows one to obtain every marked semitoric polygon of type (3c) in this way. A visual proof of Theorem 4.4.4 is given in Figure 4.17; unlike the case of type (3a) presented in the previous section, it is better here to fix n and perform a finite induction on $\ell \in \{2, \dots, n\}$.

4.4.3 Systems of type (3b)

The case of type (3b) is a bit more difficult because by performing a toric type blowup followed by a toric type blowdown on a system of type (3b), one does not obtain a system of type (3b), as illustrated in Figure 4.18.

Hence we will in fact start with the family of systems described in Lemma 4.4.3, but this time with $\alpha' > \beta'$, unless $n = 2$ in which case we need to choose $\alpha' = \beta'$. The statement of

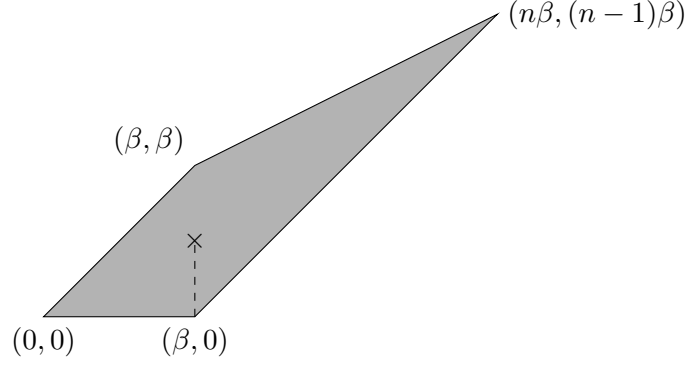


Figure 4.19: The marked weighted polygon $(\Delta_n^0(\beta), (\beta, h_n(t)), -1)$.

Lemma 4.4.3 remains valid in the former case, but in the latter case this family is not a semitoric transition family anymore. This is not a problem since in the statement and its proof we only need to consider the restriction of this family to parameters in $[0, a]$ for $a < t^+$, and this restricted family is a semitoric family with one point transitioning from elliptic-elliptic to focus-focus.

Theorem 4.4.5 ([LFP23, Theorem 6.7]). *For any $n \geq 2$, any $\beta > 0$ and any $h \in (0, \beta)$, there exist $b \in (0, 1)$ and a semitoric family*

$$(W_{n-2}(\beta, \beta), \omega_{W_{n-2}(\beta, \beta)}, F_t^n = (J, H_t^n))_{0 \leq t \leq b}$$

with one degenerate time $t_n^- < \frac{1}{2}$, such that there exists one point $p_n \in W_{n-2}(\beta, \beta)$ such that

1. $F_{t_n^-}$ has no degenerate singular point in $M \setminus \{p_n\}$;
2. if $t \in (t_n^-, b)$, the system is semitoric with one focus-focus point p_n and its marked semitoric polygon is $[(\Delta_n^0(\beta), (\beta, h_n(t)), -1)]$ as in Figure 4.19 where the image of $t \mapsto h_n(t)$ is the interval $(0, h)$ (in particular, it is of type (3b) with parameters $\beta, n, h_n(t)$);
3. if $t \in [0, t_n^-)$, the system is of toric type (p_n being elliptic-elliptic) and its (unmarked) semitoric polygon is $[(\Delta_n^0(\beta), \emptyset, \emptyset)]$, and for $t = 0$ it is even toric up to multiplication of H_0 by a constant, with Delzant polygon $\Delta_n^0(\beta)$.

Moreover, such a family can be obtained by alternatively performing blowups and blowdowns, each $n - 2$ times, to the system of Lemma 4.4.3 for some appropriate choice of α' and β' .

The proof of Theorem 4.4.5 is illustrated in Figure 4.20.

4.5 Explicit semitoric systems

In this section, we start by listing the various explicit semitoric systems constructed in [LFP22] and [LFP23] and describing some of their properties. The important message here is the fact that these systems are indeed fully explicit, rather than the precise explicit formulas which will appear. We conclude by giving a few ideas on how to come up with such explicit examples, in Section 4.5.4.

Again, we present these systems in chronological order and increasing difficulty level. Explicit systems of type (2a), (3a) or (3c) with $n = 2$ were obtained in [LFP22] and do not include any \mathbb{Z}_k -sphere. Explicit systems of type (1) and (3a), (3b) or (3c) with parameter $n \geq 3$ were constructed in [LFP23]; systems of type (1) contain a \mathbb{Z}_2 -sphere, while systems of type (3a), (3b) or (3c) with parameter $n \geq 3$ contain a \mathbb{Z}_{n-1} -sphere.

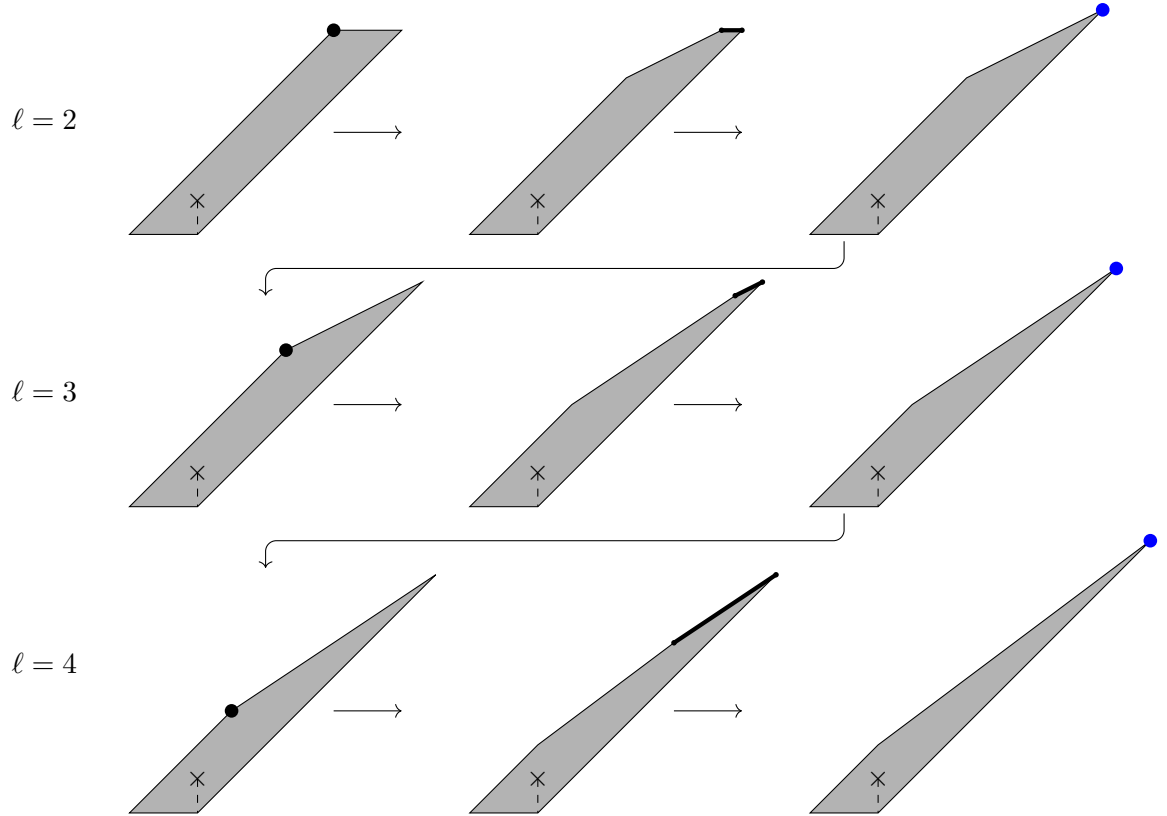


Figure 4.20: A visual proof of Theorem 4.4.5. As in Figure 4.14, we display one representative of the marked semitoric polygon of the semitoric system obtained at each step of the proof, starting from the system in Lemma 4.4.3 with $\alpha' > \beta'$. At each step, we perform a corner chop (corresponding to a toric type blowup) at the black point and then a corner unchop (corresponding to a toric type blowdown) at the bold edge, thus creating a new vertex indicated by the blue point.

We also discuss, in the relevant sections, some other important explicit systems from the literature. There are systems which we do not mention for the sake of clarity, but which are still interesting. For instance, in [LFP22] we constructed a semitoric transition family on the first Hirzebruch surface (with any scaling) which allowed us to obtain all the marked semitoric polygons of type (3a) with $n = 1$. Another example is the one-parameter family of systems from [DMH21] which transitions between systems with zero or four focus-focus points, and for some value of the parameter possesses two singular fibers with two pinches each; this system was built using the recipe from [LFP22].

4.5.1 Systems of type (2) and (3) with $n = 2$

In [LFP22, Section 7] we constructed a two-parameter family of systems on the second Hirzebruch surface, which, depending on the values of the parameters, can be semitoric of type (2a), or (3a) or (3c) with $n = 2$. By fixing one of the parameters, we obtain semitoric transition families containing systems of these types.

Recall from Section 4.4 that the second Hirzebruch surface $(W_2(\alpha, \beta), \omega_{W_2(\alpha, \beta)})$ is obtained as the symplectic reduction of \mathbb{C}^4 by the \mathbb{T}^2 -action generated by

$$N(z_1, z_2, z_3, z_4) = \frac{1}{2} (|z_1|^2 + |z_2|^2 + 2|z_3|^2 + |z_4|^2)$$

at level $N = (\alpha + 2\beta, \beta)$.

Let $J = \frac{1}{2} (|z_2|^2 + |z_3|^2)$; it is the momentum map for an effective S^1 -action on the symplectic manifold $(W_2(\alpha, \beta), \omega_{W_2(\alpha, \beta)})$, with fixed points $A = [\sqrt{2(\alpha + 2\beta)}, 0, 0, \sqrt{2\beta}]$, $B = [\sqrt{2\alpha}, 0, \sqrt{2\beta}, 0]$, $C = [0, \sqrt{2\alpha}, \sqrt{2\beta}, 0]$ and $D = [0, \sqrt{2(\alpha + 2\beta)}, 0, \sqrt{2\beta}]$. Consider moreover the Hamiltonians

$$R = \frac{1}{2} (|z_3|^2 - |z_4|^2), \quad \mathcal{X} = \Re(z_1 z_2 \bar{z}_3 z_4),$$

which also descend to the symplectic quotient.

The following statement is the object of [LFP22, Section 7.4]. Strictly speaking, in that section we only proved that the system was semitoric for the choice of parameters $(t, 1)$, $0 \leq t \leq 1$, and in a neighborhood of $(\frac{1}{2}, \frac{1}{2})$ in the parameter space, since we only checked the types of the singular points B and C there. But it is not complicated to compute these types for all values of the parameters, using the criterion from [LFP23, Proposition 7.5].

Theorem 4.5.1. *Let $\alpha, \beta > 0$ and let $\gamma > 0$ be such that*

$$\frac{1}{2(1 + 2\nu)\sqrt{\nu}} < \gamma < \frac{1}{2\sqrt{\nu}}, \quad \text{with } \nu = \frac{\beta}{\alpha}.$$

For $s_1, s_2 \in [0, 1]$, let

$$H_{s_1, s_2} = (1 - s_1)(1 - s_2)H_{00} + s_2(1 - s_1)H_{01} + s_1(1 - s_2)H_{10} + s_1 s_2 H_{11}$$

where $H_{01} = R$, $H_{10} = -R$ and

$$H_{00} = \frac{(\alpha + \beta) \left(\gamma \mathcal{X} - (2J - \alpha - 2\beta)(R + \frac{\beta^2}{\alpha + \beta}) \right)}{\alpha(\alpha + 2\beta)}, \quad H_{11} = \frac{\beta(\gamma \mathcal{X} + (2J - \alpha - 2\beta)(R + \alpha + \beta))}{\alpha(\alpha + 2\beta)}.$$

Moreover, let

$$f_{\pm}(s_1, s_2) = 2\gamma\sqrt{\nu}((1 + 2\nu)s_1 s_2 - (1 + \nu)(s_1 + s_2 - 1)) \pm (s_1 s_2 - (2 + 3\nu)s_1 + \nu s_2 + 1 + \nu)$$

and

$$g_{\pm}(s_1, s_2) = 2\gamma\sqrt{\nu}((1 + 2\nu)s_1 s_2 - (1 + \nu)(s_1 + s_2 - 1)) \mp (s_1 s_2 + \nu s_1 - (2 + 3\nu)s_2 + 1 + \nu).$$

Let $(s_1, s_2) \in [0, 1] \times [0, 1]$ be such that none of the quantities $f_{\pm}(s_1, s_2)$ and $g_{\pm}(s_1, s_2)$ vanishes. Then $(W_2(\alpha, \beta), \omega_{W_2(\alpha, \beta)}, F_{s_1, s_2} = (J, H_{s_1, s_2}))$ is

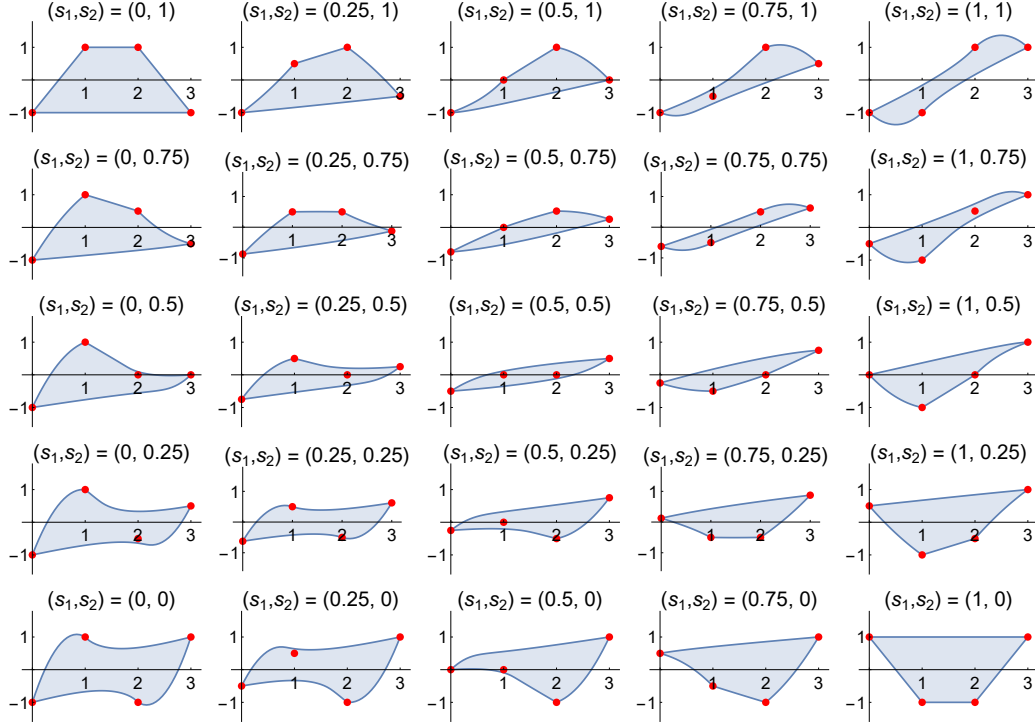


Figure 4.21: Image of the momentum map $F_{s_1, s_2} = (J, H_{s_1, s_2})$ from Theorem 4.5.1 with $\alpha = 1$, $\beta = 1$, $\gamma = \frac{9}{20\sqrt{\nu}}$ and various values of the parameters (s_1, s_2) .

- *semitoric with two focus-focus points B and C if all four quantities $f_{\pm}(s_1, s_2)$ and $g_{\pm}(s_1, s_2)$ are positive. In this case it is of type (2a) with marked semitoric polygon as in Figure 4.8b (for the same α and β);*
- *semitoric with one focus-focus point B if $f_{\pm}(s_1, s_2) > 0$ and at least one of $g_{+}(s_1, s_2)$, $g_{-}(s_1, s_2)$ is negative. In this case it is of type (3a) with $n = 2$, with marked semitoric polygon as in Figure 4.8d;*
- *semitoric with one focus-focus point C if $g_{\pm}(s_1, s_2) > 0$ and at least one of $f_{+}(s_1, s_2)$, $f_{-}(s_1, s_2)$ is negative. In this case it is of type (3c) with $n = 2$, with marked semitoric polygon as in Figure 4.8f;*
- *of toric type otherwise.*

Moreover, by fixing the value of one of the parameters s_1, s_2 and varying the other, we obtain a semitoric transition family with transition point either B or C . In particular, by varying the parameters α and β , we obtain all possible marked semitoric polygons of type (2a) or (3a) or (3c) with $n = 2$ from this system.

The image of the momentum map F_{s_1, s_2} is displayed in Figure 4.21 for some choice of α, β and γ and various values of (s_1, s_2) . The conditions involving f_{\pm} and g_{\pm} can be visualized in Figure 4.22 for a particular choice of α, β and γ . The parameters α and β give the scalings of the marked semitoric polygon. And since in a semitoric transition family, the transition point travels from one side of the boundary of the image of the momentum map to the other, all possible values of the height invariant are attained. This is why we can obtain every possible marked semitoric polygon of type (2a) or (3a) by choosing these different parameters appropriately.

The system of Theorem 4.5.1 can never be of type (2b) or (3b) because, as one can see by inspecting the marked semitoric polygons, this would require choosing $\alpha = 0$, which is impossible

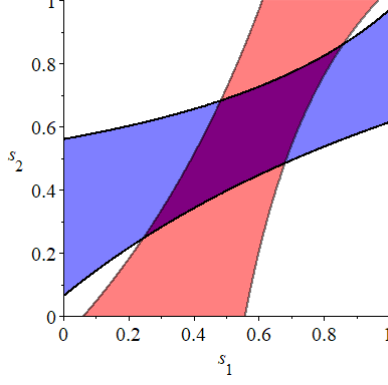


Figure 4.22: A plot showing the types of the points B and C depending on the parameters s_1 and s_2 for the system from Theorem 4.5.1, here with $\alpha = 1$, $\beta = 1$ and $\gamma = \frac{9}{20\sqrt{\nu}} = \frac{9}{20}$. In the purple region, $f_{\pm}, g_{\pm} > 0$ so both points are focus-focus. In the red region, $f_{\pm} > 0$ and either g_+ or g_- is negative so only B is focus-focus. In the blue region, the same situation applies with the roles of f_{\pm} and g_{\pm} reversed, so only C is focus-focus. In the white region, both points are elliptic-elliptic. The solid lines separating the different regions correspond to parameters for which at least one of these two points is degenerate. This can be compared with Figure 4.21.

in this setting. However, we already saw in Example 4.3.3 that when $R_1 = R_2$ and for appropriate values of the parameter t , the coupled angular momenta system from [SZ99a] is of type (3b) with parameter $n = 2$ (up to H -reflection); by varying t and R_1 , one obtains in this way all possible marked semitoric polygons of this type, as the marked semitoric polygons of systems with are part of semitoric families. Moreover, when $R_1 = R_2$, the generalized coupled momenta system introduced in [HP18] and discussed after Example 3.3.4 is actually of type (2b), and also allows one to obtain every marked semitoric polygon of this type as the polygon of a system in a semitoric family.

4.5.2 Systems of type (1)

In [LFP23], we constructed explicit systems of type (1) as members of half-semitoric transition families, and thus obtained all possible marked semitoric polygons of this type.

Concretely, we worked on $(M, \omega) = (\mathbb{CP}^2, \alpha\omega_{\text{FS}})$ where ω_{FS} is the Fubini-Study symplectic form, normalized so that the Liouville volume of \mathbb{CP}^2 equals $2\pi^2$, and $\alpha > 0$. This symplectic manifold can be obtained as the symplectic reduction of \mathbb{C}^3 by the Hamiltonian \mathbb{T}^2 -action generated by

$$N = \frac{1}{2}(|z_1|^2 + |z_2|^2 + |z_3|^2)$$

at level $N = \alpha$. Consider the invariant Hamiltonians

$$J = \frac{1}{2}(|z_1|^2 - |z_2|^2), \quad R = \frac{1}{2}(|z_1|^2 + |z_2|^2), \quad \mathcal{X} = \Re(z_1 z_2 \bar{z}_3^2).$$

Theorem 4.5.2 ([LFP23, Theorem 1.5]). *Let $\alpha > 0$ and let $0 < \gamma < \frac{1}{4\alpha}$ and $\delta > \frac{1}{2\gamma\alpha}$. Let*

$$H_t = (2t - 1) \frac{|z_3|^2}{2} - 2\gamma t(\mathcal{X} - \delta R^2) - 2\gamma \delta t \alpha^2. \quad (4.1)$$

Then the family $(\mathbb{CP}^2, \alpha\omega_{\text{FS}}, F_t = (J, H_t))_{0 \leq t \leq 1}$ is

- *of toric type when $0 \leq t < t^-$;*

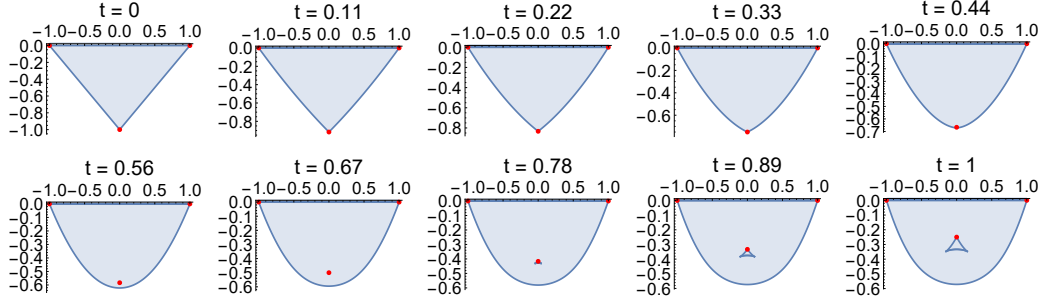


Figure 4.23: Image of (J, H_t) as in Theorem 4.5.2 with $\alpha = 1$, $\gamma = \frac{1}{8}$ and $\delta = 5$, for various values of t . Here $t^- = \frac{2}{5}$ and $t^+ = \frac{2}{3}$.

- *semitoric with one focus-focus point (at $B = [0, 0, \sqrt{2\alpha}]$) when $t^- < t < t^+$;*
- *hypersemitoric (see below) with one triangular flap with elliptic corner $F_t(B)$ when $t^+ < t \leq 1$*

where

$$t^- = \frac{1}{2(1 + 2\gamma\alpha)}, \quad t^+ = \frac{1}{2(1 - 2\gamma\alpha)}.$$

Moreover, when $t^- < t < t^+$, this system is of type (1) with parameter α as in Figure 4.8a. Furthermore, for any $h_0 \in (0, \frac{\alpha}{2})$, there exists a choice of $\gamma \in (0, \frac{1}{4\alpha})$, $\delta \in (\frac{1}{2\gamma\alpha}, +\infty)$ and $t \in (t^-, t^+)$ such that the height invariant of the system is $h = h_0$.

This statement means that this family of explicit systems forms a half-semitoric transition family (recall Definition 4.3.4), and that by varying all the parameters, we obtain all possible marked semitoric polygons of type (1) from this family. Indeed, the parameter α determines the scaling of the marked semitoric polygon, and by varying the parameters t, γ and δ we vary the height invariant.

The image of the momentum map F_t , for a given choice of α and δ and various values of t , is shown in Figure 4.23. The underlying S^1 -space (M, ω, J) has one \mathbb{Z}_2 -sphere $\{z_3 = 0\}$, and this \mathbb{Z}_2 -sphere is sent to the top boundary in the image $F_t(M)$. When $t > t^+$, the system is not semitoric anymore but hypersemitoric in the sense of [HP21]: the singular points of F_t are either non-degenerate or parabolic, which roughly means that they are of the mildest possible degenerate form (see [BGK18, Definition 2.1] for a precise definition). The flap in the image of $F_t(M)$ is the triangular region that can be observed in Figure 4.24, which corresponds to the $t = 1$ part of Figure 4.23. One of its vertices is the elliptic-elliptic value and the other two correspond to parabolic values; the edges emanating from the elliptic-elliptic vertex correspond to elliptic-regular values, and the other edge consists of hyperbolic-regular values. In [LFP23, Section 8.2.3] we study this flap and in particular give a bound on its size in terms of the parameters α, γ, δ and t .

Note that there exists another family of systems of type (1), coming from physics (more precisely from a separation of the 3D harmonic oscillator), forming semitoric families and from which one can obtain every marked semitoric polygon of type (1). These systems were studied in [CDEW19], and one crucial difference is that they do not display flaps; instead the transition point becomes degenerate exactly at one endpoint of the parameter interval. We discuss the comparison between our system and this system in more detail in [LFP23, Remark 1.7].

4.5.3 Systems of type (3a), (3b) and (3c)

Finally, in [LFP23] we constructed explicit semitoric systems of type (3a), (3b) and (3c). Since these systems are quite similar we all discuss them here.

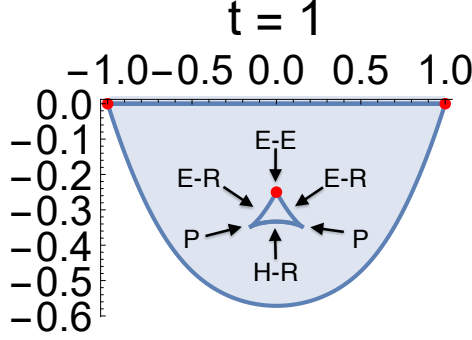


Figure 4.24: The triangular flap in the $t = 1$ system from Theorem 4.5.2, with the same choice of parameters as in Figure 4.23. Here P stands for parabolic, E-R for elliptic-regular, H-R for hyperbolic-regular and E-E for elliptic-elliptic.

Type (3a). Let $n \geq 3$ and let $\alpha, \beta > 0$. We consider the symplectic reduction $(M, \omega) = (W_{n-2}(\alpha + \beta, \beta), \omega_{W_{n-2}(\alpha + \beta, \beta)})$ of \mathbb{C}^4 by the \mathbb{T}^2 -action generated by

$$N = \frac{1}{2} (|z_1|^2 + |z_3|^2 + (n-2)|z_4|^2, |z_2|^2 + |z_4|^2)$$

at level $N = (\alpha + (n-1)\beta, \beta)$. Moreover, we consider the Hamiltonians

$$J = \frac{1}{2} (|z_1|^2 + |z_2|^2), \quad \mathcal{X} = \Re(z_1 z_2 \bar{z}_3^{n-1} z_4), \quad R = \frac{1}{2} (|z_1|^2 + (n-2)|z_4|^2),$$

which are all invariant under the action of N and hence descend to (M, ω) . Note that compared to the description of the Hirzebruch surfaces given at the beginning of Section 4.4, the coordinates z_2, z_3 and z_4 have been replaced by z_3, z_4 and z_2 respectively. This is because here we wanted the \mathbb{Z}_{n-1} -sphere of J to correspond to $\{z_3 = 0\}$, to keep a certain consistency with the explicit system of type (1) discussed in Section 4.5.2.

Theorem 4.5.3. Let $\alpha, \beta > 0$. Let $0 < \gamma < \frac{n-1}{2^{\frac{n+3}{2}} ((n-1)\beta + \alpha)^{\frac{n-1}{2}} \sqrt{2\beta}}$ and let

$$\delta > \max \left(\frac{1}{2((n-1)\beta + \alpha)\gamma}, \frac{2^{\frac{n+1}{2}} ((n-1)\beta + \alpha)^{\frac{n-3}{2}} (n(n-1)\beta + \alpha)}{(n-1)^2 \sqrt{2\beta}} \right).$$

Moreover, let

$$J = \frac{1}{2} (|z_1|^2 + |z_2|^2), \quad H_t = \frac{(2t-1)}{2} |z_3|^2 + 2\gamma t (\mathcal{X} + \delta R^2) - 2\gamma \delta t ((n-1)\beta + \alpha)^2.$$

Then $(M, \omega, F_t = (J, H_t))$ is

- of toric type when $0 \leq t < t^-$;
- semitoric with one focus-focus point (the point $D = [0, \sqrt{2\beta}, \sqrt{2(\alpha + (n-1)\beta)}, 0]$) when $t^- < t < t^+$,

where

$$t^- = \frac{1}{2 \left(1 + \frac{2^{\frac{n+1}{2}} \gamma ((n-1)\beta + \alpha)^{\frac{n-1}{2}} \sqrt{2\beta}}{n-1} \right)}, \quad t^+ = \frac{1}{2 \left(1 - \frac{2^{\frac{n+1}{2}} \gamma ((n-1)\beta + \alpha)^{\frac{n-1}{2}} \sqrt{2\beta}}{n-1} \right)}.$$

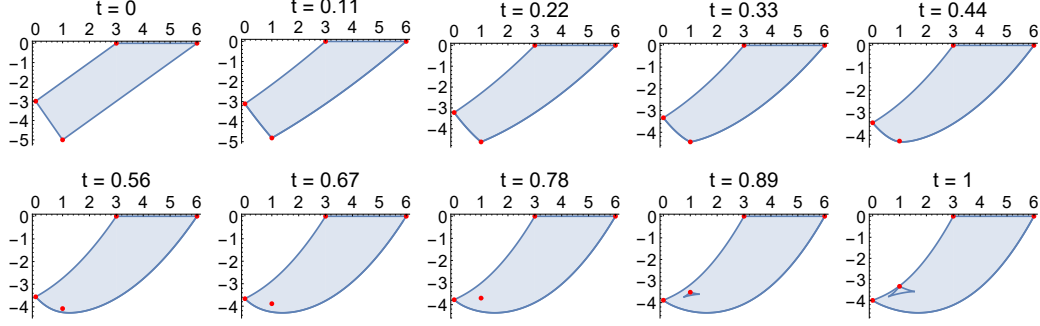


Figure 4.25: Image of (J, H_t) as in Theorem 4.5.3 with $n = 4$, $\alpha = 2$, $\beta = 1$, $\gamma = \frac{1}{90}$ and $\delta = 15$. For these values of the parameters, $t^- = \frac{27}{2(27+4\sqrt{5})} \approx 0.38$ and $t^+ = \frac{27}{2(27-4\sqrt{5})} \approx 0.75$.

Moreover, for $t \in (t^-, t^+)$ the semitoric polygon of the system is the one shown in Figure 4.8d, so it is of type (3a) with parameters α, β and n . Furthermore, if $n = 3$, for any $h_0 \in (0, h^+)$, where

$$h^+ = \begin{cases} \frac{16\beta(\alpha+2\beta) \arctan\left(\sqrt{\frac{6\beta-\alpha}{\alpha+2\beta}}\right) + 16\beta^2 \arctan\left(\frac{\sqrt{(6\beta-\alpha)(\alpha+2\beta)}}{2\beta-\alpha}\right) - (\alpha+6\beta)\sqrt{(6\beta-\alpha)(\alpha+2\beta)}}{16\pi\beta} & \text{if } \alpha < 2\beta, \\ \left(\frac{3}{2} - \frac{2}{\pi}\right)\beta & \text{if } \alpha = 2\beta, \\ \beta - \frac{(\alpha+6\beta)\sqrt{(6\beta-\alpha)(\alpha+2\beta)} + 16\beta^2 \arctan\left(\frac{\sqrt{(6\beta-\alpha)(\alpha+2\beta)}}{\alpha-2\beta}\right) - 16\beta(\alpha+2\beta) \arctan\left(\sqrt{\frac{6\beta-\alpha}{\alpha+2\beta}}\right)}{16\pi\beta} & \text{if } 2\beta < \alpha < 6\beta, \\ \beta & \text{if } \alpha \geq 6\beta, \end{cases}$$

there exists a choice of $\gamma \in \left(0, \frac{1}{4(\alpha+2\beta)\sqrt{2\beta}}\right)$, $\delta \in \left(\max\left(\frac{1}{2(\alpha+2\beta)\gamma}, \frac{\alpha+6\beta}{\sqrt{2\beta}}\right), +\infty\right)$ and $t \in (t^-, t^+)$ such that the height invariant of the system is $h = h_0$.

The last part of this statement means that for some values of the parameters α and β , when $n = 3$, we can obtain every possible marked semitoric polygon of type (3a) from a system in this family. However, in general we cannot obtain every possible value for the height invariant, hence we only obtain all possible unmarked semitoric polygon of type (3a) in this way. And for $n \geq 4$, the computation of the maximal height invariant that we can obtain by varying the parameters is too involved (this is the same for the explicit systems of type (3b) and (3c) below, except that for type (3b) the case $n = 4$ remains tractable). The image of the momentum map for this system when $n = 4$ and for some choice of parameters is displayed in Figure 4.25.

Type (3b). Let $n \geq 3$ and let $\beta > 0$. We work in the symplectic manifold $(M, \omega) = (W_{n-2}(\beta, \beta), \omega_{W_{n-2}(\beta, \beta)})$ obtained as the symplectic reduction of \mathbb{C}^4 by

$$N = \frac{1}{2} (|z_1|^2 + |z_3|^2 + (n-2)|z_4|^2, |z_2|^2 + |z_4|^2)$$

at level $N = (2\beta, \beta)$, and we consider the Hamiltonians

$$J = \frac{1}{2} (|z_1|^2 + |z_2|^2), \quad \mathcal{X} = \Re(z_1 z_2 \bar{z}_3^{n-1} z_4), \quad R = \frac{1}{2} (|z_1|^2 + (n-2)|z_4|^2).$$

Theorem 4.5.4. Let $\beta > 0$. Let $0 < \gamma < \frac{1}{4(2\beta)^{\frac{n}{2}}(n-1)^{\frac{n-3}{2}}}$ and let

$$\delta > \max\left(\frac{1}{2(n-1)\beta\gamma}, n2^{\frac{n}{2}}(n-1)^{\frac{n-5}{2}}\beta^{\frac{n}{2}-1}\right).$$

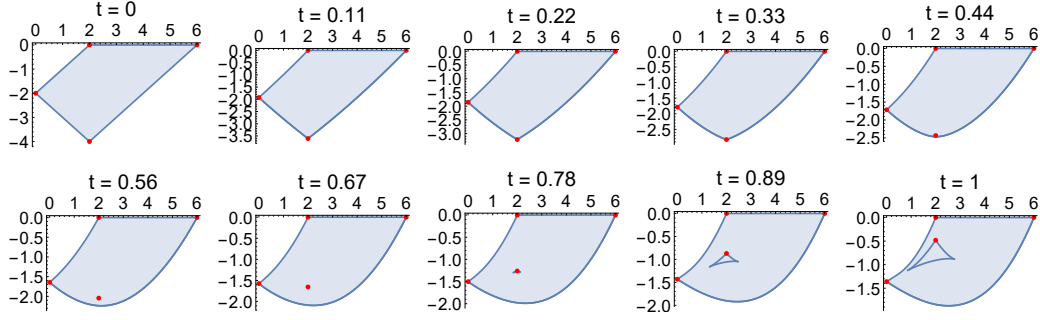


Figure 4.26: Image of (J, H_t) as in Theorem 4.5.4 with $n = 3$, $\beta = 2$, $\gamma = \frac{1}{50}$ and $\delta = 7$. For this choice of parameters, $t^- = \frac{25}{66} \approx 0.38$ and $t^+ = \frac{25}{34} \approx 0.74$.

Moreover, let

$$J = \frac{1}{2}(|z_1|^2 + |z_2|^2), \quad H_t = \frac{(2t-1)}{2}|z_3|^2 + 2\gamma t(\mathcal{X} + \delta R^2) - 2\gamma \delta t(n-1)^2 \beta^2.$$

Then $(M, \omega, F_t = (J, H_t))$ is

- of toric type when $0 \leq t < t^-$;
- semitoric with one focus-focus point when $t^- < t < t^+$,

where

$$t^- = \frac{1}{2 \left(1 + 2^{\frac{n}{2}+1} \gamma (n-1)^{\frac{n-3}{2}} \beta^{\frac{n}{2}} \right)}, \quad t^+ = \frac{1}{2 \left(1 - 2^{\frac{n}{2}+1} \gamma (n-1)^{\frac{n-3}{2}} \beta^{\frac{n}{2}} \right)}.$$

Moreover, for $t \in (t^-, t^+)$ the semitoric polygon of the system is the one shown in Figure 4.8e, so it is of type (3b) with parameters β and n . Furthermore:

- if $n = 3$, for any $h_0 \in (0, h^+)$ where

$$h^+ = \left(1 - \frac{3\sqrt{3}}{4\pi} \right) \beta,$$

there exists a choice of $\gamma \in \left(0, \frac{1}{8\beta^2\sqrt{2}\beta} \right)$, $\delta \in \left(\max \left(\frac{1}{4\beta\gamma}, 3\sqrt{2}\beta \right), +\infty \right)$ and $t \in (t^-, t^+)$ such that the height invariant of the system is $h = h_0$;

- if $n = 4$, for any $h_0 \in (0, h^+)$ where

$$h^+ = \left(1 - \frac{\ln(12 - 8\sqrt{2})}{\pi} \right) \beta,$$

there exists a choice of $\gamma \in \left(0, \frac{1}{16\beta^2\sqrt{3}} \right)$, $\delta \in \left(\max \left(\frac{1}{6\beta\gamma}, \frac{16\beta}{\sqrt{3}} \right), +\infty \right)$ and $t \in (t^-, t^+)$ such that the height invariant of the system is $h = h_0$.

Again, we can obtain every possible unmarked semitoric polygon of type (3b) by varying the parameters in this system, but not every marked semitoric polygon. The image of the momentum map for this system for a certain choice of parameters is shown in Figure 4.26.

Type (3c). Let $n \geq 3$ and let $\beta > 0$ and $0 < \alpha < \beta$. We work in the symplectic reduction $(M, \omega) = (W_{n-2}(\beta - \alpha, \beta), \omega_{W_{n-2}(\beta - \alpha, \beta)})$ of \mathbb{C}^4 by the action of

$$N = \frac{1}{2} (|z_1|^2 + |z_3|^2 + (n-2)|z_4|^2, |z_2|^2 + |z_4|^2)$$

at level $N = ((n-1)\beta - \alpha, \beta)$, and we consider

$$J = \frac{1}{2} (|z_1|^2 + |z_2|^2), \quad \mathcal{X} = \Re(z_1 \bar{z}_2 \bar{z}_3^{n-1} z_4), \quad R = \frac{1}{2} (|z_1|^2 + (n-2)|z_4|^2).$$

Theorem 4.5.5. Let $n \geq 3$. Let $\beta > 0$ and $0 < \alpha < \beta$. Let $0 < \gamma < \frac{n-1}{2^{\frac{n+3}{2}}((n-1)\beta - \alpha)^{\frac{n-1}{2}}\sqrt{2\beta}}$ and let $\delta > \max \left(\frac{1}{2((n-1)\beta - \alpha)\gamma}, \frac{2^{\frac{n+1}{2}}((n-1)\beta - \alpha)^{\frac{n-3}{2}}(n(n-1)\beta - \alpha)}{(n-1)^2\sqrt{2\beta}} \right)$. Let

$$J = \frac{1}{2} (|z_1|^2 + |z_2|^2), \quad H_t = \frac{(2t-1)}{2} |z_3|^2 + 2\gamma t(\mathcal{X} + \delta R^2) - 2\gamma \delta t((n-1)\beta - \alpha)^2.$$

Then $(M, \omega, F_t = (J, H_t))$ is

- of toric type when $0 \leq t < t^-$;
- semitoric with one focus-focus point (the point $D = [0, \sqrt{2\beta}, \sqrt{2((n-1)\beta - \alpha)}, 0]$) when $t^- < t < t^+$,

where

$$t^- = \frac{1}{2 \left(1 + \frac{2^{\frac{n+1}{2}} \gamma ((n-1)\beta - \alpha)^{\frac{n-1}{2}} \sqrt{2\beta}}{n-1} \right)}, \quad t^+ = \frac{1}{2 \left(1 - \frac{2^{\frac{n+1}{2}} \gamma ((n-1)\beta - \alpha)^{\frac{n-1}{2}} \sqrt{2\beta}}{n-1} \right)}.$$

Moreover, for $t \in (t^-, t^+)$ the semitoric polygon of the system is the one shown in Figure 4.8f, so it is of type (3c) with parameters α, β and n . Furthermore, if $n = 3$, for any $h_0 \in (0, h^+)$, where

$$h^+ = \frac{16\beta(2\beta - \alpha) \arctan \left(\sqrt{\frac{\alpha+6\beta}{2\beta-\alpha}} \right) + 16\beta^2 \arctan \left(\frac{\sqrt{(\alpha+6\beta)(2\beta-\alpha)}}{\alpha+2\beta} \right) - (6\beta - \alpha) \sqrt{(\alpha+6\beta)(2\beta-\alpha)}}{16\pi\beta},$$

there exists a choice of $\gamma \in \left(0, \frac{1}{4(2\beta-\alpha)\sqrt{2\beta}} \right)$, $\delta \in \left(\max \left(\frac{1}{2(2\beta-\alpha)\gamma}, \frac{6\beta-\alpha}{\sqrt{2\beta}} \right), +\infty \right)$ and $t \in (t^-, t^+)$ such that the height invariant of the system is $h = h_0$.

As before, we can obtain every possible unmarked semitoric polygon of type (3c) from this system by choosing the parameters appropriately, but not every marked semitoric polygon. The image of the momentum map F_t for $n = 5$ and some choice of parameters is displayed in Figure 4.27.

4.5.4 General strategy

We conclude by giving some recipes to come up with such explicit systems. Concretely, we fix a marked semitoric polygon $[(\Delta, \vec{c}, \vec{\epsilon})]$ and want to find an explicit semitoric system with this polygon as its invariant. In most examples, we looked for very particular families $(M, \omega, F_t = (J, H_t))_{0 \leq t \leq 1}$ in which the Hamiltonian H_t is obtained as a convex combination

$$H_t = (1-t)H_0 + tH_1 \quad \text{or} \quad H_t = (1-2t)H_0 + 2tH_{\frac{1}{2}};$$

in this case the question is how (M, ω) , J , H_0 and H_1 (or $H_{\frac{1}{2}}$) should be chosen.

Assume that one of the vertices in one representative of $[(\Delta, \vec{c}, \vec{\epsilon})]$

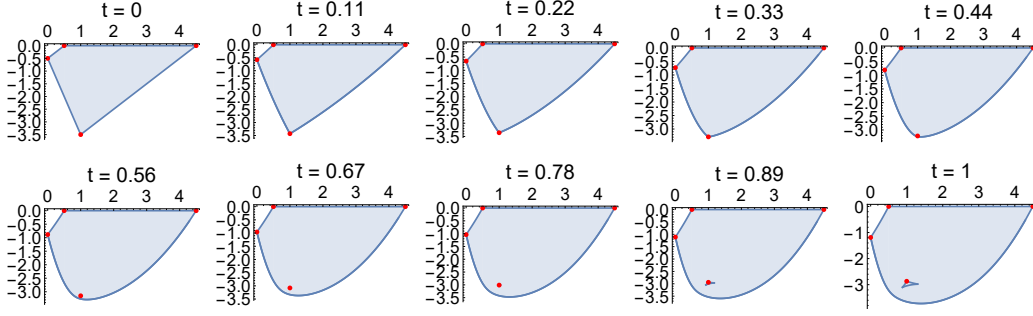


Figure 4.27: Image of (J, H_t) as in Theorem 4.5.5 with $n = 5$, $\alpha = \frac{1}{2}$, $\beta = 1$, $\gamma = \frac{1}{100}$ and $\delta = 26$. For these values of the parameters, $t^- = \frac{100}{200+49\sqrt{2}} \approx 0.37$ and $t^+ = \frac{100}{200-49\sqrt{2}} \approx 0.77$.

- either is 1-fake and at the same time satisfies the Delzant condition;
- or is k -fake for some $k \geq 2$ and at the same time satisfies the $(k-1)$ -hidden Delzant condition (see Definition 3.4.2).

Then we can erase one cut hitting this vertex and the marked point it emanates from to obtain a different marked semitoric polygon $[(\Delta', \vec{c}', \vec{\epsilon}')]$, corresponding to a semitoric system with one less focus-focus point. If we know a fully explicit semitoric system with $[(\Delta', \vec{c}', \vec{\epsilon}')] as its marked semitoric polygon, we will take this system as our $(M, \omega, (J, H_0))$. In particular, if $[(\Delta', \vec{c}', \vec{\epsilon}')] = [(\Delta', \emptyset, \emptyset)]$ with Δ' Delzant, we do know such an explicit $(M, \omega, (J, H_0))$ thanks to Delzant's algorithm (see Section 3.1). This is what happens in practice for most of our examples.$

Example 4.5.6. In this example and Examples 4.5.7 and 4.5.8 below, we will explain how we came up with the systems of type (1) from Section 4.5.2. The fake vertex of the polygon in Figure 4.8a is not Delzant, so we change the cut direction to obtain the representative shown on the left in Figure 4.28. The vertex $(\alpha, 0)$ is 1-fake and satisfies the Delzant condition, so we erase the corresponding cut and marked point. We obtain a Delzant polygon, and Delzant's algorithm yields that $(\mathbb{CP}^2, \alpha\omega_{FS}, (J, H_0))$ where

$$J = \frac{1}{2} (|z_1|^2 - |z_2|^2), \quad H_0 = \frac{1}{2} |z_1|^2,$$

is a toric system with this polygon as its momentum map image. The Hamiltonian H_0 is actually not the one that we used in Theorem 4.5.2, for a reason that will be explained in Example 4.5.8.

Now it remains to choose an appropriate H_1 (or $H_{\frac{1}{2}}$). In [LFP22, Section 3.3] we proposed to approach this question geometrically as follows. Let j be a singular level of J containing one fixed point p of the corresponding S^1 -action and embed the singular symplectic quotient $M_j^{\text{red}} = J^{-1}(j)/S^1$ in \mathbb{R}^3 in such a way that the singularity $[p]$ corresponds to the global maximum of the height function \mathcal{Z} . Let $H_t^{\text{red}, j}$ be the reduced Hamiltonian induced by H_t on M_j^{red} , and assume that \mathcal{Z} is a function of the reduced Hamiltonian $R = H_0^{\text{red}, j}$, as in Figure 4.29. Let $(\mathcal{X}, \mathcal{Y})$ be horizontal coordinates on M_j^{red} . Then by choosing $H_{\frac{1}{2}}$ in such a way that $H_{\frac{1}{2}}^{\text{red}, j} = \mathcal{X}$, we see that p transitions from elliptic-elliptic to focus-focus as the parameter t varies in $[0, \frac{1}{2}]$.

This approach requires to find good coordinates on the reduced space M_j^{red} , in a consistent way as j varies. In [LFP23] we gave another point of view, perhaps less geometric but more useful in practice. Recall from Equation (3.17) and from the fact that the weights at a focus-focus point are -1 and 1 that there exist local complex symplectic coordinates z_1, z_2 near the point p that we want to transition between elliptic-elliptic and focus-focus such that

$$J = \frac{1}{2} (|z_1|^2 - |z_2|^2)$$

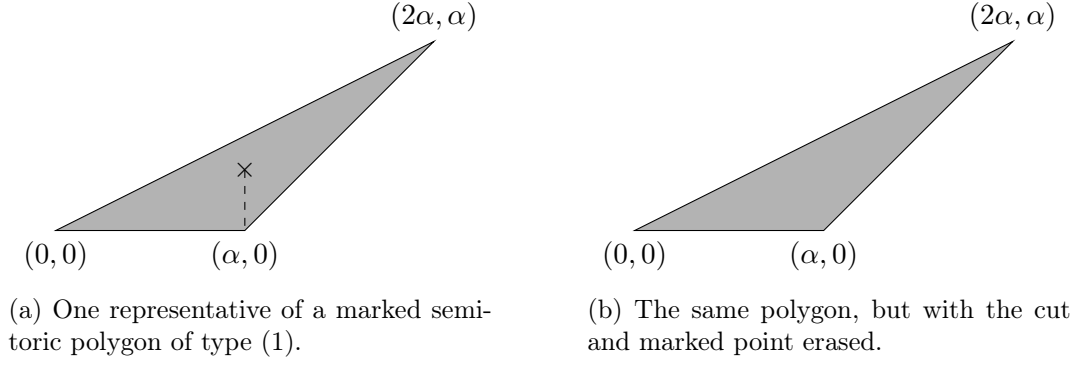


Figure 4.28: Erasing the cut incident to a 1-fake vertex satisfying the Delzant condition, and the corresponding marked point, in a representative of a marked semitoric polygon of type (1). The outcome is a Delzant polygon.

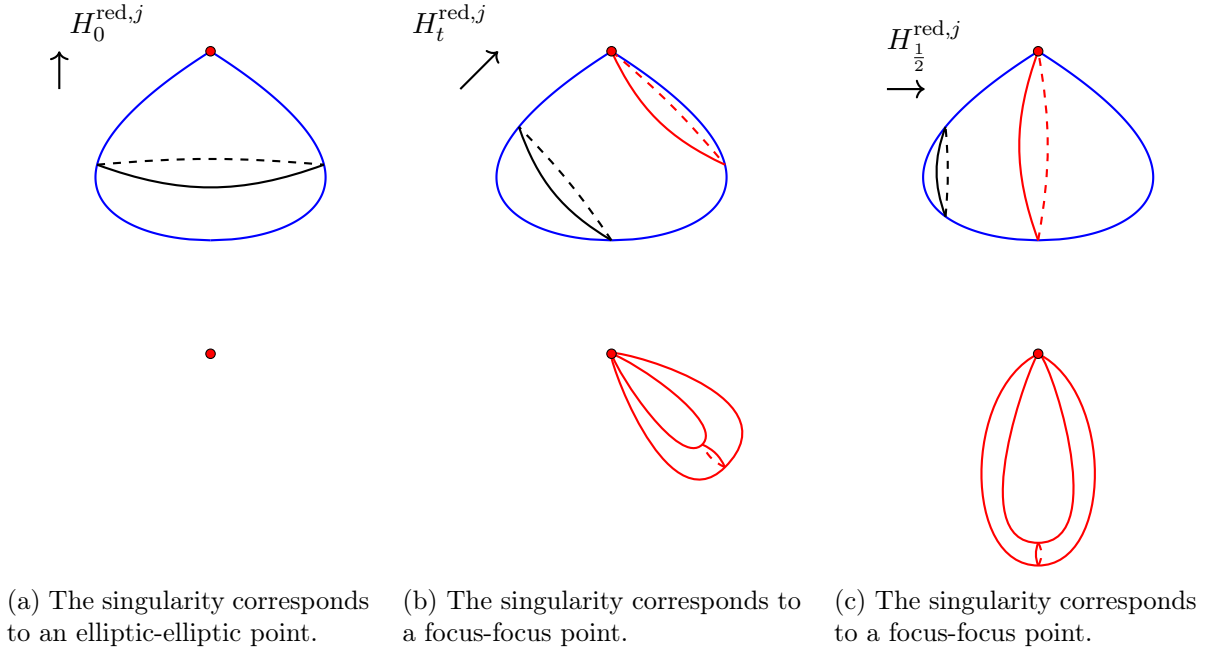


Figure 4.29: Top row: the singular level (in red, with the red circle indicating the singular point) and a regular level (in black) for the function $H_t^{\text{red},j} = (1 - 2t)H_0^{\text{red},j} + 2t\mathcal{X}$, for different values of t , on the reduced space M_j^{red} (in blue) where j is a singular value of J . Bottom row: the corresponding singular fibers in M .

(assuming that $J(p) = 0$ for the sake of simplicity). In [LFP23, Proposition 7.5] we proved that the quadratic Hamiltonians commuting with this normal form are of the form

$$H(z_1, z_2) = \mu_1 \Re(e^{i\psi} z_1 z_2) + \mu_2 |z_1|^2 + \mu_3 |z_2|^2 \quad (4.2)$$

for some $\mu_1, \mu_2, \mu_3, \psi \in \mathbb{R}$. We showed moreover that (q_1, H) is integrable if and only if $(\mu_1, \mu_2 + \mu_3) \neq (0, 0)$ and that in this case the singular point $(0, 0)$ of (q_1, H) is

- of focus-focus type if $|\mu_2 + \mu_3| < |\mu_1|$;
- of elliptic-elliptic type if $|\mu_2 + \mu_3| > |\mu_1|$;
- degenerate if $|\mu_2 + \mu_3| = |\mu_1|$.

This gives a recipe to choose $H_{\frac{1}{2}}$: put J in normal form near p , and then choose locally $H_{\frac{1}{2}}$ of the above form (4.2) with $|\mu_2 + \mu_3| < |\mu_1|$, so that p is focus-focus for $(J, H_{\frac{1}{2}})$. Then extend this to a global $H_{\frac{1}{2}}$ on M . In practice, since in most of the examples $(M, \omega, (J, H_0))$ comes from Delzant's algorithm, the coordinates of the normal form for J are very often easy to obtain.

Example 4.5.7. Let us continue investigating the constructions of Section 4.5.2. Recall from Example 4.5.6 that we consider $J = \frac{1}{2}(|z_1|^2 - |z_2|^2)$; hence J is already in normal form near the point $p = [0, 0, \sqrt{2}\alpha]$. Choosing $\psi = 0$, $\mu_1 = -\gamma$ with $\gamma > 0$ and $\mu_2 = 0 = \mu_3$ leads to considering the local Hamiltonian $-\gamma \Re(z_1 z_2)$ near p . This can be extended to a globally defined Hamiltonian $H_{\frac{1}{2}} = -\gamma \Re(z_1 z_2 \bar{z}_3^2)$ on \mathbb{CP}^2 . This is part of the actual Hamiltonian $H_{\frac{1}{2}}$ in Equation (4.1), but there is an additional term which will be justified in Example 4.5.8.

The above recipe ensures that the point p will transition from focus-focus to elliptic-elliptic as t varies, but it does not guarantee that the system $(M, \omega, F_{\frac{1}{2}} = (J, H_{\frac{1}{2}}))$ will be semitoric. Nevertheless, it is sufficient to come up with the explicit examples from [LFP22]. However, as already explained, these examples had the nice property to not include any \mathbb{Z}_k -sphere. And unfortunately, \mathbb{Z}_k -spheres can cause some trouble: it can happen that the image of some points in such a \mathbb{Z}_k -sphere lies in the interior of the image $F_t(M)$ for some $t \in [0, \frac{1}{2}]$, in which case (M, ω, F_t) cannot be semitoric (see for instance [LFP23, Lemma 2.14]). To solve this problem, it is necessary to modify H_t so that the images of the \mathbb{Z}_k -spheres lie on the boundary of $F_t(M)$ for all t , and this can be done by adding some correction terms to H_t . But these correction terms should not modify the quadratic part of H_t , to ensure that p stays of the desired type (elliptic-elliptic or focus-focus, depending on t).

Example 4.5.8. Again, we work in the setting of Section 4.5.2. Recall from Example 4.5.6 that we work with $J = \frac{1}{2}(|z_1|^2 - |z_2|^2)$; J has a \mathbb{Z}_2 -sphere given by the set of points with $z_3 = 0$. First, it is convenient to make the image of this \mathbb{Z}_2 -sphere become horizontal for $t = 0$; this is why instead of the Hamiltonian H_0 obtained in Example 4.5.6, we work with $H_0 = -\frac{1}{2}|z_3|^2$, in which case the image of the \mathbb{Z}_2 -sphere coincides with the top boundary of $F_0(\mathbb{CP}^2)$. Second, we want to make sure that this is still the case for $t \neq 0$; this is the part played by the correction term $2\gamma\delta t R^2$ in Equation (4.1), see [LFP23, Remark 8.4] for more details, and recall Figure 4.23.

Once a potentially interesting integrable system is constructed by applying this general strategy, it still remains to check that it is indeed integrable and of the desired kind depending on the value of the parameter (e.g. of toric type, semitoric with a given number of focus-focus points, or hypersemitoric as in Theorem 4.5.2). This involves computations that can be lengthy and tedious, see for instance [HP18, Section 3], [LFP19b, Section 2 and Appendix B], [DMH21] or [LFP22, Sections 6 and 7]. In [LFP23, Section 7], we introduced some general procedures to simplify these computations.

4.6 Perspectives

To conclude, we describe a few potentially interesting questions related to the contents of this chapter.

In [LFP23], we constructed fully explicit semitoric systems from all strictly minimal unmarked semitoric polygons; it would be interesting to obtain an explicit system for each strictly minimal marked semitoric polygon. This means that we would like to construct an example for every possible value of the height invariant in systems of type (3) (see Section 4.5.3); this seems difficult and may require to refine our strategies. Another possibility would be to try these strategies on systems which are not strictly minimal anymore but possess some interesting features. For instance, finding an explicit system with either one focus-focus point and two distinct \mathbb{Z}_k and \mathbb{Z}_ℓ -spheres, or two focus-focus points and one \mathbb{Z}_k -sphere, would be a good test for the recipe described in Section 4.5.4. Here we talk about the case where these three features (focus-focus point and non-trivial isotropy spheres) do not lie in the same J -fiber; if they did, this would constitute an obstruction to be part of a half-semitoric transition family.

These obstructions, which can be read on the marked semitoric polygon, for a semitoric system to be a member of a half-semitoric transition family, were obtained in [LFP23, Proposition 5.7]. A natural question is whether these obstructions can be turned into a necessary and sufficient condition: if a semitoric system (M, ω, F) does not satisfy them, can one find a half-semitoric family including it? Or at least, can one find a semitoric family including it? One possible strategy would be to perform blowdowns of toric and semitoric type on (M, ω, F) to obtain a strictly minimal system, to apply Theorem 4.3.5 that states that this strictly minimal system is a member of a semitoric family, and then to go back to the initial system (M, ω, J) by performing blowups of toric and semitoric type. The difficulty is that we do not know if there is a way to obtain a semitoric (or half-semitoric transition) family from the semitoric type blowup of a semitoric (or half-semitoric transition) family, and this would require to study closely these blowups in the manifold M and not only on marked semitoric polygons. This study will be performed in the upcoming [HSSS].

Finally, as explained in Section 4.2.3, in [LFP23] we studied the strictly minimal semitoric systems by computing all possible marked semitoric polygons associated with strictly minimal semitoric helices and using the marked polygon isomorphism from Theorem 4.2.4. For strictly minimal helices this remains tractable because the number of marked semitoric polygons associated with a given helix is relatively small, but in general the map sending a marked semitoric polygon to its helix is far from injective. Moreover as we already explained, the semitoric helix can be constructed directly from the system rather than its marked semitoric polygon. It would be interesting to study the helix invariant in more detail, in order to give a necessary and sufficient condition for two semitoric systems to possess the same helix.

Chapter 5

Inverse spectral theory for semitoric systems

In this chapter we introduce the inverse spectral problem for semitoric systems and explain its resolution in [LFVuN21] with San Vũ Ngọc. In this whole chapter, **the semitoric systems are assumed to be simple** (see Definition 3.3.2), unless stated otherwise. In Section 5.1, we introduce quantum semitoric systems and their joint spectra. In Section 5.2, we state the main result of [LFVuN21], namely the complete, constructive resolution of the inverse spectral problem for semitoric systems. In Section 5.3 we discuss two crucial ingredients of the proof of this result, namely asymptotic lattices and half-lattices and their relationship with the joint spectra of quantum integrable systems. Then in Section 5.4 we explain how to recover, using these ingredients, all symplectic invariants of a semitoric system from the joint spectrum of its quantum counterpart. Finally, in Section 5.5 we describe some potentially interesting research directions.

We believe that the results from [LFVuN21] can be extended with few modifications to the case of a semitoric system which may have several focus-focus points in the same J -fiber but not in the same F -fiber, in other words in the case where there may be several tori pinched at a single point in a given J -fiber, but no torus pinched at two or more points. In the latter case, the question remains open and it is possible that the spectral data will not be sufficient to determine all the symplectic invariants, in particular the Taylor series invariant.

5.1 Quantum semitoric systems

In order to quantize a semitoric system, we may need to consider, depending on the phase space (M, ω) , either \hbar -pseudodifferential operators or Berezin-Toeplitz operators. The former now form a very standard topic and we refer the reader to the abundant literature (a good starting point is the recent book [Zwo12]), and the latter are reviewed in Section 2.1 in the Kähler case. For our purpose, working in this Kähler setting is not restrictive, since by [Kar99, Theorem 7.1] a compact symplectic manifold endowed with an effective Hamiltonian S^1 -action is automatically Kähler.

More precisely, in [LFVuN21] we considered three settings:

1. $(M, \omega) = (T^*X, d\lambda)$ where $X = \mathbb{R}^2$ or X is a compact Riemannian surface and λ is the Liouville one-form. In this case a *semiclassical operator* is a (possibly unbounded) \hbar -pseudodifferential operator acting on $\mathcal{H}_\hbar = L^2(X)$;
2. (M, ω) is a quantizable compact Kähler manifold of dimension four, with prequantum line bundle L and auxiliary line bundle L' . In this case a *semiclassical operator* is a Berezin-Toeplitz operator acting on $\mathcal{H}_\hbar = H^0(M, L^{\otimes k} \otimes L')$ with k a positive integer and $\hbar = k^{-1}$;

3. $(M, \omega) = (\mathbb{C} \times N, \omega_0 \oplus \omega_N)$ where ω_0 is the standard symplectic form on \mathbb{C} and (N, ω_N) is a quantizable compact Kähler surface with prequantum line bundle L and auxiliary line bundle L' . In this case a *semiclassical operator* is a (possibly unbounded) Berezin-Toeplitz operator acting on

$$\mathcal{B}_k \otimes H^0(N, L^k \otimes L')$$

still with $k \geq 1$ and $\hbar = k^{-1}$. Here \mathcal{B}_k is the Bargmann space of Example 2.1.2.

The *joint principal symbol* of two commuting semiclassical operators is $(f_1, f_2) \in \mathcal{C}^\infty(M, \mathbb{R}^2)$ where f_1 and f_2 are the respective principal symbols of these operators.

Definition 5.1.1. Consider a set $\mathcal{I} \subset (0, +\infty)$ having zero as an accumulation point. A *quantum integrable system* $(\hat{J}_\hbar, \hat{H}_\hbar)_{\hbar \in \mathcal{I}}$ is the data of two commuting semiclassical operators \hat{J}_\hbar and \hat{H}_\hbar on \mathcal{H}_\hbar whose joint principal symbol $F = (J, H)$ is the momentum map of an integrable system. If moreover this system is semitoric, we call $(\hat{J}_\hbar, \hat{H}_\hbar)_{\hbar \in \mathcal{I}}$ a *quantum semitoric system*.

Throughout this chapter and to keep a certain consistency with the rest of the manuscript, we will illustrate our results on an example whose underlying phase space is compact, namely a quantization of the coupled angular momenta system described in Example 3.3.4. We refer the reader who is interested in the non-compact case to [LFVuN21], in which we also investigate the example of the Jaynes-Cummings system, which quantizes the spin-oscillator system described in Example 3.3.3. One interesting feature that both examples share is that their symplectic invariants have been computed explicitly in [ADH20, ADH19], so they provide a fertile ground to verify numerically the validity of our results. It would also be interesting to verify them on an example with two or more focus-focus points, but at the time that we wrote [LFVuN21] the literature did not contain any example with two focus-focus points for which all the invariants were computed; such an example now exists in [AHP23].

Example 5.1.2 (Coupled angular momenta.). Assume that the quantities $R_1, R_2 > 0$ introduced in Example 3.3.4 are half-integers. Then the system $(S^2 \times S^2, -(R_1 \omega_{S^2} \oplus R_2 \omega_{S^2}), (J, H_t))$, with (J, H_t) as in Equation (3.3) can be quantized as follows, using Example 2.1.1. The operators

$$\begin{cases} \hat{J}_k = R_1 \hat{Z}_{2kR_1} \otimes \text{Id} + R_2 \text{Id} \otimes \hat{Z}_{2kR_2}, \\ \hat{H}_k = (1-t) \hat{Z}_{2kR_1} \otimes \text{Id} + t \left(\hat{X}_{2kR_1} \otimes \hat{X}_{2kR_2} + \hat{Y}_{2kR_1} \otimes \hat{Y}_{2kR_2} + \hat{Z}_{2kR_1} \otimes \hat{Z}_{2kR_2} \right). \end{cases} \quad (5.1)$$

acting on $H^0(\mathbb{CP}^1, \mathcal{O}(2kR_1 - 1)) \otimes H^0(\mathbb{CP}^1, \mathcal{O}(2kR_2 - 1))$, with $\hat{X}, \hat{Y}, \hat{Z}$ as in Equation (2.8), are commuting Berezin-Toeplitz operators with joint principal symbol (J, H_t) . More details can be found in [LFP19b, Section 4], in which we used a slightly different notation.

Recall that the commuting operators $\hat{J}_\hbar, \hat{H}_\hbar$ have a *joint spectral measure* σ_\hbar such that

$$\hat{J}_\hbar = \int_{\mathbb{R}^2} s_1 \, d\sigma_\hbar(s), \quad \hat{H}_\hbar = \int_{\mathbb{R}^2} s_2 \, d\sigma_\hbar(s),$$

see for instance [SBS87, Section 6.5].

Definition 5.1.3. The *joint spectrum* Σ_\hbar of a quantum integrable system $(\hat{J}_\hbar, \hat{H}_\hbar)$ is the support of the joint spectral measure of \hat{J}_\hbar and \hat{H}_\hbar .

For instance, in the finite-dimensional case, or more generally if the joint spectrum is discrete, this joint spectrum is simply the set of all joint eigenvalues of \hat{J}_\hbar and \hat{H}_\hbar :

$$\Sigma_\hbar = \{(\lambda_1, \lambda_2) \in \mathbb{R}^2 \mid \exists \psi \in \mathcal{H}_\hbar \setminus \{0\}, \hat{J}_\hbar \psi = \lambda_1 \psi, \hat{H}_\hbar \psi = \lambda_2 \psi\}.$$

In what follows we will always assume that the joint spectrum is discrete. This can be ensured by assuming the ellipticity at infinity of the operator $\hat{J}_\hbar^2 + \hat{H}_\hbar^2$, in which case the system is called *proper*; this is well-known in the \hbar -pseudodifferential case and also works in the case of Berezin-Toeplitz operators on Bargmann spaces. Hence we will always make this assumption that $(\hat{J}_\hbar, \hat{H}_\hbar)$ is proper.

Example 5.1.4. The joint spectrum of the coupled angular momenta system (\hat{J}_k, \hat{H}_k) of Example 5.1.2 has been computed with different notation in [LFP19b, Section 4.4], and alternatively readily follows from Equations (5.1) and (2.8). It is given by

$$\Sigma_k = \bigcup_{j=0}^{\mathfrak{J}_k} \left\{ \left(-(R_1 + R_2) + \frac{j+1}{k}, E_0(j) \right), \dots, \left(-(R_1 + R_2) + \frac{j+1}{k}, E_{d(j)}(j) \right) \right\}$$

where $\mathfrak{J}_k = 2(k(R_1 + R_2) - 1)$,

$$d(j) = \begin{cases} j & \text{if } 0 \leq j \leq 2kR_1 - 1, \\ 2kR_1 - 1 & \text{if } 2kR_1 \leq j \leq 2kR_2 - 1, \\ 2k(R_1 + R_2) - j - 2 & \text{if } 2kR_2 \leq j \leq \mathfrak{J}_k, \end{cases}$$

and $E_0(j), \dots, E_{d(j)}(j)$ are the eigenvalues of the matrix

$$A_j = \frac{1}{4k^2 R_1 R_2} \begin{pmatrix} \alpha_0(j) & \beta_1(j) & 0 & \dots & 0 \\ \beta_1(j) & \alpha_1(j) & \beta_2(j) & \ddots & \vdots \\ 0 & \beta_2(j) & \alpha_2(j) & \ddots & 0 \\ \vdots & \ddots & \ddots & \ddots & \beta_{d(j)}(j) \\ 0 & \dots & 0 & \beta_{d(j)}(j) & \alpha_{d(j)}(j) \end{pmatrix}$$

with

$$\alpha_\ell(j) = (2(\ell - kR_1) + 1)(2kR_2 + (2(j - \ell) + 1)t)$$

for $0 \leq \ell \leq d(j)$ and

$$\beta_m(j) = 2t\sqrt{\ell(j - \ell + 1)(2kR_1 - \ell)(2kR_2 - (j - \ell + 1))}$$

for $1 \leq m \leq d(j)$. Here for the sake of simplicity we have assumed that $R_2 > R_1$ (when $R_1 = R_2$ there are only two cases for $d(j)$ which can be easily sorted out). This joint spectrum can then be computed by numerically diagonalizing the matrix A_j ; see Figure 5.1 in which we display this joint spectrum for the choice of parameters $R_1 = 1$, $R_2 = \frac{5}{2}$ and $t = \frac{1}{2}$ that we will keep in all the examples of this chapter.

So for each value of $\hbar \in \mathcal{I}$ we have a discrete subset of \mathbb{R}^2 given by the joint spectrum Σ_\hbar of the semiclassical operators $(\hat{J}_\hbar, \hat{H}_\hbar)$. The question that we addressed in [LFVuN21] is the semitoric case of the following more general question. Given a quantum integrable system, does this family $(\Sigma_\hbar)_{\hbar \in \mathcal{I}}$ of joint spectra determine the underlying classical integrable system (up to a good notion of isomorphism)? This was answered positively for the toric case in [CPVuN13], see also [PPVuN14], in a constructive way: Σ_\hbar converges, as $\hbar \rightarrow 0$, to the Delzant polygon of the underlying toric system.

For focus-focus fibers containing one singularity, it was proved in [PVN14] that the Taylor series invariant (see Section 3.4.2) is determined by the joint spectrum, as a uniqueness statement: if two quantum integrable systems share the same joint spectrum near the singular value, then the Taylor series invariants of the underlying semitoric systems coincide. In the semitoric case, we also obtained a uniqueness statement in [LFPVN16, LFPVN19]: we showed that if two quantum semitoric systems have the same joint spectrum, then the underlying semitoric systems must possess the same marked semitoric polygon and Taylor series invariant (hence only the twisting numbers were potentially missing, and at the time we did not know if it could be detected from the joint spectrum). In particular, this showed that two systems with only one focus-focus point, the same joint spectrum and the same twisting index must be isomorphic.

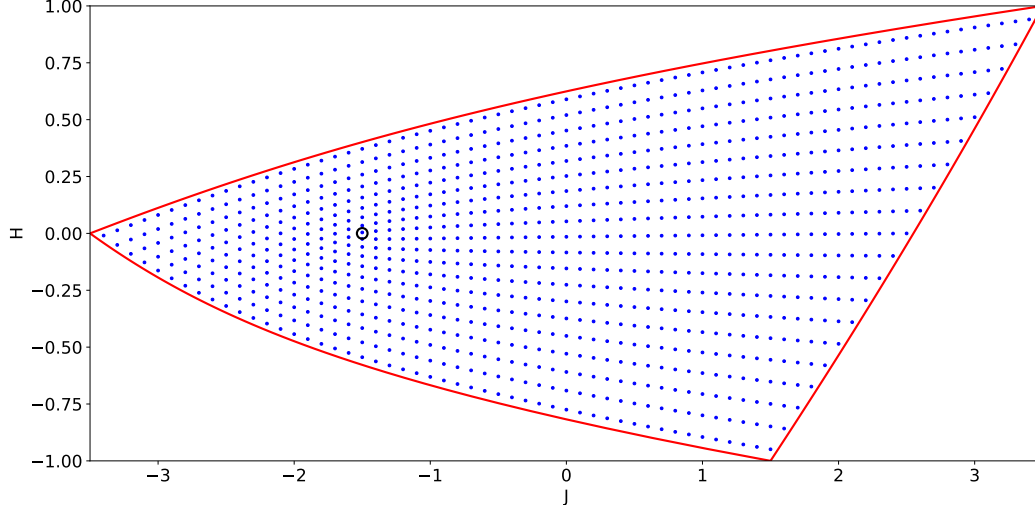


Figure 5.1: The blue dots are the joint eigenvalues of the quantum coupled angular momenta with $R_1 = 1$, $R_2 = \frac{5}{2}$ and $t = \frac{1}{2}$ for $k = 10$, see Example 5.1.4. The red line corresponds to the boundary of the image of the momentum map, and the black circle indicates the focus-focus value.

5.2 The inverse spectral result

The main result that we obtained in [LFVuN21] is a positive answer to the inverse spectral question: from the data of the family of joint spectra of a quantum semitoric system, one can recover, in a constructive way, all the symplectic invariants of the underlying semitoric system, and hence this system itself up to isomorphism. When the classical phase space is non-compact, stating this result precisely requires some care, because these joint spectra may be unbounded in the horizontal direction (recall that in a semitoric system $(M, \omega, (J, H))$ the first component J of the momentum map is proper, so these joint spectra are necessarily bounded in the vertical direction). This is why in the following statement, we need to introduce a vertical strip and restrict ourselves to the study of the joint spectrum in this strip. Of course, for a compact phase space one can simply take this strip to be large enough to contain the whole joint spectrum for all values of the semiclassical parameter.

Theorem 5.2.1 ([LFVuN21, Theorem 3.6]). *Let $\mathcal{I} \subset (0, +\infty)$ be an interval having zero as an accumulation point and let $(\Sigma_{\hbar})_{\hbar \in \mathcal{I}}$ be a collection of point sets in \mathbb{R}^2 , which is assumed to be the joint spectrum of some unknown proper quantum semitoric system $(\hat{J}_{\hbar}, \hat{H}_{\hbar})$ with joint principal symbol $F = (J, H)$. Let $S \subset \mathbb{R}^2$ be a vertical strip of bounded width. Then all symplectic invariants of the underlying classical semitoric system on $F^{-1}(S)$ can be explicitly recovered, in a constructive way, from the data of $(\Sigma_{\hbar} \cap S)_{\hbar \in \mathcal{I}}$ modulo $O(\hbar^2)$. In particular, if two proper quantum semitoric systems have the same spectrum modulo $O(\hbar^2)$, then the underlying semitoric systems are isomorphic.*

Here modulo $O(\hbar^2)$ means that we can start with a family of subsets which is not exactly $(\Sigma_{\hbar})_{\hbar \in \mathcal{I}}$ but is only $O(\hbar^2)$ -close to this joint spectrum, in the sense of the Gromov-Hausdorff distance of their intersections with compact sets, see [LFVuN21, Definition 3.8]. This means that a sufficiently small error in the measurement of this joint spectrum does not change the outcome of the theorem.

Theorem 5.2.1 is obtained by combining several results regarding the explicit recovery of the different symplectic invariants, that we describe now and until the end of this chapter. In fact, our method to recover the Taylor series invariant (see Section 5.4.1) is not specific to the semitoric case and applies to any four-dimensional integrable system with a focus-focus point

which is the only one in its F -fiber. The last statement in Theorem 5.2.1 comes from the result of [PVuN09] that a semitoric system is determined up to isomorphism from its complete list of symplectic invariants, see Theorem 3.4.16.

Here we insist on the fact that we recover constructively all the symplectic invariants of the system from the joint spectrum. Concretely, we obtain formulas and algorithms giving these invariants as limits of quantities formed by means of the joint eigenvalues. Hence we recover the uniqueness result from [LFPVN16, LFPVN19] discussed above for systems with only one focus-focus point, but we go beyond it by giving these explicit formulas and algorithms to recover all the invariants, including the twisting index, and also by handling the general case of any number of focus-focus points.

The general idea is that coming up with a good, consistent way of numbering the joint eigenvalues amounts to obtaining nice action variables for the classical system, which in turn allows us to infer the symplectic invariants. Thus, our next task is to explain this link between good quantum numbers and action variables.

5.3 Asymptotic lattices and half-lattices

Bohr-Sommerfeld conditions give a description of the joint spectrum of a proper quantum integrable system (\hat{A}_h, \hat{B}_h) near a regular value c of its joint principal symbol $F = (a_0, b_0)$. These conditions, recalled in the theorem below, state that this joint spectrum is locally a deformed lattice, and the deformation is related to a choice of action variables near c . For \hbar -pseudodifferential operators, they are due to Charbonnel [Cha88] (following Colin de Verdière [CdV80]), while they were obtained by Charles in [Cha03b] (see also [Cha06]) for Berezin-Toeplitz operators.

Theorem 5.3.1. *Let $(A_h, B_h)_{h \in \mathcal{I}}$, be a proper quantum integrable system with joint principal symbol $F = (a_0, b_0)$, and let Σ_h be its joint spectrum. Let $c \in \mathbb{R}^2$ be a regular value of F such that $F^{-1}(c)$ is connected. Then there exists an open ball $B \subset \mathbb{R}^2$ containing c such that*

1. *the joint eigenvalues in $\Sigma_h \cap B$ are simple, in the sense of [Cha88, DHVN22]: there exists $\hbar_0 > 0$ such that for every $\hbar < \hbar_0$, $\hbar \in \mathcal{I}$ and every $\lambda_h \in \Sigma_h \cap B$, the joint spectral projector of (A_h, B_h) onto the ball $B(\lambda_h, \hbar^2)$ has rank 1;*
2. *there exist a bounded open set $U \subset \mathbb{R}^n$ and a smooth function $G_h : U \rightarrow \mathbb{R}^2$ with an asymptotic expansion*

$$G_h = G_0 + \hbar G_1 + \hbar^2 G_2 + \dots$$

in the C^∞ topology, such that

$$\Sigma_h \cap B = G_h(\hbar \mathbb{Z}^2) + O(\hbar^\infty)$$

inside B , with a uniform remainder $O(\hbar^\infty)$. Moreover, $dG_0 = d\tilde{G}_0$ where \tilde{G}_0^{-1} is an oriented action diffeomorphism associated with a choice of action variables near $F^{-1}(c)$ (see the beginning of Section 3.2).

For more details, see for instance [LFVuN21, Theorem 4.3 and Definition 4.1].

In view of this description, it is quite clear that, near a regular value of the momentum map, possessing action variables (I_1, I_2) (and hence an action diffeomorphism G_0^{-1}) allows one to label the joint eigenvalues in a natural way: the joint eigenvalue corresponding to $G_0(\hbar(\ell, m))$ up to $O(\hbar^2)$ is labeled $\lambda_{\ell, m}$. In other words, $\hbar\ell$ and $\hbar m$ are the (approximate) values of the action variables I_1 and I_2 on $F^{-1}(\lambda_{\ell, m})$.

However, for the inverse question, one starts with the joint spectrum Σ_h and does not know the underlying system *a priori*, hence such action variables cannot be obtained classically. This raises the following question: from the sole knowledge of the family of joint spectra of a quantum

integrable system, can one number the joint eigenvalues in a consistent way? This question led to the introduction of asymptotic lattices and their labelings in [DHVN22].

The precise definition of an asymptotic lattice [DHVN22, Definition 3.6] is rather involved, so we will not reproduce it here. Let us simply say that this definition (here, specialized to two degrees of freedom) formalizes the notion of a local deformed lattice as the set $G_\hbar(\hbar\mathbb{Z}^2)$, where G_\hbar , called an *asymptotic chart*, admits an asymptotic expansion

$$G_\hbar = G_0 + \hbar G_1 + \hbar^2 G_2 + \dots \quad (5.2)$$

in the \mathcal{C}^∞ topology and G_0 is a local orientation-preserving diffeomorphism. In particular, the definition of asymptotic lattice is such that the joint spectrum of an integrable system near a regular value of its momentum map is an asymptotic lattice, with G_0^{-1} an oriented action diffeomorphism. And of course, the simplest example is the intersection of the rescaled lattice $\hbar\mathbb{Z}^2$ with a bounded open subset of \mathbb{R}^2 , which is an asymptotic lattice with $G_0 = \text{Id}$. Note that asymptotic charts are not unique in general; for instance, for the joint spectrum evoked above, one can always choose a different set of action variables, which results in a different action diffeomorphism G_0^{-1} and thus in a different asymptotic chart.

In [DHVN22], the authors studied asymptotic lattices and proved in particular that they all admit a preferred way, once an asymptotic chart is chosen, to label their elements consistently as $\hbar \rightarrow 0$, called a *good labeling*. They also provided some algorithms (one in the general case and one more adapted to the semitoric case) to produce a labeling of any asymptotic lattice (with the subtlety that the labeling thus obtained is not good but *linear*, i.e. good up to constants depending on \hbar). In particular, this allows one to label the joint spectrum Σ_\hbar of a proper quantum integrable system in the neighborhood of a regular value c of the underlying momentum map, and the above discussion hints at the fact that this in turns allows one to recover a pair of action variables near $F^{-1}(c)$.

An example of asymptotic lattice, with two different labelings, is displayed in Figure 5.2.

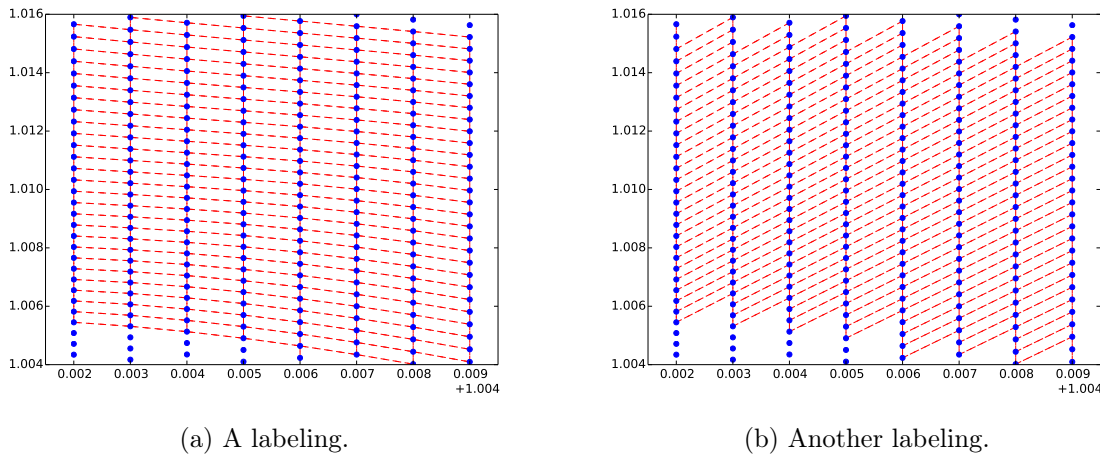


Figure 5.2: An asymptotic lattice and two labelings for it (for some fixed value of \hbar). Recall that an asymptotic lattice is a deformed rescaled lattice; the labellings are suggested by the red dashed lines.

As we will see below, in the semitoric case this idea can be realized concretely and is enough to recover the Taylor series and height invariants associated to a given focus-focus point from the joint spectrum. However, to recover the complete symplectic invariant of the system, we will need to label the whole joint spectrum, with the exception of the joint eigenvalues close to elliptic-elliptic values and to vertical half-lines above each focus-focus value. Indeed, this is quite natural since the marked semitoric polygon is constructed as the image of global action

variables on the set of regular values of F minus the cuts above or below each focus-focus value. In [LFVuN21] we came up with such a global labeling using two ingredients: the description of the joint spectrum near an elliptic-regular value as an asymptotic half-lattice, and the extension of local labelings of such asymptotic lattices and half-lattices to a global labeling for their union. The latter will be described in Section 5.4.2 below, and now we focus on the former.

Asymptotic half-lattices. The joint spectrum of a proper quantum integrable system near an elliptic-regular value is not obtained as a deformation of the rescaled lattice $\hbar\mathbb{Z}^2$ but rather of the rescaled half-lattice $\hbar(\mathbb{N} \times \mathbb{Z})$. Roughly, the joint eigenvalues only lie on one side of the boundary of the image of the underlying momentum map (see Figure 5.1). Another way to think about this is to inspect the following normal form near such an elliptic-regular singularity, which was first stated in the homogeneous setting in [CdV80], generalized to hyperbolic flows in [CdVVuN03], and extended to all non-degenerate singularities in [MZ04].

Lemma 5.3.2 ([DM91]). *Let $F = (J, H)$ be an integrable system and let $c = (c_1, c_2)$ be an elliptic-regular value of F with compact and connected fiber $F^{-1}(c)$. Then there exist a saturated neighborhood \mathcal{U} of $F^{-1}(c)$ in M , a neighborhood \mathcal{V} of $(S^1 \times \{0\}) \times \{(0, 0)\}$ in $T^*S^1 \times T^*\mathbb{R}$, a local symplectomorphism $\phi : (\mathcal{U}, \omega) \rightarrow (\mathcal{V}, \omega_0)$ and a local diffeomorphism $G_0 : (\mathbb{R}^2, 0) \rightarrow (\mathbb{R}^2, c)$ such that*

$$(F \circ \phi^{-1})(x_1, \xi_1, x_2, \xi_2) = G_0(\xi_1, q(x_2, \xi_2))$$

where $q(x_2, \xi_2) = \frac{1}{2}(x_2^2 + \xi_2^2)$. If moreover (J, H) is semitoric, then ϕ can be chosen such that $J \circ \phi^{-1} - c_1 = \xi_1$.

Here $T^*S^1 \times T^*\mathbb{R}$ is endowed with coordinates (x_1, ξ_1, x_2, ξ_2) , with x_1 as periodic coordinate, and symplectic form $\omega_0 = d\xi_1 \wedge dx_1 + d\xi_2 \wedge dx_2$. Note that near any regular value of F sufficiently close to c , G_0^{-1} is an action diffeomorphism.

Since the spectrum of the quantized version of the harmonic oscillator q consists of discrete points lying in the positive half of the real axis, this is another hint that the joint spectrum is a deformed half-lattice near such a singularity. The precise statement, which is displayed below, was initially proved in [CdV80, Theorem 6.1] for homogeneous pseudodifferential operators, while for \hbar -pseudodifferential operators it was only stated in [VN06, Théorème 5.2.4] (see also [DHVN22, Theorem 3.38]), with a sketch of proof. Moreover, to our knowledge it was not available in the literature for Berezin-Toeplitz operators. Hence, even though the statement itself is not surprising, in [LFVuN21] we needed to include a complete proof of this result.

Theorem 5.3.3 ([LFVuN21, Theorem 7.4]). *Let $(\hat{J}_\hbar, \hat{H}_\hbar)$ be a proper quantum integrable system, with momentum map $F = (J, H)$, and let c be an elliptic-regular value of F with compact and connected fiber $F^{-1}(c)$. Then there exists an open ball $B \subset \mathbb{R}^2$ around c in which the joint spectrum Σ_\hbar of $(\hat{J}_\hbar, \hat{H}_\hbar)$ has the following properties:*

1. *the joint eigenvalues are simple (in the sense of the first item in Theorem 5.3.1);*
2. *there exist a bounded open set $U \subset \mathbb{R}^2$ and a smooth map $G_\hbar : U \rightarrow \mathbb{R}^2$ with an asymptotic expansion $G_\hbar = G_0 + \hbar G_1 + \dots$ in the \mathcal{C}^∞ topology such that $\lambda_\hbar \in \Sigma_\hbar \cap B$ if and only if there exist $j(\hbar) \in \mathbb{Z}$ and $\ell(\hbar) \in \mathbb{N}$ such that $\lambda_\hbar = G_\hbar(\hbar(j(\hbar), \ell(\hbar))) + O(\hbar^\infty)$ where the remainder is uniform on B . Furthermore, G_0 is the same as in Lemma 5.3.2.*

In particular, away from the singularity this statement allows one to recover the regular Bohr-Sommerfeld conditions from Theorem 5.3.1. Note also that this statement is not restricted to semitoric systems. The idea of the proof is quite standard: by quantizing a local normal form (near one elliptic-regular point $m \in F^{-1}(c)$) derived from the one of Lemma 5.3.2 using Fourier

integral operators, we microlocally conjugate (\hat{J}_h, \hat{H}_h) to the pair $(\Xi_h, g_h(\Xi_h, Q_h))$ of operators on $L^2(\mathbb{R}^2)$, where Ξ_h, Q_h act as

$$\Xi_h = \frac{\hbar}{i} \frac{\partial}{\partial x_1}, \quad Q_h = \frac{1}{2} \left(-\hbar^2 \frac{\partial^2}{\partial x_2^2} + x_2^2 \right)$$

on compactly supported smooth functions, and g_h is a family of smooth function with an asymptotic expansion $g_h = g_0 + \hbar g_1 + \hbar^2 g_2 + \dots$ in the \mathcal{C}^∞ topology, with $\partial_y g_0 \neq 0$. The microlocal solutions of $(\Xi_h, Q_h)v_h = (\nu_h, \mu_h)v_h + O(\hbar^\infty)$ near the origin can be studied using the knowledge of the joint spectrum of the harmonic oscillator Q_h : it consists of the simple eigenvalues $\hbar(n + \frac{1}{2})$, $n \in \mathbb{N}$. This in turn gives some information on the microlocal solutions of $(\hat{J}_h, \hat{H}_h)v_h = (\tilde{\nu}_h, \tilde{\mu}_h)v_h + O(\hbar^\infty)$ near m , where the integer $\ell(\hbar) \in \mathbb{N}$ from Theorem 5.3.3 appears. To end the proof we study the microlocal solutions near the whole singular fiber $F^{-1}(c)$ by following the punctual microlocal solutions around the fiber, which gives a cocycle condition responsible for the appearance of the integer $j(\hbar)$ in Theorem 5.3.3.

In order to analyze Σ_h near an elliptic-regular singularity, we introduced the notion of asymptotic half-lattice by adapting the definition of asymptotic lattice, in such a way that Theorem 5.3.3 means that locally near the singularity, the joint spectrum is an asymptotic half-lattice. Again, we will not reproduce the full definition ([LFVuN21, Definition 4.7]) since it is rather technical. We proved that these asymptotic half-lattices also admit good labelings, and we gave an algorithm to produce linear labelings for any asymptotic half-lattice.

We insist on the fact that our proof of Theorem 5.2.1 does not necessitate the description of the joint spectrum near a focus-focus value of the system. Such a description is known in the \hbar -pseudodifferential case for a focus-focus point which is alone in its F -fiber [VN00], but not for the case of a singular fiber with multiple pinches and not at all in Berezin-Toeplitz quantization. Proving such a result would be interesting but would require more work than the elliptic-transverse case from Theorem 5.3.3, and this also explains why it was convenient to circumvent it.

5.4 Recovering the invariants

We now explain how to recover, from the joint spectrum of a proper quantum semitoric system (\hat{J}_h, \hat{H}_h) , the symplectic invariants of the underlying semitoric system $(M, \omega, (J, H))$, thanks to all the tools discussed above. As we already explained, it is natural to first study the recovery of the Taylor series and height invariants, which only uses asymptotic lattices and their labelings, and then show how to use global labelings to recover the complete symplectic invariant.

As already explained earlier, our method to reconstruct the Taylor series invariant from the joint spectrum is not specific to semitoric systems and can be applied to recover this invariant for a focus-focus fiber containing only one singular point in any four-dimensional integrable system. This invariant, in turn, completely determines (up to symplectomorphism) F in a neighborhood of the singular fiber, modulo composition on the left by a local diffeomorphism. In fact as we will see, we can also recover the full Taylor expansion at the origin of the Eliasson function defined in Section 3.4.2, and hence we recover F up to a flat term near the singular fiber.

5.4.1 Taylor series and height invariants

Let $c_0 \in \mathbb{R}^2$ be a focus-focus value of $F = (J, H)$; by replacing F with $F(c_0)$ we may, and will, assume that $c_0 = (0, 0)$. Let $c \in \mathbb{R}^2$ be a regular value of F close to c_0 , and let $B \subset \mathbb{R}^2$ be an open ball containing only regular values of F , including c ; here “close to c_0 ” means that we choose c and B such that B is contained in the simply connected open set U defined in Section 3.4.2. In view of the discussions in the previous sections, we first apply the semitoric labeling

algorithm from [DHVN22, Section 3.5.2] to obtain a labeling

$$\lambda_{j,\ell}(\hbar) = (J_{j,\ell}(\hbar), E_{j,\ell}(\hbar)) \quad (5.3)$$

of the joint eigenvalues of $(\hat{J}_\hbar, \hat{H}_\hbar)$ contained in B . This labeling is associated with an asymptotic chart G_\hbar of the form (5.2) with G_0^{-1} a semitoric action diffeomorphism, *i.e.* corresponding to action variables of the form (J, L) .

Let f_r be the Eliasson function defined in Section 3.4.2, and let τ_1, τ_2 be the two functions defined by decomposing X_L as in Equation (3.14). Then the functions a_1, a_2 defined as

$$\begin{cases} a_1 = \tau_1 + \tau_2 \partial_x f_r, \\ a_2 = \tau_2 \partial_y f_r \end{cases} \quad (5.4)$$

satisfy

$$X_L = \tilde{a}_1 X_J + \tilde{a}_2 X_H$$

with $\tilde{a}_j = a_j \circ F$ for $j = 1, 2$. A preliminary result is that these two functions can be recovered from the joint spectrum Σ_\hbar .

Lemma 5.4.1 ([LFVuN21, Lemma 5.2]). *Let j, ℓ be \hbar -dependent integers such that the joint eigenvalues $\lambda_{j,\ell}$, $\lambda_{j+1,\ell}$ and $\lambda_{j,\ell+1}$ are well-defined in an $O(\hbar)$ -neighborhood of c . Then:*

1. $\frac{E_{j,\ell}(\hbar) - E_{j+1,\ell}(\hbar)}{\hbar} = \frac{a_1(c)}{a_2(c)} + O_c(\hbar),$
2. $\frac{\hbar}{E_{j,\ell+1}(\hbar) - E_{j,\ell}(\hbar)} = a_2(c) + O_c(\hbar),$

where $E_{j,\ell}(\hbar)$ is as in Equation (5.3) and $O_c(\hbar)$ means $O(\hbar)$ with constants depending on c .

Recall from Definition 3.4.8 that the Taylor series invariant of c_0 is defined in terms of the functions σ_1 and σ_2 introduced in Proposition 3.4.7, which are known whenever τ_1, τ_2 and f_r are known. Thus, in order to recover this Taylor series invariant from Σ_\hbar , the idea is to exploit the relation (5.4) to derive these three functions from the knowledge of a_1 and a_2 ensured by the above lemma.

To make this idea more precise, recall that $\partial_y f_r > 0$ and note that Equation (5.4) implies that

$$\tau_1 = a_1 + s a_2, \quad \tau_2 = \frac{a_2}{\partial_y f_r} \quad (5.5)$$

where $s = -\frac{\partial_x f_r}{\partial_y f_r}$. To come back to σ_1 and σ_2 , we studied τ_1 and τ_2 along the image by F of the zero set of the radial Hamiltonian H_r , called the *radial curve* γ_r , and given by the equation $f_r(x, y) = 0$; note that $s(0)$ is the slope of the tangent to this curve at the origin. This allowed us to resolve the logarithmic behavior of τ_1 and τ_2 as follows. Write locally γ_r as the graph of a function φ ; then it follows from Proposition 3.4.7 that the functions

$$\nu_1 : x > 0 \mapsto \tau_1(x, \varphi(x)), \quad \nu_2 : x > 0 \mapsto \tau_2(x, \varphi(x)) + \frac{\ln x}{2\pi} \quad (5.6)$$

extend smoothly at $x = 0$ by setting $\nu_1(0) = \sigma_1(0)$ and $\nu_2(0) = \sigma_2(0)$. Indeed, for every $x > 0$, $\nu_1(x) = \sigma_1(x, \varphi(x))$ and $\nu_2(x) = \sigma_2(x, \varphi(x))$.

To sum up, if we knew the Eliasson function f_r , we would know the parametrization φ of the curve γ_r and the function s , so we could fix a small $x > 0$ and use Lemma 5.4.1 to recover $a_1(x, \varphi(x))$ and $a_2(x, \varphi(x))$ from Σ_\hbar , then Equation (5.5) to recover $\tau_1(x, \varphi(x))$ and $\tau_2(x, \varphi(x))$, and finally take the limit $x \rightarrow 0^+$ in Equation (5.6) to recover $\sigma_1(0)$ and $\sigma_2(0)$. And this would also allow us to recover the higher order terms in the Taylor series invariant.

Unfortunately, we do not know the Eliasson function, so we also need to be able to recover it from the joint spectrum. In fact, we will see that we only need to recover the Taylor expansion of this function at the origin, and this can be derived from the knowledge of a_1 and a_2 .

Linear invariants. First we explain how this idea can be applied to obtain the linear invariants $[S_{1,0}]$ and $S_{0,1}$. Note that $S_{0,1} = \sigma_2(0)$ and recall from Proposition 3.4.13 that $[S_{1,0}] = \sigma_1(0)$ modulo \mathbb{Z} . First we proved that, if γ is any curve which is tangent to the radial curve γ_r at the origin, the restrictions of σ_1 and σ_2 to γ also tend to $\sigma_1(0)$ and $\sigma_2(0)$ at the origin (see Lemmas 5.4 and 6.7 in [LFVuN21]). Consequently, it suffices to work with the tangent line to γ_r at the origin, in other words to compute its slope $s(0) = -\frac{\partial_x f_r(0)}{\partial_y f_r(0)}$.

Lemma 5.4.2 ([LFVuN21, Lemma 5.5]). *One can recover the first order derivatives $\partial_x f_r(0)$ and $\partial_y f_r(0)$ of the Eliasson function from the knowledge of a_1 and a_2 . Explicitly, for any fixed $\tau > 1$,*

$$\begin{cases} \partial_x f_r(0) = \frac{2\pi(a_1(x,0) - a_1(\tau x,0))}{\ln \tau} + O(x \ln x), \\ \partial_y f_r(0) = \frac{2\pi(a_2(x,0) - a_2(\tau x,0))}{\ln \tau} + O(x \ln x) \end{cases}$$

when $x \rightarrow 0^+$.

To obtain explicit formulas to compute this derivatives from Σ_{\hbar} , it suffices to combine this lemma with Lemma 5.4.1. Assume that both $(x,0)$ and $(\tau x,0)$ belong to the set B defined above, so that the labeling from Equation (5.3) covers them both. Let j_1, ℓ_1 (respectively j_2, ℓ_2) be \hbar -dependent integers such that the joint eigenvalues λ_{j_1, ℓ_1} , λ_{j_1+1, ℓ_1} and λ_{j_1, ℓ_1+1} (respectively λ_{j_2, ℓ_2} , λ_{j_2+1, ℓ_2} and λ_{j_2, ℓ_2+1}) are well-defined in an $O(\hbar)$ -neighborhood of $(x,0)$ (respectively of $(\tau x,0)$). Then,

$$\partial_x f_r(0) = \lim_{x \rightarrow 0^+} \lim_{\hbar \rightarrow 0} \frac{2\pi}{\ln \tau} \left(\frac{E_{j_1, \ell_1} - E_{j_1+1, \ell_1}}{E_{j_1, \ell_1+1} - E_{j_1, \ell_1}} - \frac{E_{j_2, \ell_2} - E_{j_2+1, \ell_2}}{E_{j_2, \ell_2+1} - E_{j_2, \ell_2}} \right) \quad (5.7)$$

and

$$\partial_y f_r(0) = \lim_{x \rightarrow 0^+} \lim_{\hbar \rightarrow 0} \frac{2\pi\hbar}{\ln \tau} \left(\frac{1}{E_{j_1, \ell_1+1} - E_{j_1, \ell_1}} - \frac{1}{E_{j_2, \ell_2+1} - E_{j_2, \ell_2}} \right). \quad (5.8)$$

Example 5.4.3. We work with the only focus-focus point of the coupled angular momenta system $(M, \omega, (J, H_t))$ from Example 3.3.4 with $t^- < t < t^+$. The Taylor expansion of the corresponding Eliasson function f_r can be inferred from [ADH20, Lemma 3.8] thanks to a straightforward computation (see [LFVuN21, Section 8.1] for a similar computation for the spin-oscillator system of Example 3.3.3). More precisely,

$$\partial_x f_r(0) = \frac{(2t-1)R - t}{\sqrt{C(t, R)}}, \quad \partial_y f_r(0) = \frac{2R}{\sqrt{C(t, R)}}$$

where $R = \frac{R_1}{R_2}$ and $C(t, R)$ is as in Equation (3.13). In particular when $R_1 = 1$, $R_2 = \frac{5}{2}$ and $t = \frac{1}{2}$ this yields

$$\partial_x f_r(0) = -\frac{1}{3}, \quad \partial_y f_r(0) = \frac{10}{3}. \quad (5.9)$$

We recover these quantities from the joint spectrum of the corresponding quantum system (\hat{J}_k, \hat{H}_k) from Example 5.1.2 (see also Example 5.1.4), using Equations (5.7) and (5.8), in Figures 5.3 and 5.4.

Formulas (5.7) and (5.8) allow us to recover the slope $s(0)$ from Σ_{\hbar} . Then for $x > 0$,

$$a_1(x, s(0)x) + s(0)a_2(x, s(0)x) = \tau_1(x, s(0)x) + O(x \ln x) \xrightarrow{x \rightarrow 0^+} \sigma_1(0). \quad (5.10)$$

In practice, once $s(0)$ is known, we obtain using the notation and results of Lemma 5.4.1 applied to $c = (x, s(0)x)$ that

$$\sigma_1(0) = \lim_{x \rightarrow 0^+} \lim_{\hbar \rightarrow 0} \frac{E_{j, \ell}(\hbar) - E_{j+1, \ell}(\hbar)}{E_{j, \ell+1}(\hbar) - E_{j, \ell}(\hbar)} + \frac{\hbar s(0)}{E_{j, \ell+1}(\hbar) - E_{j, \ell}(\hbar)}. \quad (5.11)$$

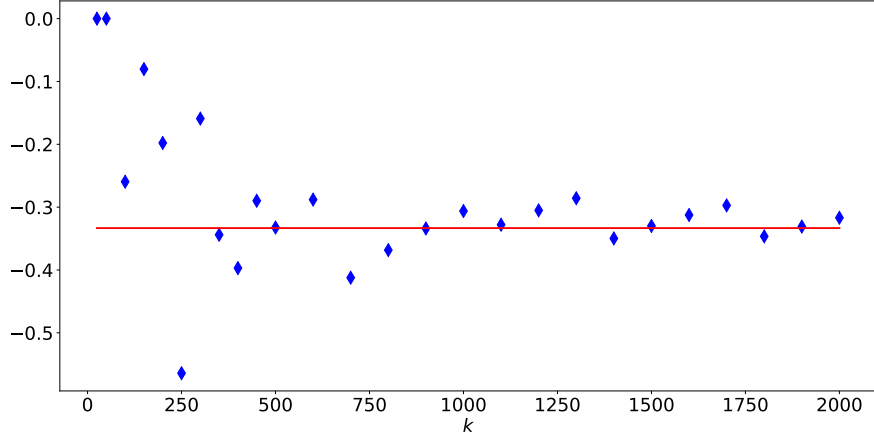


Figure 5.3: Determination of $\partial_x f_r(0)$ for the coupled angular momenta system (see Example 5.4.3) using Formula (5.7) with $x = 0.01$, $\tau = 2$ and $(j_1, \ell_1) = (0, 0) = (j_2, \ell_2)$, for different values of k . The red line corresponds to the theoretical result $\partial_x f_r(0) = -\frac{1}{3}$, see Equation (5.9).

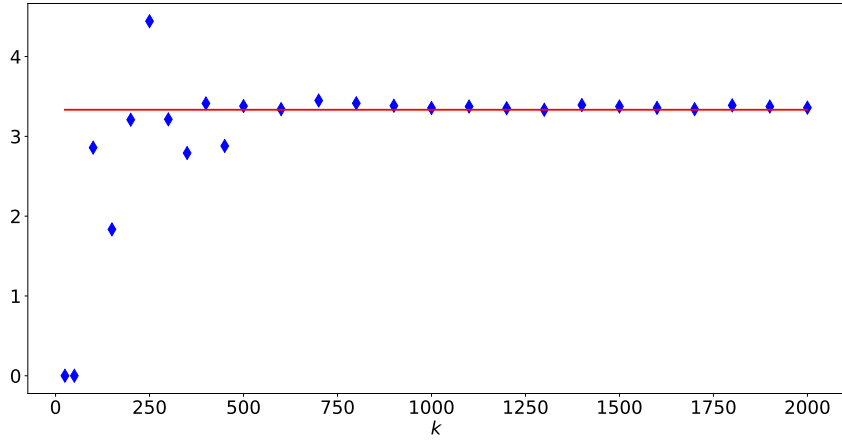


Figure 5.4: Determination of $\partial_y f_r(0)$ for the coupled angular momenta system (see Example 5.4.3) using Formula (5.8) with $x = 0.01$, $\tau = 2$ and $(j_1, \ell_1) = (0, 0) = (j_2, \ell_2)$, for different values of k . The red line corresponds to the theoretical result $\partial_y f_r(0) = \frac{10}{3}$, see Equation (5.9).

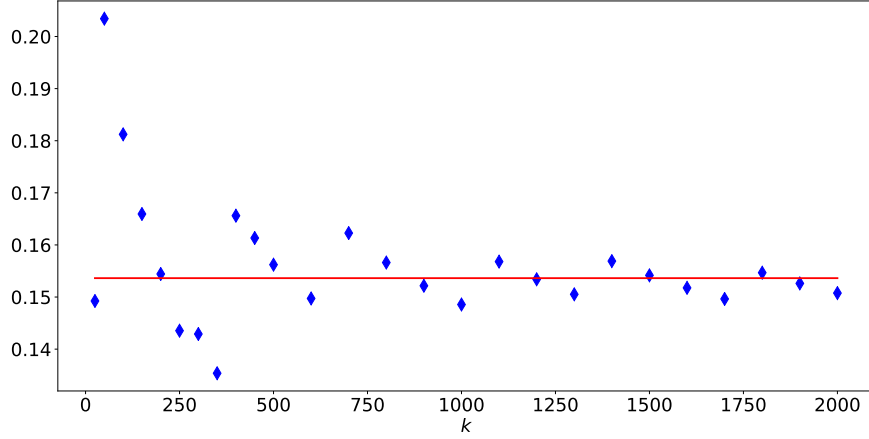


Figure 5.5: Determination of $[S_{1,0}]$ for the coupled angular momenta system (see Example 5.4.4). The blue diamonds correspond to Formula (5.11) evaluated at $(j, \ell) = (0, 0)$ with $x = 0.01$, for different values of k . Here we directly work with the privileged labeling (which can be recovered from the joint spectrum, as explained in the discussion right before Example 5.4.4) so $[S_{1,0}] = \sigma_1(0)$; the red line corresponds to the theoretical result $[S_{1,0}] = \frac{1}{2\pi} \arctan(\frac{13}{9})$, see Equation (5.12).

Thus we recover $[S_{1,0}]$ from the joint spectrum, as the fractional part of $\sigma_1(0)$. These results are summarized in [LFVuN21, Theorem 5.1].

Note that we can then recover the *privileged labeling*, i.e. the labeling corresponding to the choice of action variables (J, L_{priv}) with L_{priv} the privileged action variable defined in Section 3.4.3. Indeed, recall that we started from a labeling $\lambda_{j,\ell}(\hbar)$ as in Equation (5.3), corresponding to the pair of action variables (J, L) . Recall also that by definition of L_{priv} , the actions L and L_{priv} are related by $L_{\text{priv}} = L - \lfloor \sigma_1(0) \rfloor J$. Then the privileged labeling $\lambda_{j,\ell}^{\text{p}}(\hbar)$ is given by

$$\lambda_{j,\ell}^{\text{p}}(\hbar) = \lambda_{j,\ell+pj}(\hbar),$$

see [LFVuN21, Proposition 5.8] for more details.

Example 5.4.4. We consider once again the coupled angular momenta system from Examples 3.3.4 and 5.1.2, with parameters $R_1 = 1$, $R_2 = \frac{5}{2}$ and $t = \frac{1}{2}$. In this case we derive from Equation (5.9) that $s(0) = \frac{1}{10}$, and Equation (3.15) yields

$$[S_{1,0}] = \frac{1}{2\pi} \arctan\left(\frac{13}{9}\right). \quad (5.12)$$

We recover this linear invariant from the joint spectrum of the quantum system (\hat{J}_k, \hat{H}_k) from Example 5.1.2, using Equation (5.11), in Figure 5.5.

In [LFVuN21] we also explained how to recover the second linear invariant from the joint spectrum. Indeed, we obtained that for $x > 0$,

$$\frac{a_2(x, s(0)x)}{\partial_y f_r(0)} + \frac{\ln x}{2\pi} \xrightarrow{x \rightarrow 0^+} \sigma_2(0) = S_{0,1}.$$

Using once again the notation and results of Lemma 5.4.1 applied to $c = (x, s(0)x)$, this yields

$$S_{0,1} = \lim_{x \rightarrow 0^+} \lim_{\hbar \rightarrow 0} \left(\frac{\hbar}{\partial_y f_r(0)(E_{j,\ell+1} - E_{j,\ell})} + \frac{\ln x}{2\pi} \right). \quad (5.13)$$

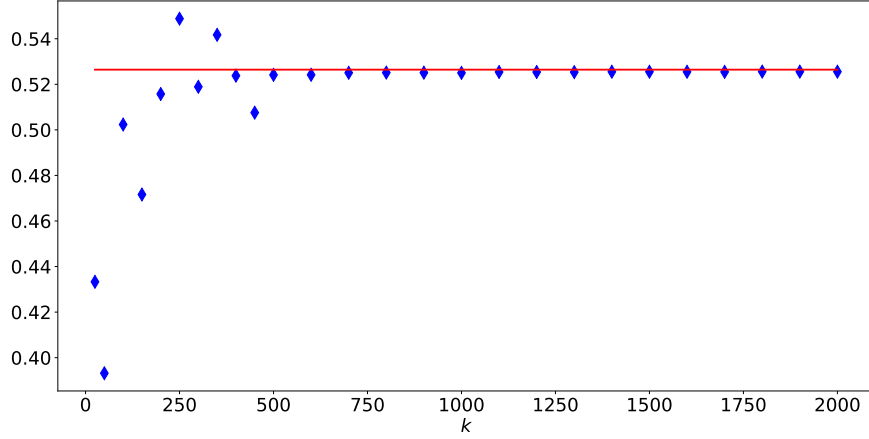


Figure 5.6: Determination of $S_{0,1}$ for the coupled angular momenta system (see Example 5.4.5). The blue diamonds correspond to Formula (5.13) evaluated at $(j, \ell) = (0, 0)$ with $x = 0.01$, for different values of k . The red line corresponds to the theoretical value $S_{0,1} = \frac{1}{2\pi} \left(\frac{7}{2} \ln 2 + 3 \ln 3 - \frac{3}{2} \ln 5 \right)$, see Equation (5.14).

Example 5.4.5. We keep working with the coupled angular momenta system from Examples 3.3.4 and 5.1.2, with parameters $R_1 = 1$, $R_2 = \frac{5}{2}$ and $t = \frac{1}{2}$. In this case Equation (3.15) yields

$$S_{0,1} = \frac{1}{2\pi} \left(\frac{7}{2} \ln 2 + 3 \ln 3 - \frac{3}{2} \ln 5 \right). \quad (5.14)$$

We recover this quantity from the joint spectrum of the quantum system (\hat{J}_k, \hat{H}_k) from Example 5.1.2, using Equation (5.13), in Figure 5.6.

Higher order terms in the Taylor series invariant. Recovering the higher order terms in the Taylor series invariant from the joint spectrum is more complicated, but the idea remains the same: in order to recover the coefficients $S_{\ell,m}$ with $\ell + m = n \geq 1$, we will first need to recover the derivatives of order n of f_r at the origin. This can be achieved by considering certain combinations of the functions a_1 and a_2 evaluated at suitable points. Recall that the functions a_1 and a_2 can be recovered from Σ_h (see Lemma 5.4.1), so from now on we assume that these functions are known.

Let μ be an additional formal parameter. For $n_1, n_2 \in \mathbb{N}$, let $\mathcal{F}_{\leq n_1, \leq n_2}$ (respectively \mathcal{F}_{n_1, n_2}) be the polynomial algebra in the variables $\partial^\beta f_r(0)$ with $|\beta| \leq n_1$ (respectively $|\beta| = n_1$), in the variables S_α with $|\alpha| \leq n_2$ (respectively $|\alpha| = n_2$), and in μ .

Proposition 5.4.6 ([LFVuN21, Proposition 6.10]). *Let $\mu \in \mathbb{R}$; the function*

$$g_\mu : x > 0 \mapsto a_1(x, \mu x) + \mu a_2(x, \mu x)$$

has an asymptotic expansion of the form

$$g_\mu(x) \sim \sum_{n \geq 0} x^n (c_n(\mu) + d_n(\mu) \ln x) \quad \text{as } x \rightarrow 0^+. \quad (5.15)$$

Moreover, for $n \geq 0$, $d_n(\mu) \in \mathcal{F}_{n+1,0}$, explicitly:

$$d_n(\mu) = -\frac{1}{2\pi n!} \sum_{\ell=0}^{n+1} \binom{n+1}{\ell} \mu^{n+1-\ell} \partial_x^\ell \partial_y^{n+1-\ell} f_r(0). \quad (5.16)$$

Furthermore, $c_n(\mu) \in \mathcal{F}_{\leq n+1, \leq n} \oplus \mathcal{F}_{1, n+1}$, explicitly:

$$c_n(\mu) = \tilde{c}_n(\mu) + \sum_{\ell=0}^{n+1} \mu^{n-\ell} \left(\mu(n+1) \partial_y f_r(0) + (n-\ell+1) \partial_x f_r(0) \right) S_{\ell, n+1-\ell}$$

with $\tilde{c}_n(\mu) \in \mathcal{F}_{\leq n+1, \leq n}$ which can be computed explicitly. Here, for the sake of simplicity, we slightly abuse notation and use the conventions $(n-\ell+1)\mu^{n-\ell} = 0$ if $\ell = n+1$ and $0^0 = 0$.

The idea of the proof of this result is that, because of Proposition 3.4.7 and Equation (5.4), there holds

$$g_\mu(x) = \sigma_1(x, \mu x) - \frac{1}{2\pi} \arctan \left(\frac{f_r(x, \mu x)}{x} \right) \\ + (\partial_x f_r(x, \mu x) + \mu \partial_y f_r(x, \mu x)) \left(\sigma_2(x, \mu x) - \frac{\ln x}{2\pi} - \frac{1}{4\pi} \ln \left(1 + \left(\frac{f_r(x, \mu x)}{x} \right)^2 \right) \right).$$

It then suffices to carefully keep track of the coefficients in the expansion of the different terms involved in this equality, using for instance Faà di Bruno's formula.

Before explaining how to employ this result to recover the Taylor expansion of the Eliasson function f_r and the higher order terms in the Taylor series invariant, let us investigate the case $n = 0$. In this case the statement means that

$$g_\mu(x) = a_1(x, \mu x) + \mu a_2(x, \mu x) = d_0(\mu) \ln x + c_0(\mu) + O(x \ln x)$$

with

$$c_0(\mu) = \tilde{c}_0(\mu) = \sigma_1(0) - \frac{1}{2\pi} \arctan(C(\mu)) + C(\mu) \left(\sigma_2(0) - \frac{1}{4\pi} \ln(1 + C(\mu)^2) \right)$$

where $C(\mu) = \partial_x f_r(0) + \mu \partial_y f_r(0)$, and

$$d_0(\mu) = -\frac{1}{2\pi} (\mu \partial_y f_r(0) + \partial_x f_r(0)) = -\frac{C(\mu)}{2\pi}.$$

In particular, for $\mu = 0$ this yields

$$a_1(x, 0) = -\frac{\partial_x f_r(0)}{2\pi} \ln x + \tilde{c}_0(0) + O(x \ln x)$$

and a straightforward computation gives the first equality in the statement of Lemma 5.4.2, allowing one to recover $\partial_x f_r(0)$. And then one can recover $\partial_y f_r(0)$ by fixing any $\mu \neq 0$ and using the limit

$$\frac{a_1(x, \mu x) + \mu a_2(x, \mu x)}{\ln x} \xrightarrow{x \rightarrow 0^+} d_0(\mu) = -\frac{1}{2\pi} (\mu \partial_y f_r(0) + \partial_x f_r(0)).$$

Subsequently, one can then choose $\mu = s(0) = -\frac{\partial_x f_r(0)}{\partial_y f_r(0)}$ to obtain

$$a_1(x, s(0)x) + s(0)a_2(x, s(0)x) = \sigma_1(0) + O(x \ln x),$$

which yields the limit in Equation (5.10). And then one can recover $S_{0,1} = \sigma_2(0)$ by choosing any $\mu \neq s(0)$ and using

$$a_1(x, \mu x) + \mu a_2(x, \mu x) - d_0(\mu) \ln x \xrightarrow{x \rightarrow 0^+} c_0(\mu)$$

to extract the value of $\sigma_2(0)$ from $c_0(\mu)$.

This illustrates the method to recover all the coefficients $S_{\ell, n-\ell}$, which constitutes the proof of [LFVuN21, Theorem 6.12] and works by induction on $n \in \mathbb{N}$. Indeed, let $n \geq 1$ and assume

that we know all the derivatives $\partial^\beta f_r(0)$ for $|\beta| \leq n$ and all the coefficients S_α for $|\alpha| \leq n$, and for any $\mu \in \mathbb{R}$, let g_μ be as in Proposition 5.4.6. Then we can compute the coefficients $c_\ell(\mu)$ and $d_\ell(\mu)$ in the asymptotic expansion (5.15) for every $\ell \leq n-1$. This allows us to obtain $d_n(\mu)$ as the limit

$$d_n(\mu) = \lim_{x \rightarrow 0^+} \frac{g_\mu(x) - \sum_{\ell=0}^{n-1} x^\ell (c_\ell(\mu) + d_\ell(\mu) \ln x)}{x^n \ln x},$$

and henceforth $c_n(\mu)$ as the limit

$$c_n(\mu) = \lim_{x \rightarrow 0^+} \frac{g_\mu(x) - \sum_{\ell=0}^{n-1} x^\ell (c_\ell(\mu) + d_\ell(\mu) \ln x) - d_n(\mu) x^n \ln x}{x^n}.$$

Recall that $d_n(\mu)$ only depends on the $n+2$ derivatives $\partial^\beta f_r(0)$ with $|\beta| = n+1$ (see Equation (5.16)). By choosing $n+2$ distinct parameters μ_0, \dots, μ_{n+1} and recovering the corresponding values $d_n(\mu_0), \dots, d_n(\mu_{n+1})$, we obtain a linear system whose unique solution is the tuple $(\partial_y^{n+1} f_r(0), \partial_x \partial_y^n f_r(0), \dots, \partial_x^{n+1} f_r(0))$.

Once this is done, a similar argument allows one to recover the coefficients S_α for $|\alpha| = n+1$. Indeed, we know all the quantities needed to compute $\tilde{c}_n(\mu)$ for any μ and then we solve a linear system of the form

$$A \begin{pmatrix} S_{0,n+1} \\ \vdots \\ S_{n+1,0} \end{pmatrix} = \begin{pmatrix} c_n(\mu_0) - \tilde{c}_n(\mu_0) \\ \vdots \\ c_n(\mu_{n+1}) - \tilde{c}_n(\mu_{n+1}) \end{pmatrix}$$

with A an invertible $(n+1) \times (n+1)$ -matrix depending only on $\partial_x f_r(0)$, $\partial_y f_r(0)$ and on the distinct parameters μ_0, \dots, μ_{n+1} .

For once, we do not illustrate this on the system of coupled angular momenta from Example 3.3.4 because the computations would be too involved and not very enlightening. However, in [LFVuN21] (in particular Figures 15 and 16), we studied the recovery of these higher order terms for the spin-oscillator system from Example 3.3.3, for which the computations are tractable since several derivatives of the Eliasson function and several coefficients of the Taylor series invariant vanish.

Height invariant. Recall that the height invariant of $c_0 = (0,0)$ can be interpreted as the volume of some submanifold in the reduced space at $J = 0$. Thus it is natural to obtain this invariant by means of a particular Weyl formula. We did so by counting the joint eigenvalues in a vertical strip of size of order \hbar^δ below c_0 , for some suitable δ .

More precisely, for $\delta \in (0, \frac{1}{2})$, $c > 0$ and $y \geq 0$, consider the quantity $N_h(\delta, c, y) = \#\Sigma_h \cap ([-c\hbar^\delta, c\hbar^\delta] \times (-\infty, -y])$.

Proposition 5.4.7 ([LFVuN21, Proposition 6.1]). *Let $\delta \in (0, \frac{1}{2})$ and $c > 0$. Then*

$$S_{0,0} = \lim_{y \rightarrow 0} \lim_{\hbar \rightarrow 0} \frac{\hbar^{2-\delta}}{2c} N_h(\delta, c, y). \quad (5.17)$$

Furthermore,

$$S_{0,0} = \lim_{\hbar \rightarrow 0} \frac{\hbar^{2-\delta}}{2c} N_h(\delta, c, 0). \quad (5.18)$$

The second equality is much nicer than the first one since it only involves one limit ($\hbar \rightarrow 0$), but it is more involved than the first one because of the singular value at $y = 0$ (see below for more details), and this is why we chose to display both.

Example 5.4.8. Again, we consider the coupled angular momenta system from Examples 3.3.4 and 5.1.2, with parameters $R_1 = 1$, $R_2 = \frac{5}{2}$ and $t = \frac{1}{2}$. For this choice of parameters, Equation (3.12) gives

$$S_{0,0} = 2 + \frac{1}{\pi} \left(3 - 5 \arctan \left(\frac{3}{4} \right) - 2 \arctan 3 \right). \quad (5.19)$$

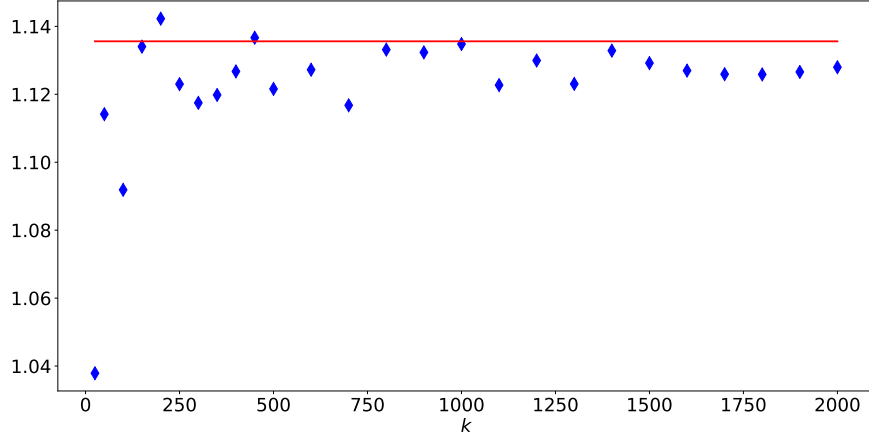


Figure 5.7: Determination of the height invariant for the coupled angular momenta (see Example 5.4.8) using Equation (5.18) in Proposition 5.4.7. The blue diamonds correspond to $\frac{\hbar^{2-\delta}}{2c} N_{\hbar}(\delta, c, 0)$ for $c = 1$, $\delta = 0.4$ and different values of $k = \hbar^{-1}$. The solid red line is the theoretical value $S_{0,0} = 2 + \frac{1}{\pi} (3 - 5 \arctan(\frac{3}{4}) - 2 \arctan 3)$ given in Equation (5.19).

In Figure 5.7, we recover this height invariant from the joint spectrum thanks to Equation (5.18).

The proof of Proposition 5.4.7 is based on results about the number of elements of an asymptotic lattice or half-lattice in a given domain. The corresponding formulas behave nicely with respect to the union of such domains, so the idea is to cover the vertical strip by rectangles in which Σ_{\hbar} is either an asymptotic lattice (from the regular Bohr-Sommerfeld conditions of Theorem 5.3.1) or an asymptotic half-lattice (from the elliptic-regular Bohr-Sommerfeld conditions of Theorem 5.3.3). This reasoning leads to Formula (5.17); Equation (5.18) requires more care since the focus-focus value, around which Σ_{\hbar} is neither an asymptotic lattice nor an asymptotic half-lattice, precisely occurs at $y = 0$. For more details, see [LFVuN21, Section 6.1].

5.4.2 Global labelings, semitoric polygons and complete invariant

As explained earlier, the reconstruction of the complete symplectic invariant from the joint spectrum Σ_{\hbar} is based on the construction of a “global labeling” of Σ_{\hbar} . More precisely, in [LFVuN21] we labeled the joint eigenvalues consistently everywhere except in a vertical strip of small width above each focus-focus value and near the elliptic-elliptic values and potential vertical walls.

Detection of singularities. Therefore, a first step is to detect these vertical walls and elliptic-elliptic and focus-focus values from the data of the joint spectrum Σ_{\hbar} only. This can be done by using the results of either [PV16], namely that Σ_{\hbar} is everywhere dense in $F(M)$ when $\hbar \rightarrow 0$ (which can already be guessed for the small value $k = 10$ in Figure 5.1), or of [LFPVN16] in which it is shown that the intersection of Σ_{\hbar} with the set of regular values of F is also dense; hence the vertical walls and elliptic-elliptic values can be located, and one can find the focus-focus values by using the logarithmic singularities of the periods at these values as in [LFPVN16]. An alternative, perhaps more satisfactory way of proceeding is to recover the Duistermaat-Heckman measure of J from the data of Σ_{\hbar} .

Recall that this Duistermaat-Heckman measure is a measure μ_J on \mathbb{R} defined as $\mu_J(I) = \text{Vol}(J^{-1}(I))$ for any interval $I \subset \mathbb{R}$. In [DH82] it is proved that $\mu_J(x) = \rho_J(x) \frac{|dx|}{2\pi}$ where the density ρ_J , called the Duistermaat-Heckman function, is continuous and piecewise affine. By [VuN07, Theorem 5.3], in the semitoric case, a positive value for ρ_J at the minimum or maximum of J indicates the presence of a vertical wall, and a change of slope for ρ_J at x_0 indicates the

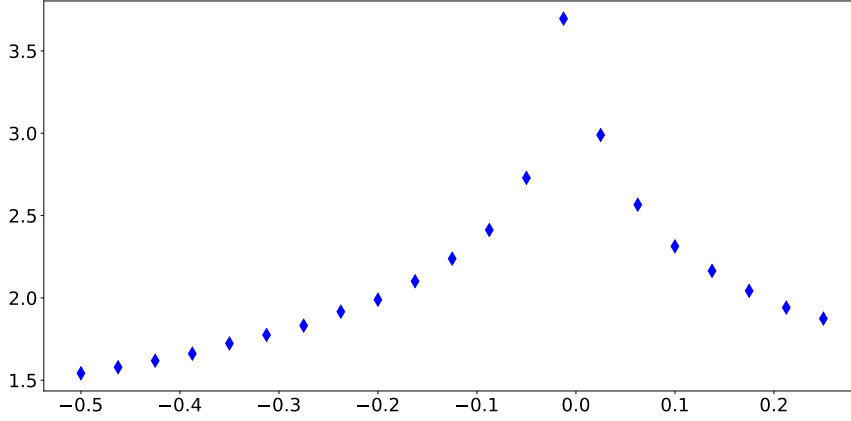


Figure 5.8: Computation of the inverse level spacings $\frac{\hbar}{E_{0,1}-E_{0,0}}$ related to the function $a_2(c)$, see Lemma 5.4.1, where $c = (-\frac{3}{2}, y)$ for various values of y ; here we work in the setting of Example 5.4.9 and $k = 50$. Notice the peak indicating the position of the focus-focus critical value at $y = 0$ (recall Equation (5.20)).

presence of elliptic-elliptic or focus-focus values of F in the fiber $J^{-1}(x_0)$. For our purpose it is not a problem to remove points on the boundary of $F(M)$ that may not be elliptic-elliptic, so each time there is such a change of slope we will simply get rid of the joint eigenvalues in small neighborhoods of the top and bottom of $\Sigma_{\hbar} \cap \{(x_0, y) \mid y \in \mathbb{R}\}$. The sole Duistermaat-Heckman function is not sufficient to obtain the location of the focus-focus values, but in order to do so we can proceed as follows. Let $x_0 \in \mathbb{R}$ be any of the points where ρ_J has a change of slope; then from the second item in Lemma 5.4.1 we can recover the restriction of the function a_2 from Equation (5.4) to the interior of $H(J^{-1}(x_0))$ minus the potential focus-focus points that it contains, and the logarithmic behavior of this function allows us to detect the focus-focus values. More precisely, if (x_0, y_0) is a focus-focus value, then, by Proposition 3.4.7 and Equation (5.4),

$$a_2(x_0, y) \sim_{y \rightarrow y_0} C \ln |y - y_0| \quad (5.20)$$

for some $C \neq 0$.

Example 5.4.9. For the coupled angular momenta system from Examples 3.3.4 and 5.1.2, with parameters $R_1 = 1$, $R_2 = \frac{5}{2}$ and $t = \frac{1}{2}$, the focus-focus value is located at $(-\frac{3}{2}, 0)$. We localize this singularity numerically from the joint spectrum by computing the inverse level spacings $\frac{\hbar}{E_{j,\ell+1}(\hbar) - E_{j,\ell}(\hbar)}$ from the second item of Lemma 5.4.1 applied to $c = (-\frac{3}{2}, y)$ for different values of y . This is shown in Figure 5.8.

The Duistermaat-Heckman function ρ_J can be recovered from the joint spectrum by using the following version of Weyl's law. Let $\delta \in (0, \frac{1}{2})$, $c > 0$ and for $x \in J(M)$, set $N_{\hbar}(x, \delta, c) = \#\Sigma_{\hbar} \cap ([x - c\hbar^{\delta}, x + c\hbar^{\delta}] \times \mathbb{R})$. Then

$$\frac{\hbar^{2-\delta}}{2c} N_{\hbar}(x, \delta, c) \xrightarrow{\hbar \rightarrow 0} \rho_J(x). \quad (5.21)$$

This version of Weyl's law for \hbar can be proved by adapting the usual case of Weyl's law in a fixed interval (see for instance [Zwo12, Theorem 14.11]), but one needs to work with semiclassical operators with symbols in appropriate classes S_{δ} . This is standard for \hbar -pseudodifferential operators (see for instance [Sjö91, Section 8]) and has been worked out recently for Berezin-Toeplitz operators in [Olt22].

Example 5.4.10. We keep considering the coupled angular momenta system from Examples 3.3.4 and 5.1.2, with parameters $R_1 = 1$, $R_2 = \frac{5}{2}$ and $t = \frac{1}{2}$. The Duistermaat-Heckman function

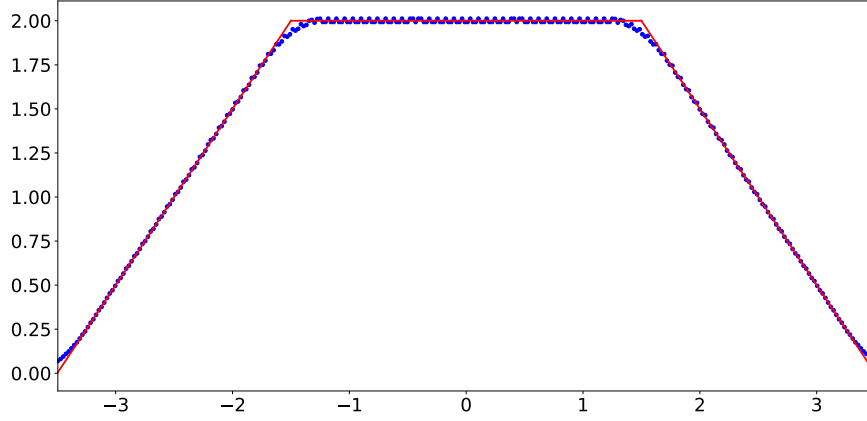


Figure 5.9: Determination of the Duistermaat-Heckman function ρ_J for the coupled angular momenta system (see Example 5.4.10) using Equation (5.21); the blue dots represent the left-hand side of this equation, with $k = 200$, $\delta = \frac{1}{4}$ and $c = 1$. The solid red line is the graph of ρ_J , see Equation (5.22).

ρ_J can easily be computed from any representative $(\Delta, \vec{c}, \vec{\epsilon})$ of the marked semitoric polygon of the system (some of these representatives are displayed in Figure 3.6). Indeed, $\rho_J(x)$ equals the length of the vertical segment obtained by intersecting the polygon Δ with the vertical line through $(x, 0)$. In our case

$$\rho_J(x) = \begin{cases} x + \frac{7}{2} & \text{if } -\frac{7}{2} \leq x \leq -\frac{3}{2}, \\ 2 & \text{if } -\frac{3}{2} \leq x \leq \frac{3}{2}, \\ \frac{7}{2} - x & \text{if } \frac{3}{2} \leq x \leq \frac{7}{2} \end{cases} \quad (5.22)$$

and $\rho_J(x) = 0$ otherwise. We recover this Duistermaat-Heckman function in Figure 5.9, thanks to Equation (5.21).

Global labelings and polygons. The next step is to remove sufficiently small neighborhoods of the vertical walls, elliptic-elliptic values and vertical half-lines above the focus-focus values. We thus obtain a new set $\tilde{\Sigma}_{\hbar}$ which is simply connected and can be written as a finite union of asymptotic lattices and half-lattices satisfying some compatibility conditions. We proved in [LFVuN21, Theorem 4.30] that any union of asymptotic lattices and half-lattices satisfying these conditions possesses a “global labeling” whose restriction to any of these asymptotic lattices or half-lattices is a linear labeling, and which is uniquely determined, in a constructive way, once we fix one of these local labelings. Furthermore, this global labeling corresponds to a “global asymptotic chart” $\tilde{\Phi}_{\hbar} = \Phi + O(\hbar)$ extending the local asymptotic charts.

In the case of $\tilde{\Sigma}_{\hbar}$, the local asymptotic charts are the inverses of action diffeomorphisms (or generalized action diffeomorphisms as in Lemma 5.3.2) and the map Φ is a cartographic homeomorphism as in Theorem 3.4.4, with $\vec{\epsilon} = (1, \dots, 1)$ (all cuts up). So starting from the labeling of any of the asymptotic lattices or half-lattices constituting $\tilde{\Sigma}_{\hbar}$, produced thanks to the algorithms discussed in Section 5.3, we obtain an explicit global labeling whose image (multiplied by \hbar) is a “discrete polygon” Δ_{\hbar} converging (in the sense of the Hausdorff distance) to a subset of the convex polygon $\Phi(M)$ (see [LFVuN21, Proposition 5.12]); the missing parts of this polygon correspond to the neighborhoods of vertical walls, elliptic-elliptic values and upwards cuts that we removed to construct $\tilde{\Sigma}_{\hbar}$. This is still sufficient to reconstruct the full polygon $\Phi(M)$, precisely because it is a polygon so we can easily draw the missing parts. There is in fact one subtlety, namely that the convergence of the discrete polygon Δ_{\hbar} is only true up to translation by a vector

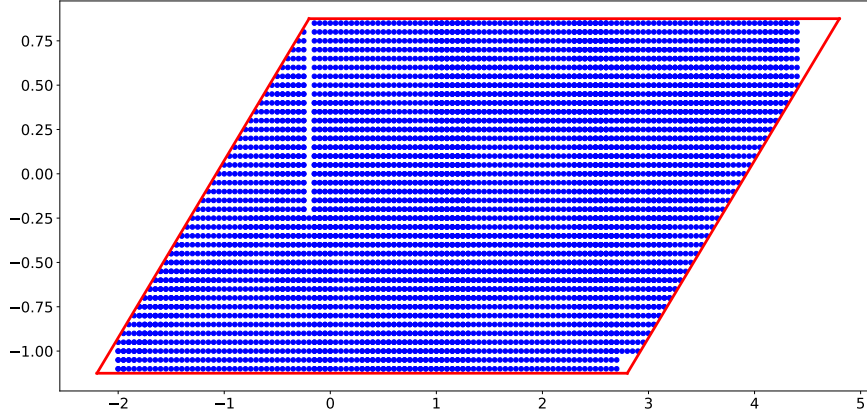


Figure 5.10: Determination of the privileged polygon for the coupled angular momenta system (see Example 5.4.11) by computing the discrete polygon Δ_{\hbar} . The blue dots represent the set Δ_{\hbar} , for $k = 20$ and $\hbar = k^{-1}$, obtained from a global labeling of the joint spectrum minus neighborhoods of the elliptic-elliptic values and of the vertical half-line above the focus-focus value. This global labeling is constructed from the initial choice of the privileged labeling near the singularity (see the discussion before Example 5.4.4). The solid red lines represent a translation of the privileged polygon shown in the top left corner of Figure 3.6.

that may depend on \hbar , but again this is not a problem (indeed, we already recovered the image of J as the support of the Duistermaat-Heckman function ρ_J).

Recall that the image $\Phi(M)$ gives one representative of the unmarked semitoric polygon which corresponds to the initial choice of action variables to be extended to a cartographic homeomorphism; here this initial choice of action variables corresponds to the initial local labeling used to construct the global labeling of $\tilde{\Sigma}_{\hbar}$. This is actually important in the next step.

Example 5.4.11. We still work with the coupled angular momenta system from Examples 3.3.4 and 5.1.2, with parameters $R_1 = 1$, $R_2 = \frac{5}{2}$ and $t = \frac{1}{2}$. Recall from Example 3.4.12 that the representative of the marked semitoric polygon of this system with upwards cut and vanishing twisting number is the polygon displayed in the top left corner of Figure 3.6. We call this polygon the *privileged polygon* of the system, and we recover it from the joint spectrum in Figure 5.10, by computing the discrete polygon Δ_{\hbar} described above.

Recovering the complete symplectic invariant. To sum up, from the joint spectrum Σ_{\hbar} we have obtained the image $\Delta = \Phi(M)$ of a cartographic homeomorphism Φ with cuts up, together with the first coordinates of the marked points in Δ which are the images by Φ of the focus-focus points. Moreover, we already saw in Section 5.4.1 how to recover the heights and Taylor series invariants of the focus-focus values from Σ_{\hbar} . Therefore, to obtain the complete symplectic invariant of (M, ω, F) it only remains to recover the twisting numbers associated with the representative Δ . This can be done as follows.

Consider the restriction of Φ to a set of regular values sufficiently close to one of the focus-focus values $F(m_0)$. Then the corresponding local labeling is associated with an asymptotic chart whose leading term is the inverse of the action diffeomorphism corresponding to the choice of action variables $(J, L_{\vec{\epsilon}})$ with $\vec{\epsilon} = (1, \dots, 1)$ (see the discussion above Definition 3.4.10). So we can recover the quantity $\sigma_1(0)$ corresponding to $L_{\vec{\epsilon}}$ using Equation (5.11). By Proposition 3.4.13, the twisting number associated with m_0 and $\vec{\epsilon} = (1, \dots, 1)$ is $\lfloor \sigma_1(0) \rfloor$.

5.5 Perspectives

We conclude this chapter by giving a few directions of research that stem naturally from the results described above.

Because we were only using the regular (or singular near a value of elliptic-regular type) Bohr-Sommerfeld conditions, the explicit formulas that we obtained in [LFVuN21] (see for instance Equations (5.7), (5.8), (5.11) and (5.13)) involve a double limit: first we fix a value $c \in F(M)$ close to a focus-focus value c_{ff} and let \hbar go to zero, and then we let c go to c_{ff} . Of course it would be better to get rid of this double limit, but for this we would need a description of the joint spectrum in a spectral window containing c_{ff} ; such singular Bohr-Sommerfeld conditions are available for \hbar -pseudodifferential operators [VN00], but not for Berezin-Toeplitz operators. And even though the results of [VN00] can surely be adapted to the latter case without too much trouble, these results only hold for a singular fiber $F^{-1}(c_{\text{ff}})$ containing exactly one focus-focus point (a torus pinched at a single point). Hence it would be interesting to directly obtain singular Bohr-Sommerfeld rules near a focus-focus value c_{ff} such that $F^{-1}(c_{\text{ff}})$ contains two or more focus-focus points, for both \hbar -pseudodifferential and Berezin-Toeplitz operators. This description of the joint spectrum would certainly involve the symplectic classification of such fibers obtained in [PT19] and, besides being of independent interest, it would allow one not only to get rid of the aforementioned double limit, but also to gain some insights regarding the inverse question in the non-simple case. As explained earlier, we believe that our proofs in [LFVuN21] can be adapted with few changes to allow for several simple focus-focus fibers in the same J -fiber; therefore the most interesting non-simple case is when there exist tori pinched at two or more focus-focus points. It is not clear whether in this case the joint spectrum determines the system, and this question would be worth investigating.

Of course, the general question of recovering an integrable system from the joint spectrum of its quantization constitutes a desirable horizon, but which is already hard to reach in dimension four. An important step towards this goal would be to understand the case of the class of hypersemitoric systems introduced in [HP21] and discussed in Section 4.5.2. These systems have been getting more and more attention in the past few years, see for instance [HP21, GH22] or the recent survey [HHM23], and are most probably generic among four-dimensional integrable systems lifting Hamiltonian S^1 -spaces (see the discussion in [HP21, Remark 1.9]). On top of singularities of elliptic and focus-focus type, hypersemitoric systems display hyperbolic-regular and parabolic singularities. A first requirement, before considering the inverse spectral problem for hypersemitoric systems, would be to produce a symplectic classification of such systems. While a complete classification is still missing, some steps have been taken towards it: in [Gul22], the author classifies hyperbolic-regular fibers in four-dimensional integrable systems lifting Hamiltonian S^1 -spaces (see also [CdVVuN03] and [BF04, BO06]), and in [KM21] the authors symplectically classify neighborhoods of parabolic orbits; this classification question is discussed in the recent survey [GH23]. As for the quantum aspects, the joint spectrum near a singular value of hyperbolic-regular type has been described in [CdVVuN03] for \hbar -pseudodifferential operators, but to our knowledge no such description has been proposed near parabolic values. In [MVuN23], the authors discuss the possibility of an inverse spectral result for A_k singularities in dimension two; for $k = 2$, these are the analogues of parabolic singularities.

Finally, another related inverse problem which would be worth studying concerns Hamiltonian S^1 -spaces (see Section 3.5). Concretely, we would consider (M, ω, J) with (M, ω) a four-dimensional compact, symplectic manifold and J the momentum map of an effective Hamiltonian S^1 -action, and a semiclassical operator $(\hat{J}_{\hbar})_{\hbar \in \mathcal{I}}$ quantizing J , and we would try to understand which properties of (M, ω, J) can be recovered from the family of spectra $(\text{Sp}(\hat{J}_{\hbar}))_{\hbar \in \mathcal{I}}$ in the semiclassical limit $\hbar \rightarrow 0$. We do not expect to recover the full Karshon graph of (M, ω, J) from these spectra, but we believe that some information can be extracted thanks to the results obtained in [CLF20, CLF23b, CLF23a] and described in Section 2.4, see also the discussion at the end of Section 2.5.

Bibliography

- [AB11] Jørgen Ellegaard Andersen and Jakob Lindblad Blaavand. Asymptotics of Toeplitz operators and applications in TQFT. In *Geometry and quantization*, volume 19 of *Trav. Math.*, pages 167–201. Univ. Luxemb., Luxembourg, 2011.
- [ADH19] Jaume Alonso, Holger R. Dullin, and Sonja Hohloch. Taylor series and twisting-index invariants of coupled spin-oscillators. *J. Geom. Phys.*, 140:131–151, 2019.
- [ADH20] Jaume Alonso, Holger R. Dullin, and Sonja Hohloch. Symplectic classification of coupled angular momenta. *Nonlinearity*, 33(1):417–468, 2020.
- [AH19] Jaume Alonso and Sonja Hohloch. Survey on recent developments in semitoric systems. *RIMS Kokyuroku*, 2137, 2019.
- [AHP23] Jaume Alonso, Sonja Hohloch, and Joseph Palmer. The twisting index in semitoric systems, 2023. Preprint, <https://arxiv.org/abs/2309.16614>.
- [ALF22] Michele Ancona and Yohann Le Floch. Berezin-Toeplitz operators, Kodaira maps, and random sections. Preprint, <https://arxiv.org/abs/2206.15112>, 32 pages, 2022.
- [Anc21] Michele Ancona. Random sections of line bundles over real Riemann surfaces. *Int. Math. Res. Not. IMRN*, (9):7004–7059, 2021.
- [Ati82] M. F. Atiyah. Convexity and commuting Hamiltonians. *Bull. London Math. Soc.*, 14(1):1–15, 1982.
- [Aur09] D. Auroux. Special Lagrangian fibrations, wall-crossing, and mirror symmetry. In *Surveys in differential geometry. Vol. XIII. Geometry, analysis, and algebraic geometry: forty years of the Journal of Differential Geometry*, volume 13 of *Surv. Differ. Geom.*, pages 1–47. Int. Press, Somerville, MA, 2009.
- [Bar61] V. Bargmann. On a Hilbert space of analytic functions and an associated integral transform I. *Comm. Pure Appl. Math.*, 19:187–214, 1961.
- [BB70] R. Balian and C. Bloch. Distribution of eigenfrequencies for the wave equation in a finite domain. I. Three-dimensional problem with smooth boundary surface. *Ann. Physics*, 60:401–447, 1970.
- [BB71] R. Balian and C. Bloch. Distribution of eigenfrequencies for the wave equation in a finite domain. II. Electromagnetic field. Riemannian spaces. *Ann. Physics*, 64:271–307, 1971.
- [BB72] R. Balian and C. Bloch. Distribution of eigenfrequencies for the wave equation in a finite domain. III. Eigenfrequency density oscillations. *Ann. Physics*, 69:76–160, 1972.

- [BBL96] E. Bogomolny, O. Bohigas, and P. Leboeuf. Quantum chaotic dynamics and random polynomials. *J. Statist. Phys.*, 85(5-6):639–679, 1996.
- [BBS08] Robert Berman, Bo Berndtsson, and Johannes Sjöstrand. A direct approach to Bergman kernel asymptotics for positive line bundles. *Ark. Mat.*, 46(2):197–217, 2008.
- [BCD09] O. Babelon, L. Cantini, and B. Douçot. A semi-classical study of the Jaynes-Cummings model. *J. Stat. Mech. Theory Exp.*, 7:P07011, 45, 2009.
- [BCHM18] Turgay Bayraktar, Dan Coman, Hendrik Herrmann, and George Marinescu. A survey on zeros of random holomorphic sections. *Dolomites Res. Notes Approx.*, 11(Special Issue Norm Levenberg):1–19, 2018.
- [BD12] O. Babelon and B. Douçot. Classical Bethe Ansatz and normal forms in an integrable version of the Dicke model. *Phys. D*, 241(23-24):2095–2108, 2012.
- [BD15] O. Babelon and B. Douçot. Higher index focus-focus singularities in the Jaynes-Cummings-Gaudin model: symplectic invariants and monodromy. *J. Geom. Phys.*, 87:3–29, 2015.
- [BdMG81] L. Boutet de Monvel and V. Guillemin. *The spectral theory of Toeplitz operators*, volume 99 of *Annals of Mathematics Studies*. Princeton University Press, Princeton, NJ, 1981.
- [Ber75] F. A. Berezin. General concept of quantization. *Comm. Math. Phys.*, 40:153–174, 1975.
- [Ber18] Robert J. Berman. Determinantal point processes and fermions on polarized complex manifolds: bulk universality. In *Algebraic and analytic microlocal analysis*, volume 269 of *Springer Proc. Math. Stat.*, pages 341–393. Springer, Cham, 2018.
- [BF04] A. V. Bolsinov and A. T. Fomenko. *Integrable Hamiltonian systems*. Chapman & Hall/CRC, Boca Raton, FL, 2004. Geometry, topology, classification, Translated from the 1999 Russian original.
- [BGK18] Alexey Bolsinov, Lorenzo Guglielmi, and Elena Kudryavtseva. Symplectic invariants for parabolic orbits and cusp singularities of integrable systems. *Philos. Trans. Roy. Soc. A*, 376(2131):20170424, 29, 2018.
- [BHMM23] Joaquim Brugués, Sonja Hohloch, Pau Mir, and Eva Miranda. Constructions of b-semitoric systems, 2023.
- [BMS94] M. Bordemann, E. Meinrenken, and M. Schlichenmaier. Toeplitz quantization of Kähler manifolds and $\mathrm{gl}(N)$, $N \rightarrow \infty$ limits. *Comm. Math. Phys.*, 165(2):281–296, 1994.
- [BMZ11] Jean-Michel Bismut, Xiaonan Ma, and Weiping Zhang. Opérateurs de Toeplitz et torsion analytique asymptotique. *C. R. Math. Acad. Sci. Paris*, 349(17-18):977–981, 2011.
- [BO06] Alexey V. Bolsinov and Andrey A. Oshemkov. Singularities of integrable Hamiltonian systems. In *Topological methods in the theory of integrable systems*, pages 1–67. Camb. Sci. Publ., Cambridge, 2006.
- [Bou90] Thierry Bouche. Convergence de la métrique de Fubini-Study d’un fibré linéaire positif. *Ann. Inst. Fourier (Grenoble)*, 40(1):117–130, 1990.

- [BP31] A. Bloch and G. Pólya. On the Roots of Certain Algebraic Equations. *Proc. London Math. Soc.* (2), 33(2):102–114, 1931.
- [BPU95] D. Borthwick, T. Paul, and A. Uribe. Legendrian distributions with applications to relative Poincaré series. *Invent. Math.*, 122(2):359–402, 1995.
- [BPU98] D. Borthwick, T. Paul, and A. Uribe. Semiclassical spectral estimates for Toeplitz operators. *Ann. Inst. Fourier (Grenoble)*, 48(4):1189–1229, 1998.
- [BU00] David Borthwick and Alejandro Uribe. Nearly Kählerian embeddings of symplectic manifolds. *Asian J. Math.*, 4(3):599–620, 2000.
- [Cat99] David Catlin. The Bergman kernel and a theorem of Tian. In *Analysis and geometry in several complex variables (Katata, 1997)*, Trends Math., pages 1–23. Birkhäuser Boston, Boston, MA, 1999.
- [CD88] R. Cushman and J. J. Duistermaat. The quantum mechanical spherical pendulum. *Bull. Am. Math. Soc., New Ser.*, 19(2):475–479, 1988.
- [CDEW19] Irina Chiscop, Holger R. Dullin, Konstantinos Efstathiou, and Holger Waalkens. A Lagrangian fibration of the isotropic 3-dimensional harmonic oscillator with monodromy. *J. Math. Phys.*, 60(3):032103, 15, 2019.
- [CdS03] A. Cannas da Silva. Symplectic toric manifolds. In *Symplectic geometry of integrable Hamiltonian systems (Barcelona, 2001)*, Adv. Courses Math. CRM Barcelona, pages 85–173. Birkhäuser, Basel, 2003.
- [CdV73] Yves Colin de Verdière. Spectre du laplacien et longueurs des géodésiques périodiques. I, II. *Compositio Math.*, 27:83–106; *ibid.* 27 (1973), 159–184, 1973.
- [CdV79] Yves Colin de Verdière. Sur le spectre des opérateurs elliptiques à bicaractéristiques toutes périodiques. *Comment. Math. Helv.*, 54(3):508–522, 1979.
- [CdV80] Y. Colin de Verdière. Spectre conjoint d’opérateurs pseudo-différentiels qui commutent II. *Math. Z.*, 171:51–73, 1980.
- [CdVV79] Y. Colin de Verdière and J. Vey. Le lemme de Morse isochore. *Topology*, 18(4):283–293, 1979.
- [CdVVuN03] Yves Colin de Verdière and San Vĩ Ngoc. Singular Bohr-Sommerfeld rules for 2D integrable systems. *Ann. Sci. École Norm. Sup. (4)*, 36(1):1–55, 2003.
- [CE20] Laurent Charles and Benoit Estienne. Entanglement entropy and Berezin-Toeplitz operators. *Comm. Math. Phys.*, 376(1):521–554, 2020.
- [Cha74] J. Chazarain. Formule de Poisson pour les variétés riemanniennes. *Invent. Math.*, 24:65–82, 1974.
- [Cha88] A.-M. Charbonnel. Comportement semi-classique du spectre conjoint d’opérateurs pseudo-différentiels qui commutent. *Asymptotic Analysis*, 1:227–261, 1988.
- [Cha03a] L. Charles. Berezin-Toeplitz operators, a semi-classical approach. *Comm. Math. Phys.*, 239(1-2):1–28, 2003.
- [Cha03b] L. Charles. Quasimodes and Bohr-Sommerfeld conditions for the Toeplitz operators. *Comm. Partial Differential Equations*, 28(9-10):1527–1566, 2003.

- [Cha06] Laurent Charles. Symbolic calculus for Toeplitz operators with half-form. *J. Symplectic Geom.*, 4(2):171–198, 2006.
- [Cha10] L. Charles. On the quantization of polygon spaces. *Asian J. Math.*, 14(1):109–152, 2010.
- [Cha13] Marc Chaperon. Normalisation of the smooth focus-focus: a simple proof. *Acta Math. Vietnam.*, 38(1):3–9, 2013.
- [Cha20] Laurent Charles. Landau levels on a compact manifold, 2020. To appear in *Annales Henri Lebesgue*, <https://arxiv.org/abs/2012.14190>.
- [Cha21a] Laurent Charles. Analytic Berezin-Toeplitz operators. *Math. Z.*, 299(1-2):1015–1035, 2021.
- [Cha21b] Laurent Charles. On the spectrum of non degenerate magnetic Laplacian, 2021. To appear in *Analysis and PDE*, <https://arxiv.org/abs/2109.05508>.
- [CLF20] Laurent Charles and Yohann Le Floch. Quantum propagation for Berezin-Toeplitz operators. Preprint, <https://arxiv.org/abs/2009.05279v2>, 43 pages, 2020.
- [CLF23a] Laurent Charles and Yohann Le Floch. The Gutzwiller trace formula for Berezin-Toeplitz operators on compact Kähler manifolds. *In preparation*, 2023+.
- [CLF23b] Laurent Charles and Yohann Le Floch. Pairings of Lagrangian states on compact Kähler manifolds. *In preparation*, 2023+.
- [CM15a] L. Charles and J. Marché. Knot state asymptotics. I: AJ conjecture and abelian representations. *Publ. Math., Inst. Hautes Étud. Sci.*, 121:279–322, 2015.
- [CM15b] L. Charles and J. Marché. Knot state asymptotics. II: Witten conjecture and irreducible representations. *Publ. Math., Inst. Hautes Étud. Sci.*, 121:323–361, 2015.
- [CP18] Laurent Charles and Leonid Polterovich. Quantum speed limit versus classical displacement energy. *Annales Henri Poincaré*, Feb 2018.
- [CP22] Laurent Charles and Leonid Polterovich. Asymptotic representations of Hamiltonian diffeomorphisms and quantization. *Groups Geom. Dyn.*, 16(4):1369–1387, 2022.
- [CPVuN13] Laurent Charles, Álvaro Pelayo, and San Vũ Ngọc. Isospectrality for quantum toric integrable systems. *Ann. Sci. Éc. Norm. Supér. (4)*, 46(5):815–849, 2013.
- [CV22] Roger Casals and Renato Vianna. Full ellipsoid embeddings and toric mutations. *Selecta Math. (N.S.)*, 28(3):Paper No. 61, 62, 2022.
- [Del88] Thomas Delzant. Hamiltoniens périodiques et images convexes de l’application moment. *Bull. Soc. Math. France*, 116(3):315–339, 1988.
- [Del21] Alix Deleporte. Toeplitz operators with analytic symbols. *J. Geom. Anal.*, 31(4):3915–3967, 2021.
- [Det18] Renaud Detcherry. Geometric quantization and asymptotics of pairings in TQFT. *Ann. Sci. Éc. Norm. Supér. (4)*, 51(6):1599–1630, 2018.
- [DG75] J. J. Duistermaat and V. W. Guillemin. The spectrum of positive elliptic operators and periodic bicharacteristics. *Invent. Math.*, 29:39–79, 1975.

- [DH82] J. J. Duistermaat and G. J. Heckman. On the variation in the cohomology of the symplectic form of the reduced phase space. *Invent. Math.*, 69:259–268, 1982.
- [DH13] Kiril Datchev and Hamid Hezari. Inverse problems in spectral geometry. In *Inverse problems and applications: inside out. II*, volume 60 of *Math. Sci. Res. Inst. Publ.*, pages 455–485. Cambridge Univ. Press, Cambridge, 2013.
- [DHS20] Alix Deleporte, Michael Hitrik, and Johannes Sjostrand. A direct approach to the analytic Bergman projection, 2020. To appear in *Annales de la Faculté des Sciences de Toulouse*, <https://arxiv.org/abs/2004.14606>.
- [DHVN22] Monique Dauge, Michael A. Hall, and San Vũ Ngọc. Asymptotic lattices, good labellings, and the rotation number for quantum integrable systems. *Discrete and Continuous Dynamical Systems*, 42(12):5683–5735, 2022.
- [DKL⁺22] Yu Du, Gabriel Kosmacher, Yichen Liu, Jeff Massman, Joseph Palmer, Timothy Thieme, Jerry Wu, and Zheyu Zhang. Packing densities of Delzant and semitoric polygons, 2022. To appear in *SIGMA*, <https://arxiv.org/abs/2210.06415>.
- [DLM04] Xianzhe Dai, Kefeng Liu, and Xiaonan Ma. On the asymptotic expansion of Bergman kernel. *C. R. Math. Acad. Sci. Paris*, 339(3):193–198, 2004.
- [DLM23] Alexander Drewitz, Bingxiao Liu, and George Marinescu. Gaussian holomorphic sections on noncompact complex manifolds, 2023. Preprint, <https://arxiv.org/abs/2302.08426>.
- [DM91] J.-P. Dufour and P. Molino. Compactification d’actions de \mathbf{R}^n et variables action-angle avec singularités. In *Symplectic geometry, groupoids, and integrable systems (Berkeley, CA, 1989)*, volume 20 of *Math. Sci. Res. Inst. Publ.*, pages 151–167. Springer, New York, 1991.
- [DMH21] Annelies De Meulenaere and Sonja Hohloch. A family of semitoric systems with four focus-focus singularities and two double pinched tori. *J. Nonlinear Sci.*, 31(4):Paper No. 66, 56, 2021.
- [DMSD16] Emily B. Dryden, Diana Macedo, and Rosa Sena-Dias. Recovering S^1 -invariant metrics on S^2 from the equivariant spectrum. *Int. Math. Res. Not. IMRN*, 16:4882–4902, 2016.
- [Don01] S. K. Donaldson. Scalar curvature and projective embeddings. I. *J. Differential Geom.*, 59(3):479–522, 2001.
- [Dui80] J. J. Duistermaat. On global action-angle coordinates. *Comm. Pure Appl. Math.*, 33(6):687–706, 1980.
- [DZ22] Alix Deleporte and Steve Zelditch. Real-analytic geodesics in the Mabuchi space of Kähler metrics and quantization, 2022. Preprint, <https://arxiv.org/abs/2210.00763>.
- [Eli84] L. H. Eliasson. *Hamiltonian systems with Poisson commuting integrals*. PhD thesis, University of Stockholm, 1984.
- [Eli90] L. H. Eliasson. Normal forms for Hamiltonian systems with Poisson commuting integrals—elliptic case. *Comment. Math. Helv.*, 65(1):4–35, 1990.
- [ES18] Jonathan David Evans and Ivan Smith. Markov numbers and Lagrangian cell complexes in the complex projective plane. *Geom. Topol.*, 22(2):1143–1180, 2018.

- [Eva23] Jonny Evans. *Lectures on Lagrangian Torus Fibrations*. London Mathematical Society Student Texts. Cambridge University Press, 2023.
- [Fin12] Joel Fine. Quantization and the Hessian of Mabuchi energy. *Duke Math. J.*, 161(14):2753–2798, 2012.
- [Ful93] William Fulton. *Introduction to toric varieties*, volume 131 of *Annals of Mathematics Studies*. Princeton University Press, Princeton, NJ, 1993. The William H. Roever Lectures in Geometry.
- [GH78] Phillip Griffiths and Joseph Harris. *Principles of algebraic geometry*. Pure and Applied Mathematics. Wiley-Interscience [John Wiley & Sons], New York, 1978.
- [GH22] Yannick Gullentops and Sonja Hohloch. Creating hyperbolic-regular singularities in the presence of an \mathbb{S}^1 -symmetry, 2022. Preprint, <https://arxiv.org/abs/2209.15631>.
- [GH23] Yannick Gullentops and Sonja Hohloch. Recent examples of hypersemitoric systems and first steps towards a classification: a brief survey, 2023. Preprint, <https://arxiv.org/abs/2308.16346>.
- [GS82] V. Guillemin and S. Sternberg. Convexity properties of the moment mapping. *Invent. Math.*, 67(3):491–513, 1982.
- [Gui95] V. Guillemin. Star products on compact pre-quantizable symplectic manifolds. *Lett. Math. Phys.*, 35(1):85–89, 1995.
- [Gul22] Yannick Gullentops. *Hyperbolic singularities in the presence of S^1 -actions and Hamiltonian PDEs*. PhD thesis, Universiteit Antwerpen, 2022. <https://repository.uantwerpen.be/docman/irua/fb8845/186212.pdf>.
- [Gut71] Martin C. Gutzwiller. Periodic orbits and classical quantization conditions. *Journal of Mathematical Physics*, 12(3):343–358, 1971.
- [GW11] Damien Gayet and Jean-Yves Welschinger. Exponential rarefaction of real curves with many components. *Publ. Math. Inst. Hautes Études Sci.*, (113):69–96, 2011.
- [HHM23] Tobias Våge Henriksen, Sonja Hohloch, and Nikolay Martynchuk. Towards hypersemitoric systems. To appear in *Conference Proceedings of RIMS Kokyuroku*, <https://arxiv.org/abs/2307.04483>, 2023.
- [Hör83] Lars Hörmander. *The analysis of linear partial differential operators. I*, volume 256 of *Grundlehren der Mathematischen Wissenschaften [Fundamental Principles of Mathematical Sciences]*. Springer-Verlag, Berlin, 1983. Distribution theory and Fourier analysis.
- [HP18] S. Hohloch and J. Palmer. A family of compact semitoric systems with two focus-focus singularities. *Journal of Geometric Mechanics*, 10(3):331–357, 2018.
- [HP21] S. Hohloch and J. Palmer. Extending compact Hamiltonian S^1 -spaces to integrable systems with mild degeneracies in dimension four. Preprint, <https://arxiv.org/abs/2105.00523>, 2021.
- [HSS15] S. Hohloch, S. Sabatini, and D. Sepe. From compact semi-toric systems to Hamiltonian S^1 -spaces. *Discrete Contin. Dyn. Syst.*, 35(1):247–281, 2015.
- [HSSS] S. Hohloch, S. Sabatini, D. Sepe, and M. Symington. From Hamiltonian S^1 -spaces to compact semi-toric systems. *In preparation*.

- [ILMM20] Louis Ioos, Wen Lu, Xiaonan Ma, and George Marinescu. Berezin-Toeplitz quantization for eigenstates of the Bochner Laplacian on symplectic manifolds. *J. Geom. Anal.*, 30(3):2615–2646, 2020.
- [Ioo20] Louis Ioos. Geometric quantization of Hamiltonian flows and the Gutzwiller trace formula. *Lett. Math. Phys.*, 110(7):1585–1621, 2020.
- [Ioo22] Louis Ioos. Balanced metrics for Kähler-Ricci solitons and quantized Futaki invariants. *J. Funct. Anal.*, 282(8):Paper No. 109400, 58, 2022.
- [IP23] Louis Ioos and Leonid Polterovich. Quantization of symplectic fibrations and canonical metrics. *Internat. J. Math.*, 34(8):Paper No. 2350043, 47, 2023.
- [JC64] E.T. Jaynes and F.W. Cummings. Comparison of quantum and semiclassical radiation theories with application to the beam maser. *Proc. IEEE*, 51(1):89–109, 1963–1964.
- [Joz94] Richard Jozsa. Fidelity for mixed quantum states. *Journal of Modern Optics*, 41(12):2315–2323, 1994.
- [Kac43] M. Kac. On the average number of real roots of a random algebraic equation. *Bull. Amer. Math. Soc.*, 49:314–320, 1943.
- [Kac66] Mark Kac. Can one hear the shape of a drum? *Amer. Math. Monthly*, 73(4, part II):1–23, 1966.
- [Kar99] Y. Karshon. Periodic Hamiltonian flows on four-dimensional manifolds. *Mem. Amer. Math. Soc.*, 141(672):viii+71, 1999.
- [Kle16] Semyon Klevtsov. Geometry and large N limits in Laughlin states. In *Travaux mathématiques. Vol. XXIV*, volume 24 of *Trav. Math.*, pages 63–127. Fac. Sci. Technol. Commun. Univ. Luxemb., Luxembourg, 2016.
- [KM21] Elena Kudryavtseva and Nikolay Martynchuk. C^∞ symplectic invariants of parabolic orbits and flaps in integrable Hamiltonian systems. Preprint, <https://arxiv.org/abs/2110.13758>, 2021.
- [KMM19] Yuri A. Kordyukov, Xiaonan Ma, and George Marinescu. Generalized Bergman kernels on symplectic manifolds of bounded geometry. *Comm. Partial Differential Equations*, 44(11):1037–1071, 2019.
- [KMMW17] Semyon Klevtsov, Xiaonan Ma, George Marinescu, and Paul Wiegmann. Quantum Hall effect and Quillen metric. *Comm. Math. Phys.*, 349(3):819–855, 2017.
- [Kor18] Yu. A. Kordyukov. On asymptotic expansions of generalized Bergman kernels on symplectic manifolds. *Algebra i Analiz*, 30(2):163–187, 2018.
- [Kor22] Yuri A. Kordyukov. Berezin-Toeplitz quantization associated with higher Landau levels of the Bochner Laplacian. *J. Spectr. Theory*, 12(1):143–167, 2022.
- [Kos70] Bertram Kostant. Quantization and unitary representations. I. Prequantization. In *Lectures in modern analysis and applications, III*, volume Vol. 170 of *Lecture Notes in Math*, pages pp 87–208. Springer, Berlin, 1970.
- [KPP18] D. M. Kane, J. Palmer, and Á. Pelayo. Minimal models of compact symplectic semitoric manifolds. *J. Geom. Phys.*, 125:49–74, 2018.

- [Lel57] Pierre Lelong. Intégration sur un ensemble analytique complexe. *Bull. Soc. Math. France*, 85:239–262, 1957.
- [LF14a] Yohann Le Floch. Singular Bohr-Sommerfeld conditions for 1D Toeplitz operators: elliptic case. *Comm. Partial Differential Equations*, 39(2):213–243, 2014.
- [LF14b] Yohann Le Floch. Singular Bohr-Sommerfeld conditions for 1D Toeplitz operators: hyperbolic case. *Anal. PDE*, 7(7):1595–1637, 2014.
- [LF18a] Yohann Le Floch. Bounds for fidelity of semiclassical Lagrangian states in Kähler quantization. *J. Math. Phys.*, 59(8):082103, 35, 2018.
- [LF18b] Yohann Le Floch. *A brief introduction to Berezin-Toeplitz operators on compact Kähler manifolds*. CRM Short Courses. Springer, Cham, 2018.
- [LFP16] Yohann Le Floch and Álvaro Pelayo. Euler–MacLaurin formulas via differential operators. *Adv. in Appl. Math.*, 73:99–124, 2016.
- [LFP19a] Yohann Le Floch and Álvaro Pelayo. Spectral asymptotics of semiclassical unitary operators. *Journal of Mathematical Analysis and Applications*, 473(2):1174–1202, 2019.
- [LFP19b] Yohann Le Floch and Álvaro Pelayo. Symplectic geometry and spectral properties of classical and quantum coupled angular momenta. *J. Nonlinear Sci.*, 29(2):655–708, 2019.
- [LFP22] Yohann Le Floch and Joseph Palmer. Semitoric families. To appear in *Mem. Amer. Math. Soc.*, <https://arxiv.org/abs/1810.06915>, 2022.
- [LFP23] Yohann Le Floch and Joseph Palmer. Families of four-dimensional integrable systems with S^1 -symmetries. Preprint, <https://arxiv.org/abs/2307.10670>, 145 pages, 2023.
- [LFPVN16] Yohann Le Floch, Álvaro Pelayo, and San Vũ Ngọc. Inverse spectral theory for semiclassical Jaynes–Cummings systems. *Mathematische Annalen*, 364(3):1393–1413, 2016.
- [LFPVN19] Yohann Le Floch, Álvaro Pelayo, and San Vũ Ngọc. Correction to: “Inverse spectral theory for semiclassical Jaynes–Cummings systems”. *Math. Ann.*, 375(1-2):917–920, 2019.
- [LFVuN21] Yohann Le Floch and San Vũ Ngọc. The inverse spectral problem for quantum semitoric systems. Preprint, <https://arxiv.org/abs/2104.06704>, 105 pages, 2021.
- [LMTW98] Eugene Lerman, Eckhard Meinrenken, Sue Tolman, and Chris Woodward. Non-abelian convexity by symplectic cuts. *Topology*, 37(2):245–259, 1998.
- [LO38] J. E. Littlewood and A. C. Offord. On the Number of Real Roots of a Random Algebraic Equation. *J. London Math. Soc.*, 13(4):288–295, 1938.
- [Lu00] Zhiqin Lu. On the lower order terms of the asymptotic expansion of Tian-Yau-Zelditch. *Amer. J. Math.*, 122(2):235–273, 2000.
- [Mat96] V. S. Matveev. Integrable Hamiltonian systems with two degrees of freedom. Topological structure of saturated neighborhoods of points of focus-focus and saddle-saddle types. *Mat. Sb.*, 187(4):29–58, 1996.

- [Min47] Henri Mineur. Sur les systèmes mécaniques dont les intégrales premières sont définies par des équations implicites. *C. R. Acad. Sci. Paris*, 224:26–27, 1947.
- [MM07] Xiaonan Ma and George Marinescu. *Holomorphic Morse inequalities and Bergman kernels*, volume 254 of *Progress in Mathematics*. Birkhäuser Verlag, Basel, 2007.
- [MM08a] X. Ma and G. Marinescu. Toeplitz operators on symplectic manifolds. *J. Geom. Anal.*, 18(2):565–611, 2008.
- [MM08b] Xiaonan Ma and George Marinescu. Generalized Bergman kernels on symplectic manifolds. *Adv. Math.*, 217(4):1756–1815, 2008.
- [MP15] Julien Marché and Thierry Paul. Toeplitz operators in TQFT via skein theory. *Trans. Am. Math. Soc.*, 367(5):3669–3704, 2015.
- [MPH⁺09] Jarosław Adam Miszcza, Zbigniew Puchała, Paweł Horodecki, Armin Uhlmann, and Karol Życzkowski. Sub- and super-fidelity as bounds for quantum fidelity. *Quantum Inf. Comput.*, 9(1-2):103–130, 2009.
- [MS17] Dusa McDuff and Dietmar Salamon. *Introduction to symplectic topology*. Oxford Graduate Texts in Mathematics. Oxford University Press, Oxford, third edition, 2017.
- [MVuN23] Nikolay Martynchuk and San Vũ Ngọc. On the symplectic geometry of A_k singularities, 2023. Preprint, <https://arxiv.org/abs/2105.00523>.
- [MZ04] E. Miranda and N. T. Zung. Equivariant normal form for nondegenerate singular orbits of integrable Hamiltonian systems. *Ann. Sci. École Norm. Sup. (4)*, 37(6):819–839, 2004.
- [MZ08] Xiaonan Ma and Weiping Zhang. Bergman kernels and symplectic reduction. *Astérisque*, (318):viii+154, 2008.
- [Olt22] Izak Oltman. An exotic calculus of Berezin-Toeplitz operators. Preprint, <https://arxiv.org/abs/2207.09596>, 2022.
- [Pao18] Roberto Paoletti. Local scaling asymptotics for the Gutzwiller trace formula in Berezin-Toeplitz quantization. *J. Geom. Anal.*, 28(2):1548–1596, 2018.
- [PEU20] Salvador Pérez-Esteva and Alejandro Uribe. Szegő limit theorems for singular Berezin-Toeplitz operators. *J. Funct. Anal.*, 278(1):108301, 45, 2020.
- [Pol12] Leonid Polterovich. Quantum unsharpness and symplectic rigidity. *Lett. Math. Phys.*, 102(3):245–264, 2012.
- [Pol14] Leonid Polterovich. Symplectic geometry of quantum noise. *Comm. Math. Phys.*, 327(2):481–519, 2014.
- [PPT19] Joseph Palmer, Álvaro Pelayo, and Xiudi Tang. Semitoric systems of non-simple type. Preprint, <https://arxiv.org/abs/1909.03501>, 2019.
- [PPVuN14] Álvaro Pelayo, Leonid Polterovich, and San Vũ Ngọc. Semiclassical quantization and spectral limits of \hbar -pseudodifferential and Berezin-Toeplitz operators. *Proc. Lond. Math. Soc. (3)*, 109(3):676–696, 2014.
- [PT19] Álvaro Pelayo and Xiudi Tang. Vũ Ngọc’s conjecture on focus-focus singular fibers with multiple pinched points. Preprint, <https://arxiv.org/abs/1803.00998v3>, 2019.

- [PV16] Álvaro Pelayo and San Vũ Ngọc. Spectral limits of semiclassical commuting self-adjoint operators. In *A mathematical tribute to Professor José María Montesinos Amilibia on the occasion of his seventieth birthday*, pages 527–546. Madrid: Universidad Complutense de Madrid, Facultad de Ciencias Matemáticas, Departamento de Geometría y Topología, 2016.
- [PVN11] Álvaro Pelayo and San Vũ Ngọc. Symplectic theory of completely integrable Hamiltonian systems. *Bull. Amer. Math. Soc. (N.S.)*, 48(3):409–455, 2011.
- [PVN12] Álvaro Pelayo and San Vũ Ngọc. Hamiltonian dynamics and spectral theory for spin-oscillators. *Comm. Math. Phys.*, 309(1):123–154, 2012.
- [PVN14] Álvaro Pelayo and San Vũ Ngọc. Semiclassical inverse spectral theory for singularities of focus-focus type. *Comm. Math. Phys.*, 329(2):809–820, 2014.
- [PVuN09] Á. Pelayo and S. Vũ Ngọc. Semitoric integrable systems on symplectic 4-manifolds. *Invent. Math.*, 177(3):571–597, 2009.
- [PVuN11] Á. Pelayo and S. Vũ Ngọc. Constructing integrable systems of semitoric type. *Acta Math.*, 206(1):93–125, 2011.
- [RS93] Joel Robbin and Dietmar Salamon. The Maslov index for paths. *Topology*, 32(4):827–844, 1993.
- [RSN20] Ophélie Rouby, Johannes Sjöstrand, and San Vũ Ngọc. Analytic Bergman operators in the semiclassical limit. *Duke Math. J.*, 169(16):3033–3097, 2020.
- [Rüs64] Helmut Rüssmann. Über das Verhalten analytischer Hamiltonscher Differentialgleichungen in der Nähe einer Gleichgewichtslösung. *Math. Ann.*, 154:285–300, 1964.
- [RZ12] Yanir A. Rubinstein and Steve Zelditch. The Cauchy problem for the homogeneous Monge-Ampère equation, I. Toeplitz quantization. *J. Differential Geom.*, 90(2):303–327, 2012.
- [SBS87] Michael Sh. Birman and M.Z. Solomjak. *Spectral Theory of Self-Adjoint Operators in Hilbert Space*. Mathematics and its applications. D. Reidel Pub. Co.; Sold and distributed in the U.S.A. and Canada by Kluwer Academic Publishers, 1 edition, 1987.
- [Sjö91] Johannes Sjöstrand. Microlocal analysis for the periodic magnetic Schrödinger equation and related questions. In *Microlocal analysis and applications. Lectures given at the 2nd session of the Centro Internazionale Matematico Estivo (C.I.M.E.), held at Montecatini Terme, Italy, July 3-11, 1989*, pages 237–332. Berlin etc.: Springer-Verlag, 1991.
- [Sou66] J.-M. Souriau. Quantification géométrique. *Comm. Math. Phys.*, 1:374–398, 1966.
- [SVuN18] D. Sepe and S. Vũ Ngọc. Integrable systems, symmetries, and quantization. *Lett. Math. Phys.*, 108(3):499–571, 2018.
- [Sym03] Margaret Symington. Four dimensions from two in symplectic topology. In *Topology and geometry of manifolds (Athens, GA, 2001)*, volume 71 of *Proc. Sympos. Pure Math.*, pages 153–208. Amer. Math. Soc., Providence, RI, 2003.
- [SZ99a] D. A. Sadovskii and B. I. Zhilinskiĭ. Monodromy, diabolic points, and angular momentum coupling. *Phys. Lett. A*, 256(4):235–244, 1999.

- [SZ99b] Bernard Shiffman and Steve Zelditch. Distribution of zeros of random and quantum chaotic sections of positive line bundles. *Comm. Math. Phys.*, 200(3):661–683, 1999.
- [SZ02] Bernard Shiffman and Steve Zelditch. Asymptotics of almost holomorphic sections of ample line bundles on symplectic manifolds. *J. Reine Angew. Math.*, 544:181–222, 2002.
- [Tia90] Gang Tian. On a set of polarized Kähler metrics on algebraic manifolds. *J. Differential Geom.*, 32(1):99–130, 1990.
- [Uhl76] A. Uhlmann. The “transition probability” in the state space of a $*$ -algebra. *Rep. Mathematical Phys.*, 9(2):273–279, 1976.
- [vdM85] Jan-Cees van der Meer. *The Hamiltonian Hopf bifurcation*, volume 1160 of *Lecture Notes in Mathematics*. Springer-Verlag, Berlin, 1985.
- [Vey78] J. Vey. Sur certains systèmes dynamiques séparables. *Amer. J. Math.*, 100(3):591–614, 1978.
- [Via14] Renato Vianna. On exotic Lagrangian tori in \mathbb{CP}^2 . *Geom. Topol.*, 18(4):2419–2476, 2014.
- [Via16] Renato Ferreira de Velloso Vianna. Infinitely many exotic monotone Lagrangian tori in \mathbb{CP}^2 . *J. Topol.*, 9(2):535–551, 2016.
- [VN00] San Vũ Ngọc. Bohr-Sommerfeld conditions for integrable systems with critical manifolds of focus-focus type. *Comm. Pure Appl. Math.*, 53(2):143–217, 2000.
- [VN06] San Vũ Ngọc. *Systèmes intégrables semi-classiques: du local au global*, volume 22 of *Panoramas et Synthèses*. Société Mathématique de France, Paris, 2006.
- [VuN03] San Vũ Ngọc. On semi-global invariants for focus-focus singularities. *Topology*, 42(2):365–380, 2003.
- [VuN07] San Vũ Ngọc. Moment polytopes for symplectic manifolds with monodromy. *Adv. Math.*, 208(2):909–934, 2007.
- [VuN11] San Vũ Ngọc. Symplectic inverse spectral theory for pseudodifferential operators. In *Geometric aspects of analysis and mechanics*, volume 292 of *Progr. Math.*, pages 353–372. Birkhäuser/Springer, New York, 2011.
- [VuNW13] San Vũ Ngọc and Christophe Wacheux. Smooth normal forms for integrable Hamiltonian systems near a focus-focus singularity. *Acta Math. Vietnam.*, 38(1):107–122, 2013.
- [Zel98a] S. Zelditch. The Inverse Spectral Problem for Surfaces of Revolution. *J. Differential Geom.*, 49:207–264, 1998.
- [Zel98b] Steve Zelditch. Szegő kernels and a theorem of Tian. *Internat. Math. Res. Notices*, (6):317–331, 1998.
- [Zou92] Maorong Zou. Monodromy in two degrees of freedom integrable systems. *J. Geom. Phys.*, 10(1):37–45, 1992.
- [Zun97] Nguyen Tien Zung. A note on focus-focus singularities. *Differential Geom. Appl.*, 7(2):123–130, 1997.


- [Zun02] Nguyen Tien Zung. Another note on focus-focus singularities. *Lett. Math. Phys.*, 60(1):87–99, 2002.
- [Zun03] Nguyen Tien Zung. Symplectic topology of integrable Hamiltonian systems. II. Topological classification. *Compositio Math.*, 138(2):125–156, 2003.
- [Zwo12] Maciej Zworski. *Semiclassical analysis*, volume 138 of *Graduate Studies in Mathematics*. American Mathematical Society, Providence, RI, 2012.
- [ZZ18] Steve Zelditch and Peng Zhou. Pointwise Weyl law for partial Bergman kernels. In *Algebraic and analytic microlocal analysis*, volume 269 of *Springer Proc. Math. Stat.*, pages 589–634. Springer, Cham, 2018.

Dans ce mémoire, nous présentons quelques-unes de nos contributions dans le cadre de la quantification de Berezin-Toeplitz, qui correspond à la limite semi-classique de la quantification des espaces de phases compacts, et de l'étude des systèmes semi-toriques, qui sont des systèmes intégrables en dimension quatre avec une symétrie S^1 sous-jacente.


Ce manuscrit est divisé en cinq chapitres, incluant un premier chapitre introductif. Le deuxième chapitre expose des résultats purement semi-classiques: une estimation de la fidélité d'états lagrangiens mixtes, l'étude de la distribution des zéros de certaines sections holomorphes, et une description du propagateur quantique d'un opérateur de Berezin-Toeplitz avec des applications aux formules de traces. Le troisième chapitre constitue une préparation aux chapitres suivants en présentant les prérequis sur les systèmes semi-toriques. Dans le quatrième chapitre, nous décrivons nos résultats concernant la construction d'exemples explicites de systèmes semi-toriques avec certains invariants symplectiques donnés. Enfin, dans le cinquième chapitre, nous présentons un résultat spectral inverse pour les systèmes semi-toriques quantiques, qui combine l'analyse semi-classique et la géométrie des systèmes semi-toriques.

INSTITUT DE RECHERCHE MATHÉMATIQUE AVANCÉE
UMR 7501
 Université de Strasbourg et CNRS
 7 Rue René Descartes
 67 084 STRASBOURG CEDEX

Tél. 03 68 85 01 29
 Fax 03 68 85 03 28
<https://irma.math.unistra.fr>
irma@math.unistra.fr



Université
 de Strasbourg



Institut de Recherche
 Mathématique Avancée

ISSN 0755-3390

IRMA 2023/008
<https://tel.archives-ouvertes.fr/tel-04265111>